MATTEO ACHILLI

MODIFICATION DE LA MICROSTRUCTURE ET DES PROPRIÉTÉS MÉCANIQUES D'ÉCHAFAUDAGES À BASE DE GELS DE COLLAGÈNE POUR LA RÉGÉNÉRATION DU TISSU VASCULAIRE

Thèse présentée
à la Faculté des études supérieures et postdoctorales de l'Université Laval
dans le cadre du programme de doctorat en génie de la métallurgie
pour l'obtention du grade de Philosophiae Doctor (Ph.D.)

DÉPARTEMENT DE GÉNIE DES MINES, MÉTALLURGIE ET MATÉRIAUX
FACULTÉ DES SCIENCES ET GÉNIE
UNIVERSITÉ LAVAL
QUÉBEC

2012

Résumé

Le besoin de substituts pour vaisseaux sanguins de petit calibre a attiré une attention considérable sur le développement de constructions artérielles dans des bioréacteurs à partir de systèmes d'échafaudage. Les gels formés à partir de collagène reconstitué représentent des substrats idéaux pour le remodelage du à l'activité cellulaire, mais leur faible résistance et élasticité limitent leur utilisation comme échafaudages pour la régénération du tissu vasculaire. Ces caractéristiques proviennent de la perte d'organisation structurelle liée au processus d'extraction du collagène. Dans ce contexte, l'objectif de ce projet était d'améliorer les propriétés mécaniques des gels de collagène afin de supporter la croissance et la maturation du tissu vasculaire sous contrainte cyclique.

En considérant l'importance de l'état d'agrégation du collagène pour les propriétés mécaniques des tissus natifs, la stratégie de ce projet a été de modifier la microstructure des matrices de collagène reconstitué en agissant sur trois aspects : 1) les interactions intermoléculaires et la fibrillogenèse ont été ajustées en variant les paramètres expérimentaux (pH, température, force ionique et concentration du collagène); 2) des liaisons covalentes ont été introduites afin de fixer des fibrilles voisines; 3) les gels ont été compactés et les fibrilles alignées grâce à l'action de remodelage des cellules. Des mesures de spectrophotométrie et des images par MEB ont confirmé les effets des conditions expérimentales et du remodelage sur la microstructure des gels. Notamment, la présence des cellules a permis la formation de matrices plus compactes et orientées, surtout en présence de contraintes mécaniques. Des essais mécaniques ont démontré que les stratégies adoptées ont engendré le renforcement de la structure. En particulier, des essais cycliques ont établi que la variation des conditions expérimentales combinée à la réticulation ont produit des matrices dont l'hystérèse diminue et l'élasticité augmente.

En conclusion, l'ensemble de ces études a permis la réalisation à court terme (24-48 h) de structures à base de collagène présentant une résistance mécanique, une rigidité et une élasticité accrues. Ces résultats suggèrent que ces matrices sont de bons candidats comme supports pour la régénération de tissus vasculaires sous conditionnement cyclique.

Abstract

The need for small-caliber vascular replacements has attracted considerable attention on the development of scaffold-based vascular constructs in bioreactors. Reconstituted collagen gels represent ideal substrates for cell-mediated remodeling, but their low strength and low elasticity, limits their application as scaffold for the regeneration of the vascular tissue. These features result from collagen extraction and the consequent loss of structural organization. The objective of this project was to improve the mechanical performances of collagen gels in order to support the growth and the maturation of the vascular tissue under cyclic conditioning.

Considering how fundamental collagen assembly is for the mechanical behavior of native tissues, the microstructure of reconstituted collagen lattices was modified by working on three aspects: 1) The intermolecular interactions and the aggregation of collagen monomers were tailored by modulating the experimental conditions, including pH, temperature, ionic strength and collagen concentration; 2) Inter-fibril crosslinking was carried out in order to fix neighboring collagen fibrils through their reactive side chains; 3) Gels were compacted and fibrils were aligned through cell-mediated remodeling. Spectrophotometric analyses and SEM confirmed the effects of changes in experimental conditions and cell-mediated remodeling on collagen gels microstructure. Notably, the presence of SMCs lead to tighter and highly oriented lattices, moreover in the presence of mechanical constraints. Mechanical tests showed that the adopted procedures contributed to the stiffening of collagen lattices. In particular, the modulation of the experimental conditions combined with crosslinking lead to lattices presenting lower hysteresis and higher elasticity as shown by cyclic tests.

In conclusion, this study produced, in a short time (24-48 h), collagen gel-based lattices with improved stiffness, strength, and elastic recoil. The results suggest that these lattices are serious candidates for the role of temporary supports during the maturation period under cyclic loading.

Preface

This doctoral project is part of a wider research aiming to produce tissue-engineered replacements for small-caliber blood vessels. The overall objective is to recreate in vitro a fully functional blood vessel, i.e. a tubular construct showing the histological – presence of intima, media, and adventitia – and functional features of natural vessels, with the aid of three main characters: One, a scaffold – collagen gel – two, the cellular types that characterize the three different layers – respectively endothelial cells (ECs), smooth muscle cells (SMCs) and fibroblasts – and three, a bioreactor, i.e. a device developed to promote the growth and the maturation of the engineered tissue. This project, in particular, aimed to improve the mechanical performances of collagen gels and derived tissue equivalents in prevision of the maturation process in the bioreactor.

Collagen gels potential for playing the role of temporary templates for tissue regeneration had already been assessed in vascular tissue engineering (VTE). Collagen gels are highly hydrated lattices which result from the reconstitution in vitro of collagen fibrils through a process of self-assembly. This process spontaneously occurs under proper environmental conditions and is mainly defined by the molecular structure of collagen monomers. The reconstituted lattices lack the microstructural organization that dictates the mechanical properties of collagenous tissues in vivo, and show an unsatisfactory structural stability considering the mechanical requirements for VTE scaffolds. Consisting of a network of highly entangled fibrils immersed in a fluid, collagen gels microstructure is defined by the water content and the size, orientation, and intermolecular interactions of the fibrils. The control of the processes that regulate these parameters leads to the definition of the viscoelastic behavior of collagen gels.

This project present an improved control of collagen gel microstructure through: 1) The development of new protocols for collagen gels, involving an extensive rationalization of the components and the procedures leading to collagen gelation; 2) UV-C and chemical crosslinking, which were used to stiffen the microstructure of collagen gels; 3) Cell-

mediated remodeling, for the purpose of reorganizing the collagen lattices in terms of fibril alignment and gel compaction.

This interdisciplinary project was prominently experimental. It was carried out under the supervision of Prof. Diego Mantovani, a professor at the Laboratory for Biomaterials and Bioengineering (LBB), and was developed mainly at the Research Center of the Quebec University Hospital (CHUQ), and in part at the Department of Mining, Metallurgy and Materials Engineering. The project was based on the expertise developed in the last years at the LBB concerning the extraction of collagen from rat-tail tendons (RTTs) and the preparation of collagen gels.

This thesis is structured on the insertion of three journal articles in which I am the first author. The first article entitled "On the Effects of UV-C and pH on the Mechanical Behavior, Molecular Conformation and Cell Viability of Collagen-Based Scaffold for Vascular Tissue Engineering", co-authored by Dr. Jean Lagueux and Prof. Diego Mantovani, was published in *Macromolecular Bioscience* (Vol. 10(3), P. 307-316) on March 10th, 2010. This article discussed the potential of pH modulation and UV-C crosslinking in stiffening collagen gels. While Dr. Lagueux and Prof. Mantovani contributed to the definition of the experimental protocol as well as the revision of the manuscript, the student defined the majority of the experimental plan and carried out the experimental part along with the redaction of the manuscript. The student would also like to acknowledge Dr. Pascale Chevallier and Prof. Gaétan Laroche for their suggestions concerning the FT-IR analyses and Marie-France Côté for her suggestions about the viability tests.

The second article entitled "Tailoring Mechanical Properties of Collagen-Based Scaffolds for Vascular Tissue Engineering: The Effects of pH, Temperature and Ionic Strength on Gelation " was published in *Polymers* (Vol. 2(4), P. 664-680), on December 6th, 2010, and was co-authored by Prof. Mantovani. This article discussed the influence of the experimental conditions on the microstructure of collagen gels, providing new clues about how to modulate these conditions in order to improve the mechanical performances of collagen gels. The student defined the experimental protocol and carried out the

experimental part as well as the redaction of the manuscript. Prof. Mantovani contributed to the revision of the manuscript.

The third article entitled "On the Viscoelastic Properties of Collagen Gel-Based Lattices under Cyclic Loading: Applications for Vascular Tissue Engineering" was submitted to *Macromolecular Materials & Engineering* on October 27th, 2011, and was co-authored by Ph.D student Sébastien Meghezi and Prof. Mantovani. This article compared the improvements in terms of strength and elasticity of collagen gel-based lattices resulting from two different approaches. Sébastien provided the thermoregulated bath and along with Prof. Mantovani contributed to the revision of the manuscript.

I'd like to thank Professor Diego Mantovani for the possibility that he gave me to develop an experimental project in the field of tissue engineering, moreover for his patience and the freedom I was allowed in defining the project and conducting the experiments.

I'd also like to thank Prof. Alberto Redaelli, professor at the Polytechnic of Milan. Even though the collaboration didn't work as expected, I really appreciated the opportunity of having access to his laboratory.

A special acknowledgement for the people of my research group at the Laboratory for Biomaterials and Bioengineering, who, in different moments and different ways, have been part of my path towards the completion of this project. I think about Sébastien Meghezi, a greathearted person with whom I had many discussions about common problems concerning the research, and with whom I kept the laboratory functioning well. A special thanks to Benedetto Marelli, a great friend and a great person that I had the chance to know and appreciate. Thanks to all the other people from the group, present and past, in particular Frédéric Couet, Dr. Jean Lagueux, Betül Celebi, Laure Menville, Manuela Boschelle, Marta Amadei, Ramiro Irastorza, Raquel Weska, and Navneeta Rajan.

I'm deeply grateful to Bernard Drouin, a really special person, and to Marie-France Côté and Jacques Lacroix, for their unconditioned help, kindness and availability.

Many thanks to Pascale Chevallier and to Stéphane Turgeon, research assistants at the LBB, and to their families; their presence at the laboratory and their company outside made

my stay in Quebec more comfortable, more valuable and more pleasant, and this was because I could always consider them as my reference.

Thanks to Prof. Gaétan Laroche and Prof. Éric Peticlerc, for their suggestions and their participation at our meetings. Thanks to Daniel Marcotte, for his assistance in manufacturing most of the parts of the experimental setup concerning the mechanical tests, and to the secretaries at the LBB and at the University Laval – AnnBarbara Forgues, Ginette Cadieux, and Renée Roy – for their kind help. Thanks to Servaas Holvoet, Paula Horny and once more Frédéric, for their suggestions about my manuscripts. Finally thanks to Maryam Moravej, Christian Sarra-Bournet, Marie Haïdopoulos and Karine Vallières, because by reading their theses I had many interesting inputs for this report.

Many many thanks to all the people that outside the laboratory made my life richer, more interesting and made me feel more at home with their hospitality and kindness: again Sébastien and Servaas, Marie, Sébastien François and Sandra, the Saraïlis family, Slawek and Johanna, Anna, Nadia, Daniela and Cesar, Davide, Enrico, and Mauro. Thanks especially to Maurizio, a really good friend, always present to hang out and have fun.

A big hug to my family, for their love and the possibility they gave me to join them on every Christmas. In the last five years I've realized more and more the importance of sharing moments with family and the efforts and renounces that a parent can make for his son. Thanks to my uncle Fabio, Mac, Maria, and our friends Gabriella, Guido, Joe and their families, because they have always made me feel at home.

Plein de bisous à ma princesse, because without her I wouldn't be here writing the same story. Thank you for your patience, your tireless love and understanding. I hope to be worth of all of it, and I hope to be there when you will need me the most as you did for me.

Table of contents

List of Tables

List of Figures

List of Abbreviations

AFM: Atomic Force Microscopy
CHUQ: Centre Hospitalier Universitaire de Québec
CS: Chondroitin Sulfate
DS:Dermatan Sulfate
EC: Endothelial Cell
ECM: Extra-Cellular Matrix
EDC: 1-ethyl-3-(3-dimethylaminopropyl) carbodiimide hydrochloride
FT-IR: Fourier Transform Infrared
GTA: Glutaraldehyde
Gly: Glycine
HA: Hyaluronic Acid
HS: Heparan Sulfate
Hyp: Hydroxyproline
KS: Keratan Sulfate
Lys: Lysine
MMP: Matrix Metalloproteinase
NHS: N-hydroxysuccinimide
PGA: Poly(Glycolic Acid)
Pro: Proline
RTT: Rat Tail Tendon
SEM: Scanning Electron Microscopy
SIS: Small Intestinal Submucosa
SMC: Smooth Muscle Cell – **VSMC**: Vascular Smooth Muscle Cell
TE: Tissue Engineering
TGF: Tissue Growth Factors
TEBV: Tissue-Engineered Blood Vessel
VTE: Vascular Tissue Engineering

Introduction

The replacement of diseased or destroyed tissues and organs along with the shortage of natural substitutes, constitute the main problems addressed by tissue engineering (TE), a multidisciplinary field where engineering, materials science and life sciences converge to either repair, replace, maintain, or enhance the function of a particular tissue or organ.[1,2] In particular, TE relies on the capacity of cells to regenerate living tissues as well as on driving this process by controlling cell function.[3] In this context, biomaterials, defined as materials intended to interact with biological systems, play a fundamental role.[4] In scaffold-based TE for example, biomaterials of natural or synthetic origin are shaped to form scaffolds and support cell proliferation and differentiation by mimicking the extra-cellular matrix (ECM) in terms of physical and chemical stimuli.[5] While cells alone are only able to migrate and form two-dimensional (2D) layers, scaffolds provide three-dimensional (3D) framework and an initial support for the cells to attach, proliferate, differentiate, form an ECM and develop into the desired organ or tissue prior to implantation.[6-8] Also, a number of critical cell functions, including adhesion to the matrix and other cells, migration, proliferation, differentiation, and apoptosis, can be controlled by defining the scaffold morphology and composition.[9] Ideally, in order to ensure tissue regeneration, the design of a scaffold should take into account the following requirements:[6,7,10-12]

- Biomechanical behavior: A scaffold should possess the adequate structural strength in order to match the handling and the mechanical stimulations until the cells produce a suitable ECM. Moreover, the scaffold should be able to transfer the mechanical stimuli to cells.
- High porosity: A scaffold should possess interconnecting pores of appropriate scale to favor cell migration, matrix remodeling, tissue integration and vascularisation. In particular, a large area would be available for cell interactions and biochemical modifications.

- Surface properties: A scaffold should have the appropriate surface chemistry to favor cellular attachment, migration onto or into the scaffold, proliferation, regulation of the phenotype and synthesis of the required proteins and molecules.
- Specific 3D shape: A scaffold should present a shape that matches that of the tissue to replace.
- Biodegradability: Depending on the application, long-term stability for scaffold may not be desired. In case the scaffold is either degraded or metabolized, its material should:
    - Present controlled biodegradability or bioresorbability so that tissue will eventually replace the scaffold.
    - Induce negligible toxicity from degradation products.
- Manufacturing feasibility: A scaffold should be easy to fabricate into a variety of shapes and sizes.

The replacement of small-caliber blood vessels represents an impelling problem considering the organ shortage and the suboptimal performances of current prosthetic or biological grafts.[13,14] The goal of VTE is to provide an alternative solution by producing viable and fully functional vascular substitutes according the previously cited principles. In the scaffold-based approach, vascular constructs are obtained by seeding vascular cells into a scaffold and by fostering tissue growth and maturation. The latter is normally conducted inside bioreactors, which are devices developed to reproduce a suitable environment where specific physical and chemical stimuli promote matrix remodeling and tissue regeneration.[15,16] The mechanical and the morphological properties of the construct are initially defined by the scaffold, but they change over time as a function of the cell-mediated remodeling that is promoted by the environment.[17] Ideally, after this step, vascular constructs possess the required properties to be implanted inside the human body.

Rationale and Objectives of the Project

Tissue-engineered vascular substitutes should present the three layers – intima, media and adventitia – that compose a natural vessel. Each layer is characterized by a different cellular type and consequently by different structure and functions.[18,19] The vascular tissue has a peculiar behavior in responding to mechanical solicitations like those imparted by the blood flow. This behavior is mediated by the inner layer, but it is the medial layer that accounts for the strength, elasticity and vasoactive response in arteries.[20,21] It follows that the first concern in assembling a vascular construct consists in recreating a tissue equivalent with mechanical and biological properties that mimic those of the native media. The ECM of the media is mainly made of fibrous proteins – e.g., collagen, elastin – cells – SMCs – and other macromolecules – e.g., proteoglycans (PGs), glycosaminoglycans (GAGs).[19,20,22] Collagen, in particular, was selected as scaffold material for the preparation of tissue equivalents because of its biological properties and biomechanical role in the ECM.[23] Type I collagen is present in nature in highly hierarchical assemblies and is responsible for the structural integrity of tissues like bones, skin and blood vessel.[24] It can be extracted from different sources but this procedure compromises the structural organization of collagen and consequently the peculiar mechanical strength.[25] Collagen spontaneously polymerizes in vitro when the experimental conditions are suitable, resulting in highly hydrated lattices that present an elevated potential in terms of cell-mediated remodeling and tissue regeneration.[26-28] At the same time, collagen gels do not present adequate mechanical properties for handling and even less for implantation.[29]

The objective of this doctoral project was to improve the mechanical performances of collagen gel-based lattices in terms of strength and elasticity. In particular, considering that the vascular construct is to experience a maturation period, the mechanical properties have to match the mechanical solicitations that are applied in the bioreactor. Finally, considering that collagen represents an ideal substrate for tissue regeneration because of its biological properties, it was desirable that the methods applied to achieve the objective would preserve these features.

Structure of the Thesis

The thesis is composed of six chapters. In the first chapter, the problems that engender the need for tissue-engineered blood vessels (TEBVs) are discussed. The main concepts of VTE and a literature review are then presented. In the second chapter the principles regarding matrix remodeling, maturation and regeneration of the vascular tissue are developed. Moreover, the processes and the conditions that affect the mechanical properties of collagen gels are presented in order to elucidate the strategies adopted in this project. The control and modulation of these processes constitute the core of this project and are the subject of the three articles presented in the third, fourth and fifth chapter respectively. These chapters include the experimental procedures as well as the results of the thesis.

The third chapter discusses the effects of pH and UV-C crosslinking on the stiffness of collagen gel. In addition, the effects of these parameters on the swelling properties and on the molecular conformation are shown. FT-IR spectroscopy confirmed the effects of UV-C radiation on the conformational changes of the collagen triple helix, while colorimetric tests assessed the viability of fibroblasts on these substrates.

The fourth chapter discusses the influence of the experimental conditions on collagen gelation and on the final mechanical properties of collagen gels. These effects were investigated by turbidimetric analyses and mechanical tests. Moreover, because gelation generally occurred in non-physiological conditions, viability tests assessed the suitability of these gels as substrates for SMCs adhesion and proliferation.

The fifth chapter reports the results of cyclic tests on collagen lattices prepared according to two different approaches. The outcomes in terms of strength, hysteresis, permanent deformation and matrix remodeling by SMCs are then discussed, highlighting the potential of these lattices in supporting tissue regeneration under mechanical conditioning.

The sixth and final chapter proposes a general discussion, the conclusion, and the future perspectives for the methods and protocols developed during this project.

CHAPTER 1. Context

This chapter presents the vascular system and the problems that engender the need for biological substitutes of small-diameter blood vessel. The structure of the blood vessel wall is discussed with particular attention to the composition of the ECM and its mechanical implications. Finally, a review of the literature concerning the developments in the field of VTE discusses the advantages and drawbacks of each approach, focusing on the steps that are required to generate a fully functional TEBV.

1.1 Vascular System

The cardiovascular system is a closed circulatory system formed by the heart and the vascular system, that ensures the maintenance of an optimal environment for the survival and proper functioning of cells and tissues by driving the blood through the body.[30] The blood flow in turn regulates:[31]

- The transport of oxygen, nutrients, hormones and vitamins, and the removal of carbon dioxide and metabolites.
- Control of the homeostasis, intended as control of the body fluid, of the concentration of dissolved particles, of the level of temperature and pH.
- Mediation of the immune response.

The vascular system is divided into pulmonary – the portion transporting oxygenated-depleted blood to the lungs and oxygenated blood back to the heart – and systemic – the portion transporting oxygenated blood to the rest of the body and oxygenated-depleted blood back to the heart – circulation. It consists of a branched network of blood vessels divided into five major types (**Fig. 1.1**): the arteries, the arterioles, the capillaries, the venules, and the veins.[18] Starting from the ventricles of the heart, elastic arteries transform the pulsatile output into a more stable flow, then branch into arteries of decreasing diameter and finally into muscular arteries. The blood then passes through the microcirculatory system, consisting of the arterioles, capillaries, post-capillary venules, and muscular

venules.[19,32] The exchange of gas, cells and molecules with the surrounding tissues occurs at the capillary level.

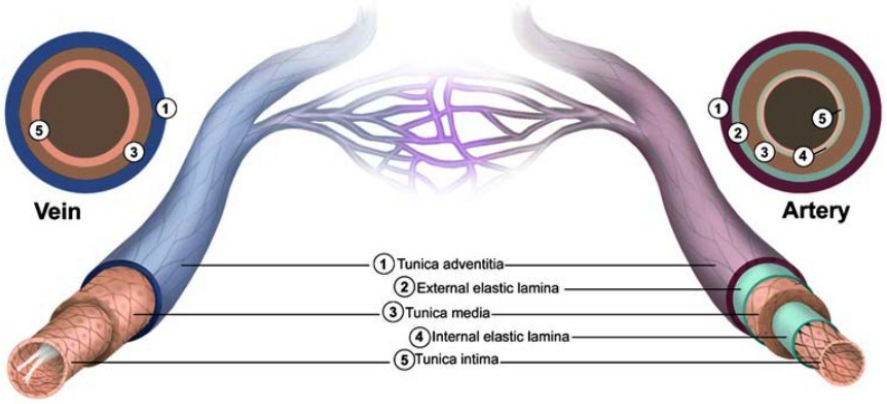

Figure 1.1: Structure and layers of arteries and veins.[33]

The microcirculation ends in the venous system where venules and veins merge into larger vessels transporting blood back to the atria of the heart.[19,34,35] The blood vessel walls have a concentric layered structure, with each layer being distinct in its cell and ECM composition and conferring specific functional properties. Arteries and veins present three layers – tunica intima, tunica media, and tunica adventitia – while capillaries are just composed of the intima. The specific microstructures of arteries and veins vary with age, disease, and location along the vascular tree.[22] Elastic arteries present a media with both SMCs and elastic laminae while in muscular arteries SMCs prevail. Arteries are an important component of proper cardiac function by serving as elastic reservoirs and pushing the blood down the vascular tree during contraction.[36] In the arteries, fenestrated, cylindrical sheets of elastin separate the intima from the media (internal elastic lamina) and the media from the adventitia (external elastic lamina).[19,20,22] The veins are divided into large and medium-sized vessels and possess a different layered configuration than arteries because of the lower intraluminal pressures.[37] Veins present thinner walls – with a thinner media and thicker adventitia – and larger cross-sectional diameters than corresponding segments of the arteries. There is little distinction in their histological details, as between the media and the adventitia, and great variation in the arrangement of the SMCs, which may be longitudinal as in the adventitia of some veins.[19,37]

1.1.1 Tunica intima

The tunica intima constitutes the innermost layer of blood vessels and consists of an endothelium and an underlying basal lamina composed of type IV collagen, laminin, fibronectin, and PGs.[38] The endothelium is a single, confluent layer of flat, elongated ECs generally aligned in the direction of the flow.[37] In addition to being a smooth, nonthrombogenic interface between the blood and the underlying vascular wall, the endothelium is a selective barrier against plasma lipids and lipoproteins, it controls nutrient and water transport across the vessel wall, and is biologically active, for example by regulating the vessel tone via SMCs contraction or by promoting cell replication, migration or synthesis of proteins. In fact, in response to chemical and mechanical stimuli, ECs produce various vasoactive molecules, growth factors, and factors that regulate the clotting process, like platelet activation, adhesion and aggregation and leukocyte adhesion.[19,21,39] The endothelium can also modify substances for transport into the wall (e.g., white blood cells or lipids), which thereby play important roles in atherosclerosis and restenosis.[20,22] Even though ECs play a pivotal role in mediating the mechanical response, in young, healthy humans, the intima contributes negligibly to the mechanical properties of the vessel.[20,37,39]

1.1.2 Tunica media

The tunica media is the dominant layer in the arteries in terms of volume and contribution to the mechanical behavior.[21,37] It is primarily responsible for maintaining the vascular tone via SMCs' vasoactivity, which in turn dictates blood pressure and shear stress. This layer is thicker in arteries than in veins.[19] The media is composed of alternating concentrical layers of SMCs embedded in various types of collagen (I, III, V), PGs, and elastin-based lamellae, whose number is higher in the larger, more proximal vessels that experience the highest wall tension.[19,20,37] Thin elastic fibrils connect the lamellae and the lamellae with the SMCs.[20,21] Collagen provides high-strain stiffness and strength to the tissue, while elastin yields resilience and low-strain elasticity, which prevents the wall from permanently deforming as a result of cyclic stretching. Collagen and SMCs are arranged in a helical herringbone pattern around the circumference of the vessel, with a pitch that

changes between different vessels and different segments of the same vessel, and whose direction alternates between successive layers.[19] This arrangement provides enhanced circumferential load-bearing properties and torsional stability to the tissue.[21] SMCs have secretory capabilities and are primarily responsible for synthesizing collagen fibers, elastic fibers, elastic lamellae and PGs of the media.[39] Smooth muscle contraction, hypertrophy (increase in size), hyperplasia (increase in number), apoptosis, and migration (often from the media to the subintima) play essential roles in diseases such as aneurysms, atherosclerosis, and hypertension.[22]

1.1.3 Tunica adventitia

The tunica adventitia is the outermost layer and is composed of fibroblasts and axially oriented type I collagen fibers that reinforce the vessel and anchor it to the perivascular tissue. The fibroblasts are primarily responsible for regulating the ECM of the adventitia via the synthesis and degradation of collagens. The high relative collagen content helps prevent over-distension and vascular rupture at extremely high pressures.[20,22] The tunica adventitia is infiltrated with nerve fibers, lymphatic vessels and (in larger veins) a network of elastin fibers. In large vessels the tunica adventitia contains a small vasculature, the vasa vasorum, which nourishes the external tissue of the vessel wall and is needed when the thickness of the wall is too great to allow a sufficient transmural diffusion of oxygen directly from the blood.[18,20,21] The fibroblasts are responsible primarily for regulating the matrix, particularly the collagen, but they can be stimulated to migrate, proliferate, and differentiate when needed.[22]

1.2 Extra-cellular matrix

The ECM endows tissues with their specific mechanical and biochemical properties. The organization and biochemistry of ECM components determine mechanical strength, cell response, and tissue organization.[40] The ECM regulates the cellular metabolism – adhesion, migration, proliferation, gene expression – by mediating the mechanical stimuli that are transmitted to cell cytoplasm via integrins, which are cellular transmembrane receptors that connect the cytoskeleton to the ECM, or by sequestering and releasing

growth factors and cytokines.[3] On the other hand, cells are responsible for the synthesis of ECM components, degrading enzymes and their inhibitors.[9,23,40] It follows that ECM and resident cells have a mutual influence on maintenance, synthesis and remodeling, cell attachment, migration and differentiation. The ECM, particularly that of connective tissues such as cartilage, tendon, skin, and blood vessel walls, consists of fibrous proteins like collagen and elastin embedded in the ground substance, a gel-like matrix that is primarily composed of water, GAGs, glycoproteins and PGs.[41]

The passive mechanical properties of a native vessel derive from the composition of the ECM and the orientation of ECM components, in particular collagen and elastin. These components contribute with PGs to appropriate strength, stiffness, elasticity and compressibility, and their combination determines the ultimate viscoelastic behavior of a normal blood vessel.[9]

Collagen is the most abundant protein in mammals and serves for the maintenance of the structural integrity of tissues and organs. Moreover, collagen is also involved in the interaction with specific receptors that define cellular adhesion, differentiation, growth and survival. Collagen also contributes to the entrapment, local storage and delivery of growth factors and cytokines, playing important roles during organ development and tissue regeneration.[23] It is organized into insoluble fibrillar structures and acts as the major stress-bearing component of connective tissues and of the fibrous matrices of skin and blood vessels.[24] Type I collagen is, with very few exceptions, the major collagen of many tissues, and its highly oriented structure is responsible for the high tensile stiffness imparted to tissues like tendons. It can be found in combination with type III collagen, which in turn is an important component of reticular fibers and elastic tissues and contributes to the extensibility of blood vessels.[23,42]

Elastin is the dominant ECM protein in the arterial wall and confers elasticity and recoiling to the blood vessel. Elastin is insoluble and is the result of the crosslinking of tropoelastin – the soluble, non-glycosylated and hydrophobic precursor synthesized by SMCs – and other extracellular proteins – the fibrillin-rich microfibrils. Elastin prevents tissue creep under load and is responsible for the mechanical behavior at low strains before stiffer collagen

fibers are engaged. In addition, elastin regulates SMCs activity and this regulation is important in preventing overexpression of fibrous proteins.[20,24,40,43]

Most proteins are covalently associated with carbohydrates to form **glycoproteins**. Glycoproteins vary in carbohydrate content from <1% to >90% by weight. They have functions that span the entire spectrum of protein activities, including those of enzymes, receptors, hormones and transport, adhesion (e.g., laminin, fibronectin), and structural proteins.[40,41]

GAGs (alternatively, mucopolysaccharides) are linear, negatively charged polysaccharides of alternating uronic acid and hexosamine residues. GAGs interact with a wide range of proteins involved in physiological and pathological processes. The negative charges are responsible for the high hydrophilicity of GAG chains, resulting in an enormous hydration in aqueous solution and a viscous behavior under mechanical solicitations, particularly compression.[24,44]

GAGs can be sulphated – chondroitin sulfate (CS), dermatan sulfate (DS), keratan sulfate (KS), heparin and heparan sulfate (HS) – or non-sulphated – hyaluronic acid (HA). These disaccharide chains occur in proportions that are both tissue and species dependent.[24,44]

In nature, all GAG chains, with the exception of HA, are covalently linked to a core protein to give a **PG**. A PG includes one or more GAG chain. They are found in the ground substance, in basement membranes (basal laminae) and in cell-surface membranes. PGs play multiple roles. They act as:

- Organizers in tissue remodeling (e.g. decorin, biglycan) by interacting with molecules such as collagen and elastin and regulating their assembly and the mechanical properties of the ECM.
- Inter-fibrillar bridges and tensile stress-transfers between neighboring fibrils.
- Biological filters selecting molecules according to their size and/or charge.
- Regulators of intracellular signaling and cellular metabolism, by presenting domains that mediate binding to cytokines, other ECM proteins, growth factors, enzymes and lipoproteins.

- Regulators of tumor cell growth and invasion.

Some of the PGs (e.g. versican) can form huge complexes by attaching noncovalently to HA, sequestering large volumes of water, and determining the compressibility of the matrix.[20,24,38,44-49]

1.3 Vascular Diseases and Clinical Solutions

Cardiovascular diseases (CVDs) are a group of disorders concerning the heart and blood vessels and represent the major cause of death globally.[50] Blood vessels can fail because of aneurysms, dissections, or most commonly because of atherosclerosis, an inflammatory disease that causes a hardening and thickening of the vessel wall by the formation of plaques – which consist of a deposition of fatty substances, calcium, collagen fibers, cellular waste products and fibrin – beneath the intimal layer. This ultimately leads to the narrowing of the lumen and can thereby decrease blood flow to the downstream tissues.[32,51]

When drugs or regulation of the life style are not sufficient in preventing the occlusion of the arteries, surgical intervention is needed. The less invasive options regard balloon angioplasty and eventually inflation of stents in the clogged region. On the contrary, when the substitution of the vessel is required, a bypass is applied. The gold standard of bypass arteries is constituted by autologous bypass grafts, obtained by displacing the saphenous vein, the internal mammary artery, or the radial artery. Arterial grafts are the preferred conduits due to their ability to provide better blood supply via vasa vasorum as well as their long-term patency. In contrast, venous grafts are susceptible to stenosis caused by intimal hyperplasia or fibrosis, secondary atherosclerosis, and aneurysm formation. Their patency is typically not long, lasting only about few years, after which surgery is again indicated. The use of autologous grafts is limited by concomitant disease or previous surgery, and hence artificial grafts must also be used.[13,14,40,52]

Synthetic grafts made of polyethylene terephthalate (PET, Dacron) and expanded polytetrafluoroethylene (ePTFE, Teflon) have had success only in high-flow or low-resistance conditions.[14] These grafts show limits concerning compliance mismatch,

favoring intimal hyperplasia at the site of anastomoses. They also show flow instabilities, which promote thrombus formation, evoke cellular and humoral foreign body response, including the deposition of plasma proteins and platelets, the infiltration of neutrophils and monocytes, and the migration of ECs and SMCs. They may experience events leading to the failure of the graft, like calcium deposition, chronic inflammation, and increased risk for microbial infections.[40,53-55] When dealing with small diameter (< 6 mm, e.g. coronary, lower leg arteries) vessels in low-flow and high-resistance conditions, these problems are accentuated. In particular, the patency rates have been disappointing and the majority of bypasses failed due to the rapid occurring of thrombotic events.[53,54,56-60] Surface-induced thrombogenicity may be reduced by engineering and coating the luminal surface of the graft with a ECs' monolayer.[53,57] Notwithstanding this approach is considered to be one of the TE methodologies for the replacement of blood vessels, it lacks potential for complete tissue regeneration, vasoactivity and consequently the full functionality of a native vessel.[25,57]

1.4 VTE and the Regeneration of the Vascular Tissue

Considering the shortcomings of current therapies in small diameter applications, the clinical need for completely biological living vascular replacements, with the ability to remodel and grow, and with the physiologic and functional characteristics of native blood vessels, drives the research in VTE.[51,61]

The full functionality of a TEBV depends on the integration of SMCs – contractility – and ECs – nonthrombogenic interface – along with the reproduction of some or all the three layers.[25,62] This process relies heavily on the ability of cells to adhere, migrate into the construct, and remodel its structure; and on an in vitro maturation period to improve construct integrity, vasoactive response, and EC stabilization. Consequently, it is extremely important to understand and control the factors – cell source, scaffold, bioreactor design, culture medium composition, and culture conditions – that regulate the synthesis, deposition, and remodeling of ECM.[60,63]

1.4.1 Requirements

A living TEBV should satisfy a number of critical requirements prior to implantation into the host system:[9,25,62,63]

- Be nonimmunogenic and resistant to infection. Because both ECs and SMCs are immunogenic cell types, current approaches rely on autologous strategies. However, critical issues like the low proliferative potential (ECs) or the time required for cell separation and expansion, may limit the clinical impact at a relevant scale. Alternatively, allogenic cells could be genetically modified to improve the immune acceptance and exploited.[57] Otherwise, autologous adult stem cells or progenitor cells may provide a valuable cell source for VTE: They can be easily obtained (bone marrow, peripheral blood) and present a high proliferative capacity as well as the potential to differentiate into multiple vascular phenotypes.[9,59,64] However, further understanding of the mechanisms – growth factors, cell-cell contact, mechanical stresses – involved in differentiation of stem cells and progenitor cells is required.[40]

- Present a confluent, quiescent endothelium in order to be nonthrombogenic. The quiescent phenotype of ECs would prevent the activation of platelets and other clotting factors. A fully functional endothelium would also enable EC-mediated vasoactivity by acting as a signaling interface between the blood flow in the vessel lumen and the underlying SMCs.

- Present a medial layer with SMCs organized circumferentially in the direction of the collagen and elastin fibers and expressing a contractile phenotype, even though both phenotypes are needed for the formation of TEBVs. The synthetic phenotype being desired during the development because of the increased cell proliferation and matrix synthesis, and the contractile phenotype being desired at the end of the development in order to provide the TEBV with vasoactivity, reduce the secretion of ECM proteins and promote the formation of intracellular myofilaments. For an implanted TEBV, SMCs expressing a synthetic phenotype would result in an excess of proliferation, migration, and ECM production, which could lead to intimal

thickening and occlusion, reproducing the pattern of certain pathological conditions like atherosclerosis and restenosis. Thus, the control of SMCs plasticity, i.e. their ability to assume synthetic or contractile phenotypes, becomes fundamental in order to avoid unwanted remodeling, as well as to provide a suitable substrate for normal EC function, and to promote normal physiological function.[3,58,65]

- Present sufficient mechanical strength (burst strength > 1700 mmHg as in safenous vein) to withstand long-term hemodynamic stresses (physiological pressure ~ 80-120 mmHg) without failure, along with presenting proper elasticity as to not experience permanent creep that can lead to aneurysm (stable diameter after 30 days of pulsatile loading). Moreover, a matched impedance (physiological compliance ~ 4-8%/mmHg x 10^{-2} at 150 mmHg) of the TEBV to the native system would be a critical factor for long-term in vivo success.[66]
- Induce an acceptable healing response; not being carcinogenic, allergenic, or resulting in infection, toxicity, inflammation, hyperplasia, or fibrous capsule formation. Ideally, remodeling of the TEBV should occur in response to the local and systemic vascular conditions, leading to the integration of the graft into the body such that it eventually becomes indistinguishable from a native vessel.
- Possess appropriate permeability to water, solutes, and cells.
- Present ease of handling and suturability (suture retention strength ~ 3 N).[66]

In addition, from a commercial standpoint and to have a clinical impact, a TEBV should be fabricated in large-scale quantities, at reasonable costs, with specifications (diameter, length) that fit the requirements of each patient, as well as being easily shipped and stored, for an off-the-shelf availability.

1.5 State of the Art

There are different methodologies for the generation of TEBV. The following paragraphs are not intended to exhaustively treat all the studies concerning VTE but to report the most significant examples for each methodology.

1.5.1 Decellularized Tissues

This approach consists of implanting a decellularized and in some cases a crosslinked tissue, which can be seeded with autologous cells before implantation or which recruits cells directly from the surrounding host tissue. These matrices already have proper composition and architecture, they offer advantages of simple manufacturing and ease of handling, and prevent the immune acceptance issues that come with allogenic cells. Nonetheless, recruiting cells into an acellular vascular construct is not trivial, and there are critical issues considering that the success of this method depends on the capacity to recruit ECs to form a nonthrombogenic endothelium on the lumen of the graft. In the case of cell seeding before implantation, the main drawbacks regard the difficulties of isolating and expanding autologous human cells.[25,51] This approach was followed in the works reported in **Table 1.1**.

Table 1.1: Decellularized tissues used as TEBV.

	Features	Observations
Badylak et al. [67] **Lantz et al.** [68] **Sandusky** [69]	Rolled small intestinal submucosa implanted in dogs	High burst pressure (3517 mmHg) No complications at 5 years
Wilson et al. [70]	Decellularized arteries from cadavers	94 % patency at 6 years (into dogs)
Huynh et al. [71]	Decellularized intestinal collagen layer coated with type I collagen and crosslinked with EDC and complexed with heparin on the luminal surface	Burst pressure ~ 1000 mmHg Suture retention twofold the surgical requirement 100 % patency after 13 weeks Infiltration of SMCs and ECs Responsiveness to vasoactive agents
Inoue et al. [72]	Rolled human acellular dermal matrix	

1.5.2 Peritoneal Granulation Tissue

This approach consists of using the body's natural healing response to produce a tubular construct (**Table 1.2**). A silicone tube is inserted in the peritoneal cavity and is progressively encapsulated in a granulation tissue consisting largely of type I collagen and myofibroblasts and then covered by mesothelial cells, which possess antithrombotic properties. The capsule is then removed and everted such that the mesothelium lines the lumen. Alternatively, this step may be avoided in presence of antithrombotic therapy.[51,73-76]

Table 1.2: Application of the body's fibrotic response to foreign materials for the construction of TEBV.

	Features	Observations
Campbell et al. [74,75]	Silastic tubing in the peritoneal cavity to promote the formation of a tubular granulation tissue (2-3 weeks)	Responsiveness to vasoactive agents Patent at 4 months Production of collagen and elastin Burst pressure ~ 2500 mmHg

Notwithstanding the high promises of this technique, the possibility to use the pleural and peritoneal cavities of human beings as in vivo bioreactors still has to be confirmed, moreover in pathological subjects. In addition, this method doesn't provide off-the-shelf available vascular grafts.

1.5.3 Biodegradable Scaffolds in Synthetic Polymers

In this approach (**Table 1.3**), cells are seeded into a biodegradable polymeric scaffold that supports cell proliferation, production of ECM proteins and tissue remodeling.

Table 1.3: TEBVs obtained using biodegradable synthetic polymers as scaffold.

	Features	Observations
Niklason et al. [77]	PGA scaffold seeded with SMCs on silicon tubes Following seeding with ECs Use of a bioreactor to impart 5 % radial strain at 60-165 beats/min Endothelialization after 8 weeks	Native-like histological features High rupture strength (> 2000 mmHg) and high collagen content compared to nonpulsed vessels (< 300 mmHg) Response to vasoactive substances Patency reduced at 4 weeks
Shum-Tim et al. [78]	PGA-polyglactin blends seeded with ECs, SMCs and fibroblasts	Patent at 5 months
Watanabe et al. [79]	PGA – L-lactides or ε-caprolactone blends seeded with vascular cells	Patent for up to 13 months
Shin'oka et al. [80]	Autologous bone marrow cells seeded onto polycaprolactone–polylactic acid blend reinforced with PGA (ø = 10 mm) Implanted in pediatric patient	No graft-related complications at 7 months
Gong et al. [64]	Constructs based on PGA scaffold and bone marrow-derived mesenchymal stem cells	Differentiation in SMCs through chemical and mechanical stimuli Histological resemblance to native vessels
Dahl et al. [81]	Constructs based on PGA scaffold and xenogenic SMCs Successive decellularization and implantation in animal models	No aneurysm or hyperplasia and 88% patency at 6 months in the arteriovenous model 1-year patency as carotid replacement SMC infiltration and EC covering in the luminal surface

Ideally, the polymer progressively degrades in culture or after implantation, transforming from a synthetic to a biological tissue analogue with an SMC medial layer. ECs are then seeded to form an endothelial lining.

1.5.4 Cell Sheets via the 'Cell Self-Assembly' Method

In this approach (**Table 1.4**), human humbilical vein SMCs and human dermal fibroblasts are cultured in the presence of high doses of ascorbic acid, producing great amounts of type I collagen and forming viable sheets of cells and ECM. These sheets are wrapped around a porous, tubular mandrel to form the media and the adventitia. After further maturation, ECs are seeded on the luminal surface. In this method, autologous human cells make the construct completely from secreted human proteins, eliminating immunological mismatch and concerns about remaining synthetic polymer in the vessel wall.

The main drawbacks are the time required to produce a fully mature construct (>13 weeks) and the complexity of the manufacturing process.[25,51]

Table 1.4: TEBVs generated via the cell-sheets approach.

	Features	Observations
L'Heureux et al. [82]	Three layered structure by autologous cells and ECM	Circumferentially oriented ECM containing collagen and elastin (in the adventitia) Burst pressure higher than 2000 mmHg (main contribution from the adventitia) 50 % patency at 1 week after implantation Intramural blood infiltration
L'Heureux et al. [83-85]	As before but without the medial layer Mechanical conditioning Implanted as hemodialysis access	Nonthrombogenic and mechanically stable at 8 months ~ 28 weeks fabrication 85 % patency at 6 month Response to vascular agonists Burst pressure ~ 3500 mmHg Lower compliance than arteries (~1.5%/mmHg x 10^{-2}), but increasing in vivo
Konig et al. [86]	Use as an A-V shunt	Mechanical stability Mechanical properties close to those of the internal mammary artery

1.5.5 Biopolymer Scaffolds

This approach (**Table 1.5**) consists of creating tubular constructs with vascular cells (SMCs, fibroblasts) seeded onto or embedded into a biopolymer-based matrix. Biopolymers can be processed under different forms, including hydrogels, freeze-dried sponges, and

electrospun matrices. In the case of hydrogels, a suspension of vascular cells is incorporated in a solubilized natural polymer (collagen, fibrin, HA). Polymerization (gelation) then occurs in tubular moulds by changing the environmental conditions (pH, temperature, addition of enzymes), resulting with the cells entrapped and uniformly dispersed in the network of the hydrogel. In the following days, the cells are responsible for the compaction and remodeling of the scaffold, and the production of a dense and organized tissue. ECs are then seeded onto the luminal surface of the constructs. These matrices have the advantage of resembling to the ECM of native tissues and the potential to be recognized by vascular cells. Indeed, by controlling their composition it is possible to direct cell differentiation, function, and remodeling in desired ways.

The major limit of this approach remains the difficulty in achieving appropriate mechanical properties for use in the arterial system.[56] Longer maturation (weeks to months) in the presence of the appropriate medium supplements or mechanical stimulation, has been shown to change the structure of the matrix, direct cell function, and increase the mechanical properties.[25,51]

Table 1.5: TEBVs obtained using biopolymers as scaffolds for vascular cells.

	Features	Observations
Weinberg et al. [87]	Adventitia anlogue made from fibroblasts and collagen Media analogue made from SMCs and collagen Intima-like monolayer of ECs, Molded into a tubular configuration Dacron sleeves as reinforcement	Lack of mechanical integrity - Low burst pressure (<10 mmHg without Dacron meshes, ~300 mmHg with Dacron sleeves) Low production of elastin - poor elasticity
L'Heureux et al. [88]	Collagen gel contracted over a central mandrel	Circumferential alignment of collagen fibrils and SMCs Burst pressure <120 mmHg
Kanda et al. [89]	Polyurethane - SMC-seeded collagen construct subjected to pulsatile flow	Longitudinal orientation for ECs and circumgerantial for SMCs and collagen Switch of SMCs from a synthetic to a contractile phenotype
Hirai et al. [90]	SMCs in type I collagen - Variation of the initial collagen concentration to improve the burst strength ECs lining Dacron sleeve	Burst pressure ~ 110 mmHg High compliance
Tranquillo et al. [91]	Magnetic prealignment in the circumferential direction of the collagen fibrils during fibrillogenesis	Mandrel compaction more beneficial than magnetic prealignment

		Still poor mechanical integrity
Girton et al. [92]	Stiffening and strengthening of collagen gels constructs through glycation (elevated dose of glucose or ribose)	Predicted burst pressure ~ 225 mmHg
Seliktar et al. [93]	Improved remodeling of SMCs seeded collagen constructs by applying cyclic distensions (10 % - 1 Hz)	Enhancement of mechanical properties and histological organization
Ye et al. [94]	Human myofibroblasts embedded in fibrin gel	
Grassl et al. [95]	Fibroblasts and neonatal SMC embedded in fibrin gel Stimulation with TGF and insulin	Higher deposition of ECM than in collagen scaffolds
Long et al. [96]	Fibroblasts and neonatal SMC embedded in fibrin gel	Deposition of elastic fibers
Cummings et al. [97]	SMCs embedded in collagen-fibrin constructs	The presence of fibrin influences compaction and final mechanical properties
Zavan et al. [98]	Hyaff scaffolds implanted for 5 months	Degraded and replaced by a neoartery Proper histological organization, no need for chemical or cellular preconditioning in vitro
Lepidi et al. [99]	Hyaff-11 construct seeded with ECs and implanted in rats	Construct degraded in 6 months and substituted by regenerated vascular tissue
Berglund et al. [100]	Organized intact elastin incorporated in collagen-based TEBV	Higher elasticity Estimated burst pressure ~ 80 mmHg at 23 days
Buttafoco et al. [101]	Freeze-dried collagen-elastin scaffolds, crosslinked, seeded with SMCs, and cultured under pulsatile flow	Improvement of the mechanical properties Cell-mediated alignment visible in 14 days

1.6 Biochemical and Biomechanical Stimulation

Cell function and phenotype are regulated by a series of environmental cues, including cell-cell interactions, biochemical – ECM composition, ions, small proteins, humoral factors, growth factors – and biomechanical – compressive, tensile or shear stress – stimuli.[3,57]

Cardiovascular cells experience 10 % strains on average with every heartbeat (~ 1 Hz). Mechanical stimuli are transduced to the cell interior through integrins and cause cytoskeletal rearrangements, activation of ion channels and membrane-bound enzymes, and the releasing of growth factors. Mechanical stimulation affects cell function, orientation, growth and differentiation, playing a critical role during tissue development and repair by modulating the synthesis of almost all major components of the ECM (collagen, elastin, PGs, GAGs, matrix metalloproteinases (MMPs), glycoproteins, growth factors).[45]

Vascular tissues are subjected to three principal hemodynamic forces, which exert their effects both independently and synergistically:[57,62]

- Shear stresses: The blood flow exerts tangential frictional stresses that act directly on ECs. Secondary signals released by ECs and transmitted to other regions of the vessel wall can modulate SMC behavior and induce changes in vessel diameter and tone, SMC proliferation, and ECM organization.[62]
- Luminal pressure: The cyclic inflation provokes the circumferential stretching and the radial compression of the vessel wall. The circumferential stretching influences directly both ECs and SMCs, and represents the dominant mechanical stimulus that the media perceives.[3,45,62]
- Tension in the longitudinal direction: In the coronary system, for example, blood vessels are exposed to cyclic bending, twisting and stretching due to their attachment to the heart.[58]

Table 1.6: Examples of TEBV conditioning via biochemical and biomechanical stimuli.

	Features	Observations
Kanda et al. [89,102]	SMC-collagen constructs cyclically stretched at 1 Hz with a strain amplitude of 10 % for up to 4 weeks	Increases in contractile components – SMC reversion to a more contractile phenotype Changes of cells and fibrils orientation
L'Heureux et al. [82]	Cell-sheets based TEBV, cultured in presence of high doses of ascorbic acid and proline	Increased production of ECM proteins, in particular type I collagen
Niklason et al. [77]	SMC-PGA constructs on silicone tubes distended for 8 weeks at 5 % radial distension at a rate of 165 beats/min to simulate the fetal environment Medium supplemented with ascorbic acid and proline	Burst pressure ~2150 mmHg Low compliance Contractility
Seliktar et al. [93]	SMC-collagen constructs distended during the compaction period at 1 Hz and a strain of 10 % for 8 days	Increased strength compared to maturation in static conditions Upregulation of MMPs expression
Isenberg et al. [103]	SMC-collagen constructs cyclically stretched for 5 weeks	Increased strength compared to maturation in static conditions
Hoerstrup et al. [53]	PGA-poly-4-hydroxybutyrate blend seeded with SMCs and ECs exposed to shear and cyclic distension	Burst pressure ~ 326 mmHg after 4 weeks Cell proliferation and collagen deposition
Kim et al. [104]	PGA scaffolds crosslinked with poly-L-lactic acid, seeded with SMC and stretched to a strain of 7 % at 1 Hz for up to 20 weeks	Increased mechanical stiffness and strength Increased collagen and elastin synthesis

The development of TEBV in vitro is inspired by the consideration that vascular cells are exposed to pulsatile forces during most of vasculogenesis and throughout life. Hence, bioreactors have been designed to provide engineered vessels with mechanical stimulation

and enhanced nutrient and oxygen delivery. Different authors (**Table 1.6**) used such systems to promote tissue growth by enhancing ECM synthesis and/or increasing cell proliferation.[57,58,60,62] The development and maturation – intended as improvement of mechanical properties, functionality, and histological organization – of TEBVs can be enhanced by mechanical stretching, which has profound effects on SMC phenotype, orientation, ECM deposition, growth factor release, proliferation, and vascular tone.[9,62] Overall, cyclic strains applied to SMCs increase the synthesis of elastin, PGs, GAGs, degrading proteases, growth factors, and contractile proteins. Static strains downregulate ECM degrading proteases and lead to a loss of the contractile phenotype, while large strains (e.g. pathological conditions) promote the synthetic phenotype and matrix synthesis.[3] ECM synthesis also depends on the magnitude, frequency, and duration of the applied strain.[3,9,45] An optimal dynamic conditioning – mimicking the strains of the in vivo environment – would promote a contractile phenotype and would avoid the change from contractile to synthetic, though a synthetic phenotype may be desired during TEBV development.[58]

Biochemical factors have a profound impact on tissue remodeling. Growth factors, glycoproteins (e.g. fibronectin, laminin) cytokines, amino acids, ions (e.g. copper), and vitamins (e.g. ascorbic acid) play key roles in triggering a large number of processes that determine cell proliferation and differentiation, collagen synthesis and crosslink formation. Optimal combinations and concentrations of these factors are important to the development of TEBVs.[57,58]

1.7 Vascularization

Long-term viability of thick 3D engineered tissues is a major challenge. It requires the development of a functional nerve network and microvasculature that will support the survival of the construct in vitro and will develop after implantation, promoting its integration.[60] Even the small-diameter TEBV, with walls ranging from 300 to 1000 μm, cannot count on the diffusion of nutrients and oxygen, and require some degree of microvasculature for proper oxygenation.[56,58] Four main approaches were developed for aiming the vascularization of engineered tissue:[105]

- Use of scaffolds with controlled release of angiogenesis growth factors.
- Coculture of ECs with target tissue cells and angiogenesis signaling cells.
- Use of microfabrication methods for creating designed channels that allow nutrients to flow and/or that direct endothelial cells attachment.
- Exploitation of decellularized tissues.

Up to now, none of the currently available TE approaches have resulted in a small-diameter TEBV that satisfies all the requirements previously reported – considering the need for acute/emergency therapy and the time required to develop a vascular construct. – with a significant clinical impact.[9,13]

CHAPTER 2. The Project: Strategies and Methodologies

This chapter presents the structure and functions of collagen, with particular attention to the features that encourage or limit the application of collagen gels in TE. The discussion on collagen self-assembly and on the viscoelastic behavior of collagenous tissues opens up for the presentation of the methodologies defined to improve the mechanical stability of collagen gels by acting on the microstructure.

2.1 Collagen: From Molecular Structure to Function

Collagen is abundant in many tissues representing about 25 % of the total body protein of mammals. The highly hierarchical organization of collagen assemblies provides the major structural support of all vertebrate tissues.[23,106]

At least 20 distinct collagen types occur in different tissue of the same individual and all of them share the same monomeric structure. A single molecule of collagen (tropocollagen) has a rodlike shape with a length of ~ 300 nm, a width of ~ 1.5 nm, and a molecular mass of ~ 285 kD.[24,42] Tropocollagen is composed of three left-handed α-helices twisted together around a central axis to form a right-handed superhelical structure. Short non-helical telopeptides flank each α-chain at the beginning (N-terminus) and at the end (C-terminus).[23] Each α-chain is staggered by one amino acid residue with respect to the neighboring chain and the three chains may be identical (homotrimers, e.g. type III collagen) or different (heterotrimers, e.g. type I collagen). These α-chains have a distinctive amino acid sequence that consists of repeating Gly-X-Y triplets over a continuous, ~1000-residue polypeptide. X is often Pro and Y is often Hyp. Inter-chain hydrogen bonds between Gly residues and Pro residues stabilize the triple helix. Enzymatic modification of Lys may occur in the third position. Collagen is synthesized within the cell as soluble procollagen, which is converted extracellularly into the collagen monomer by specific enzymatic cleavage of terminal propeptides. Without this passage, collagen monomers wouldn't assemble into fibrils.[23,24,26,42,107,108]

Type I (**Figure 2.1**) and type III collagens are fibril-forming collagens, i.e. their monomers assemble side by side in the axial direction to form fibrils with diameters of ~ 100-200 nm. Collagen fibrils present a characteristic 67 nm banding pattern (*D*-period), which derives from the monomers packing laterally with an axial stagger that is an integer multiple of the *D*-period. This stagger is due to the longitudinal clustering of polar and of hydrophobic residues, which present a periodicity of ~ 234 residues, i.e. ~ 67 nm. Since the *D*-period is not an integral division of the molecule length, a gap region separates the end of a molecule from the beginning of the next one. The association between collagen molecules is driven by electrostatic and hydrophobic interactions. These interactions are further stabilized by intermolecular, lysyl oxidase-induced crosslinks. These occur between sites in the N- and C-telopeptides and the helical part of neighboring molecules, and depend on the extent of hydroxylation of both the telopeptide and triple helical lysines involved in the crosslink. Fibrils can assemble in a parallel way to form fibers or lamellae at the micron level in tendon, bone and other tissues.[24,42,49,109-111]

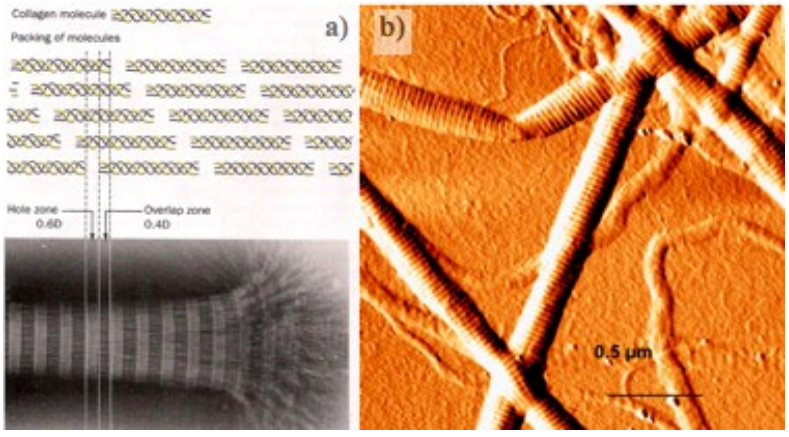

Figure 2.1: Collagen molecules packing into fibrils (a)[24]; AFM image of collagen fibrils (b) - (unpublished image from Luca Amadori).

2.1.1 Extraction

Different forms of collagen-based biomaterials are used for biomedical applications:[112-114]

- Collagenous matrices retaining the original tissue structure.
- Collagen fibers.

- Biomaterials obtained from purified collagen molecules in association, or not, with other macromolecular components and prepared in different forms depending on their applications: gels, sponges, and membranes (films or sheets).

Type I collagen is the most abundant and also the most used as a biomaterial. There are several tissues from which it can be isolated, like dermis, tendons, bone, amnion, blood vessels, pericardium, placenta, etc.[51,113] This protein is usually extracted from dermis (notably bovine, e.g. calf skin) or tendons of young animals by acid treatment, and by enzyme extraction (pepsin) in acid, for the case of more mature tissues. In fact, in this case, less labile crosslinks render collagen insoluble to simple acid solubilization, while pepsin cuts the telopeptides (atelocollagen) and consequently the covalently linked ends of collagen monomers.[28,106,112,113] The nature of the collagen crosslinking introduced by the enzyme lysyl oxidase is tissue specific. In tissues such as RTT where the telopetide lysines are barely hydroxylated and the predominant crosslink is the aldimine formed between lysine-aldehyde and hydroxylysine, the crosslink is stable under physiological conditions but can be cleaved in vitro by diluted acetic acid.[111,115] Diluted acids (e.g., acetic acid) generate repelling charges on the triple helices leading to the swelling of fibrillar structures.[42] This procedure results in a viscous liquid in which small aggregates of collagen monomers are dispersed in acetic acid.

2.1.2 Antigenicity and Immunogenicity

The animal origin of many collagen-based biomaterials has always raised concerns regarding their potential to evoke immune responses. Collagen antigenicity – i.e., the ability to interact with secreted antibodies – is linked to macromolecular features not common to the host species. Macromolecular features interacting with antibodies are referred to as antigenic determinants. In the case of collagen, they can be classified as:[116]

- Helical. The recognition by antibodies occurs only in the presence of an intact triple helix.

- Central, located within the triple helical portion of native collagen. The recognition is possible only on amino acid sequence, and therefore only when collagen is denatured and the triple helix unwound.
- Terminal, located in the nonhelical terminal regions (telopeptides) of the molecule. In these regions the major interspecies variation occurs and thus the major antigenic determinants.

Antigenicity can be reduced by pepsin treatment or by the introduction of crosslinks.[106,116] Immunogenicity is intended as the ability to induce an immune response, which implies the synthesis of antibodies. The immune response to an antigen depends both on the site of implantation and the species in which the biomaterial is implanted. It involves a complex interaction between the humoral (antibody-mediated) and cell-mediated response. These lead to binding of antibodies and targeting by cytotoxic cells, and ultimately to elimination of antigens and antigen-infected cells.[113,116] From a practical point of view, collagen is weakly immunogenic compared with other proteins, and adverse immunological responses to xenograft (e.g., bovine or porcine dermal collagen) are extremely infrequent.[116] Moreover, the use of human collagen may solve the remaining concerns about the immune acceptance of nonhuman collagen.[25]

2.1.3 Crosslinking

Natural intermolecular crosslinks are extremely important in ensuring the structural integrity of collagen fibers. For example, the inhibition of lysyl oxidase by copper deficiency or by β-aminopropionitrile, a lathyritic agent, leads to an abnormal fragility of bones, joints, and large blood vessels.[24,111] These crosslinks are disrupted during collagen extraction and purification procedures, thereby depriving the reconstituted collagen-based material of the typical strength of native collagenous tissues.[42] These reconstituted collagen lattices may then need crosslinking treatments at some stage in order to show adequate biomechanical properties.[112]

Synthetic, covalent crosslinks between collagen fibrils result in stabilization of the fibrillar network and serve to:[111,112,117]

- Reduce antigenicity and foreign body response.
- Attenuate the susceptibility to enzyme (e.g. MMPs) degradation – due to decreased accessibility for the enzyme and reduced hydration of the fibers – and host cells.
- Enhance mechanical properties – the crosslinks preventing the molecules/fibrils sliding past each other under load.

The objective is to produce a biomaterial with tailored properties and a controlled rate of degradation according to the process of regeneration of the tissue. There are several crosslinking strategies for creating covalent bonds between the reactive moieties (lysine, glutamic and aspartic acid, hydroxyl groups, etc.) in the side chains that project radially from neighboring fibrils, thus leading to intermolecular and interfibrillar crosslinking.[111] The most common strategies involve:[42,106,112,113]

- **Introduction of exogenous chemical agents** – formaldehyde, glutaraldehyde (GTA), epoxy compounds, and isocyanates – that are incorporated as part of the crosslink, forming chemical entities that are not normally present in biological tissues. Thus, these materials may result cytotoxic or may induce inflammation or immune response in situ, as well as, when degraded, in the organs involved in their metabolism or excretion. In the case of GTA, the number and effectiveness of crosslinks depends on the number of available primary amines (ε-amino groups of lysine residues) and their intermolecular distance, which in turn are determined by collagen concentration and fibril disposition.
- **Catalysis of crosslink formation by physicochemical means** (photo-oxidation, γ-radiation, microwave irradiation, dehydration, freeze-drying, and dehydrothermal treatment). These methods eliminate concerns about nonbiological agents, residual precursor, intermediates, and derivatives. Dehydration leads to densification of collagen matrices and formation of covalent and noncovalent corsslinks. Dehydrothermal treatment, which consists of drying at 110 ºC under vacuum, produces concentrated crosslinked matrices through condensation reactions (esterification or amide link formation), although there are risks of denaturation and

degradation. UV-C (λ = 254 nm) rays generate free radicals in the core of aromatic residues as in tyrosine and phenylalanine. Intensity, distance from the source and duration of irradiation must be carefully chosen in the case of UV-C because it may adversely affect the integrity of collagen molecules. In fact, UV-C light has two competing effects: crosslinking increases with increased radiation, but, prolonged exposure leads to fragmentation of the collagen triple helix and denaturation.

- **Catalysis by chemical agents** – carbodiimide (e.g., EDC) and azyl azide – that are removed after the reaction. In this case, the catalytic agent is not incorporated into the crosslink and can be completely washed out of the biomaterial. EDC (**Figure 2.2**) reacts with the carboxyl groups of aspartic acid and glutamic acid side chains and mediates the link with primary amines of lysine to form an amide link. The addition of N-hydroxysuccinimide (NHS) makes the reaction more efficient by reducing the intermediates of the reaction. No residual agent remains and the resulting iso-peptide bond mimics the natural peptide bond in proteins.

- **Introduction of biological crosslinking compounds** – genipin, nordihydroguaiaretic acid (NDGA). Genipin becomes incorporated after a reaction between its aldehydes and the primary amines of collagen, as in GTA crosslinking. On the other hand, the fact of being a biological molecule renders the fixed tissues less cytotoxic than in the case of GTA. NDGA does not form crosslinks with side chains of collagen but polymerizes and interpolates within the collagen network.

- **Naturally occurring crosslinking reactions** (glycation, via lysyl oxydase, via transglutaminase). Glycation, i.e. non-enzymatic, carbohydrate-mediated (glucose or ribose) crosslinking, occurs in connective tissues with aging and is accelerated in cases of diabetes. When reproduced in vitro, glycation does not elicit an inflammatory response nor does it prevent normal cell activity. The effectiveness of glycation may be improved by coupling this method with UV-C radiation. Lysyl oxidase induces crosslinking by the conversion of lysine and hydroxylysine to allysine and hydroxyallysine. SMCs need to be transfected to overexpress lysyl oxidase and cofactors like pyridoxal phosphate, Cu^{2+}, and O_2 are necessary.[118]

Crosslinking by glycation or lysyl oxidase does not damage the cellular component of cell-seeded gels. On the contrary, the other methodes require procedures or agents that result cytotoxic. In these cases, the approach consists in creating a scaffold, carry out the crosslinking, and subsequently seed the cells. This approach is similar to the one combining cells with a preformed synthetic scaffold, with the important distinction that the scaffold is made of collagen.[25,51]

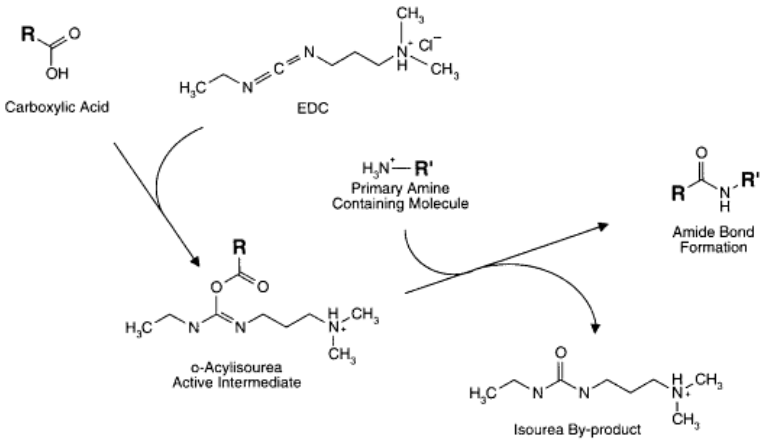

Figure 2.2: EDC-mediated crosslinking. EDC reacts with carboxylic groups to form highly active, o-acylisourea intermediates that can react with a nucleophile (e.g., primary amine) to form an amide bond. Both the reagent and the isourea formed as the by-product of the reaction can be washed out.[119]

2.1.4 Degradation

Collagen is naturally degraded by MMPs, specifically collagenase and phagocytosis, and leaves no permanent foreign residue. The rate of degradation of collagen depends heavily on the site chosen for implantation in the organism, and can be tailored by the introduction of crosslinks.[23,108,113]

2.1.5 Denaturation

Collagen triple helix can unfold to the random coil conformation (gelatin) following physical treatments (e.g., UV-C) or by heating. In particular, the denaturation temperature depends on the origin and on the degree of assembly of collagen molecules: The mammalian collagens denature at about 40 ºC, while the aggregated fibers denature at

about 65 ºC. The denaturation temperature is indicative of the degree of stability of collagen lattices and is often measured to evaluate the efficacy of crosslinking treatments.[111]

The degree of denaturation of collagen molecules can be followed by Fourier Transform Infrared (FT-IR) analysis. The shift of the peaks of specific bands (e.g., Amide I, II), generally to lower frequencies, is indicative of the triple helix-random coil transition that affects collagen lattices subjected to thermal or UV-C treatments.[120-126]

2.2 Hydrogels as Scaffolding Systems

Scaffolds serve as 3D networks which address cell function and metabolism, and mediate stimuli, which in turn direct growth and formation of a desired tissue. In this regard, hydrogels, i.e. highly hydrated polymers (water content ≥ 30 wt.-%), represent ideal templates for tissue regeneration. This is because they present high permeability to dissolved solutes, provide a place for cells to adhere, proliferate, and differentiate, and mediate chemical signals through the incorporation of growth factors, and mechanical signals to the cells.[108] Hydrogels are composed of hydrophilic chains, of either synthetic or natural origin. The structural integrity of hydrogels depends on various chemical bonds and physical interactions formed between polymer chains. Hydrogels are typically degradable, can be processed under mild conditions, and have mechanical and structural properties similar to the ECM. Naturally derived hydrogels can be formed from agarose, alginate, chitosan, collagen, fibrin, gelatin, and HA. They have been frequently used in TE applications because they are either components of, or present affinities to, the natural ECM, and can be easily molded into specific geometries.[108] Mechanical properties are affected by polymer and crosslinker characteristics, gelling conditions (e.g. temperature and pH), swelling, and degradation.[108] Gels in which the inter-chain interactions are not covalent (i.e., without crosslinking) can present viscous properties, since, under stress, the molecular chains can slide past each other.[28] The success of scaffolds depends on the appropriate transport of gases, nutrients, proteins, cells, and waste products into, out of, and/or within the scaffold. In the case of hydrogels, this transport occurs by diffusion and represents one of the advantages of this type of biomaterial.

Reconstituted collagen gels provide a biomimetic, 3D environment that promotes, through mechanical (mediated by integrins) and chemical (regulating the entrapment, local storage and delivery of growth factors and cytokines) stimuli, in-vivo-like cellular (e.g., fibroblasts, SMCs) activity (adhesion, proliferation, differentiation, protein synthesis and migration), which differs from that of 2D cultures. Besides, these biological scaffolds are particularly attractive because of the capability of cells to remodel the collagenous lattice, when they are added either during or after reconstitution, leading to the fast formation of a tissue-equivalent easy to manipulate.[25,51,57,113,127]

2.2.1 In Vitro Self-Assembly

It was shown that collagen monomers – obtained from acidic or enzymatic treatments and solubilized in cold (4 ºC) dilute acetic acid – spontaneously self-assemble under suitable experimental conditions (21-37 ºC, physiologic pH and salt concentration), by both linear and lateral growth, forming fibrils identical to those observed in vivo (e.g., same *D*-period). This self-assembly (also referred as fibrillogenesis) results in gels where randomly oriented, highly entangled collagen fibrils are suspended in aqueous buffer. The typical collagen concentration is between 0.1 and 0.5 % by weight, which is substantially lower than in native tissues (e.g., skin > 5 %). The kinetics of self-assembly, fibrils' final structure, and mechanical properties all depend on the initial concentration of collagen, as well as the temperature of the reaction, the properties of the buffer (pH, ionic strength, electrolyte species and concentrations), the presence of other molecules (e.g., GAGs, PGs), and the retention of the N- and C-telopeptides.[24-26,28,42,127-132]

The contribution of the N- and C-telopeptides is clear when comparing the self-assembly of collagen monomers obtained by solubilization in dilute acid, to the self-assembly of monomers whose non-helical telopeptides have been cleaved by pepsin-digestion. It was shown that the telopeptides help both the initiation and the development of well-packed long fibrils.[127,128,133]

Self-assembly proceeds by a nucleation and growth mechanism and can be monitored by rheological tests and turbidity measurements (λ = 300-400 nm). The final microstructure

can be observed by different microscopic techniques, including electron microscopy (SEM or TEM), atomic force microscopy (AFM), confocal microscopy, second harmonic generation and multiphoton microscopy.[24,129,134-141] Turbidity (or optical density) is proportional to collagen concentration, fibril size, number, and bundling. A typical curve shows three phases (**Figure 2.3**): an initial lag phase with no change in turbidity – where small numbers of collagen molecules associate to form nuclei (5-17 molecules) – a sigmoidal growth phase – where the nuclei (otherwise identified as microfibrils) grow into fibrils by longitudinal and lateral accretion of more molecules or microfibrils – and finally a plateau region. The rate of self-assembly is normally expressed in terms of time between the start of the process and the moment in which the turbidity reaches the half of its value at the steady state (half-time or $t_{1/2}$). Fibril diameter is determined during the lag phase, by the rate of nucleation and the step of the nuclei.[26,49,127-129,131,135,138,139,142-145]

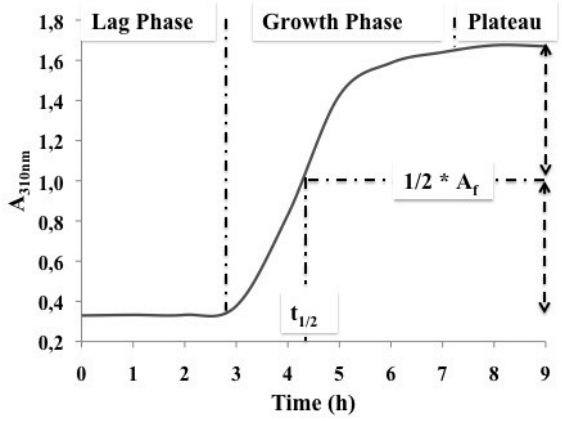

Figure 2.3: Turbidity during collagen self-assembly.

Fibrillogenesis is determined by the intrinsic properties of the collagen molecules themselves.[107,146] It is driven by the entropy of the solvent and more generally depends on the hydrogen bonding, as well as on the hydrophobic and electrostatic interactions between neighboring collagen molecules. While hydrophobic residues tend to associate in order to minimize the contact with the solvent, ionizable residues participate in electrostatic interactions that are sensitive to the pH and ionic strength of the solution. Hydrophobic interactions are strongly influenced by the mobility of water molecules and consequently by the temperature. On the other hand, electrostatic interactions depend on the net charge of

collagen molecules, which in turn is a consequence of pH and salt concentration, i.e. ionic strength.[127,129-131,138,142,147-149]

2.2.2 Effects of Collagen Concentration

An increase in collagen concentration accelerates the self-assembly process (both lag and growth phase) and results in higher fibril density and more interactions between fibrils. This leads to greater fibril recruitment and a stiffer response to mechanical solicitations.[127,129,132]

2.2.3 Effects of pH

The pH value exerts a significant effect on the net charges and number of ionized amino acids (e.g., histidine) along adjacent collagen triple helices. It was proposed that an increase of pH leads to the deprotonation of amino acid side chains as well as to the decrease of the net positive charge on each collagen monomer. This thereby increases the intermolecular attractive forces and stabilizes the fibril.[130,141,149,150] In general, the increase of pH results in thinner and longer fibrils, in a lower turbidity (**Figure 2.4**), and in higher mechanical properties.[129,130,132,141,151]

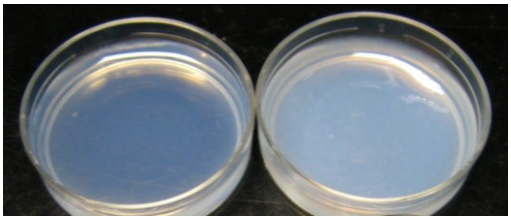

Figure 2.4: Macroscopical appearance of collagen gels prepared at pH 10 (left) and 7 (right).

2.2.4 Effects of Ionic Strength

The ionic strength depends on the type and concentration of electrolytes in the solution. These ions can be adsorbed by charged residues and consequently can reduce the number of attractive or repulsive interactions between charged groups.[149,150] At low concentrations, the ions screen the similarly charged groups and favor self-assembly, while at high concentration the ions screen the oppositely charged groups as well and hinder the process (salting in). Given the pH (normally ~ 7), high ionic strengths (compared to 140-150 mM)

lead to a lower rate of self-assembly, and increase the extent of lateral aggregation thus producing thicker fibrils. The last point is confirmed by the higher turbidity. Fibrils are more flexible and have a higher water content. The intermolecular interactions are weaker and the mechanical properties lower.[129,130,148,152]

In addition, it was shown that the isoelectric point shifts as a function of the salt concentration and ion species (e.g., Na^{+}, K^{+}, Ca^{2+}, $HPO4^{2-}$, etc.), which is probably for the adsorption of ions by the collagen molecules. In general, collagen molecules are less soluble at the isoelectric point because the surface charge of the collagen monomers is reduced, minimizing the electrostatic repulsion and favoring fibril formation.[149,152]

2.2.5 Effects of Temperature

The increase of temperature favors hydrophobic interactions between nonpolar amino acids (including phenylalanine, valine, leucine, isoleucine, and methionine) of adjacent molecules. The increase of temperature leads to a faster self-assembly, a lower turbidity, and thinner fibrils. Generally, mechanical properties are higher at lower temperatures.[129,130,138-140,144,148,153]

An increase of fibril diameter along with decreasing temperature is consistent with the nucleation-growth mechanism. At higher temperatures nucleation is faster, and so more nucleation centers form and compete with each other for aggregation of remaining collagen molecules, resulting in slender fibrils.[139,153]

2.2.6 Mechanical Implications of the Microstructure

Collagen fibril density, dimensions (diameter, length) and organization depend on the assembly conditions and define the gel microstructure, thereby impacting the bulk mechanical properties (and biological activity) of the resulting gels. For a given collagen concentration, mechanical properties generally increase in gels with longer thinner fibrils. This determines a higher surface area for inter-fibril interactions and thus a more interconnected and continuous network.[127,132,139,140]

2.2.7 Preparation of Collagen Gels

The composition of collagen gels is defined according to the desired microstructure and is conditioned by the presence of cells. For example, blends of collagen and cells are usually prepared with a physiologic salt concentration and at physiologic pH, eventually with the addition of culture medium.[91,93,103,154,155]

Table 2.1: Different protocols adopted to promote collagen self-assembly.

	Regulation of pH	Regulation of ionic strength
Gross et al. [156]	HCl - phosphate buffer	NaCl - phosphate buffer
Wood et al. [142]	NaOH – KH_2PO_4	NaCl
Cooper et al. [157]	Acetic acid diluted against water - Na_2HPO_4 - KH_2PO_4	Na_2HPO_4 - KH_2PO_4
Comper et al. [133]	NaOH - KH_2PO_4	NaCl
Williams et al. [144]	TES - HEPES - Na_2HPO_4 - NaH_2PO_4 - NaOH - HCl	NaCl
Gelman et al. [158]	TES - Na_2HPO_4	NaCl
Helseth et al. [135]	NaOH	NaCl
Na et al. [159,160]	NaPi (not specified phosphate solution)	NaCl
Rosenblatt et al. [130]	Na_2HPO_4	NaCl
Roeder et al. [132]	Na_2HPO_4 - KH_2PO_4	PBS -
Silver et al. [161]	Tris - Na_2HPO_4	NaCl
Freudenberg et al. [149]	PBS - NaOH	PBS - KCl / $CaCl_2$
Raub et al. [140,141]	NaOH	PBS - NaCl
Li et al. [152]	NaOH	PBS
"Physiologic" gels		
Tranquillo et al. [91]	NaOH - HEPES	MEM
Wakatsuki et al. [155]	NaOH	DMEM
Seliktar et al. [93]	NaOH	DMEM
Rajan et al. [29]	NaHCO3	DMEM
Yang et al. [139]	HEPES - NaOH	DMEM

The preparation of collagen gels proceeds through three main steps:

1. The neutralization of the cold (4 ºC) diluted acid (acetic acid, hydrochloric acid - HCl) in which collagen is solubilized through the addition of the proper amount of strong (sodium hydroxide - NaOH) or weak (e.g., sodium bicarbonate - $NaHCO_3$)

bases. Buffers can be added to further stabilize the pH (e.g., Tris[1], PBS[2], TES[3], HEPES[4], DMEM[5]).

2. The addition of an electrolyte (salt) solution to raise the ionic strength and promote the electrostatic interactions that favor collagen self-assembly.
3. Blending in ice and increasing of the temperature to foster the hydrophobic interactions that favor the self-assembly process as well.

Different "recipes" (**Table 2.1**) have been adopted to obtain collagen gels; most of them aimed to reproduce the conditions that promote collagen fibrillogenesis in vivo (physiological conditions, i.e. pH ~ 7-7.4, ionic strength ~ 140 mM, temperature ~ 37 ºC), while others vary base and salt concentrations in order to investigate the effects of pH and ionic strength. The choice of base and electrolytes is not trivial: for example, weak bases (Na_2HPO_4, $NaHCO_3$) normally imply a higher contribution in terms of ionic strength, which in turn has to be compensated by reducing the salt concentration, and only a lower range of pH that can be achieved. On the other hand, the effects of the salt content depend not only on the concentration but also on the type of ions diluted: monovalent (e.g., NaCl, KCl) or divalent (e.g., $CaCl_2$) ions influence the electrostatic interactions differently.

Finally, the selection of buffers or salt type may affect the efficacy of crosslinking treatments on collagen gels. It was shown that phosphates are responsible for the electrolysis of EDC and hinder crosslinking.[162-165]

2.3 Applications of Collagen Gels in VTE

Bell and al. were the first to present the process by which fibroblasts recognize collagen gels and compact the fibril network.[166] This approach was subjected to developments but the basic principles remain: It consists in blending a suspension of cell (fibroblasts or SMCs), solubilized collagen (especially type I), and growth supplements. The resulting

[1] Tris: Tris(hydroxymethyl)aminomethane
[2] PBS: Phosphate Buffered Saline
[3] TES: N-(tris(hydroxymethyl)methyl-2-amino)-ethanesulfonic acid
[4] HEPES: 4-(2-Hydroxyethyl)piperazine-1-ethanesulfonic acid
[5] DMEM: Dulbecco's Modified Eagle Medium

solution can be cast in moulds with the desired geometry (e.g., annular mould) and gelation is carried out in physiological conditions. Once the gel is formed, cells result entrapped in the lattice and they are fed with culture medium. The cells extend processes, spread out in 3D, become anchored to the surrounding fibrils through integrins, and start to exert tensile forces. Of initial round shape, they then develop stellate or bipolar morphologies. It follows a process of contraction, rearrangement and densification that begins within hours and continues for days. It is visible at macroscopic level as a marked reduction in gel volume – up to 85-99 % – and an increase in solid volume fraction through matrix compaction and fluid syneresis (**Figure 2.5**). From a mechanical point of view, this process produces tissue-equivalent with higher mechanical properties than the first gel. Cells rearrange the fibril network in a reciprocal manner, in ways and with rates that depend on several factors including: physical constraints; presence of serum and composition of the culture medium; concentration, age and type of cells; concentration and type of collagen.[25,51,113,127]

Total gel contraction and relative rate are higher in low-collagen, high-cell-density constructs and lower in high-collagen, low-cell-density constructs. Above a certain cell number, contraction does not change, potentially due to a lack of binding sites.[127]

The combination of mold geometry and mechanical constraints (e.g., adherent or free-slip surfaces) can be used to control cell and fibril alignment, which in turn strongly influences the mechanical properties. Unconstrained gels are compacted into random, isotropic fibrillar networks because the fibrils are pulled freely in the direction of cell traction. Their mechanical properties improve following densification over the first few weeks of culture but eventually decline.[127]

Mechanical constraints exist when placing local boundaries on network rearrangement, which lead to the anisotropic distribution of collagen fibrils and mechanical properties. In this case, mechanical properties generally improve over time, following densification, fibril alignment, and ECM remodeling.[127] Free-slip surfaces are used to promote circumferential alignment in TEBVs.[88,167] In these studies, collagen is reconstituted in annular molds with a non-adherent inner mandrel. This redistributes the strain field induced by cells in the

circumferential direction, leading to fibrils alignment (as in the media of blood vessels) and the consequent improvement of the mechanical stability in this direction.[25,62,63,127]

Pre-aligned fibril networks can influence cell-mediated compaction by contact guidance, where cell preferentially align in the direction of the matrix and exert tractions along this axes.[127]

Gel compaction can be stimulated by growth factors and can be inhibited by the absence of serum – serum free gels do not generate force – or agents preventing the organization of actin filaments.[51,113,127]

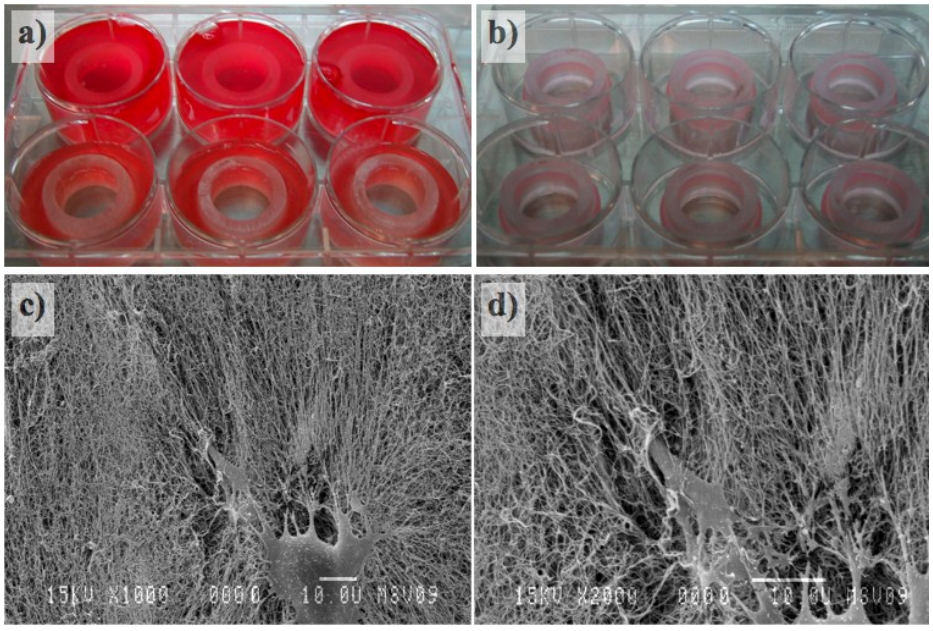

Figure 2.5: Collagen gels prepared embedding SMCs and cast in annular moulds (a); same samples compacted after 24 h (b). Collagen fibrils pulled and aligned by SMCs (c - 1000x, d - 2000x)

During compaction, cell proliferation and collagen synthesis decrease (contractile phenotype), while the expression of MMPs significantly increases compared to monolayer culture or seeded collagen sponges. This is probably a result of the number and the 3D distribution of contact sites between collagen and cells.[113] The initial collagen is progressively degraded (5 % in ~ 3 days, ~ 80 % in 4 weeks) and collagen synthesis depends on whether the gel is constrained. Unconstrained floating gels induce quiescence and apoptotic cell death, while constrained gels compact significantly more and present an

increased cell number. Other matrix components are synthesized in a manner dependent on the cell type and culture conditions. While PGs and GAGs are rapidly synthesized, elastin is almost absent.[127]

2.3.1 Drawbacks

Cell-seeded gel compaction is insufficient to produce a functional tissue replacement. Collagen gel-based constructs are characterized by unsatisfactory mechanical performances (e.g., strength, elasticity) that derive from the low structural integrity of the reconstituted collagen gels, as well as the composition and structure of the matrix, which differ from the one of native tissues. In particular, without the integration of elastin, the constructs would probably experience permanent deformation and mechanical failure.[25,127]

2.3.2 Tissue Maturation

A fully mature vascular construct should present mechanical and histological features specific of native vessels. These features can be achieved by tailoring the organization and composition of the matrix as well as the function of cells.[51] In this regard, different methods have been investigated to promote this development. Different techniques attempt to reproduce mechanical and chemical cues that occur in vivo during development.[127]

Supplementation of the culture medium with growth factors, amino acids and ascorbic acid have been shown to alter SMC metabolism and in particular to increase the synthesis of ECM proteins (e.g., collagen).[51,62,117]

Mechanical stimulation is an important trigger for cellular response, thus cyclic circumferential stretch was explored with the intent to mimic the pulsatile solicitations in the cardiovascular system and to address cell function. This conditioning has been shown to alter cell phenotype and consequently matrix synthesis, organization, and degradation, and finally tissue histology in a manner dependent on the loading protocol (preload, stretch magnitude and rest time, frequency, experiment duration) and the cell type. It has also been shown to improve the mechanical properties compared to statically loaded controls and to promote the synthesis and integration of circumferentially aligned elastin, practically absent in static control.[25,51,127]

2.4 Biomechanical Profile of Collagen-based Tissues

Soft biologic tissues (e.g., skin, blood vessels) usually present a viscoelastic behavior, i.e. they show a non-linear, time-dependent stress-strain relationship with the features of both elastic solids – time-independent behavior, elastic energy storage – and viscous liquids – time-dependent behavior, viscous dissipation of the energy. The viscoelasticity and the anisotropy of these tissues depend on the hierarchical structure of the ECM at the molecular and supramolecular level, and in particular on the preferential orientation of the fibrous component. In this regard, the impact of collagen structures – fibrils, fibers – is of primary importance. The energy storage and the elastic behavior during deformation involve the reversible axial stretching of collagen at the molecular – triple helix – and supramolecular levels – increase of the *D*-period, inter-fibril stretching. On the other hand, the viscous dissipation involves the plastic sliding of molecular and fibrillar units by each other. The absence of intermolecular and inter-fibrils crosslinks precludes the elastic recovery to the state before deformation, accentuating the viscous character and the occurring of permanent deformations.[32,168-171]

The mechanical properties of collagenous tissues and collagen gels can be investigated through rheological, compression, or tensile tests, and depend on the loading conditions. Rheological oscillatory tests have been conducted to show the elastic – represented by the storage modulus (G') – and viscous – represented by the loss modulus (G") – components of the material. The amount of phase shift defines the loss tangent ($\tan \delta = G''/G'$), where $\tan \delta = 0$ for an elastic material and $\tan \delta = \infty$ for a completely viscous material.[127,130,138-141,147,153]

In the case of tensile tests, mechanical properties are often expressed in terms of stiffness (the resistance to deformation for a given stress), strength (the maximum stress sustained before breaking), toughness (the energy stored or dissipated before breaking), failure strain and yield stress. On the other hand, the viscoelastic behavior is normally shown with stress-relaxation – decay of the stress in a sample held at a fixed strain – or creep – increase of the strain in a sample held at a fixed stress – tests, while the energy dissipation (by heat) in a

cycle, is expressed in terms of hysteresis, i.e. the loop area formed by the loading and unloading curves (**Figure 2.6 a**).[155,169,172-176]

Uniaxial tensile tests on reconstituted collagen lattices may involve dog bone or ring-shaped samples (**Figure 2.6 b-c**), as in the case of gels, tissue-equivalents, or fibers.

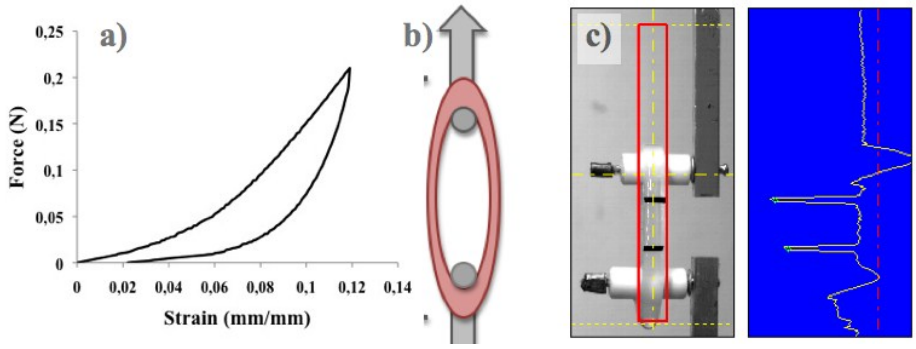

Figure 2.6: (a) Loop hysteresis of a collagen gel sample in a tensile test. (b) Setup of a tensile test on a ring-shaped sample. (c) Collagen gel ring (frontal perspective) with markers (black strips) mounted on two cylindrical hooks and ready for tensile tests; a camera recognizes and follows the markers shown as the two peaks in the diagram.

These tests generate nonlinear stress-strain curves similar to those of native soft tissue and exhibit three regions (**Figure 2.7**):[93,127,132,161,172]

1. A nonlinear "toe" region at low strain: At the beginning, low stress generates large deformation. Fibrils are not stretched but uncrimp and realign in the load direction.
2. A stiff "linear" region: Fibrils are aligned in the load direction and stretched axially.
3. An exponential yield and failure region: Its presence depends on the microstructure and the type of breaking – plastic or brittle – of the sample.

Acellular gels and tissue-equivalents have a mechanical behavior that is dependent on the strain magnitude, strain rate, rest period, and preconditioning protocol, probably because the changes in fibril alignment, interfibrillar associations and water flow are sensitive to the aforementioned parameters. Preconditioning may work to stabilize the mechanical properties of gels but it was shown not to be so effective in the case of tissue-equivalents.[172]

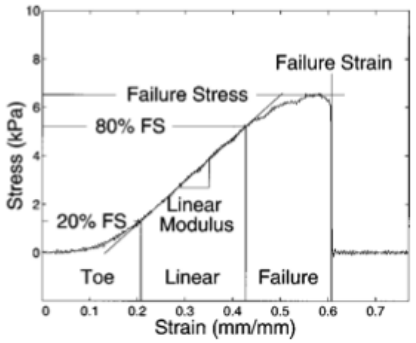

Figure 2.7: Typical stress-strain relationship in collagen gels.[132]

From a mechanical point of view, tissue-equivalents represent a higher level of complexity compared to acellular gels. This is generally because they are anisotropic, present a modified ECM, and their mechanical behavior is affected by cell activity in response to mechanical and chemical stimuli.[93,127,155]

The strength and stiffness of collagen gel-based constructs can be tested by shaping tubular samples and subjecting them to intraluminal pressure: In this case, the investigated parameters are compliance and burst pressure, where the compliance represents the radial deformation per unit of pressure, and the burst pressure represents the pressure at break of the sample.[87,154]

In compression (confined or unconfined) tests, the viscoelastic behavior is more complex compared to shear and tensile tests because of the poroelastic mechanism: For this case, the viscous dissipation is not only caused by the slippage within the fibril network but also by the dissipation via interstitial flow.[127,177-180]

2.5 Blends of collagen and natural polymers

The mechanical properties of collagen scaffolds can be enhanced by combining collagen with synthetic or natural polymers (e.g., elastin, GAG, fibrin, chitosan, fibroin). These biomaterials have been investigated for different TE applications and can be obtained by associating the polymers in separate phases or by blending them. In this case, different processing lead to either electrospun matrices, freeze-dried sponges, films or gels.[10,87,108,181] The blends may eventually be crosslinked to increase their mechanical

integrity.[51] The combination of collagen with natural polymers may also improve the biological performances of the scaffold, even considering the fact that they are degraded in vivo by normal enzymatic processes.[108]

2.5.1 Collagen-Chitosan Scaffolds

Chitosan is a linear polysaccharide derived from chitin, it is found in arthropod exoskeletons, and is structurally similar to GAGs. As collagen it is soluble in dilute acids and gels at a physiologic pH, so that these two components can be easily blended. Chitosan-collagen blends are often processed to form sponges and have been widely investigated in the TE of tissues including skin, periodontal ligament and cartilage.[182-185]

2.5.2 Collagen-Fibrin Scaffolds

The use of fibrin has given interesting results with and without collagen.[96,97,186-188] Fibrin is a wound-healing protein and it is known to stimulate regenerative and remodeling responses in a variety of cell types. Insoluble fibrin fibrils can be obtained by enzyme (thrombin) cleavage from fibrinogen, which is abundant in blood, and can be isolated, purified, and solubilized.[51] Fibrin gels present similar microstructures – fibril diameter ~ 40-400 nm – and the same potential to undergo cell-mediated remodeling compared to collagen gels, but have two main advantages:[62]

- Autologous fibrin can be easily extracted from the blood of the patient.
- Culture of SMCs in fibrin gels showed higher synthesis of collagen and elastin, which is promising for the production of the elastic component that is so critical for the full-functionality of TEBVs.

From a mechanical point of view, fibrin gels appear weaker than pure collagen gels but their blending, moreover in combination with cell-mediated remodeling, leads to interesting results.[97,189]

2.5.3 Collagen-Fibroin Scaffolds

Fibroin is a natural protein that composes the backbone of silk, a material with extremely high mechanical properties and excellent biocompatibility. Collagen and fibroin have been combined to form porous or electrospun scaffolds.[190,191]

2.5.4 Collagen-Elastin Scaffolds

Elastin is the protein responsible for the elastic recoil of native vessels. Even though it is naturally insoluble, crosslinked elastin can be hydrolized and used as scaffold material. This protein is interesting not only for the fundamental contribution it provides to the mechanical profile of the scaffold, but also for the role that elastin peptides exert in cell signaling, chemotaxis, proliferation, and protease expression.[190] Collagen-elastin blends are normally prepared by electrospinning or freeze-drying – two cases in which they are crosslinked to increase their mechanical integrity before being seeded with cells.[51,192-197]

2.5.5 Collagen-GAG Scaffolds

The GAGs content of the ECM determines the mechanical behavior in compression and strongly influences cell metabolism as well as the development of the microstructure.[44]

HA (**Figure 2.8**) is an important GAG component of the ground substance where it plays an important role in the binding of growth factors and cytokines along with regulating cell migration and proliferation.[198] HA molecules are composed of 250 to 25000 disaccharide units that consist of D-glucuronic acid and N-acetyl-D-glucosamine. Its high molecular mass and numerous mutually repelling anionic groups make HA a rigid and highly hydrated molecule, which, in solution, occupies a volume ~1000 times that in its dry state. HA solutions therefore have a viscoelastic behavior.[41]

Collagen-HA blends, which are generally obtained by freeze-drying and often crosslinked with EDC, have been studied for several applications.[199-202] HA can be blended with collagen to form gel as well, and as for GAGs, this polymer showed the capacity to affect collagen fibrillogenesis.[138]

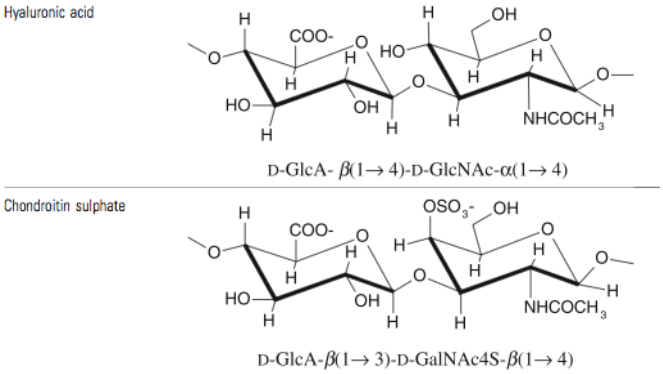

Figure 2.8: Disaccharide units of HA and CS.[44]

Sulphated GAGs are normally found in combination with proteins (PG) and have been shown to contribute to the stress distribution in collagen lattices.[48,109] Moreover, they affect the organization and structure of collagen fibrils in vivo and in vitro.[203-209] CS (**Figure 2.8**) is the most abundant sulphated GAG in the body and is found in cartilage, tendon, ligament and blood vessels. CS has been extensively used in combination with collagen for TE applications, predominanlty for skin and cartilage replacements. These blends are obtained in gel form or by freeze-drying and are eventually crosslinked with EDC. In this way, CS is covalently crosslinked to collagen and works for the stress transfer between different fibrils. CS has been widely used also for its biological features, in particular the capacity to promote cell (e.g., fibroblasts) colonization.[210-221]

In conclusion, several natural polymers can be blended with collagen, but only some of them – GAGs, fibrin – in the gel form. In particular, HA and CS are natural components of the ECM of blood vessels and deserved more attention for their potential to increase of the structural integrity of collagen gel-based scaffolds.

2.6 Methodologies

The highly viscous behavior as well as the low strength are responsible for the mechanical failure of reconstituted collagen lattices, in terms of break or permanent deformation, so making the latter unsuitable for cyclic conditioning. Several authors have tried to overcome this problem by shaping collagen constructs under different forms (mainly sponge) as well as in combination with natural and synthetic polymers, the latter mainly with the role of

additional mechanical supports (e.g., silastic tubes, Dacron meshes).[87,195] On the other hand, exogenous crosslinkers, with or without copolymers (e.g., GAGs), have been introduced to increase the strength and stiffness of collagen gels with some success. However these improvements are not important enough to ensure the structural integrity under extensive conditioning.[111,127]

To the best of our knowledge, there is no collagen gel showing adequate strength and recoil to support alone the regeneration of the vascular tissue during the maturation period. Nonetheless, a biological scaffold with these features may simplify and fasten the production as well the manipulation of engineered constructs, for example by eliminating the need for synthetic supports or for maturation periods in static conditions.

The present work aimed to develop collagen gel-based lattices which promote cell-mediated remodeling and are mechanically compatible with the maturation process, ultimately leading to a fully functional TEBV. The mechanical behavior of collagen lattices depends on the structure and interactions of collagen fibrils, which in turn are determined by the extraction and the self-assembly of collagen monomers. The proper definition of the self-assembly process allows an important control over the ultimate microstructure and mechanical properties. In particular, specific combinations of the experimental conditions favor the mechanical stability of the collagen lattices. Nonetheless, collagen self-assembly is incapable of recreating the organization and the crosslinks that determine the mechanical profile of collagenous tissues in vivo. In this context, a synthetic crosslinking may reduce the sliding of collagen fibrils and therefore the viscous behavior of collagen gels. Optimization of the experimental conditions and crosslinking are the leitmotif of this research project. In addition, copolymers like GAGs were investigated in order to increase the biological and mechanical potential of collagen gel-based scaffolds.

CHAPTER 3. On the Effects of UV-C and pH on the Mechanical Behavior, Molecular Conformation and Cell Viability of Collagen-Based Scaffold for Vascular Tissue Engineering

This chapter presents the first article[6] as published in the journal *Macromolecular Bioscience* on March 10th, 2010. Small modifications were made in order to adapt the paper to the thesis. This study originates from the work of Boccafoschi et al. for the preparation of collagen gels, and from the work of Rajan et al. for the use of UV-C radiation as a means to generate covalent crosslinks between neighboring fibrils.[29,154] With respect to these works, the following study investigates collagen gels with a higher collagen concentration and submitted to higher doses of UV-C radiation. The protocols and the setup of the mechanical tests are detailed in the Appendix.

3.1 Résumé

Les substituts vasculaires à base de collagène représentent dans le domaine du génie du tissu vasculaire une alternative valide pour le remplacement de vaisseaux sanguins de petit calibre affectés par des pathologies. Dans cet étude, des échafaudages à base de gel de collagène ont été réticulés en combinant la variation du pH et la radiation UV-C. Les effets sur les propriétés mécaniques, sur la structure moléculaire et sur la viabilité et la morphologie cellulaire ont été étudiés. Les propriétés mécaniques ont augmenté avec le pH et la dose d'UV-C et dépendaient fortement de la vitesse des tests. La conformation des molécules de collagène a été légèrement affectée. Pendant que l'adhésion cellulaire n'a pas été altérée significativement, la prolifération a diminué en fonction du pH et des doses de UV-C. Ces résultats suggèrent que les gels de collagène irradiés avec UV-C peuvent représenter un substrat adéquat pour des applications dans le génie du tissu vasculaire.

---

[6] Matteo Achilli, Jean Lagueux, Diego Mantovani, Laboratory for Biomaterials and Bioengineering, Department of Materials Engineering & Research Centre, Quebec University Hospital, Laval University, Quebec City, G1K 7P4, Canada

3.2 Abstract

Collagen-based vascular substitutes represent in VTE a valid alternative for the replacement of diseased small-caliber blood vessels. In this study, collagen gel-based scaffolds were crosslinked combining modulation of pH and UV-C radiation. The effects on the mechanical properties, on the molecular structure and on cell viability and morphology were investigated. The mechanical response increased as a function of pH or UV-C dose and strongly depended on the test speed. Collagen molecular conformation resulted only slightly modified. While cell adhesion was not significantly altered, cell proliferation partially decreased in function of pH and UV-C. These findings suggest that UV-C treated collagen gels can represent an adequate substrate for VTE applications.

3.3 Introduction

Cardiovascular diseases are responsible of the death of more than 17 million people each year.[222] When the replacement of a diseased vessel becomes necessary, synthetic vascular grafts result unsuccessful in cases where the lumen of the diseased vessel is smaller than 6 mm.[54,59,62,223] In this regard, vascular tissue engineering (VTE) takes advantage of cell activity in the process of generation of small-caliber blood vessels.[62] Scaffold-based VTE assumes that scaffolding structures, made of both synthetic and/or natural, degradable and/or permanent materials, can be successfully used to promote three-dimensional (3D) vascular cell growth and generate small-caliber vascular substitutes.[59] Among all the materials of natural origin, collagen surely represents one of the most interesting because of its biological and mechanical properties.[62]

The collagen family is constituted by more than 20 known extracellular proteins whose common feature is their molecular structure: a right-handed triple helix composed of three left-handed twists of α-chains where each α-chain is a monotonously repeating sequence of amino acids (Gly-X-Y). Nearly one-third of its residues is Gly, and another 15 to 30% are Pro (in X position) and Hyp or Hyl (in Y position).[23] Because of its well packed, triple helical structure, collagen represents the major stress-bearing component of connective tissues such as bone, cartilage, tendons and the fibrous matrices of skin and blood

vessels.[24] Collagen types III and I are fibril-forming collagens and are two of the main components of blood vessels. These collagens assemble into highly orientated aggregates with the typical quarter-staggered fibril-array, which presents a characteristic banding pattern with a periodicity of about 70 nm (the D-period) based on a staggered arrangement of individual collagen monomers.[23]

Collagen has wide medical applications because of its biological properties.[106,113] Collagen can be extracted from rat-tail tendons (RTT) by solubilization and mechanical disruption of collagen fibers.[224] This process results in loss of the structural organization and mechanical features of the collagen matrix, however good biological properties are preserved.[115,224,225] This solubilized collagen can polymerize to become a gel and can be shaped in disks, which is a suitable shape for characterization, or in tubular structures, which is the final shape of the VTE construct.[154] Collagen gelation depends on different factors such as temperature and pH.[42] The latter influences the formation of electric charges in the amino acids of collagen causing electrostatic attractions or repulsions between different fibrils.[24] The neutralization of the global charge of a collagen molecule is normally reached at the isoelectric point, which for collagen is 6.5–7, even if amino acid side chains could be still ionized.[24,130] With this pH and at 37 ºC the self-assembly of collagen fibrils takes place.[115] Wood et al. proved that collagen fibrillogenesis can be favored by a pH higher than the isoelectric point,[129] while Roeder et al.,[132] Usha et al. and Rosenblatt et al. discussed the improvement of mechanical properties for collagen matrices when the pH was higher than 7.[130,151]

Collagen matrices and collagen gel in particular are known to present a time-dependent mechanical behavior.[176,178,226] These viscoelastic properties can be shown by tensile, compression or rheological tests.[176-178,226,227] Moreover, collagen mechanical properties can be modulated by different crosslinking methods.[42,112] One of these methods is UV-C irradiation (λ = 254 nm), a physical treatment that increases the number of crosslinks in collagen gels. The effects of UV-C on collagen depend on irradiation doses, pH, degree of hydration of the sample and presence of other components that can interact with collagen during the formation of free radicals.[123-125,228-230] UV-C radiation affects the triple helical

structure by creating free radicals and crosslinking the aromatic side chains of tyrosine or phenylalanine, or by unraveling the hydrogen bonds that normally stabilize the triple helix.[42,120,126,228,231-237] These opposite effects alter collagen mechanical properties respectively by stiffening the collagen matrix or by leading to the triple helix-random coil transition and consequently to denaturation.[229,234,236-238] The degree of crosslinking can be detected by different methods, for example by evaluating the stiffening of collagen samples, or by measuring the variation of the swelling ratio.[239,240]

As discussed by several authors, UV-C can cause unfolding of the collagen triple helical structure and protein fragmentation.[120,126,228,231-233] Fourier-transform infrared (FT-IR) spectroscopy is a technique that can be used to detect collagen conformational changes.[225] The degree of triple helix-random coil transition can be evaluated by the shifting of the Amide I band (1650–1665 cm^{-1}) of IR spectra of collagen to lower frequencies.[121,122,125,241] Indeed for heat-denatured collagen, i.e. gelatine, the peak of Amide I band can be found around 1635-1640 cm^{-1}.[241]

UV-C radiation can affect cell viability as well. In fact it has been shown that UV radiation causes damage to DNA by the formation of free radicals.[242,243] Consequently it would be preferable to irradiate collagen gels with UV-C first, and only then to add cells.

Collagen extracted from RTT has been widely investigated and characterized from a biological and morphological point of view.[137,154,224,225] Even though RTT collagen presents good biological properties, collagen gels do not fulfill the mechanical requirements for VTE applications yet. In particular, once these gels are seeded with cells and placed in a bioreactor for the maturation process, they do not present the elastic properties required to stand the mechanical solicitations imposed by a pulsatile flow.

While an exploratory work has already evaluated the effect of low doses of UV-C on the biological properties of collagen gel, in the present study the specific effects of pH, UV-C irradiation and test speed were investigated from a mechanical point of view through confined compression tests of two-dimensional (2D) collagen gel samples.[29] The key rationale behind the process of stiffening collagen gels adopted here was the following: an increase in pH affects the electrostatic bonds and decreases the distances between the fibrils

and their UV-C reactive side chains.[129,130] In this way more crosslinks can be formed by UV-C radiations. Finally, opportune rinsing could re-establish a physiological pH in order to improve cell growth. By this approach, it was expected to reach a compromise between stiffening and preservation of the biological properties. FT-IR analyses were carried out to assess the degree of denaturation due to UV-C treatments.[125,225] Finally colorimetric assays and scanning electron microscopy (SEM) analyses evaluated the viability and the morphology of fibroblasts on collagen gels in function of UV-C dose and pH respectively.

3.4 Experimental Part

The present study aimed to characterize collagen gels that were prepared at pH 7.5 or 10 and then irradiated at 0, 35 or 70 $J \cdot cm^{-2}$.

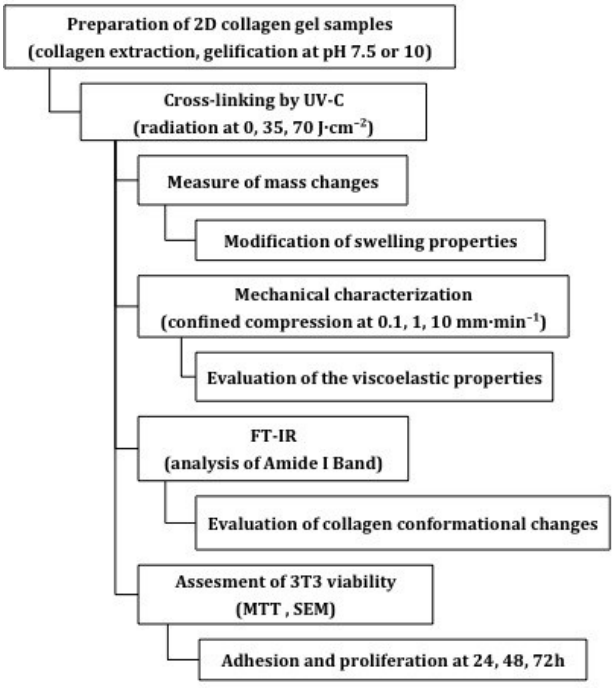

Figure 3.1: Plan of the experimental methods.

The range of pH and the range of UV-C doses were defined according to preliminary results that investigated the influence of pH and UV-C on collagen gel mechanical performances. Each group of treatment corresponds to a specific combination of pH and UV-C dose. Figure 3.1 presents the plan of the experimental methods.

3.4.1 Preparation of 2D Collagen Gels

A solution of type I collagen (4 $g \cdot L^{-1}$) and 0.02 M acetic acid was obtained from RTTs according to a procedure previously developed in our laboratory.[115] Collagen gels were prepared at pH 7.5 or 10. The acidified collagen solution was mixed with Dulbecco's Modified Eagle Medium 5X (DMEM, Gibco, Invitrogen Corporation, Burlington, ON, Canada) and 0.45 M $NaHCO_3$ (Fisher Scientific, Nepean, ON, Canada) at a ratio of 5:2:1 in order to obtain a solution of pH 7.5. The solution at pH 10 was obtained by adding 4 M NaOH (MAT, Quebec City, QC, Canada). Collagen solutions were poured into Petri dishes (35 x 10 mm^2 Cell Culture Dishes, Corning Inc., Wilkes Barre, PA, USA) and gels were allowed to set overnight at 37 ºC, 5% of CO_2 and 100% humidity. The resulting disk-shaped samples had a collagen concentration of 2 $g \cdot L^{-1}$. This geometry was chosen because it facilitates both UV-C treatment and characterization.

3.4.2 UV-C Treatment

Samples were weighed and then irradiated by UV-C radiation with a UV-C-Hg lamp (TUV G30T8, 30W, Philips, main peak at 253.7 nm) at three different doses of 0, 35 (2h 42min of irradiation) and 70 $J \cdot cm^{-2}$ (5 h 24 min of irradiation). The temperature of the samples was controlled in order to prevent heat-denaturation. The power of the UV-C lamp (3.6 $mW \cdot cm^{-2}$) was tested with a UVX Radiometer (UVP Inc., Upland, CA, USA). Samples were weighed a second time and then soaked overnight in buffer solutions in order to stabilize the pH to the physiological level and prepare collagen gels to cell seeding. In particular, samples at pH 7.5 were soaked in DMEM 1x solution while samples at pH 10 were soaked in a solution of DMEM 1X /0.050 M 4-(2-hydroxyethyl)piperazine-1-ethanesulfonic acid (HEPES, Sigma Aldrich, St. Louis, MO, USA); in the latter case HEPES was chosen because it was the most effective in stabilizing the pH at 7.5. Once that pH was stabilized at 7.5, all the samples were soaked in normal culture medium in order to remove HEPES and the undesired effects of its ionic strength on cell viability. Medium in excess was removed and samples were weighed a last time. Mass was expressed in % according to the equation:

$$\text{mass}_i(\%) = \frac{\text{mass}_i}{\text{mass}_0} \quad (3.1)$$

where mass_0 represents the mass before UV-C treatment, and mass_i represents the mass measured at two different time points: immediately after UV-C irradiation (i = 1), or after soaking the samples in buffer solutions (i=2). The water uptake was defined by the equation:

$$\text{Water Uptake}(\%) = \text{Mass}_2(\%) - \text{Mass}_1(\%) \quad (3.2)$$

3.4.3 Mechanical Tests

The mechanical behaviour of collagen gels was evaluated with an Instron 5848 Microtester (Instron Corporation, Norwood, MA, USA) in a confined compression test mode. Collagen gels were confined by the Petri dishes and were compressed by a circular plate (d = 2 cm) that was fixed to a 5 N load cell. Time-dependency of the mechanical properties was investigated adopting three different test speeds, 0.1, 1 and 10 $\text{mm}\cdot\text{min}^{-1}$. Samples were tested at room temperature without mechanical preconditioning and with a single compression run. Results were expressed in terms of stress/strain and stiffness/strain where the stiffness is defined by the equation:

$$\text{Stiffness} = \frac{\partial(\text{Stress})}{\partial(\text{Strain})} \quad (3.3)$$

3.4.4 FT-IR Analysis

UV-C-induced modifications to the triple helical structure of collagen were investigated by analyzing the IR spectra of collagen gels. Samples were dried in a vacuum oven for 24 h at 20 ºC. A denatured collagen sample was produced by warming collagen gel in a vacuum oven for 1 week at 40 ºC; thereafter its IR spectrum was compared with the one of gelatin Type B from Bovine Skin (Sigma Aldrich, St. Louis, MO, USA). The IR spectra were collected on a Nicolet Magna-IR 550 FT spectrometer (Thermo Nicolet, Madison, WI, USA) equipped with a deuterated triglycine sulfate (DTGS) detector and a germanium-coated KBr beam splitter. One hundred scans were routinely acquired with a spectral

resolution of 4 cm^{-1} in the attenuated total reflectance (ATR) mode. A split pea attachment (Harrick Scientific Corp., Ossining, NY, USA) equipped with a hemispherical 3 mm-diameter silicon internal reflection element was used. Variations in the position of the Amide I band were monitored in the 1600 to 1720 cm^{-1} range; all spectra were normalized. IR data were treated with Omnic E.S.P. 5.1 (Thermo Nicolet, Madison, WI, USA) and Grams 32 (Spectral Notebase version 4.11, Galactic Industries Corporation, Salem, NH, USA).

3.4.5 Cell Viability: MTT Assay and SEM Analysis

NIH 3T3 fibroblasts were cultured in culture medium consisting of DMEM 1X supplemented with 10% Fetal Bovine Serum (FBS, Multicell, Wisent Inc., St-Bruno, QC, Canada). Each sample was seeded with $1x10^6$ cells diluted in culture medium and was incubated. Culture medium was changed every day.

Cell adhesion after 1h of incubation and cell proliferation at three time points (after 24, 48 or 72 h of incubation), were evaluated by colorimetric assays.[29,224,225] 3-(4,5-dimethylthiazol-2-yl)-2,5-diphenyl-2H-tetrazolium bromide (MTT, Sigma Aldrich, St. Louis, MO, USA) is reduced to purple formazan by mitochondrial dehydrogenase in cells indicating normal cell metabolism. At each time point, MTT was solubilized in culture medium (1 $g \cdot L^{-1}$) and added to cells; samples were therefore incubated for 4 h. Subsequently the medium was removed, samples were extensively rinsed with phosphate buffered saline (PBS) and dried overnight in an oven; then the purple formazan crystals were solubilised with pure dimethyl sulfoxide (DMSO, Sigma Aldrich, St. Louis, MO, USA) at room temperature. The optical density at 570 nm was determined using a 96-well plate reader (BioRad Model 450 Microplate Reader, Mississauga, ON, Canada). Samples consisting of $1x10^6$ fibroblasts seeded in Petri dishes and without collagen were used as positive control while collagen samples without cells were used as negative control. Results are expressed as % of the control, where the negative control represents the 0% and the positive control the 100% of the scale.

Cell morphology was investigated by SEM.[29] Samples seeded with fibroblasts were incubated for 24 hours. Culture medium was then removed, samples were washed in 0.1 M cacodylate buffer and fixed at 4 ºC for 2 hours with 2.5% glutaraldehyde in 0.1 M cacodylate buffer solution. After fixation, samples were rinsed with 0.1 M cacodylate buffer and treated with 0.25% osmium tetroxide in 0.1 M cacodylate buffer solution. Samples were rinsed once again at 4 ºC with 0.1 M cacodylate buffer, dehydrated at three different levels of ethanol (70, 95, 100%), and dried with the critical point drying method (Polaron CPD 7501, VG Microtech, East Grinstead, W Sussex, UK). Samples were then sputter-coated with gold-palladium and images were captured with a JSM-35CF (Jeol Ltd., Tokyo, Japan).

3.4.6 Statistical Analysis

Statistical analyses were carried out with the software SAS (SAS Institute Inc., Cary, NC, USA). All tests were made in triplicate with the exception of tests investigating mass change and cell proliferation that were executed with nine repetitions; all the experiments were repeated twice. Data are expressed as mean ± standard deviation. Two-way analyses of variance (ANOVA) were carried out to evaluate the effects of pH and UV-C on mass change and cell adhesion. Three-way ANOVA were employed to evaluate the effects of pH, UV-C and test speed on the mechanical behavior, and of pH, UV-C and time point on cell proliferation. Concerning the cell proliferation test, differences between individual treatments were also analyzed by Tukey's pairwise multiple comparison procedure. All the graphs were represented with Prism 5 (GraphPad Software Inc., La Jolla, CA, USA). Results were considered statistically significant for $p < 0.05$.

3.5 Results and Discussion

3.5.1 Mass Change

The possibility to evaluate the effects of crosslinking techniques on collagen by the analysis of the swelling properties has been already reported in literature.[240] Figure 3.2A shows how the mass at the time point 2 changes as a function of pH and UV-C doses.

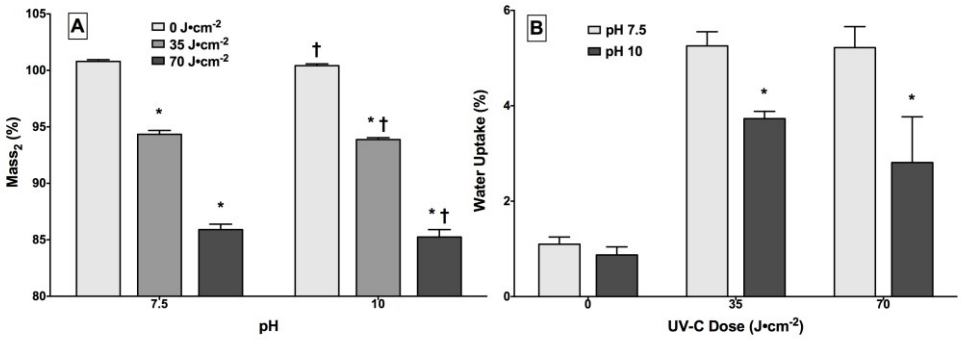

Figure 3.2: Effects of pH and UV-C dose on collagen gel mass. Results are expressed as % of the mass of collagen gel before UV-C treatment. (A) Change of mass after soaking the samples in buffer solution (time point 2). *: significant difference ($p<0.01$) between groups with same pH but different UV-C treatment. †: significant difference ($p<0.01$) between groups with same UV-C treatment but different pH. (B) Difference of mass between time point 2 and 1. *: significant difference ($p<0.01$) between groups with same UV-C treatment but different pH.

Both of these parameters were found to significantly affect the mass of collagen gels ($p<0.01$). On the contrary, the interaction of these parameters was not statistically significant. UV-C had mostly an inversely proportional linear effect on mass, which decreased to 94% and 86% for UV-C doses of 35 and 70 $J \cdot cm^{-2}$ respectively. The pH had a significant effect even if it was considerably less important than that of UV-C radiation. In response to an increase of pH from 7.5 to 10, the mass generally decreased of the 0.4% independently of UV-C radiation. Figure 3.2B shows the water uptake as a function of pH and UV-C dose. When UV-C radiations were applied, the water uptake of collagen gels prepared at pH 10 was 1.9% less than in case of samples prepared at pH 7.5 ($p < 0.01$).

The decrease or increase of mass is probably due to the evaporation or absorption of buffer solution respectively. This hypothesis is coherent with the work of Kaminska et al.,[232] where it was found that UV-C radiation could cause release of water from collagen structures by evaporation. During the irradiation process, collagen gels lost a part of their water content, a decrease directly proportional with the UV-C dose. However, after soaking in buffered culture medium, the samples recovered a part of the water content by swelling, although the mass never reached its initial value. This effect is probably due to UV-C, which formed crosslinks in collagen gels reducing the swelling. At the same time the difference in water uptake revealed that collagen gels prepared at pH 10 swelled less than

samples prepared at pH 7.5, likely because samples prepared at pH 10 resulted to be more crosslinked. Different authors discussed the effect of pH on swelling properties. Usha et al. studied the swelling ratio of RTT collagen in acid condition,[151] while Nam et al. studied the swelling ratio of collagen gels in function of pH.[240] Even though the pH range was different from the one considered in this work, both these works showed that the swelling ratio was strongly dependent of pH. Rosenblatt et al. discussed the effect of pH (6÷9) on deprotonation of side chain moieties of collagen hydrogels, supposing that this could lead to the formation of net attractive interactions, fiber dehydration and consequently decrease of the global swelling.[130] Finally it can be assumed that pH can affect the formation of intra and inter fibrillar bonds therefore influencing the swelling properties. This assumption is coherent with the results presented in this work concerning the effects of pH on collagen gel mass.

3.5.2 Mechanical Tests

Figure 3.3 shows the representative stress/strain and stiffness/strain curves. The stress/strain curve presents a non-linear behaviour, while three different regions can be clearly distinguished in the Stiffness-Strain curve.

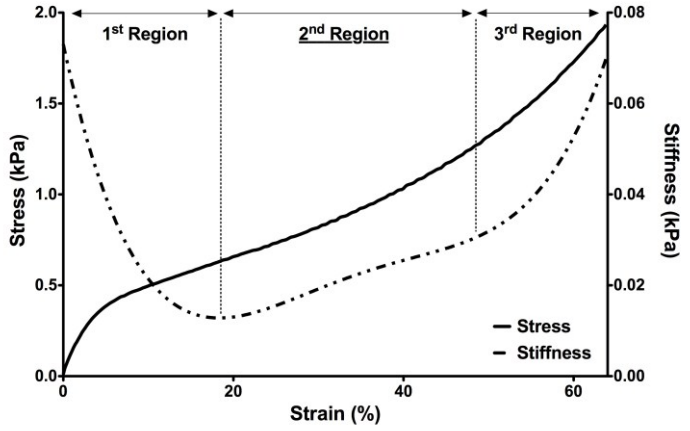

Figure 3.3: Stress/strain (solid line) and stiffness/strain (dash-dotted line) curve of collagen gels prepared at pH 10, irradiated at 70 J·cm^{-2} and compressed at 1 mm·min^{-1}. The three regions are clearly identified. These curves and their shapes are a typical feature of collagen gel samples for any combination of pH, UV-C dose or test speed.

In the first region (up to 15-20% strain) the mechanical response is strongly influenced by the resistance of water to come out of the gel because of the deformation. The third region (from 50-60% up to the end of the strain range) reflects the approaching of the compressive plate to the bottom of the Petri dish, as can be seen from the increase of the slope, and can be considered a board effect. These two regions, therefore, were not considered the most representative of the mechanical behavior of the matrix of collagen fibrils. Finally, the second region (around 15-20% to 50% strain) was taken into account to study the mechanical properties of collagen gels. The mean stiffness in the second region (average stiffness, AS) was calculated and used as an indicative parameter to evaluate the effects of pH, UV-C and test speed on the mechanical response. Results are represented in Figure 3.4, while in Table 3.1 the values of AS are detailed in function of pH, UV-C dose and test speed. The AS increased when pH, UV-C dose or test speed increased ($p < 0.01$). UV-C radiation had a linear effect on AS while test speed had mainly a linear effect. In order to further understand the nature of this effect, further tests at different speeds should be carried out. No interaction between pH, UV-C and test speed, was statistically significant.

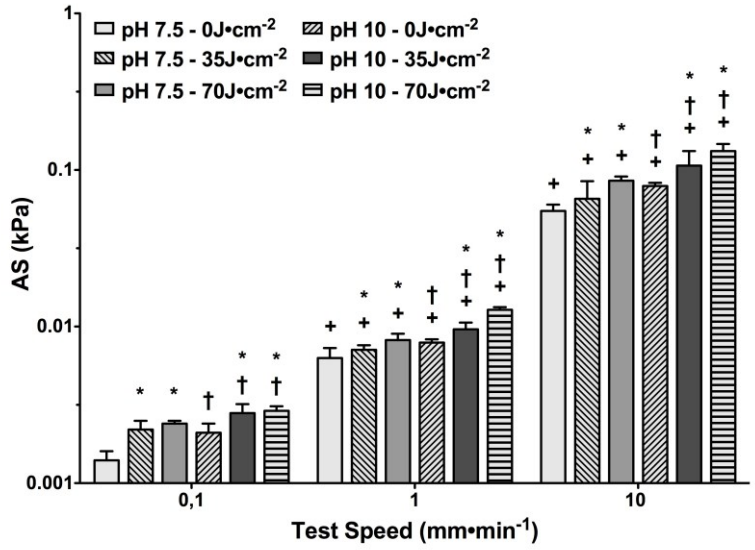

Figure 3.4: Averaged stiffness (AS) as a function of pH, UV-C dose and test speed. *: significant difference between groups with different UV-C doses. †: significant difference between groups with different pH. +: significant difference between groups with different test speed.

The dependency on test speed yields evidence for viscoelastic behavior. AS increased on average of a factor 3.8 when test speed passed from 0.1 to 1 mm·min^{-1} and tenfold between 1 and 10 mm·min^{-1}. Samples were not preconditioned because the water loss was found to affect the reproducibility of tests and no specific analysis studied the recovery of the original state after load removal.

Table 3.1: Average stiffness (10^{-3} kPa) as a function of pH, UV-C dose, and test speed.

pH	UV-C dose	Test Speed		
	J·cm^{-2}	(mm·min^{-1})		
		0.1	1	10
7.5	0	1.4 ± 0.2	6.3 ± 1.0	54.8 ± 5.3
	35	2.2 ± 0.3	7.1± 0.5	65.5 ± 19.3
	70	2.4 ± 0.1	8.2 ± 0.8	85.4 ± 5.4
10	0	2.1 ± 0.3	7.9 ± 0.4	79.0 ± 3.8
	35	2.8 ± 0.4	9.6 ± 1.0	106.7 ± 25.5
	70	2.9 ± 0.2	12.8 ± 0.5	132.1 ± 14.5

From our observations collagen gel samples reabsorbed part of the water content that was expelled during compression tests. This partial recovery might suggest that collagen gel samples manifested a viscoelastic character rather than a viscoplastic one (results not shown). The type of curve for stress-strain (Figure 3.2), with the exception of the first region, is in accordance with the results obtained by Neel et al.[178] This study analyzed the mechanical behaviour of collagen gels in unconfined compression with the aim to produce dense matrices. The viscoelastic character was evidenced and two main regions were clearly distinguishable, where the second one reflected the approaching of the two plates of the compressive apparatus. Those collagen gels were stiffer than those we investigated in this study mainly because they were previously compressed and compacted. The importance of the water content and its recovery was discussed and the mechanical response was shown to depend on the water content. The latter is in accordance with what was assumed in the present study about the importance of the water content in the reproducibility of mechanical tests.

As shown in Figure 3.4, the increase of pH from 7.5 to 10 lead to an average increase of AS of 40%. As discussed in the previous section, pH ranging from 6 to 9 influences the formation of attractive forces between different collagen fibrils.[130] Roeder et al. and

Rosenblatt et al., studied the effects of pH in the range 6-9 on the tensile mechanical properties of collagen matrices and on the rheological properties of collagen hydrogels respectively.[130,132] In both of these studies, an increase of pH resulted in an increase of the mechanical properties. Usha et al. studied the effect of pH in the range 4-8 on RTT collagen fibers. Even in this case an increase of pH resulted in an increase of tensile mechanical properties.

UV-C irradiation at 35 and 70 $J \cdot cm^{-2}$ increased on average the AS of 30% and 56% respectively. As discussed by previous works, UV-C radiation promotes the formation of free radicals in the aromatic side chains and therefore the formation of crosslinks. One of the consequences of crosslinking is the stiffening of the collagen structure. Lee et al. irradiated collagen membranes with UV-C doses ranging from 2.8 to 11.2, 22.4, 44.8 and 134.4 $J \cdot cm^{-2}$, measuring the higher improvement of mechanical properties in the case of 22.4 $J \cdot cm^{-2}$.[236] In the work of Weadock et al. two different crosslinking techniques were compared,[237] UV-C radiation and dehydro-thermal treatment, by means of enzymatic digestion. Irradiating extruded collagen fibres at 3.6, 7.2, 14.4, 28.8 and 57.6 $J \cdot cm^{-2}$ they found that an improved resistance to digestion was obtained for 3.6 $J \cdot cm^{-2}$. Sionkowska et al. irradiated collagen tendons and collagen films at 63.12 and 126.24 $J \cdot cm^{-2}$ and evidenced a decrease in mechanical properties mainly due to collagen denaturation.[234,238] Ohan et al. treated collagen films in presence of glucose (3, 6 and 9 mM) at 26 $J \cdot cm^{-2}$ showing an improvement in the mechanical properties.[229] In the present study, the applied UV-C doses seem to be considerably higher than in other studies, and a decrease of the mechanical properties could be expected. At the same time some important points have to be considered. As previously mentioned UV-C effects on collagen depend on UV-C doses, presence of other molecules, degree of hydration, pH and type of collagen sample.

The collagen gels discussed here contain a concentration of glucose (5×10^{-3} M) that is relevant considering the work of Ohan et al.[229] In this work the presence of glucose was due to the addition of DMEM, which was used to prepare a suitable substrate for cells. Even though further studies are required to clarify its role, glucose may have acted as a synergistic factor in the process of collagen crosslinking.

Collagen denaturation consists in the unravelling of hydrogen bonds that stabilize the triple helical structure: the consequence is the transition from a triple helical to a random coil organization by unfolding. The amount of inter-helical hydrogen bonds depends on the degree of hydration of the molecule. Collagen films or membranes are less hydrated than gel samples. Consequently collagen gel may be less affected by water evaporation and the risk of the rupture of hydrogen bonds. Additional evidences about the concern regarding denaturation of collagen gels have been provided by FT-IR analysis.

3.5.3 FT-IR Analysis

The degree of denaturation of collagen can be interpreted from the shifting of the peak of the Amide I band of FI-TR absorbance spectra.[121,122,125,241] Therefore, Amide I bands of collagen gel samples differing for pH or UV-C irradiation were compared. Thermally denaturated collagen displayed the same spectrum as the gelatin control (data not shown) and consequently was used as positive control to evaluate the degree of denaturation of collagen due to different UV-C doses. Figure 3.5 presents the spectra of samples prepared at pH 7.5 (A) or 10 (B) and irradiated at 0, 35 or 70 $J \cdot cm^{-2}$, and the spectrum of denatured collagen. During the period of irradiation, the temperature of collagen gel samples was not significantly different from room temperature (22-26 ºC); therefore it was assumed that there was no risk for heat-denaturation due to UV-C irradiation. In case of UV-C irradiation at 0 or 35 $J \cdot cm^{-2}$ and for both levels of pH, the peak of the Amide I band was found in 1656 cm^{-1}. Mainly because IR spectra didn't show the shifting of the Amide I band, it can be assumed that there was no triple helix-random coil transition. On the contrary, concerning UV-C radiation at 70 $J \cdot cm^{-2}$, the shifting became evident in the case of samples prepared at pH 7.5, while for samples prepared at pH 10, there was just a slight shifting. In any case, none of the samples showed a degree of denaturation similar to the one of thermally denatured collagen, whose peak was found in 1637 cm^{-1}.

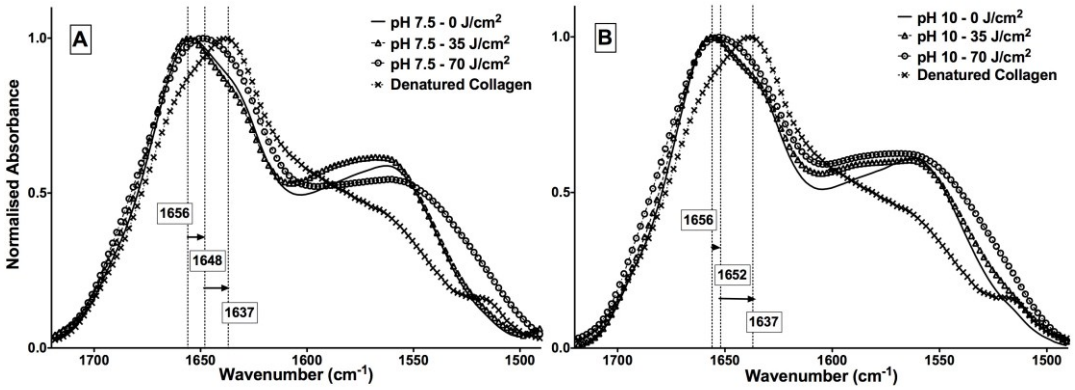

Figure 3.5: Amide I band: detail of FT-IR spectra of collagen gel samples prepared at pH 7.5 (A) and 10 (B) in function of the UV-C doses 0 (–), 35 (Λ), 70 J·cm^{-2} (o). The spectrum of denatured collagen (x) is also presented. The arrows indicate the shifting between the peaks of different groups.

Kaminska et al. irradiated pieces of tendon or films up to 128 J·cm^{-2} noticing a progressive shifting of the Amide I band.[125] However the complete shifting to a gelatin-like state was never reached. Here collagen gel samples were irradiated up to 70 J·cm^{-2} without the shifting characteristic of the triple helix-random coil transition. As discussed in the previous section, different authors irradiated collagen at lower doses attaining denaturation, even though we stressed on the role of different parameters in collagen conformational changes.[126,228] In terms of Amide I band shifting, collagen gel samples prepared at pH 7.5 seemed to be more affected by high levels of UV-C radiation than samples prepared at pH 10. This effect is probably related to the higher degree of crosslinking. In fact, as discussed by several authors,[244-247] the resistance to denaturation increases with the degree of crosslinking.

3.5.4 MTT Assay and SEM Analysis

Figure 3.6 presents the cellular adhesion in function of pH and UV-C irradiation of collagen gels. The differences between collagen gels with cells and the negative control (0% of the scale) was statistically significant ($p < 0.01$). Cellular adhesion was detected on collagen gels for every combination of pH or UV-C dose; no significant difference between groups was found.

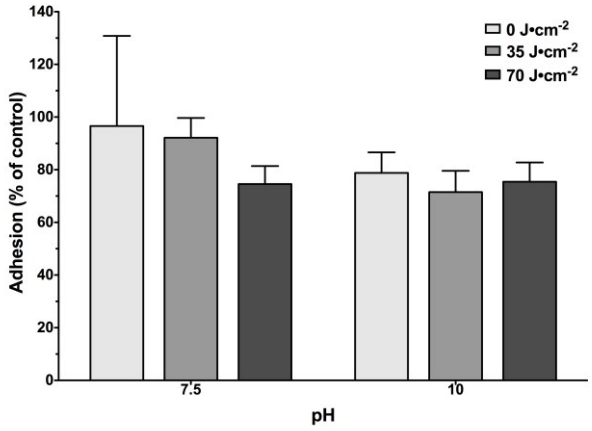

Figure 3.6: Results of MTT test for cell adhesion (1h of incubation) on collagen gel samples prepared at different pH (7.5, 10) and irradiated at different UV-C doses (0, 35, 70 J·cm^{-2}). Adhesion is expressed in percent; 0% and 100% correspond to the negative control (collagen gels without cells) and to the positive control (cells seeded in Petri dishes) respectively.

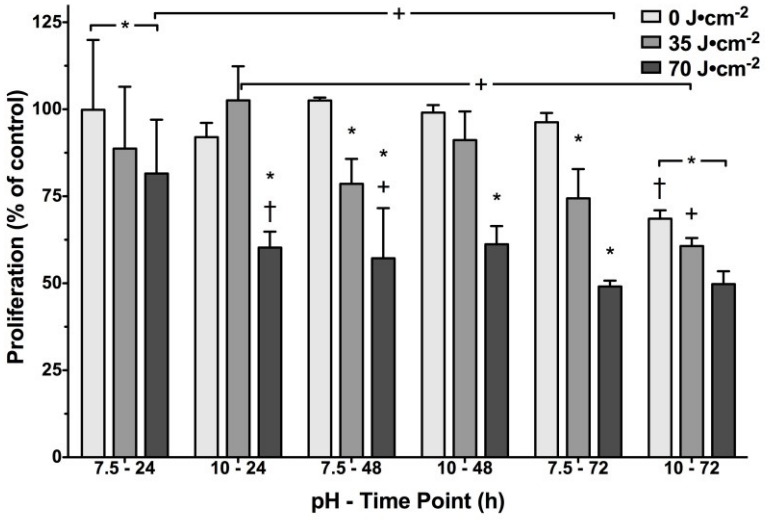

Figure 3.7: Results of MTT test for cell proliferation (time point: 24, 48 and 72 h of incubation) on collagen gel samples prepared at different pH (7.5, 10) and irradiated at different UV-C doses (0, 35, 70 J·cm^{-2}). *: significant difference between groups with different UV-C doses. †: significant difference between groups with different pH, +: significant difference between groups at different time point.

Figure 3.7 presents the results of the cell proliferation test. Collagen gel samples seeded with fibroblasts were compared in function of pH, UV-C dose and the time point at which proliferation was evaluated. Cell proliferation was once again significantly different from the negative control (0% of the scale, $p < 0.01$); moreover cell proliferation depended on

the type of treatment applied on collagen gels (combination pH – UV-C dose), time point, and on the interaction of these parameters ($p < 0.01$). Because of this interaction, the Tukey's pairwise comparison procedure was employed to evidence significant differences between groups. In general it can be observed that cell proliferation decreased progressively with pH and UV-C dose.

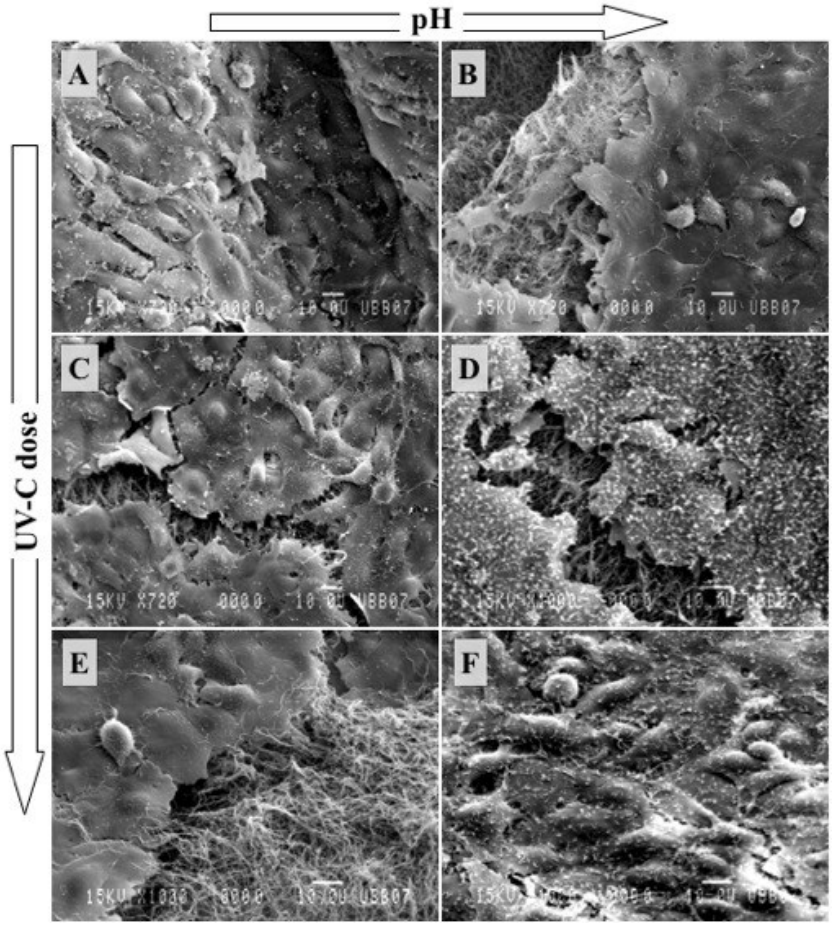

Figure 3.8: SEM images of fibroblasts on collagen gels in function of pH and UV-C doses. (A) Cells on non-irradiated collagen gel prepared at pH 7.5 (720x). (B) Cells on non-irradiated collagen gel prepared at pH 10 (720x). (C) Cells on collagen gel prepared at pH 7.5 and irradiated at 35 J·cm^{-2} (720x). (D) Cells on collagen gel prepared at pH 10 and irradiated at 35 J·cm^{-2} (1000x). (E) Cells on collagen gel prepared at pH 7.5 and irradiated at 70 J·cm^{-2} (1000x). (F) Cells on collagen gel prepared at pH 10 and irradiated at 70 J·cm^{-2} (1000x).

Figure 3.8 presents SEM images of fibroblasts on collagen gel samples in function of pH and UV-C radiation. These images show that fibroblasts adhered and spread over all the types of samples, therefore the effects of different pH or UV-C doses was not evident. The

number of seeded cells and the time of incubation proved to be sufficient for a complete covering of the upper surface of collagen gels. At the same time some images were chosen to show the matrix of collagen fibrils underlying the cell layer. Collagen fibrils were visible only on the boards of the samples (Figure 3.8B, 3.8E) and in specific regions where the manipulation of samples most probably caused some cracks in the cell layer (Figure 3.8C, 3.8D). Other studies assessed cell viability on UV-C treated collagen samples by colorimetric or morphological assays. Bellincampi et al. and Caruso et al. showed that fibroblasts were able to proliferate on UV-C treated collagen matrices,[248,249] while Rajan et al. discussed the potential of UV-C irradiation on collagen gels by studying fibroblasts viability.[29] All these studies showed that cell growth could be supported by UV-C-treated collagen substrates. Coherently, the results of the present work show that UV-C treated collagen gels represent an adequate substrate for cell growth, even though proliferation is affected by the dose of UV-C.

3.6 Conclusion

This work investigated the effects of test speed, UV-C and pH on the mechanical properties of 2D collagen gels and analyzed the influence of UV-C and pH on cell viability and molecular conformation of collagen gels.

Weight analysis and mechanical tests showed that collagen gels were progressively crosslinked by increasing doses of UV-C and that pH acted as a synergistic factor. In particular mechanical tests assessed that mechanical properties depended on test speed as well. Collagen gel stiffness resulted to be time-dependent and increased in function of pH and UV-C dose.

FT-IR analysis detected no denaturation for non-irradiated collagen gels and gels irradiated at 35 $J \cdot cm^{-2}$. In the case of UV-C treatment at 70 $J \cdot cm^{-2}$, the shifting of the Amide I band depended on pH and was more important for samples prepared at pH 7.5. Notwithstanding this shifting, the molecule of collagen was not affected by a complete triple helix-random coil transition.

Colorimetric (MTT) and morphological (SEM) analyses assessed that UV-C treated collagen gel can be a suitable substrate for cell growth, even though proliferation was negatively affected by increasing UV-C doses.

Collagen gel prepared at pH 10 and irradiated at 70 $J \cdot cm^{-2}$ was the most interesting from a mechanical point of view. Even though FT-IR analysis detected slight changes concerning collagen conformation and MTT tests evidenced some drawbacks concerning cell proliferation, this type of substrate seems to be a good compromise between improvement of mechanical properties and preservation of good biological properties.

In the future, further studies will be focused to define the optimal treatment (combination of pH and UV-C) to apply in terms of improvement of mechanical properties and preservation of good biological properties. Moreover, other types of mechanical tests will be defined in order to confirm the findings of this work while the role of glucose will be further investigated.

3.7 Acknowledgements

We would like to thank *Pascale Chevallier*, research associate at the *Laboratory for Biomaterials and Bioengineering*, for her kind help in FT-IR analysis; *Benedetto Marelli*, MSc student at the *Polytechnic of Milan* (Italy), for his assistance during SEM analysis; *Sébastien Meghezi* and *Frédéric Couet*, Ph.D. students at the *Laboratory for Biomaterials and Bioengineering*, for their assistance in the preparation of collagen and mechanical testing; and *Marie-France Côté*, research assistant at the *Bioengineering Unit of the Research Center* at the St François d'Assise Hospital, for her advices in the definition of the protocol for MTT tests. We also acknowledge the *Canadian Bureau for International Education (CBIE)* for the award during the first year of Ph.D., the *Natural Science and Engineering Research Council of Canada* and the *Centre Hospitalier Universitaire de Québec, Hôpital Saint-François d'Assise* for partially funding this research.

CHAPTER 4. Tailoring Mechanical Properties of Collagen-Based Scaffolds for Vascular Tissue Engineering: The Effects of pH, Temperature and Ionic Strength on Gelation

This chapter presents the second article[7] as published in the journal *Polymers* on December 6th, 2010, with small differences in the captions of the figures 4.3 and 4.5. The protocols for collagen gelation as presented in the previous chapter include a variety of components (phosphate buffers, amino acids, glucose) that may limit the control of the experimental conditions (pH, ionic strength, collagen concentration, inclusion of copolymers) and so of the final microstructure. Moreover, the presence of specific agents (e.g., phosphate groups) may hinder the interactions induced by chemical agents and the formation of covalent bonds. In relation to these considerations, the protocols for collagen gelation were re-defined by simplifying the composition of collagen gels in order to ensure a deeper control on the mechanisms of self-assembly. The protocols and the setup of the mechanical tests are detailed in the Appendix.

4.1 Résumé

Les gels de collagène ont été amplement étudiés pour des applications en génie tissulaire en raison de leurs propriétés biologiques. Dans les cas où ils ont été utilisés comme échafaudages pour le génie du tissu vasculaire, la limite majeure a toujours été leurs faibles propriétés mécaniques. Pendant le processus de fibrillogenèse *in vitro* qui amène à la formation des gels, la taille des fibrilles, leurs interactions chimiques, et la microstructure résultante sont régulés principalement par trois conditions expérimentales : pH, force ionique et température. Dans cette étude, ces trois paramètres ont été modulés afin d'augmenter les propriétés mécaniques des gels. Les effets sur la gélification ont été étudiés par turbidimétrie et par microscopie électronique à balayage. Les tests de turbidimétrie ont

[7] Matteo Achilli and Diego Mantovani, Laboratory for Biomaterials and Bioengineering, Department of Materials Engineering & Research Centre, Quebec University Hospital, Laval University, Quebec City, G1K 7P4, Canada

démontré que la gélification était affectée par les trois facteurs et les images par microscopie ont confirmé que altérations majeures s'étaient produites au niveau de la microstructure. Les tests mécaniques ont démontré que les modules en compression et traction augmentaient respectivement de quatre et trois fois comparés au contrôle. Enfin, des tests de viabilité ont confirmé que ces gels sont adaptés comme échafaudages pour l'adhésion et la prolifération cellulaire.

4.2 Abstract

Collagen gels have been widely studied for applications in tissue engineering because of their biological implications. Considering their use as scaffolds for vascular tissue engineering, the main limitation has always been related to their low mechanical properties. During the process of *in vitro* self-assembly, which leads to collagen gelation, the size of the fibrils, their chemical interactions, as well as the resulting microstructure are regulated by three main experimental conditions: pH, ionic strength and temperature. In this work, these three parameters were modulated in order to increase the mechanical properties of collagen gels. The effects on the gelation process were assessed by turbidimetric and scanning electron microscopy analyses. Turbidity measurements showed that gelation was affected by all three factors and scanning electron images confirmed that major changes occurred at the microstructural level. Mechanical tests showed that the compressive and tensile moduli increased by four- and three-fold, respectively, compared to the control. Finally, viability tests confirmed that these gels are suitable as scaffolds for cellular adhesion and proliferation.

4.3 Introduction

According to the World Health Organization, cardiovascular diseases constitute one of the most important causes of mortality throughout the world.[250] When small caliber (ø < 6 mm) blood vessels have to be replaced and autologous substitutes are unavailable, synthetic grafts do not represent a long-term alternative and other options have to be

considered.[54,59,62,223] Scaffold-based vascular tissue engineering (VTE) proposes to combine cells and scaffolding systems in order to obtain vascular constructs[62]. Concerning the choice of the material for the scaffolds, collagen in particular is of significant interest because of its biological properties.[113,224]

The collagen family includes more than 20 types of extracellular proteins. All these types present the same molecular structure, *i.e.*, a right-handed triple helix composed of three left-handed twists of α-chains, where each α-chain is a monotonously repeating sequence of amino acids (Gly-X-Y). Nearly one-third of its residues are Gly, another 15 to 30% are Pro (in X position) and Hyp or Hyl (in Y position).[23] Collagen types III and I are fibril-forming collagens and represent the major stress-bearing component of the fibrous matrices of blood vessels.[24] These collagens assemble into well-packed, highly-orientated aggregates, which present a characteristic banding pattern with a periodicity of about 70 nm (the D-period).[23]

Type I collagen can be obtained from the collagen fibers of rat-tail tendons (RTT) by solubilization in acetic acid.[115] This process results in the decomposition of collagen fibers and fibrils into small aggregates of collagen monomers dispersed in the acid solution. It has been widely documented that these small aggregates undergo *in vitro* "self-assembly" at neutral pH, in salt solution and at 37 °C or room temperature, forming fibrils with the typical banding pattern.[26] These gels show good biological properties and can be formed into tubular structures or into any shape suitable for further characterization.[154,224,225] On the other hand, the process of solubilization determines the loss of the structural organization and mechanical features of the original collagen matrix. The main drawback of collagen gel-based constructs resides in their low mechanical properties, in terms of low stiffness and low elasticity, which make them unsuitable for implantation.[251] At the same time, cell-driven remodeling of the collagen matrix under dynamic conditioning has been shown to have potential in order to overcome this limitation.[77,93]

Collagen fibrillogenesis depends on electrostatic and hydrophobic interactions.[26,42,130,138,142] Ionization and electrostatic interactions between amino acid residues are regulated by factors such as pH and ionic strength. The formation of net

charges between collagen molecules of neighboring fibrils may determine electrostatic attractions that can stabilize the matrix as well as affect the size of the fibrils and consequently the structure of the matrix.[129,130,132,252] Moreover, temperature affects the hydrophobic interactions and therefore the kinetics of collagen fibrillogenesis as well as pH and ionic strength.[129,130,144]

The previously adopted protocols for collagen gels were conceived to favor the inclusion of cells in the gel as well as their proliferation and the remodeling of the collagen microstructure. This approach implies three experimental conditions: preparation of the gel solution with culture medium, gelation in the incubator and neutral pH.[154,253] These conditions fix the ionic strength, the pH and the temperature at which fibrillogenesis occurs and affect the size of the fibrils, the interactions between neighboring fibrils and, consequently, the type of microstructure and the mechanical properties of the scaffold. The resulting tubular construct is expected to be remodeled by cellular activity within one week in static culture after which the construct is to be placed in a bioreactor for dynamic conditioning and final maturation.[154] At the same time, the gel used in this approach does not seem to be sufficiently resistant to ensure the integrity of the construct, neither during the procedures of manipulation and mounting in the bioreactor, nor during the first period of dynamic conditioning while the mechanical resistance of the construct is mainly provided by the scaffold.[17] Other works showed the possibility of associating additional supports to the collagen gel-based construct in order to preserve its structural integrity during these steps.[93,97,254]

Another approach consists of seeding cells on collagen gel-based scaffolds whose mechanical properties have been increased by physical or chemical crosslinking.[112]

As an alternative to improve the mechanical performances of collagen gel scaffolds without crosslinking treatments, this work aimed at tailoring and finally increasing the mechanical properties of collagen gels by modulating ionic strength, pH and temperature of gelation. The effects of these parameters on collagen gelation were characterized with turbidity measurements, scanning electron microscopy (SEM) and mechanical tests. Particular attention was focused on the role of pH 10 in increasing the mechanical properties. These

scaffolds were then rinsed with buffer medium in order to set the pH to a physiological level, cells were seeded on top and the construct incubated to favor cell proliferation. The suitability of these gels as scaffolds for vascular cells was assessed using colorimetric assays. Though not discussed in this work, an eventual tubular construct could be mounted in a bioreactor for dynamic conditioning and maturation.

4.4 Experimental Part

Collagen was obtained from RTT and solubilized at 4 mg/mL in 0.02 M acetic acid according to a previously developed protocol.[115] Collagen gels were prepared on ice at two different pHs, with seven different salt concentrations corresponding to different ionic strengths, and gelled at three different temperatures. Collagen was mixed with different concentrations of sodium chloride (NaCl, Sigma Aldrich, St. Louis, MO, U.S.) and 1 M sodium hydroxide (NaOH, Laboratoire MAT Inc., Quebec City, QC, Canada). The final volume was adjusted with deionized water and the resulting solution was at pH 10 with a collagen concentration of 2.8 mg/mL. The final concentrations of NaCl as well as an outline of the experimental plan are presented in Table 4.1. Gels at pH 7 were obtained by including Hepes (Sigma Aldrich, St. Louis, MO, U.S.) solution at a final concentration of 17 mM.

Table 4.1: Experimental plan for the preparation of collagen gels. Samples were prepared combining each level of each of the three factors: pH, temperature and ionic strength. The levels of ionic strength were defined by modulating the salt concentration.

Factors	Levels						
pH	7	10					
T (°C)	4 (T1)	21 (T2)	37 (T3)				
Salt Conc. (mM)	64.2 (c1)	82.6 (c2)	101 (c3)	119 (c4)	138 (c5)	156 (c6)	174 (c7)

Except for turbidimetric assays, once that gelation was complete the samples were soaked overnight in phosphate-buffered saline (PBS 1×, Sigma Aldrich, St. Louis, MO, U.S.), in order to carry out the tests at physiological pH and ionic strength.

Collagen solutions (200 µL) were poured into 96 multiwell plates (96 Well Cell Culture Cluster, Corning, NY, U.S.) and gelled at the three different temperatures. Each combination of pH, ionic strength and temperature was repeated four times (n = 4). While

collagen solutions were poured in the central wells of the plates, 1× PBS was poured in the surrounding wells in order to prevent evaporation from the samples. The kinetics of fibrillogenesis of gels prepared at pH 10 was monitored by measuring the turbidity, defined here as the absorbance at 310 nm, with a μQuant Spectrophotometer (BioTek Instruments Inc., Highland Park, U.S.) and the related software KC4. The measurements were ended when the values of the absorbance stopped showing statistically significant changes. In order to evaluate the rate of fibrillogenesis, the half-time ($t_{1/2}$), defined as the time at which the absorbance reached half of its final value, was calculated. Only the final absorbance, defined as the absorbance at the steady state, was measured in the case of gels prepared at pH 7.

The different microstructures of collagen gels as a function of pH and ionic strength were observed by SEM. Collagen gel disks (200 μL, ø = 11 mm) were prepared at different ionic strengths (c1, c4 or c7) and pHs (7 or 10) and set at 21 °C. Each combination of pH and ionic strength was repeated four times (n = 4). Samples were soaked in 1× PBS overnight, washed in 0.1 M cacodylate buffer (sodium cacodylate trihydrate, Sigma Aldrich, St. Louis, MO, U.S.) and fixed at 4 °C for 2 hours with 2.5% glutaraldehyde (Sigma Aldrich, St. Louis, MO, U.S.) in 0.1 M cacodylate buffer solution. After fixation, samples were rinsed with 0.1 M cacodylate buffer and treated with 0.25% osmium tetroxide in 0.1 M cacodylate buffer solution. Samples were rinsed once again at 4 °C with 0.1 M cacodylate buffer, dehydrated at three different concentrations of ethanol (70, 95, 100%), and dried with the critical point drying method (Polaron CPD 7501, VG Microtech, East Grinstead, W Sussex, UK). Samples were then sputter-coated with gold-palladium and images were captured with a scanning electron microscope JSM-35CF (Jeol Ltd., Tokyo, Japan).

Collagen solutions for all combinations of pH and ionic strength were poured into 48 multiwell plates (48 Well Cell Culture Cluster, Corning, NY, U.S.) and gelled at 4, 21 and 37 °C. Each combination of pH, ionic strength and temperature was repeated three times (n = 3). The resulting cylindrical samples (height = 5.5 mm, ø = 11 mm) were then soaked in 1× PBS overnight and tested in compression mode with a piston (ø = 20 mm) attached to a 5 N load cell and connected to an Instron 5848 Microtester (Instron Corporation, Norwood,

MA, U.S.). Samples were preconditioned with three cycles (0–2%) and tested at 0.2 mm/s and room temperature. The mechanical behavior was evaluated by considering the compressive modulus (CM), defined as the linear regression between 15 and 30% of strain, and the compressive strain energy (CSE), defined as the integral of the curve between 0 and 40% of strain. The gel prepared at pH 7, at an ionic strength corresponding to c4 and set at 37 °C was used as a control because, except for the concentration of collagen, it presented the same experimental conditions as the one previously studied in our laboratory.[253]

Square-section toroidal samples (cross-sectional area: 5 mm × 6 mm, i.d. = 22 mm, n = 2) were obtained by pouring collagen solutions in specific plastic molds and were tested in tensile mode in the same conditions as compression tests. Two black strips (1 mm × 5 mm) were applied on the samples and the deformation was followed using a video camera. The mechanical behavior was evaluated in terms of tensile modulus (TM), defined as the linear regression of the final part of the curve before break, and ultimate tensile stress (UTS).

Collagen gels prepared at pH 10 and three different ionic strengths (c1, c4 or c7) were set in 48 multiwell plates at the three different temperatures. Each combination of ionic strength and temperature was repeated three times (n = 3). Samples were then soaked overnight in 1× PBS and then in culture medium (79% Dulbecco's Modified Eagle Medium (DMEM High Glucose, HyClone Laboratories Inc., Logan, UT, U.S.), 10% Fetal Bovine Serum (FBS, Multicell Wisent Inc., Saint-Jean-Baptiste de Rouville, QC, Canada), 10% Porcine Serum (PS, Multicell Wisent Inc., Saint-Jean-Baptiste de Rouville, QC, Canada) and 1% Penicillin-Streptomycin (PenStrep, Invotrogen Corp., Carlsbad, CA, U.S.)). 3× E05 porcine smooth muscle cells (pSMCs) between the second and seventh passage were seeded on each sample and covered with culture medium. Samples were incubated and colorimetric assays were carried out after 24 or 48 h. 3-(4,5-dimethylthiazol-2-yl)-2,5-diphenyl-2H-tetrazolium bromide (MTT, Sigma Aldrich, St. Louis, MO, U.S.) is reduced to purple formazan by mitochondrial dehydrogenase in cells indicating normal cell metabolism. At each time point, culture medium was removed and each sample was rinsed with PBS in order to remove dead cells. MTT was solubilized in culture medium (1 mg/mL) and added to cells; samples were subsequently incubated for 4 h. The medium was then removed, samples were extensively

rinsed with 1× PBS and dried overnight in a vacuum oven at 21 °C; the purple formazan crystals were solubilized with pure dimethyl sulfoxide (DMSO, Sigma Aldrich, St. Louis, MO, U.S.) at room temperature. The optical density at 595 nm was determined using a 96-well plate reader (BioRad Model 450 Microplate Reader, Mississauga, ON, Canada). Cell viability was expressed as a % of the control, corresponding in this case to the collagen gel previously developed and whose biological properties have already been assessed.[224] Even though this gel presented a lower concentration of collagen (2 mg/mL) because of the presence of serum and culture medium, it was considered the best choice as a positive control in order to evaluate the potential of the new gels in terms of biological performances.

ANOVA tests were carried out in order to evaluate statistically significant differences between treatments. Two-way and three-way ANOVA were used to analyze the results from turbidity measurements, compression and viability tests. The Tukey's test was adopted to analyze the results from tensile tests. Differences between treatments were considered statistically significant for $p < 0.05$. All the experiments were repeated at least twice and the results are expressed as mean ± standard deviation (SD).

4.5 Results and Discussion

Collagen gels prepared at different pHs, ionic strengths and set at different temperatures were evaluated by turbidity measurements, mechanical tests and SEM imaging in order to assess the effects of these three factors on the process of self-assembly.

4.5.1 Turbidity Measurements

The results from the turbidity measurements are presented in Figure 4.1. For all the treatments, the absorbance increased with time and finally reached a plateau (Figure 1(a–c)). No syneresis was observed macroscopically. The value of this final absorbance was used to define the $t_{1/2}$ (Figure 2(d)) and consequently to estimate the time required for gelation. In particular, it can be noticed that the increase of the absorbance or reaching of the plateau was delayed by increasing the ionic strength. On the contrary, an increase in the temperature led to a faster gelation.

The collagen gels prepared at c5, c6 or c7 and set at T = 4 °C had not completely gelled by day 38. They were held at 21 °C (T1*) and their turbidity increased and reached steady state in three days. In this case, the $t_{1/2}$ was extrapolated. The results regarding the final absorbance and the $t_{1/2}$ are presented in Table 4.2. The final absorbance was higher and the kinetics faster (data not shown) for gels prepared at pH 7 than for gels prepared at pH 10. In particular, collagen gels prepared at pH 7 and set at 37 °C presented too many bubbles that invalidated the spectrophotometric measurements, so these results were not reported.

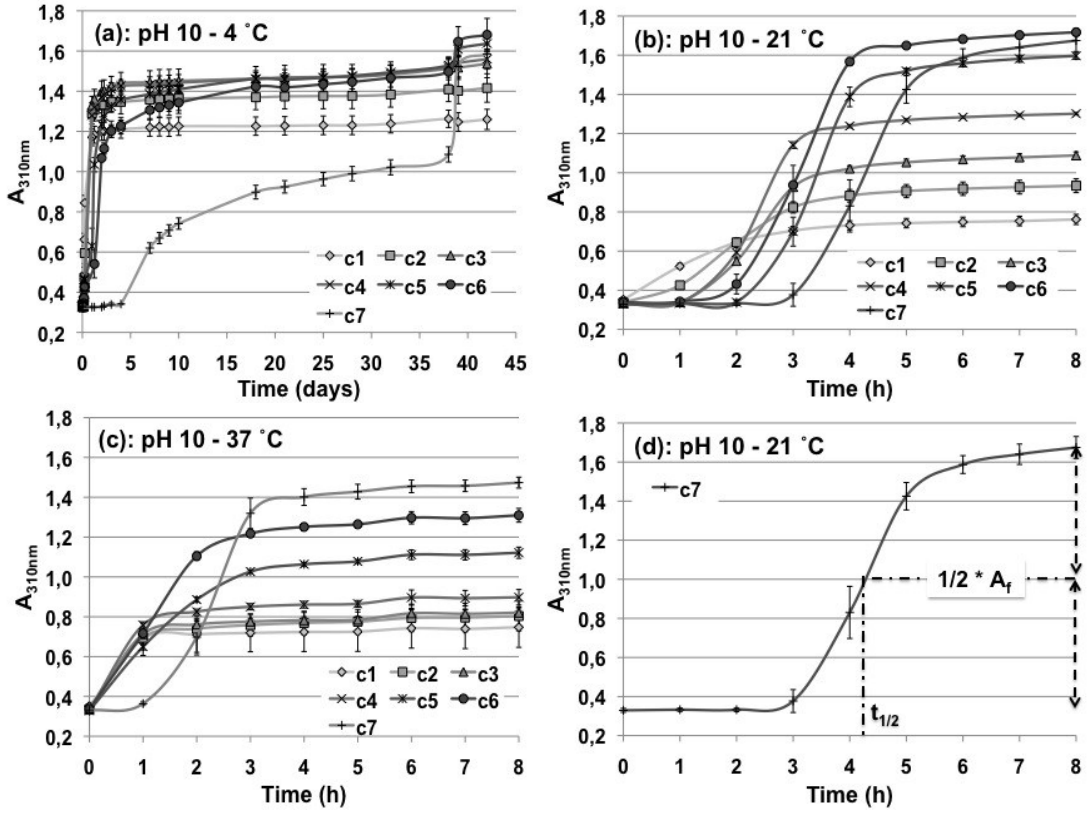

Figure 4.1: (a) Turbidity measurements for collagen gels prepared at pH 10, different ionic strengths (c1, c2, c3, c4, c5, c6, c7) and T = 4 °C. (b) Turbidity measurements for collagen gels prepared at pH 10, different ionic strengths (c1, c2, c3, c4, c5, c6, c7) and T = 21 °C. (c) Turbidity measurements for collagen gels prepared at pH 10, different ionic strengths (c1, c2, c3, c4, c5, c6, c7) and T = 37 °C. (d) Example of $t_{1/2}$ defined as the time required to reach half of the final absorbance.

This situation did not compromise other types of characterization and these samples were otherwise tested. The kinetics of gels prepared at pH 7 as a function of collagen concentration, temperature and ionic strength has already been widely discussed by several

authors.[129,135,144,159]Considering that the conclusions of these authors were consistent with the results concerning the kinetics of gelation of samples prepared at pH 7, it was chosen not to report them here in detail. In general, turbidity assays have already been used to assess collagen self-assembly *in vitro*.[129,135,144,159] In particular, Wood *et al.* and Williams *et al.* have already shown that the precipitation of collagen molecules is regulated by concentration, pH, ionic strength and temperature.[129,144] Both authors showed that collagen self-assembly is faster at lower ionic strengths or at higher temperatures. On the contrary, these works presented different conclusions concerning the effects of pH (range 6–8) on gelation rate: Wood *et al.* stated that an increase of pH led to a decrease in the gelation rate while Williams *et al.* stated the opposite. It has to be considered that collagen gels were prepared at different concentrations: 1 mg/mL in the case of Wood *et al.* and 0.1 mg/mL in the case of Williams *et al.*

This work studied collagen gels prepared at a higher concentration (2.8 mg/mL) and a higher pH (10) than those discussed by the previously cited authors, and the results concerning the effects of temperature and ionic strength are consistent with both these works. In the case of the effect of pH, the results presented here agree with the conclusions from Wood *et al.*[129]. All the factors had a statistically significant effect on gelation, in terms of kinetics or final absorbance ($p < 0.05$).

Table 4.2: Results from the turbidity measurements as a function of pH (7, 10), ionic strength (c1, c2, c3, c4, c5, c6, c7) and temperature (T1 = 4 °C, T1* = 4 °C and 21 °C after 38 days, T2 = 21 °C, T3 = 37 °C): Final absorbance for all the types of gels and $t_{1/2}$ for gels prepared at pH 10.

	pH 7		pH 10						
	A_{310nm} (T1)	A_{310nm} (T2)	A_{310nm} (T1*)	A_{310nm} (T1)	$t_{1/2}$	A_{310nm} (T2)	$t_{1/2}$	A_{310nm} (T3)	$t_{1/2}$
c1	1.501 ± 0.050	1.604 ± 0.073	1.256 ± 0.050	1.263 ± 0.043	5.6 h	0.792 ± 0.030	1.4 h	0.797 ± 0.121	21 min
c2	1.763 ± 0.023	1.831 ± 0.092	1.414 ± 0.069	1.409 ± 0.061	9 h	0.970 ± 0.035	2 h	0.880 ± 0.094	33 min
c3	1.868 ± 0.031	1.959 ± 0.026	1.529 ± 0.064	1.512 ± 0.054	13 h	1.134 ± 0.021	2.4 h	0.864 ± 0.012	28 min
c4	2.002 ± 0.020	2.056 ± 0.076	1.553 ± 0.044	1.520 ± 0.038	14 h	1.355 ± 0.013	2.4 h	0.944 ± 0.042	31 min
c5	2.020 ± 0.044	2.105 ± 0.019	1.639 ± 0.039	1.530 ± 0.041	29 h	1.663 ± 0.016	3.4 h	1.208 ± 0.027	1.5 h
c6	2.184 ± 0.030	2.041 ± 0.067	1.684 ± 0.077	1.497 ± 0.065	44 h	1.776 ± 0.017	3.2 h	1.414 ± 0.039	1.35 h
c7	2.159 ± 0.051	2.136 ± 0.051	1.591 ± 0.049	1.086 ± 0.038	24 d	1.783 ± 0.064	4.34 h	1.545 ± 0.028	2.3 h

The modulation of these three factors could make the $t_{1/2}$ shift by several hours or days while the turbidity measures could change by a factor of three. The precipitation of collagen fibrils is an endothermic process whose rate increases with temperature.[157] This effect can be considered in terms of an increase of hydrophobic interactions due to an increase of temperature. As well, a decrease of ionic strength can prevent the phenomenon of salting in and enhance bonding between electrostatically charged amino acid side chains.[130] The difference in the gelation rate in some cases could be observed macroscopically by the presence of bubbles that generally remained trapped in the gel when gelation was completed in less than one hour. In general, samples prepared at lower pH, lower temperature and higher ionic strength presented a higher turbidity, as observed by Wood *et al.*[129] As discussed in the next section, these authors observed that gels with ticker fibrils caused by a lower pH or temperature or a higher ionic strength presented a higher turbidity. In order to show the effects of the three parameters on collagen gels microstructure, SEM analyses were carried out.

4.5.2 SEM

Figure 4.2 shows the microstructure of collagen gels as a function of pH and ionic strength, as imaged by SEM.

As can be observed, the microstructure of collagen gels changed as a function of pH and ionic strength. The matrices appear tighter at higher pH for all the considered levels of ionic strength. The same observation can be found in the work of Rosenblatt *et al.*[130] This effect is probably due to the formation of net electrostatic interactions between charged residues, resulting in tighter packing of the fibrils.

Even though fibril diameters were not measured here, some observations can be made. For example, collagen fibrils of samples prepared at c1 seem to be thinner at both pHs when compared to the other gels prepared at c4 or c7 and the same pH. At the same time, for c1 and c4, samples prepared at pH 7 seem to present thicker fibrils than samples prepared at pH 10.

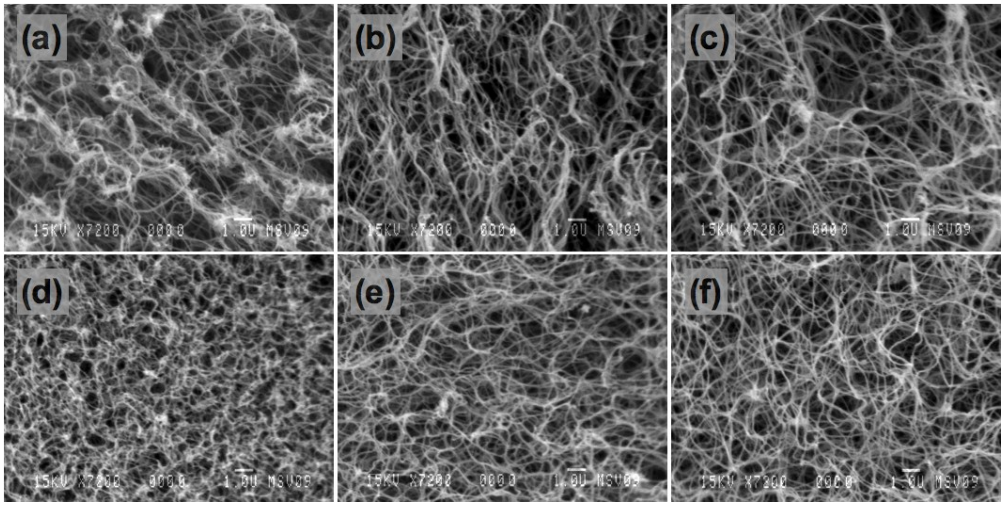

Figure 4.2: SEM images (7200×) of samples prepared at different pHs, ionic strengths and set at T = 21 °C. (a) Sample prepared at pH 7 and ionic strength c1. (b) Sample prepared at pH 7 and ionic strength c4. (c) Sample prepared at pH 7 and ionic strength c7. (d) Sample prepared at pH 10 and ionic strength c1. (e) Sample prepared at pH 10 and ionic strength c4. (f) Sample prepared at pH 10 and ionic strength c7.

Several authors have pointed out the importance of pH, ionic strength and temperature in changing the dimensions of the fibrils and consequently the microstructure of collagen gels.[129,132,144] Roeder *et al.* showed that fibril diameter decreases at more basic pH values and Wood *et al.* showed that fibril diameter generally increases at lower pH, higher ionic strength or lower temperature.[129,132] In particular, as discussed in the previous section, lower ionic strength and higher temperature increase electrostatic and hydrophobic interactions, which enhance fibril precipitation and limit lateral aggregation, resulting in thinner fibrils. The same authors observed that matrices with thicker fibrils resulted in higher turbidity as discussed in this work. Yang *et al.* and Raub *et al.* focused on the microstructure of collagen gels as a function of temperature.[139,140] In both cases, collagen gels were prepared at pH 7.4 but at different concentrations: 2 mg/mL by Yang *et al.* and 4 mg/mL by Raub *et al.* While Yang *et al.* observed that fibrils were thinner at higher temperature; Raub *et al.* observed that fiber diameter increased at lower temperature. The difference in collagen concentration may explain why Raub *et al.* observed fibril bundles. The present work does not present SEM images for collagen gels prepared at pH 7 and set at different temperatures. From the final absorbance results (Table 4.2), it can be observed that there were no significant differences between gels prepared at pH 7 and set at different

temperatures; consequently no major differences at the microstructural level could be assumed. In a following work, Raub *et al.* considered the effects of pH (range 5.5–8.5) on fiber size.[141] The authors observed that fiber diameter as well as the pore size and the pore area fraction decreased by increasing the pH. While these considerations are regarding gels with a final collagen concentration of 4 mg/mL, this work proposes similar conclusions concerning the effect of pH on the final microstructure, where slender and more tightly packed fibrils occur in the case of higher pH.

The different organization and size of collagen fibrils resulted in microstructures with different mechanical properties.

4.5.3 Mechanical Tests

Figure 4.3 shows the typical mechanical behavior in the compression and tension of collagen gels as well as the slopes and the area under the curve used to define the parameters that have been adopted to compare the different treatments. Both CM and TM were calculated out of the toe region that is typical of collagen-based materials.[93,132,254,255]

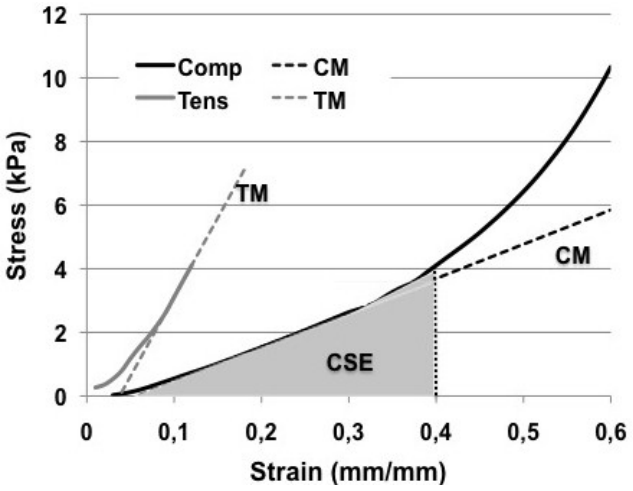

Figure 4.3: Mechanical behavior of collagen gels in terms of compression and tension with the slopes that were used to define the compressive modulus (CM) and tensile modulus (TM), respectively. The compressive strain energy (CSE) was defined as the integral between 0 and 40% of strain.

The CM was defined between 15 and 30% of strain where a linear region could be identified for all the treatments, while the CSE was evaluated up to the 40% of strain

because the approach of the piston to the plate was considered to affect the results for strain higher than 40%. In this case, the presence of the toe region in the strain range in which the CSE was calculated did not affect the results. The results concerning the CM and CSE are presented in Figure 4.4 and restated in Table 4.3 as a function of ionic strength, pH and temperature. Higher pH, particularly at lower temperature, significantly increased both CM and CSE ($p < 0.01$). At the same time, the interactions between the three factors and the effects of the ionic strength on the mechanical properties were statistically significant ($p < 0.05$), which depended on the combination of temperature and pH.

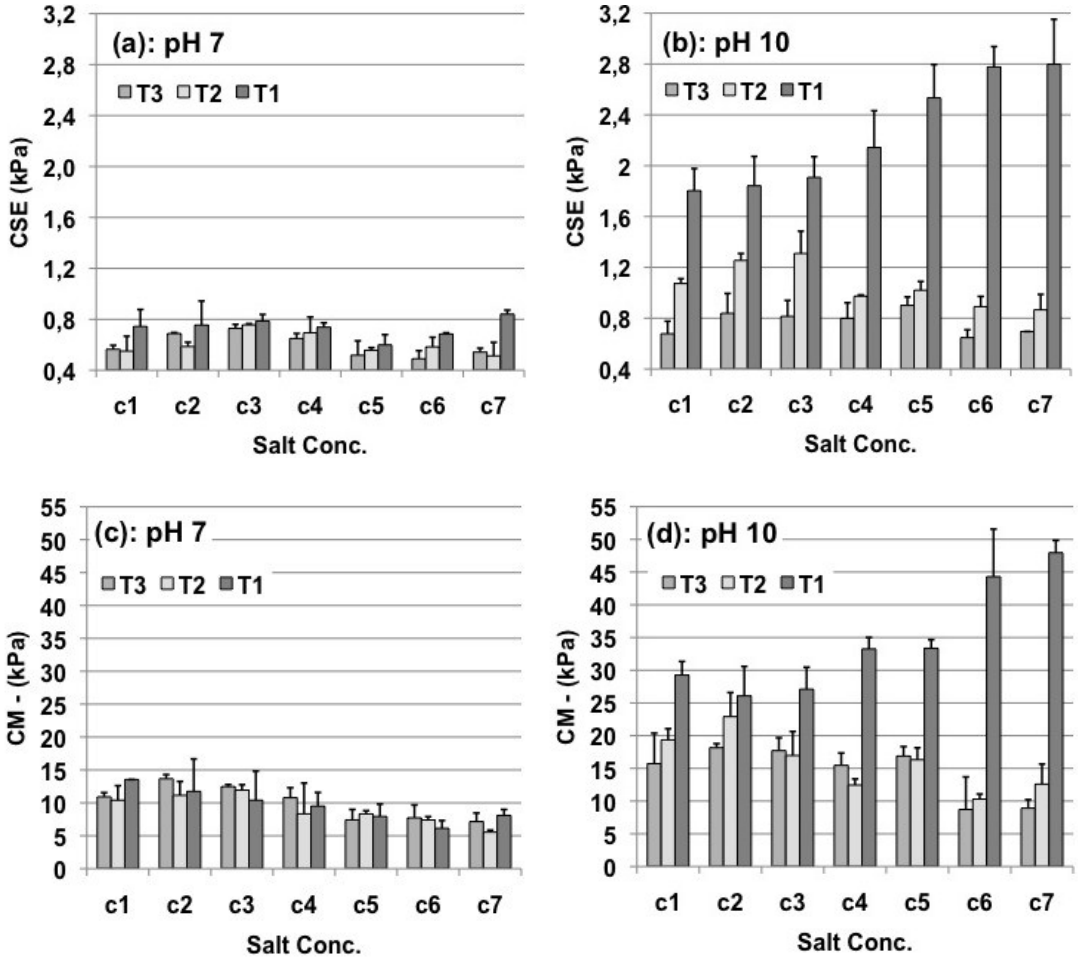

Figure 4.4: Compressive strain energy (CSE) (a) and compressive modulus (CM) (c) as a function of ionic strength (salt conc., c1, c2, c3, c4, c5, c6, c7) and temperature (T1 = 4 °C, T2 = 21 °C, T3 = 37 °C) for samples prepared at pH 7. CSE (b) and CM (d) as a function of ionic strength (salt conc., c1, c2, c3, c4, c5, c6, c7) and temperature (T1 = 4 °C, T2 = 21 °C, T3 = 37 °C) for samples prepared at pH 10.

Except for samples prepared at pH 10 and set at 4 °C, where the mechanical properties increased with the ionic strength, the samples generally presented a maximum for the ionic strengths corresponding to c2-c3-c4 for any level of temperature. The improvement of the mechanical properties of the gel prepared at pH 10, c7 and 4 °C was almost four-fold when compared to the control, and almost six-times when compared to the gel with the lowest mechanical properties. Tensile tests were conducted only on the types of gel that were considered the most interesting in regard to the improvement of the mechanical properties shown in compression. Figure 4.5 presents the results in terms of TM and UTS. Considering the TM, the group of gels prepared at pH 10 and set at 21 °C presented a maximum for c4. Consistent with the results from the compression tests (Figure 4(d)), collagen gels prepared at pH 10, c4 and 21 °C as well as the gel prepared at pH 10, c7 and 4 °C, were significantly more resistant than the control ($p < 0.01$). Regarding the gel prepared at pH 10, c7 and 4 °C, the UTS was significantly higher than the one of the control ($p < 0.05$).

Table 4.3: CM and CSE as a function of ionic strength (c1, c2, c3, c4, c5, c6, c7), pH (7, 10) and temperature (T1 = 4 °C, T2 = 21 °C, T3 = 37 °C) and expressed as mean ± SD.

	CM (kPa)					
	pH 7			***pH 10***		
Salt Conc.	*T3*	*T2*	*T1*	*T3*	*T2*	*T1*
c1	10.913 ± 0.633	10.401 ± 2.204	13.539 ± 0.004	15.722 ± 4.652	19.361 ± 1.702	29.255 ± 2.084
c2	13.666 ± 0.629	11.144 ± 2.112	11.742 ± 4.929	18.157 ± 0.628	22.912 ± 3.674	26.078 ± 4.507
c3	12.466 ± 0.307	11.936 ± 0.818	10.399 ± 4.420	17.713 ± 1.970	16.967 ± 3.674	27.099 ± 3.361
c4	10.778 ± 1.521	8.330 ± 4.677	9.501 ± 2.072	15.462 ± 1.886	12.451 ± 0.932	33.256 ± 1.747
c5	7.411 ± 1.580	8.324 ± 0.483	7.932 ± 1.868	16.880 ± 1.457	16.329 ± 1.818	33.360 ± 1.305
c6	7.726 ± 1.951	7.386 ± 0.513	6.130 ± 1.182	8.719 ± 4.974	10.305 ± 0.772	44.299 ± 7.266
c7	7.149 ± 1.299	5.543 ± 0.305	8.094 ± 0.895	8.920 ± 1.301	12.592 ± 3.064	47.960 ± 1.885
	CSE (kPa)					
c1	0.565 ± 0.031	0.550 ± 0.117	0.744 ± 0.133	0.677 ± 0.099	1.073 ± 0.038	1.803 ± 0.174
c2	0.688 ± 0.008	0.586 ± 0.034	0.755 ± 0.189	0.838 ± 0.156	1.254 ± 0.054	1.842 ± 0.231
c3	0.729 ± 0.031	0.757 ± 0.009	0.786 ± 0.052	0.814 ± 0.125	1.309 ± 0.175	1.908 ± 0.164
c4	0.649 ± 0.040	0.694 ± 0.125	0.738 ± 0.034	0.799 ± 0.122	0.973 ± 0.010	2.143 ± 0.289
c5	0.518 ± 0.113	0.557 ± 0.020	0.599 ± 0.081	0.901 ± 0.066	1.020 ± 0.069	2.534 ± 0.262
c6	0.491 ± 0.064	0.584 ± 0.076	0.685 ± 0.010	0.647 ± 0.062	0.891 ± 0.080	2.777 ± 0.160
c7	0.543 ± 0.031	0.513 ± 0.106	0.841 ± 0.032	0.695 ± 0.001	0.866 ± 0.122	2.798 ± 0.354

As discussed in the previous section, several authors have studied the effects of parameters like pH, ionic strength and temperature on fibrillogenesis.[26,129,144,252,256] Some of them

already pointed out that, regarding the process of self-assembly, the modulation of these parameters can determine modifications at the micro-structural level in terms of the fibril size and the electrostatic interactions between neighboring fibrils.[129,130,132,139-141,147] Roeder *et al.* showed, in agreement with the conclusions from Wood *et al.*, that the fibril diameter decreases and the fibril length increases by increasing the pH, conjecturing that this change could explain the improvement in the mechanical properties.[129,132] While the mechanical properties increased as expected by increasing collagen concentration, collagen gels prepared at 2 mg/mL and different pH (6–9) were stiffer at higher pH. The values of the linear modulus reported by these authors are lower than those presented in this work most probably for three reasons: a lower concentration of collagen in the gels, a lower pH during gel preparation and a lower testing rate. Rosenblatt *et al.* (pH range 6–9) focused on the role of pH and ionic strength in generating collagen intermolecular attractive forces. These electrostatic forces finally stabilize the matrix yielding higher mechanical properties as shown by rheological tests.[130] Raub *et al.* (pH range 5.5–8.5) confirmed by similar tests that collagen gels are stiffer when prepared at higher pH[141]. While it is difficult to compare the absolute values of the results of rheological tests with the ones of compression or tensile tests, it can be noted that the general conclusions about the effects of pH are consistent. Considering the findings of the previous section, the present study confirms that a more alkaline pH during gelation leads to a tighter packing of collagen fibrils and a more rigid microstructure. Even though the fibril diameter seems to decrease at higher pH, a higher volume fraction of fibrils, more than the presence of thicker fibrils, may determine the increase of the mechanical properties, as proposed by the previously cited authors.[132,140] It has to be considered that while the present work reports the results of mechanical tests conducted on gels whose pH and ionic strength were stabilized at the physiological level by soaking the samples in 1× PBS, all the previously cited works discussed the mechanical properties of collagen gels prepared and tested at alkaline pH. Because a higher pH implies more electrostatic bonds between fibrils, gels prepared and tested at alkaline pH values are expected to show higher mechanical properties than gels prepared at basic pH but then stabilized at pH 7–7.5.

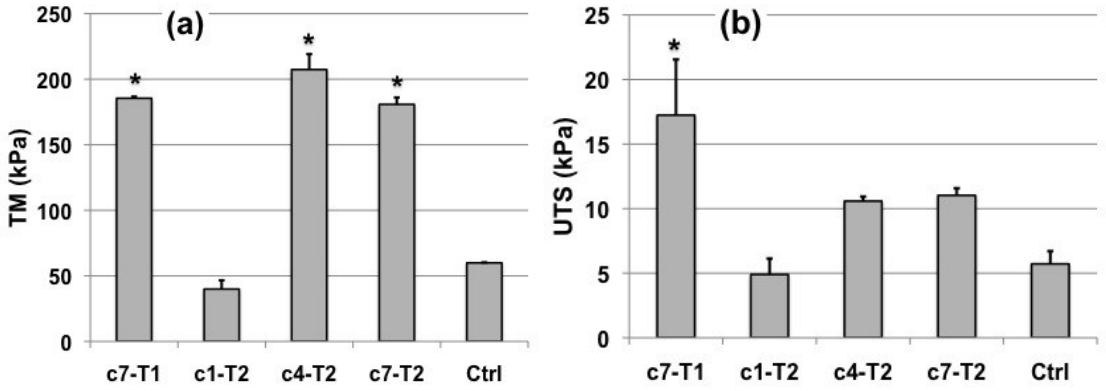

Figure 4.5: (a) Tensile modulus (TM) for the control and for some of the gels prepared at pH 10: these treatments were selected to feature the range obtained by modulating ionic strength and temperature. * denotes treatments with statistically significant differences as compared to the control ($p < 0.01$). (b) Ultimate tensile stress (UTS) for the control and for some of the gels prepared at pH 10. * denotes treatments with statistically significant differences as compared to the control ($p < 0.05$).

Yang *et al.* and Raub *et al.* discussed the effects of temperature on the mechanical properties of collagen gels prepared at pH 7.4 by rheological tests.[139,140] While Yang *et al.* observed that a temperature decrease resulted in higher stiffness, Raub *et al.* showed that gel stiffness decreased by decreasing the temperature. These works differed in the final concentration of collagen in the samples tested, 2 and 4 mg/mL respectively. In this work, from the results of the compression tests, no significant differences were observed between gels prepared at pH 7 as a function of temperature. On the contrary, the temperature profoundly affected the mechanical properties of gel prepared at pH 10.

Seliktar *et al.*, Berglund *et al.* and Cummings *et al.* discussed the mechanical properties of collagen-based constructs under tensile tests.[93,97,254] The values of the tensile modulus of cell-compacted collagen gels without crosslinking, sleeves or support, are interestingly close to those reported in this work. In this case, cell-driven remodeling has not yet occurred and the mechanical properties could be further increased.

Another factor that could partially explain the difference of mechanical properties observed between gels prepared at different pHs, ionic strengths or temperatures, is the presence of air bubbles. These bubbles could remain trapped in the case of rapid gelation (<1 h), resulting in discontinuities in the structure and preferential sites for fracture propagation.

The present study was mainly devoted to define collagen gels that could satisfy the mechanical requirements following the pulsatile flow of a bioreactor.[15,257] In particular, during the early stages of conditioning, a collagen gel-based construct should resist up to 10 kPa of circumferential stress and present a linear region with a circumferential modulus of at least 100 kPa. As can be observed in Figure 4.5, collagen gels prepared at pH 10, c7 and 4 °C and gels prepared at pH 10, 21 °C and c4 or c7, present TM and UTS equal or higher than 100 and 10 kPa, respectively. On the contrary, the gels prepared under physiological conditions (control) do not satisfy these requirements.

In conclusion, although further attention should be addressed to the mechanical behavior of these constructs after several cycles, the collagen gels proposed in this work represent a valid scaffolding system to support cell proliferation and remodeling during the early stages of maturation in a bioreactor.

4.5.4 Viability Test

Viability tests were conducted only on gels prepared at pH 10 because they were the most interesting considering their higher mechanical properties. These tests were carried out in order to validate the potential of these scaffolds to support cell adhesion and proliferation once they are installed in a bioreactor. The results of the MTT test are shown in Figure 4.6. Cell viability did not significantly change as a function of ionic strength or the temperature at which samples were prepared, nor as a function of the time point. The viability of pSMCs on any type of gel seemed to be lower when compared to the control, at almost 80%. This could be explained by two differences regarding the preparation of collagen gels and the preparation of the control. The control was gelled with culture medium and serum already inside. Even if the collagen gels discussed here were rinsed with culture medium, they could not be expected to have equivalent diffusion with these components. Moreover, the control had a final concentration of 2 mg/mL of collagen while the other gels had a final concentration of 2.8 mg/mL. These tighter matrices could have diminished cell infiltration and proliferation. Notwithstanding this point, the gels presented in this work seem compatible with cell adhesion and proliferation.

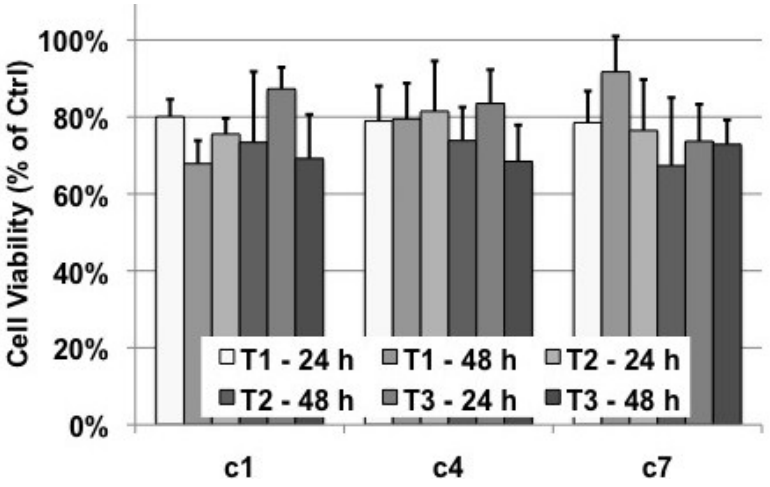

Figure 4.6: Results of the MTT test on collagen gels prepared at pH 10 as a function of ionic strength, temperature of gelation and the time point (24 or 48 h) at which cell viability was assessed. The results are expressed as % cell viability of the control.

4.6 Conclusion

The aim of this work was to improve the mechanical properties of collagen gels that are expected to support vascular cell adhesion and proliferation under dynamic conditioning. This could be achieved by increasing pH, lowering temperature and modulating ionic strength.

In particular, this work focused on the effects of preparing collagen gels at pH 10 and the interactions of this parameter with different levels of temperature or ionic strength. As shown by turbidity measurements and SEM, these parameters affected collagen self-assembly and consequently, the microstructure. Collagen fibril packing, in particular, became more important at higher pH. These tighter matrices proved to be stiffer with significant increases in the compressive and tensile modulus as well as in compressive strain energy and ultimate tensile stress. The values of the tensile modulus were comparable to those of cellularized collagen gel. All the gels were tested under physiological conditions and the results of the mechanical tests confirmed the importance of different experimental conditions at the moment of collagen preparation. Collagen gel prepared at pH 10 showed increasing mechanical properties when set at 4 °C as a function of ionic strength. In particular, collagen gels prepared at pH 10, 174 mM and set at 4 °C presented the highest

mechanical properties. Among others, this work proposes an interesting method to tailor not only the mechanical properties but also the gelation time, which can be considerably increased by increasing the ionic strength of gels set at 4 °C.

Further improvements can be obtained. While biological molecules like glycosaminoglycans can be added in order to favor cell proliferation as well as to further increase the mechanical properties in combination with chemical cross-linkers, the mechanical properties of collagen gels should be evaluated under cyclic testing in order to better mimic the cyclic solicitations imposed by the bioreactor to the vascular construct.

In conclusion, while all the collagen gels supported pSMC proliferation, some of them showed interesting mechanical properties, and therefore express a great potential as scaffolds for pSMCs in VTE applications.

4.7 Acknowledgements

We would like to thank Pascale Chevallier, Stéphane Turgeon and Jean Lagueux, at the Laboratory for Biomaterials and Bioengineering (LBB), for their kind help regarding the SEM, and Frédéric Couet, at Laval University, and Raquel Weska, at the University of Campinas, Brasil, in training at LBB, for their assistance in revising the article. We also acknowledge the Canadian Bureau for International Education (CBIE) for the award during the first year of Ph.D., the Natural Science and Engineering Research Council of Canada, the Canadian Institutes for Health Research and the Centre Hospitalier Universitaire de Québec, Hopital Saint-François d'Assise for partially funding this research.

CHAPTER 5. On the Viscoelastic Properties of Collagen Gel-Based Lattices under Cyclic Loading: Applications for Vascular Tissue Engineering

This chapter presents the third article[8] as submitted to *Macromolecular Materials & Engineering* on October 27th, 2011. The collagen gels presented in this study take advantage of the findings discussed in the previous chapter and of those concerning cell-mediated remodeling in the presence of mechanical constraints. The protocol for collagen gels where collagen and cells are blended in physiological conditions – Boccafoschi et al.[154] – was modified and the pH was stabilized with Hepes. The pH of collagen gels prepared in basic conditions was further stabilized by including Na_2CO_3. In the case of these gels, collagen concentration was increased or HA was introduced. Samples were tested under cyclic loading in physiologic conditions.

This article represents the natural conclusion to the series of investigations aiming to improve the mechanical performances of collagen gels through the modification of the microstructure.

5.1 Résumé

Les gels à base de collagène reconstitué ont été largement utilisés comme échafaudages même si leurs faibles résistance et élasticité limitent leur application dans le domaine du génie du tissu vasculaire. Dans cette étude, deux approches ont été adoptées afin de modifier leur comportement mécanique : dans la première, des gels préparés en conditions physiologiques ont été remodelés par contraction et étirement cellulaire ; dans la deuxième, des gels ont été préparés dans des conditions non physiologiques et ont été réticulés chimiquement. Les échantillons ont été testés sur des charges mécaniques cycliques et le comportement viscoélastique a été évalué. Les résultats ont démontré que les deux approches génèrent des réseaux avec résistance adéquate, pendant que la réticulation réduit

[8] Matteo Achilli, Sébastien Meghezi, Diego Mantovani, Laboratory for Biomaterials and Bioengineering, Department of Materials Engineering & Research Centre, Quebec University Hospital, Laval University, Quebec City, G1K 7P4, Canada

significativement l'hystérèse et la déformation permanente. Enfin, des images par microscopie électronique à balayage ont démontré que les cellules musculaires lisses étaient capables de contracter et remodeler tous les types de réseau, confirmant que ceux-ci sont des supports adéquats pour la régénération du tissu.

5.2 Abstract

Reconstituted collagen gels are widely used as scaffolds even though their low strength and poor elasticity limit their applications in VTE. In this study, two approaches were adopted to modify the mechanical behavior: in the first one, gels prepared in physiologic conditions were remodeled by cell-mediated contraction; in the second one, gels prepared in non-physiologic conditions were chemically crosslinked. Samples were tested under cyclic loading and the viscoelastic behavior was assessed. The results showed that both of these approaches resulted in lattices with adequate strength, while crosslinking significantly reduced hysteresis and permanent deformation. Finally, SEM showed that SMCs were capable of contracting and remodeling all the lattices, confirming that these are suitable supports for tissue regeneration.

5.3 Introduction

Collagen constitutes a natural substrate for cell attachment, proliferation and signaling, and its potential in the regeneration of small caliber (ø < 6 mm) blood vessels has been widely investigated. In particular, in scaffold-based vascular tissue engineering (VTE) collagen is one of the materials used as scaffold for vascular cells in order to develop a vascular construct – where a construct is defined as the whole of scaffold and vascular cells – and eventually a tissue-engineered blood vessel (TEBV) through a process of maturation.[25,57,59,62,113] Considering that the media is the major load-bearing layer in a natural artery, it follows that a TEBV should be developed starting from a media-equivalent (ME) with adequate mechanical properties.[21,103]

Collagen is the most abundant extracellular protein of vertebrates. Even though more than 20 types of collagen have been identified, all these types present a similar molecular structure, i.e. three twisted α-chains where each α-chain is a monotonously repeating

sequence of more than 1000 amino acids (Gly-X-Y). Even though the X and Y positions are normally occupied by proline and hydroxyproline respectively, positively charged (lysine or hydroxylysine) or negatively charged (glutamic acid or aspartic acid) amino acids may be present. Collagen types III and I are fibril-forming collagens that assemble into the well-packed highly-oriented aggregates that represent the major stress-bearing component of the fibrous matrices of blood vessels.[23,24,109]

Type I collagen can be obtained from rat-tail tendons (RTT) by solubilization in acetic acid.[28,115] This process reduces the highly hierarchical collagen structures to small aggregates of collagen monomers. It has been shown that these small aggregates undergo in vitro "self-assembly" at neutral pH, in salt solution, and at 37 ºC or room temperature, forming fibrils with the typical banding pattern.[26] From another standpoint, the process of solubilization leads to the structural weakness of reconstituted collagen gels, making them unsuitable for implantation.[25,154,224,225] Cell-mediated remodeling has been shown to have potential in increasing the strength of collagen gels.[88,91,93,103] In this case, an ME is obtained by suspending smooth muscle cells (SMCs) in a collagen solution prepared at physiological pH and ionic strength, which is then cast in a specific mould and gels in an incubator. In the days following preparation, cell-mediated remodeling yields gel contraction as well as the reorganization of the network of collagen fibrils.[88,91,93,103,137,154] The maturation of the ME greatly benefits from cyclic conditioning in a bioreactor, with the expectation that this could contribute to the formation of a TEBV with the mechanical and structural features of a natural vessel.[103,258] Nonetheless, this step requires that the ME possess adequate strength and elasticity in order not to experience creep deformation or structural failures. MEs with these properties may be achieved by having an early remodeling in static conditions or by modulating the bulk properties of bare collagen gels and seeding cells successively.

In relation to the last point, it was reported that collagen gel strength is increased by affecting collagen gelation or by crosslinking treatments.[112,259] One of the most widely used chemical methods for the crosslinking of collagen lattices is based on 1-ethyl-3-(3-dimethylaminopropyl)carbodiimide (EDC). EDC is a water-soluble crosslinking agent that

mediates the amide crosslinks between the carboxyl groups of aspartic and glutamic acid side chains and the primary amines of lysine and hydroxylysine side chains of collagen. N-hydroxysuccinimide (NHS) can be associated to EDC to make the reaction more efficient. The residual crosslinking agents are not incorporated in the macromolecule and are washed away at the end of the reaction, therefore avoiding problems of cytotoxicity.[112]

The mechanical as well as the biological profile of collagen lattices can be modified by the inclusion of copolymers. In this context, the composition of the ECM of blood vessels is inspiring.[20] Hyaluronic acid (HA), for example, is a non-sulphated glycosaminoglycan (GAG) and is a rigid and highly hydrated molecule with a high molecular mass.[41] HA regulates cell migration and proliferation and its presence also strongly influences the mechanical behavior in compression and the visoelastic properties of the ECM.[45,198] Collagen and HA have already been used as copolymers in tissue engineering.[201,260,261] Moreover, the structural stability of HA-collagen gels can be enhanced by EDC crosslinking, which leads to amide and ester bond formation between the side groups of these polymers.[199,200,202,262,263]

Given the importance for MEs to withstand the cyclic solicitations incurring during the maturation process in the bioreactor, this work aimed to characterize the viscoelastic properties of collagen gel-based lattices deriving from two different approaches. In the first one, the experimental conditions concerning collagen self-assembly were defined in order to foster prompt cell-mediated remodeling; in the second one, the experimental conditions were optimized and EDC crosslinking carried out in order to maximize the strength of the gels. In this case, the contribution of HA was also studied. The potential of these lattices in promoting maturation and remodeling was investigated by assessing cell-mediated contraction and by scanning electron microscopy (SEM). Then, the different lattices were tested under cyclic loading, with the intent to simulate the cyclic solicitations that may occur during the maturation process, and to evaluate the viscoelastic behavior in terms of hysteresis and permanent deformation.

5.4 Experimental Part

5.4.1 Cell Isolation

Porcine SMCs were isolated from the medial layer of a young pig aorta. The media was separated from the intima and the adventitia, and cut in small pieces; these were placed in Petri dishes (100 mm TC-Treated Culture Dishes, Corning, NY, U.S.) and cultured with Medium 199 (Invotrogen Corp., Carlsbad, CA, U.S.) supplemented with 10 vol.-% Fetal Bovine Serum (FBS, Multicell Wisent Inc., Saint-Jean-Baptiste de Rouville, QC, Canada) and 1 vol.-% Penicillin-Streptomycin (PenStrep, 10,000 units of penicillin + 10,000 μg of streptomycin $\cdot mL^{-1}$, Invotrogen Corp., Carlsbad, CA, U.S.). Once SMCs had populated the Petri dishes, they were cultured with Smooth Muscle Grow Medium (SmGM-2, Lonza, Walkersville, MD, U.S.). When confluency was observed, cells were detached and frozen or suspended in a culture medium consisting of 79 vol.-% Dulbecco's Modified Eagle Medium (DMEM High Glucose, HyClone Laboratories Inc., Logan, UT, U.S.) supplemented with 10 vol.-% FBS, 10 vol.-% Porcine Serum (PS, Multicell Wisent Inc., Saint-Jean-Baptiste de Rouville, QC, Canada) and 1 vol.-% PenStrep. SMCs were used between the 2^{nd} and the 5^{th} passage.

5.4.2 Preparation of Collagen Lattices

Collagen lattices were prepared using two different approaches. In the first one, samples (type A) were prepared by suspending SMCs in a physiological medium with solubilized collagen. In the second approach, samples (type B) were prepared without cells and at higher pH, ionic strength, and with a higher collagen concentration; a part of these samples was then crosslinked. All the gels were prepared using an acid solution of type I collagen (4 $g \cdot L^{-1}$) obtained as previously reported.[115] The experimental plan is presented in **Table 5.1**. Because the two approaches imply different procedures regarding gelation and cell seeding, specific subsections will detail the differences in the preparation of the samples.

Table 5.1: Experimental plan for the preparation of collagen samples. Cr: crosslinked.

Type of Collagen Lattice	# of Cells Included	pH	Coll. conc.	HA conc.	Crosslinking
	$10^6 \cdot mL^{-1}$ of collagen		$g \cdot L^{-1}$	$g \cdot L^{-1}$	
Type A	2	7.4	2	–	–
Type B (–)	–	10	3.6	–	–
Type B (Cr)	–	10	3.6	–	x
Type B (+ HA)	–	10	2.8	0.8	–
Type B (+ HA Cr)	–	10	2.8	0.8	x

Type A Samples

Samples were obtained by mixing 5 mL of the acid collagen solution, 0.2 mL of 1 M HEPES buffer solution (Sigma Aldrich, St. Louis, MO, U.S.), 0.15 mL of 1 M sodium hydroxide (NaOH, Laboratoire MAT Inc., Quebec City, QC, Canada), 2 mL of 5X DMEM, and 2.65 mL of SMCs suspension. The final concentrations of collagen and cells were 2 $g \cdot L^{-1}$ and $2x10^6 \cdot mL^{-1}$ of collagen gel respectively. The final pH was 7.4. Ring-shaped samples were obtained by pouring this solution in annular moulds (i.d. = 22 mm, cross-sectional area = 5 mm x 6 mm). Gels were set at 37 ºC, 5 % CO_2, and 100 % humidity.

Type B Samples

Samples were prepared with (type B (+HA)) or without (type B (–)) HA (Sigma Aldrich, St. Louis, MO, U.S.). Type B (–) samples were obtained by mixing 9 mL of the acid solution of collagen, 0.2 mL of 1 M sodium carbonate (Na_2CO_3, Sigma Aldrich, St. Louis, MO, U.S.), 0.14 mL of 1 M NaOH, and 0.295 mL of 4 M sodium chloride (NaCl, Sigma Aldrich, St. Louis, MO, U.S.). The final volume was adjusted with 0.365 mL of deionized water. Type B (+HA) samples were prepared by mixing 7 mL of the solubilized collagen, 2 mL of 4 $g \cdot L^{-1}$ HA, 0.2 mL of 1 M Na_2CO_3, 0.1 mL of 1 M NaOH, and 0.3 mL of 4 M NaCl. The final volume was adjusted with 0.4 mL of deionized water. The pH for both these gels was 10. Depending on the type of characterization, these solutions were poured in specific moulds and left at 4 ºC overnight, and then at 21 ºC for at least 6 hours to accomplish the gelation process. Part of the samples with (type B (+HA Cr)) or without (type B (Cr)) HA was crosslinked in a 50 mM HEPES solution of 50 mM EDC (Sigma

Aldrich, St. Louis, MO, U.S.) – 50 mM NHS (Sigma Aldrich, St. Louis, MO, U.S.) for 12 hours at room temperature. Meanwhile, the uncrosslinked samples were soaked in 50 mM HEPES solution. All the samples were then soaked in 1X phosphate-buffered saline (PBS, Sigma Aldrich, St. Louis, MO, U.S.) for at least 4 hours. The final pH resulted to be 7.

5.4.3 Cell-mediated contraction

The cell-mediated contraction of each lattice was evaluated by measuring the mass change. This parameter was defined as the ratio between the mass of the sample ($mass_i$) at different time points, and the mass at the beginning of cell-mediated contraction ($mass_0$). Each 24 hour culture medium in excess was removed, samples were weighed and fresh culture medium poured to completely cover the samples. This procedure was repeated for 1 week. Mass change is expressed by the Equation (5.1):

$$mass\ change\ (\%) = \frac{mass_i}{mass_0}\ x\ 100 \qquad (5.1).$$

Samples were set differently according to the two approaches.

Type A Samples

Ring-shaped samples (n = 5) were set for 30 minutes, then weighed and immersed in culture medium. This moment was considered the starting point for cell-mediated contraction.

Type B samples

Disk-shaped samples (1 mL per sample, n = 5) were prepared in 12 multi-well plates (12-well Multiwell Plate, Becton Dickinson, Franklin Lakes, NJ, U.S.) and then $2x10^6$ SMCs were seeded on top. Samples were removed after 24 hours, placed in small Petri dishes (35 mm TC-Treated Culture Dishes, Corning, NY, U.S.), weighed and then immersed in culture medium. This moment was considered the starting point for cell-mediated contraction.

5.4.4 Mechanical Tests

Cyclic uniaxial tensile tests were carried out on type A samples (n = 5) after 24 hours of contraction and on type B samples without cells (n = 5) with an Instron 5848 Microtester (Instron Corporation, Norwood, MA, U.S.). All the samples were ring-shaped (i.d. = 22 mm) and were soaked in 1X PBS for at least 2 hours before testing. Samples were placed between two hooks (ø = 8 mm), the upper one being fixed to a 10 N load cell, in a thermoregulated bath (T = 37 ºC) with 1X PBS. The samples were put in tension by separating the hooks up to a distance (= 22 mm) corresponding to the complete extension of the rings, and then left for 10 minutes to reach the temperature of the bath. They were then cyclically tested at 5 %·s^{-1} according to two different stretching protocols. In the first one (SP1), samples were stretched with up to five different loads for ten cycles each. This test was intended to show the strength and the viscoelastic behavior as a function of the cycle number and of the increasing load. In the second one (SP2), samples were stretched one hundred times at a fixed load. This test was intended to show the viscoelastic behavior over a longer period. The applied loads were defined upon the transmural pressures that act on a tubular construct during cyclic conditioning. The ring-shaped samples were considered as sections of a vessel in which the wall tension was calculated according to Equation (5.2).[264,265]

$$T = p_{\text{int}} r_{\text{int}} - p_{\text{ext}}(r_{\text{int}} + h) \tag{5.2}$$

where T is the wall tension, p_{int} and p_{ext} are respectively the pressure inside and outside the vessel and r_{int} and h represent the internal radius of the vessel and the wall thickness. The Equation (5.2) can be rewritten in the following form (Equation (5.3)):

$$T = \Delta p\, r_{\text{int}} - p_{\text{ext}} h \tag{5.3}$$

where Δp represents the transmural pressure across the vessel wall.

In a ring test configuration as presented in **Figure 5.1**, the relation between the applied load (*Load*), the force (F), and T, which is defined as force per unit length (N·m^{-1}), can be expressed by the Equation (5.4):

$$Load = 2\,F = 2\,T\,l \tag{5.4}$$

where l represents the width of the ring-shaped sample, i.e. the dimension in the longitudinal direction of a hypothetic vessel. Equation (5.3) and (5.4) can be related in the Equation (5.5):

$$Load = 2\,l\,(\Delta p\,r_{\text{int}} - p_{\text{ext}}h) \tag{5.5}.$$

Equation (5.5) was used to calculate the loads applied to ring-shaped samples with different width (l) and thickness (h), and given the transmural pressure (Δp), the internal radius (r_{int}), and the external pressure (p_{ext}).

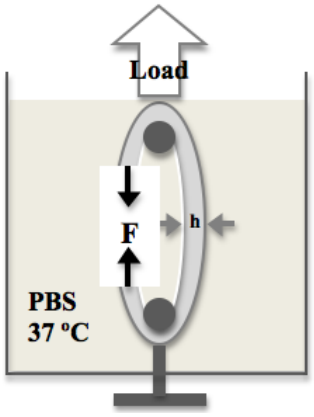

Figure 5.1: Experimental setup for tensile test. A ring-shaped specimen (cross section l x h) is mounted on two cylindrical hooks in a thermoregulated bath, and stretched by the Instron Microtester. The force (F) in each side of the ring corresponds to half the load (Load) applied.

The viscoelastic properties were evaluated in terms of hysteresis, defined as the loop area divided by the area under the loading curve, maximal strain (Max Strain) and permanent deformation (PDef) after each cycle.[168,172,266] The tension and the strain at break of each sample were defined as ultimate tension (UT) and ultimate strain (US).

5.4.5 Lattice Morphology

The different microstructures were observed by SEM before the mechanical tests and after 1 week of cell-mediated contraction. The samples were fixed and dehydrated as previously reported.[259] Briefly, samples were washed in 0.1 M cacodylate buffer (sodium cacodylate trihydrate, Sigma Aldrich, St. Louis, MO, U.S.) and fixed at 4 °C for 2 hours with 2.5% glutaraldehyde (Sigma Aldrich, St. Louis, MO, U.S.) in 0.1 M cacodylate buffer solution.

After fixation, samples were rinsed with 0.1 M cacodylate buffer and treated with 0.25% osmium tetroxide in 0.1 M cacodylate buffer solution. Samples were rinsed once again at 4 °C with 0.1 M cacodylate buffer, dehydrated at three different concentrations of ethanol (70, 95, 100%), and dried with the critical point drying method (Polaron CPD 7501, VG Microtech, East Grinstead, W Sussex, UK). Samples were then sputter-coated with gold-palladium and images were captured with a scanning electron microscope JSM-35CF (Jeol Ltd., Tokyo, Japan).

Type A Samples

Specimens consisted of strips cut from ring-shaped samples after 24 hours or 1 week of cell-mediated contraction.

Type B Samples

Samples without cells were prepared in 48 multiwell plates (48 Well Cell Culture Cluster, Corning, NY, U.S.). Samples resulting from 1-week contraction were obtained as reported in the section “Cell-mediated contraction”.

5.4.6 Statistical Analysis

ANOVA tests were carried out with the software SAS (vers. 9.2, SAS Institute Inc., Cary, NC, USA). Statistically significant differences concerning mass changes were evaluated with the repeated measures test. Tukey’s pair-wise multiple comparison procedure was used to analyze the UT and the US, and the results concerning the SP2 were fitted by polynomial regression. In particular, results concerning the hysteresis were fitted with tenth order polynomials, while Max Strain and PDef were fitted with fourth order polynomials. Differences between treatments were considered statistically significant for $p < 0.05$. All the tests were performed at least in triplicate. Results are expressed as mean ± SD.

5.5 Results and Discussion

The improvement of the mechanical properties of collagen-gel based MEs was attempted through two different approaches.

In the first one (type A), the protocol for collagen gels was defined – physiologic pH and ionic strength, presence of sera and culture medium, gelation in an incubator at 37 ºC, 5 % CO_2, 100% humidity – in order to foster a prompt gel remodeling by SMCs. In fact, notwithstanding the structural weakness of bare collagen gels deriving from this protocol, this approach counts on compaction and fibrils realignment in the circumferential direction for an increase of the strength.[88,93]

In the second approach (type B), the interest was focused on the parameters that affect the mechanical properties of collagen gels. It was clear that the modification of the experimental conditions of collagen gelation – increase of ionic strength and pH (= 10), decrease of the temperature (= 4 ºC) – in combination with chemical crosslinking were not compatible with cell survival. This situation implied that SMCs could be seeded only after a proper rinsing. Ideally, in order to shorten the time between gel preparation and the start of cyclic conditioning, these gels were required to show adequate mechanical properties before cell-mediated remodeling. For this reason, mechanical tests were conducted on type B samples without cells.

The differences in these two approaches lead to different ways of combining SMCs and collagen gels. Therefore, the authors preferred to address cell-mediated remodeling separately for each approach, with the intent to show their potential for tissue remodeling.

5.5.1 Cell-Mediated Contraction

The results of mass change as a consequence of the remodeling by SMCs are shown in **Figure 5.2**. Cell-mediated contraction led to compaction of the lattices and expulsion of part of the liquid content, thus resulting in a decrease of samples' weight.

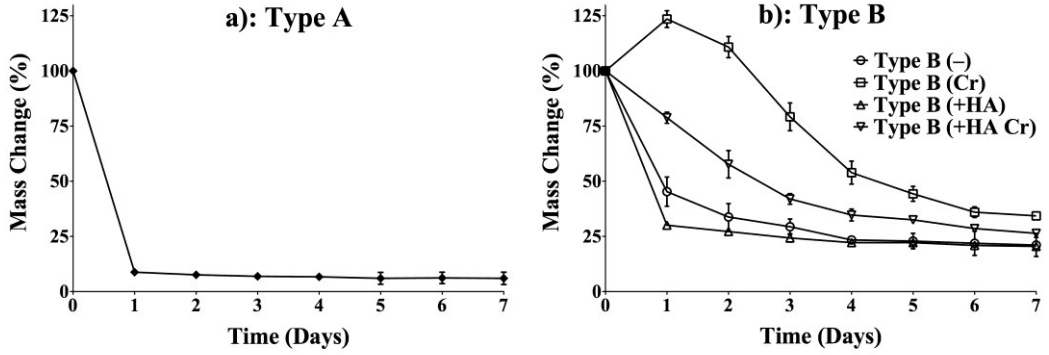

Figure 5.2: Mass Change (%) for type A samples (a) and type B samples (b) as a function of time.

Type A Samples

As can be observed (Figure 2.a) type A samples contracted by ~ 90 % in 24 hours ($p < 0.01$), after which no major changes were observed. Cell-mediated contraction of collagen gels has already been reported.[88,91,93,97,154,155,254,267,268] The central mandrel represents a geometrical constraint that redistributes the cell-generated forces in the circumferential direction promoting alignment of SMCs and collagen fibrils. The degree and rate of cell-mediated contraction depend on parameters like cell type (SMCs or fibroblasts), cell source (species, age), cell concentration, geometry of the construct, and culture conditions.[113] These lattices contracted quite fast compared to what was reported before.[92,93,269] The differences with the work of Seliktar et al. (70 % in 48 hours) may be explained by the lower cell concentration (10^6 cells), and the age of the subject (adult) from which they were isolated. The last point may explain as well the lower contraction rates measured in the work of Baguneid et al. (~ 70 % in 24 hours) and in the work of Girton et al. (~ 60 % in 48 hours).

Type B Samples

Samples were detached from the original mould only 24 hours after cells were seeded and the weight was measured. At this moment, the lattices did not present any sign of contraction, most probably because the forces generated by the cells seeded on the top were hindered by the adhesion forces acting between the board of the sample and the original

mould. Therefore this moment was used as a starting point to measure cell-mediated contraction. The differences were statistically significant ($p < 0.01$). After day 7 no major contraction had been observed for all the lattices. In general, crosslinked lattices were contracted more slowly than the uncrosslinked ones. In fact, as discussed by several authors, crosslinking increases the mechanical as well as the biological stability of collagen lattices to enzymatic degradation and cell remodeling.[112,113,162,262,270-274] Type B (Cr) samples' weight increased at day 1. In this case, the higher collagen density and the effect of crosslinking increased samples' stability and retarded cell-mediated contraction. In this interval, swelling was more important than liquid outflow and samples' weight increased rather than decreased. The rate of contraction for samples with HA contracted was more important compared to samples without HA. As reported by Travis et al., the presence of HA may affect the phenotype and so the activity of SMCs, resulting, in this case, in a faster remodeling.[261]

5.5.2 Mechanical Tests

The different loads applied to ring-shaped collagen samples were calculated according to the Equation (5.5), considering the different dimensions for contracted and uncontracted lattices. After 24 hours of contraction, type A samples presented a width (l) of 2.725 ± 0.339 mm and a thickness (h) of 1.221 ± 0.189 mm.

Table 5.2: Calculation according to Equation (5) of the loads (*Load*) applied to the different collagen samples as a function of sample width (*l*) and thickness (*h*).

Δp	Type A			Type B		
mmHg	$l - h$ / mm	T / $N \cdot m^{-1}$	*Load* / N	$l - h$ / mm	T / $N \cdot m^{-1}$	*Load* / N
50	2.8. – 1.3	19.361	0.108	6 – 5	17.548	0.210
100		39.3597	0.220		37.546	0.450
150		59.358	0.332		57.545	0.690
200		79.356	0.444		77.543	0.930
250		99.354	0.556		97.541	1.170

Table 5.2 presents an example of the calculation considering l = 2.8 mm and h = 1.3 mm. The p_{ext} was obtained by making the hypothesis that in a culture chamber a tubular ME is located under 50 mm of culture medium, resulting in a hydrostatic pressure of 490 Pa. In

order to consider the solicitations acting on a tubular ME with an inner diameter of 6 mm, the r_{int} was set at 3 mm.

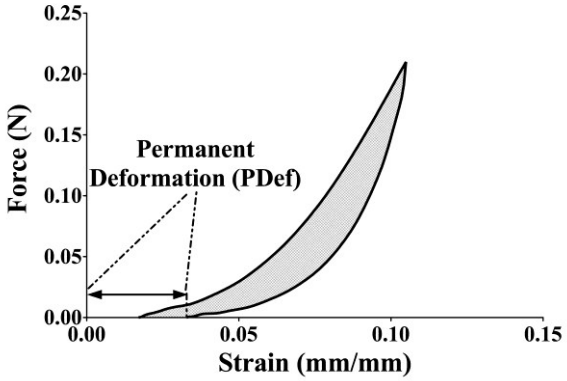

Figure 5.3: Loop at the second cycle for a type B (–) sample tested according to the SP1. The hysteresis was calculated as the loop area divided by the area under the loading curve. Permanent deformation was defined according to the definition of Silver et al.[168]

Even though some authors have discussed the importance of pre-conditioning in testing collagen lattices, in the present work no pre-cycling was carried out: the intent was to test the lattices in the same conditions in which a tubular ME would be subjected to cyclic conditioning after being installed in the culture chamber, i.e. without pre-cycling.[172,176] **Figure 5.3** shows a typical loop that was considered to calculate the hysteresis. **Figure 5.4** shows examples of the mechanical response for different lattices under cyclic loading according to the SP1 (Figure 5.4 a, c, e) and according to the SP2 (Figure 5.4 b, d, f). Considering the SP1, the graphs report only the cycles that were completed before break. Type B (–) samples didn't break during the test, showing on the other side an important elongation: As can be observed, the strains shift more towards the right side of the graph compared the other types of sample. Type A and type B (Cr) samples broke before the end of the test, with the second being more brittle and the less stretched. In the case of the SP2, all the samples didn't break and their final elongation followed the trends shown in the SP1: Type B (–) samples present the most important elongation while type B (Cr) present the less important one.

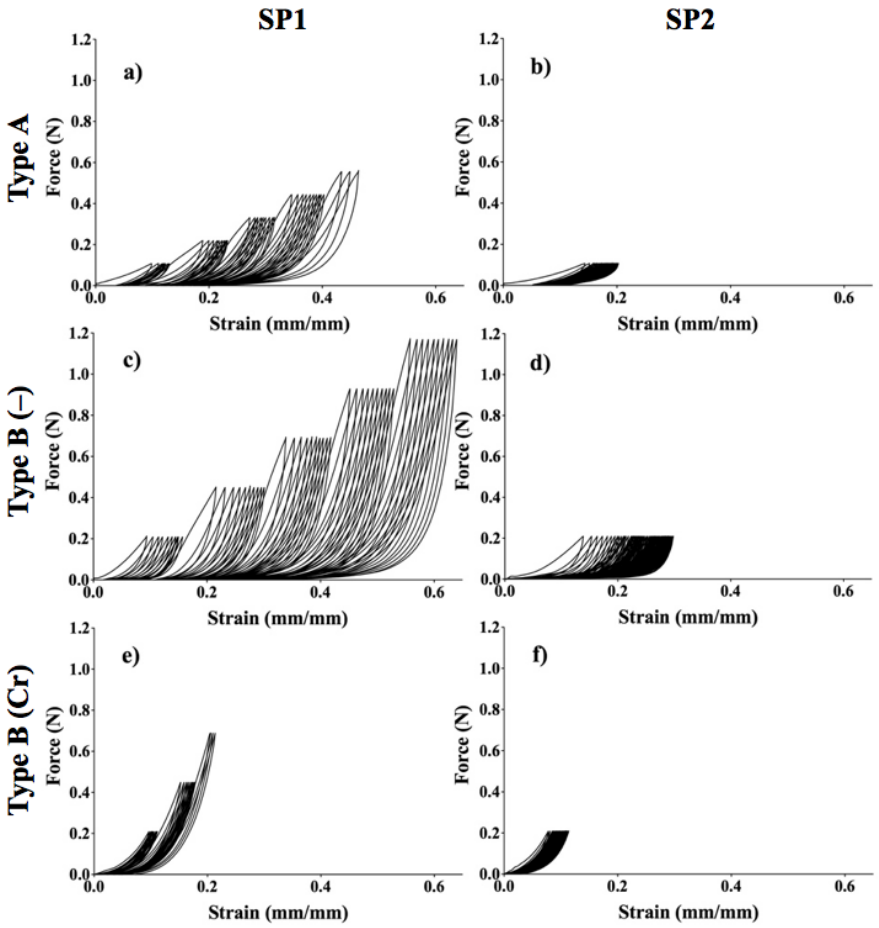

Figure 5.4: Mechanical response of type A samples (a, b), type B (–) samples (c, d), and type B (Cr) samples (e, f) to cyclic loading applied according to the SP1 (a, c, e) and to the SP2 (b, d, f). The curves regarding crosslinked and uncrosslinked type B (+HA) samples were omitted because of similarity to those of type B (–) and type B (Cr) samples respectively.

Tension and Strain at Break

Figure 5.5 shows the UT and the US of the different samples tested according to the SP1. Type A samples break at lower strain (0.49 $mm \cdot mm^{-1}$, $p < 0.05$) than type B (–) samples (~ 0.63 $mm \cdot mm^{-1}$), even though they present similar values in terms of UT (~ 95 $N \cdot m^{-1}$). Crosslinked samples were more brittle and broke at lower tension (~ 50 $N \cdot m^{-1}$) and lower strain (0.18 $mm \cdot mm^{-1}$) than type A and uncrosslinked type B ($p < 0.05$). Moreover, in the case of uncrosslinked samples, the introduction of HA at the place of a higher concentration of collagen results in a decrease of the UT (76 $N \cdot m^{-1}$, $p < 0.05$).

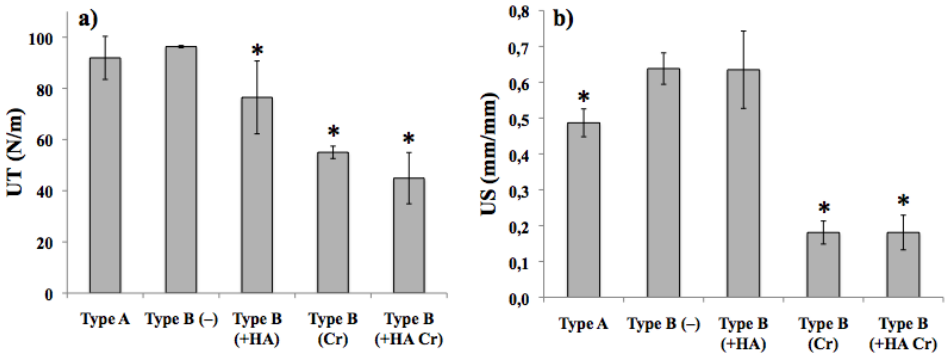

Figure 5.5: UT (a) and US (b) of different collagen lattices. * denotes statistically significant differences between type B (–) samples and other treatments ($p < 0.05$).

According to Equation (3), the wall tension is linearly proportional to the internal diameter. Therefore, MEs incurring in permanent deformation would experience higher wall tension for the same transmural pressure. Considering how the applied loads were defined, the changes in wall tension due to increasing permanent deformation were not taken into account. Consequently, the authors were cautious in comparing these results with those reported for burst testing. Nonetheless, considering just the first cycle for each test, it is clear that all the samples are able to resist a transmural pressure higher than 50 mmHg. Boccafoschi et al. previously reported lower burst pressures (~ 18 mmHg) for collagen gel-based constructs.[154] These constructs differed from the type A lattices discussed in this work for a lower collagen concentration and a slightly different conception of the protocol for collagen gels. Above all, it is likely that the reasons that lead to the different contraction rates – i.e. a different perfusion of the culture medium and the different age of SMCs' source – affected the remodeling of the microstructure as well, resulting in a higher strength of the structure.

Viscoelastic Properties

The viscoelastic properties were analyzed in terms of hysteresis, maximal strain, and permanent deformation at each cycle. The results are shown in **Figure 5.6** for the SP1 (a-c-e) and for the SP2 (b-d-f). In the case of the SP1, the results were calculated over the number of cycles that was common to samples of the same type. All the samples present hysteresis (Figure 5.6 a) and permanent deformation (Figure 5.6 e), even at different levels.

The hysteresis generally decreases along each set of ten cycles while it increases when the load is increased. Crosslinked samples present lower hysteresis, lower strains, and considerably lower permanent deformations, showing a more elastic behavior than uncrosslinked samples. For example, considering cycle 10, hysteresis, Max Strain and PDef for crosslinked samples are 40-57 %, 35-45 %, and 80 % lower compared to uncrosslinked samples.

In the case of the SP2, the results for the different types of collagen lattices – in the order, type A, type B (–), type B (+HA), type B (Cr), type B (+HA Cr) – were fitted by polynomial regression. The hysteresis (Figure 5.6 b, R^2 = 0.94, 0.85, 0.77, 0.93, 0.8) gradually decreases from the first cycle on, reaching a steady state during the test. Crosslinked samples show a hysteresis 30-40 % lower compared to uncrosslinked samples. The Max Strain (Figure 5.6 d, R^2 = 0.99 for all the types of samples) and the PDef (Figure 5.6 f, R^2 = 0.97, 0.98, 0.75, 0.99, 0.96) generally increase as a function of cycle number. At the end of the tests, crosslinked samples present a 70-75 % lower PDef compared to uncrosslinked type B samples, and a 50 % lower PDef compared to type A samples.

Crosslinking increases the rigidity and reduces the PDef in type B samples (Figure 5.6 c-d-e-f). In fact, it has been reported that EDC mediates the formation of amide bonds between collagen-collagen and collagen-HA side groups, and the formation of ester bonds between HA-HA side groups, consequently increasing the structural stability of the composite.[199,200,202,262,263]

This effect is responsible for the different contribution of HA to the PDef and Max Strain of uncrosslinked or crosslinked type B samples (Figure 5.6 c-d-e-f). In the first case, the lower collagen concentration – type B (+HA) – and the fact that HA is not covalently bound to collagen, but acts as filler, leads to a higher plasticity compared to type B (–) samples (Figure 5.6 e-f). In the second case, the newly formed covalent interactions between collagen and HA lead to a similar behavior of type B (Cr) and type B (+HA Cr) samples. Type A samples show an intermediate behavior between uncrosslinked and crosslinked type B samples. While the PDef is twofold compared to type B (Cr) samples in the case of

the SP2, the same parameter presents a 4.5-fold increase in the case of the SP1 (cycle 20), showing that the lower elastic recovery may limit the interest in type A lattices.

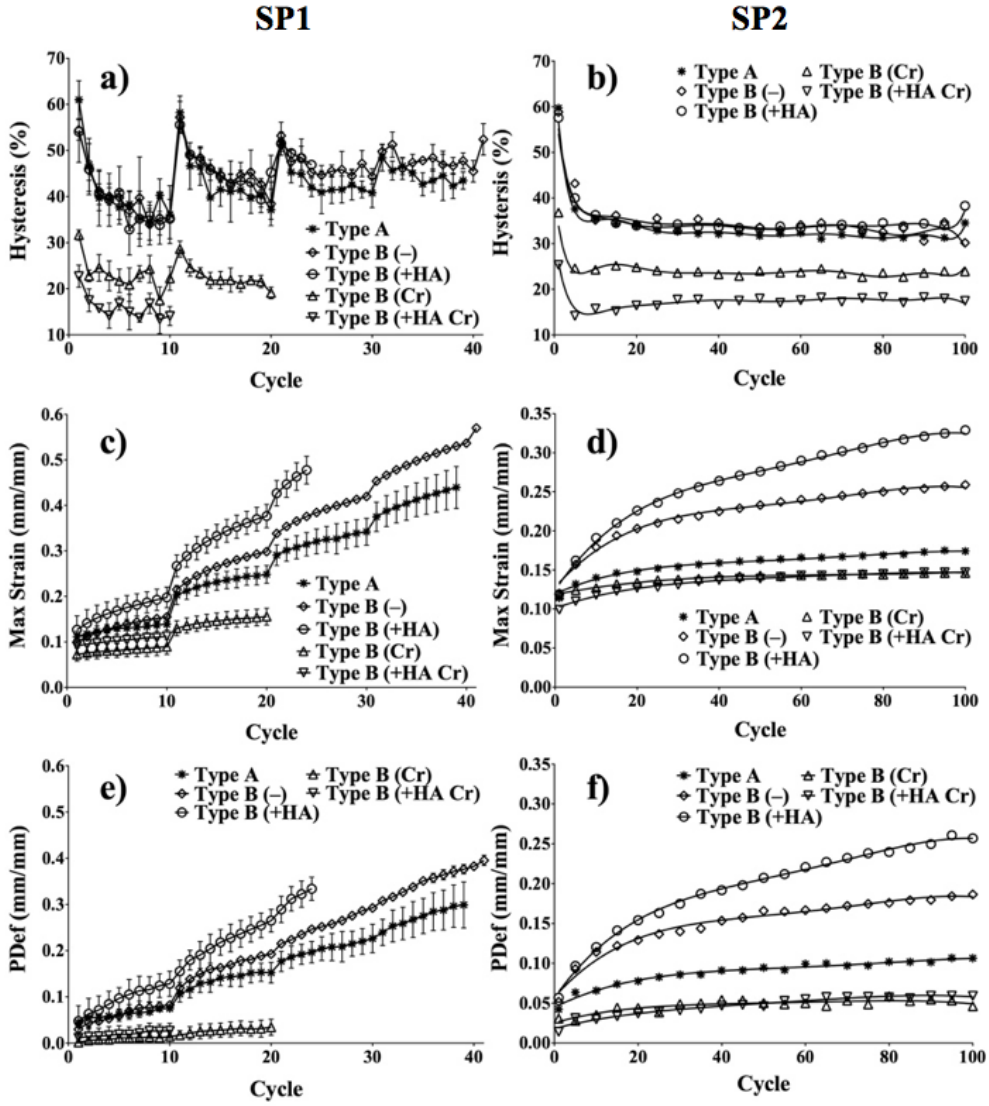

Figure 5.6: Hysteresis (a-b), Max Strain (c-d), and PDef (e-f) as a function of cycle number in the case of the SP1 (a-c-e) and the SP2 (b-d-f) for different collagen lattices. Curves concerning the hysteresis (b) were fitted with tenth order polynomials with R^2 = 0.94, 0.85, 0.77, 0.93, 0.8 for type A, type B (–), type B (Cr), type B (+HA) and type B (+HA Cr) samples respectively. Curves concerning the maximal strain (d) were fitted with fourth order polynomials with R^2 = 0.99 for all the types of samples. Curves concerning the permanent deformation (f) were fitted with fourth order polynomials with R^2 = 0.97, 0.98, 0.75, 0.99, 0.96 for type A, type B (–), type B (Cr), type B (+HA) and type B (+HA Cr) samples respectively.

The viscoelastic properties of ring-shaped collagen samples have already been investigated.[155,172,176,268] Even though the stretching protocols were defined by these authors in order to test the samples as a function of the applied strain instead of the applied tension, similarities in the mechanical behavior can be found. For example, by fixing the strain, Wagenseil et al. showed that the hysteresis and the peak force decrease as a function of cycle number.[172] The decrease of the peak force can be seen as a relaxation of the lattice during the test, as well as in this study the increase of the Max Strain and PDef recall a creep phenomenon. Consequently, even though the protocols differ in the initial settings, in both these works a consistent viscoelastic behavior is observed.

While Wille et al. investigated the contribution of the active response of cells to the final mechanical properties of the constructs, this work investigated only the contribution of the different collagen lattices.[268] In the present work, the manipulation of the samples before the mechanical tests didn't ensure cell survival, therefore it was assumed that the SMCs embedded in type A samples were not in the condition to actively contribute to the mechanical behavior of the ME.

In general, the tests on ring-shaped samples provided relevant information on the strength and on the viscoelastic properties of the different collagen-based lattices.

It has been reported that the morphological and mechanical features of ME are strongly improved by the maturation process under cyclic conditioning.[53,77,93,103,275-277] Because the success of this procedure depends on the capability to support the remodeling, ME are required to show adequate strength and elasticity in order to stand the cyclic solicitations and prevent any mechanical failure. In general, in the blood vessel wall vascular cells experience a 10 % circumferential strain on average at the frequency of 1 Hz (= 1 heartbeat). Several authors investigated the effects of cyclic circumferential strain on vascular constructs, spanning between 2.5 to 20 % circumferential strain and between 0.33 and 2.75 Hz regarding the frequency.[45] In this study, collagen-based lattices are tested at $5\%\cdot s^{-1}$ and show no rupture up to 10 % circumferential strain (Figure 5.5 b, 5.6 c-d). In addition, crosslinked gels show a lower permanent deformation as a consequence of the higher elasticity. In this regard, ME generated according to the approach of type A, or of

type B without crosslinking, may not be able to support the remodeling process by experiencing extensive creep deformation and so mechanical failure.

All the samples possess the sufficient structural integrity in order to be handled. This condition is achieved in 24-48 hours without need of long periods of maturation in static conditions or supporting materials or sleeves to ensure the integrity of the ME.[93,154,254,275] The definition of the stretching protocols during the cyclic conditioning may then match the mechanical properties of MEs by applying appropriate transmural pressure (50-100 mmHg) in the early stages. The strength of the ME would then increase during the maturation process.

In conclusion, type B (Cr) lattices represent the best compromise for the generation of collagen gel-based ME. The reasons reside in the lower plastic deformation compared to type A and uncrosslinked type B samples, and in the wider range of wall tension that can be applied before break compared to type B (+HA Cr) samples.

5.5.3 Lattice Morphology

Type A Samples

Figure 5.7 presents the inner (a-b) and outer (c-d) surfaces of type A rings after 24 hours (before mechanical tests, a-c) and after 1 week of cell-mediated contraction (b-d). SMCs and the collagen network can be observed in all the micrographs, where the vertical direction corresponds to the circumferential direction in the ring samples. Considering the samples after 24 hours of cell-mediated contraction, it can be noticed that while in the inner surface a preferential orientation cannot be detected, in the outer surface SMCs and collagen fibrils are clearly oriented in the vertical direction. This finding is in contrast with the observations of Wille et al., who showed that a preferential orientation in the circumferential direction is clearer in the inner more than in the outer surface of compacted ring samples.[268] Any consideration should take into account that the two protocols differ in collagen and cell concentrations, and in the conditions in which the compaction occurred, with consequences on the dynamics of gel compaction. In fact, the higher cell concentration is responsible for the faster compaction – ~ 90% in 24 hours against 70 % in 2 days for

Wille et al. – and may explain the more evident alignment in the outer surface. Concerning the inner surface, the alignment in the circumferential direction may have been hindered by the combination of compressive forces from the outer layers and adhesive forces with the central mandrel. It has to be considered that in the work of Wille et al. gel compaction occurred without a central mandrel. Micrographs 5.7 b and 5.7 d show the inner and outer surfaces after 1 week of cell-mediated contraction. While compaction has progressed in the inner surface, the outer surface is covered by SMCs and the underlying network is hardly visible.

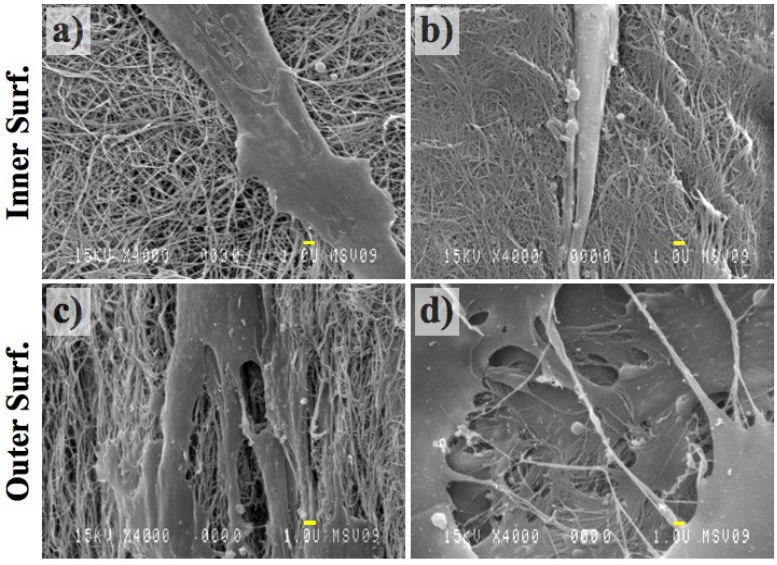

Figure 5.7: Micrographs (x4000) of type A lattices with the yellow bar representing 1 µm. Inner (a) and outer (c) surface of ring samples after 24 hours of cell-mediated contraction as before mechanical tests. Inner (b) and outer (d) surface of ring samples after 1 week of cell-mediated contraction. The circumferential direction in ring samples corresponds to the vertical direction in the micrographs.

Type B Samples

Figure 5.8 presents the microstructures of type B (–) (a-b), type B (Cr) (c-d), type B (+HA) (e-f) and type B (+HA Cr) (g-h) samples before mechanical tests (a-c-e-g) and after 1 week of cell-mediated contraction (b-d-f-h). Because the latter was carried out without mandrels or geometrical constraints, compaction and realignment of collagen fibrils occurred according to the local orientation of SMCs. Finally, even though at different rates, all the

lattices were compacted and reorganized by SMCs. This confirms that type B as well as type A lattices support tissue remodeling.

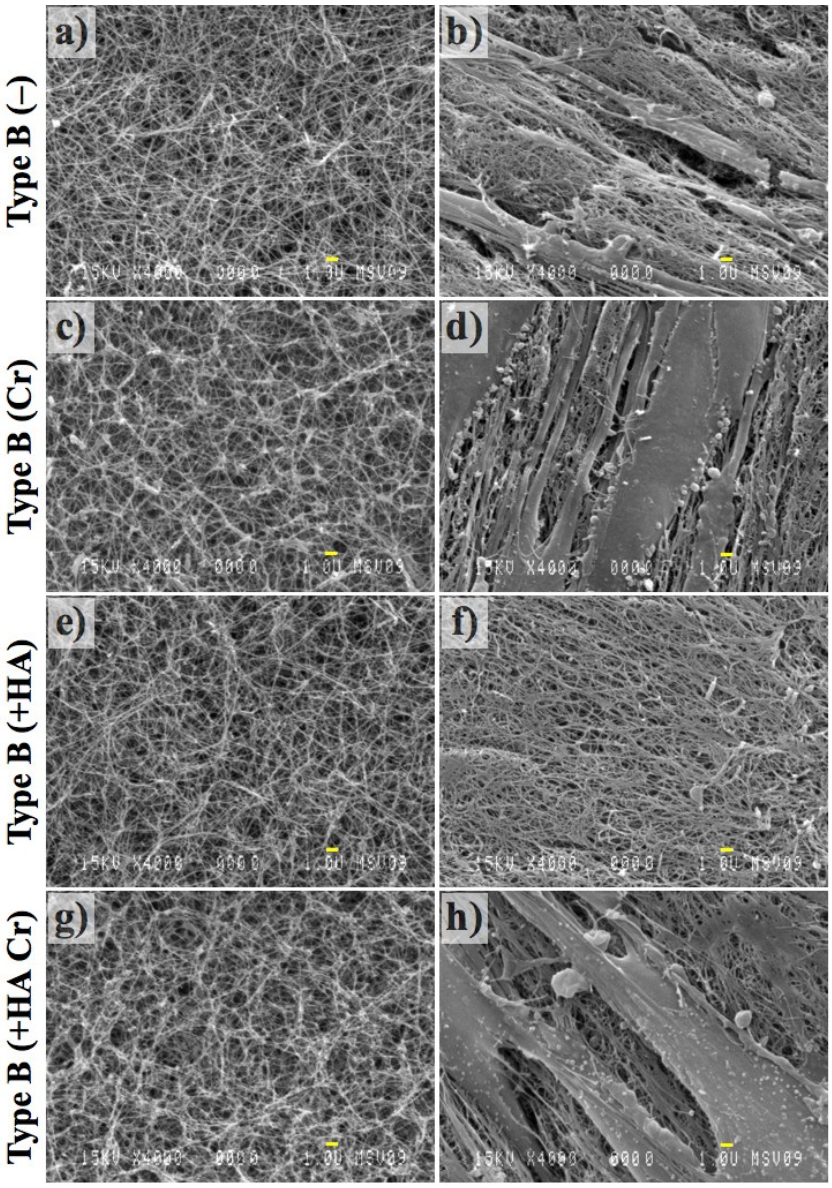

Figure 5.8: Micrographs (x4000) of type B lattices with the yellow bar representing 1 µm. Type B (–) (a) and type B (Cr) (c) lattices as before mechanical tests. Type B (–) (b) and type B (Cr) (d) lattices after 1 week of cell-mediated contraction. Type B (+HA) (e) and type B (+HA Cr) (g) lattices as before mechanical tests. Type B (+HA) (f) and type B (+HA Cr) (h) lattices after 1 week of cell-mediated contraction.

5.6 Conclusion

The present work investigated the potential of two different approaches for the generation of collagen gel-based MEs. MEs have to experience extensive cyclic conditioning and further manipulation before becoming TEBVs. It follows that they are required to show adequate mechanical properties in terms of strength and elasticity. The two approaches aimed to improve these properties by fostering cell-mediated remodeling or by combining crosslinking with an alternative procedure of collagen gelation.

The results show that it is possible to obtain collagen-based lattices with adequate strength in 24-48 hours. Moreover, EDC-mediated crosslinking increases the elasticity as shown by the decrease of hysteresis and permanent deformation, suggesting that these lattices may represent valid candidates for the production of MEs. Contraction tests and SEM confirm that both the approaches presented in this study support remodeling by SMCs.

Further developments would regard the evaluation of the mechanical properties as well as of lattice remodeling during cyclic conditioning in a bioreactor. At the same time, it would be interesting to investigate the contribution of cells to the mechanical behavior of MEs in response to circumferential stretching. These steps may lead to a mature ME and prelude to a fully functional TEBV.

5.7 Acknowledgements

We would like to thank *Élise Roussel*, at the *Centre de recherche de l'Institut universitaire de cardiologie et de pneumologie de* Québec, and *Betül Celebi*, at the *Laboratory for Biomaterials and Bioengineering*, for their kind help during the extraction of SMCs, and *Frédéric Couet* and *Bernard Drouin*, at the *Laboratory for Biomaterials and Bioengineering*, for their kind help in revising the article. We also acknowledge the *Canadian Bureau for International Education* (*CBIE*) for the award during the first year of Ph.D., the *Natural Science and Engineering Research Council of Canada*, the *Canadian Institutes for Health Research* and the *Centre Hospitalier Universitaire de Québec*, *Hopital Saint-François d'Assise* for partially funding this research.

CHAPTER 6. General Discussions and Conclusions

This chapter provides a conclusive overview on the results obtained in this doctoral project. The different sections recall the context and the rationale of the project, present the developments concerning the preparation of collagen gels, and resume and discuss the main findings concerning the modification of the microstructure and of the mechanical properties. Finally, the limits and the future perspectives are proposed.

6.1 Collagen Gels and VTE

It is generally accepted that a fully functional TEBV can be generated only through the maturation process of a vascular construct, i.e. a tubular assembly of vascular cells and endogenous and/or exogenous (e.g., scaffold material) molecules.[16,60,62] As a matter of fact, this construct can be initiated with or without a scaffold. In the case where a scaffolding material is used, it is required to present adequate mechanical and biological properties in order to support cell adhesion, proliferation, migration, and cell-mediated remodeling during the process of maturation. Regarding the biological properties, collagen represents an ideal material:

- It is a naturally occurring polymer and one of the main components of the ECM; consequently it is recognized by the cells, addressing their metabolism and functions.
- It self-assembles in vitro by opportunely setting the environmental conditions and can be shaped according to need.
- It can be remodeled in vitro and in vivo in presence of cells, fostering the regeneration of the targeted tissue.
- It is normally accepted and naturally degraded by hosts with very low risks of immune rejection or complications.

In vivo, several types of collagen are organized in highly hierarchical structures that determine the mechanical behavior of different tissues. Collagen has always attracted

researchers for being a natural scaffold. On the other hand, the mechanical profile of reconstituted collagen lattices has limited their applications and the enthusiasm about this material. The different mechanical behavior between collagen in vivo and reconstituted collagen is determined by the degree of structural organization and bonding between the supramolecular structures. Native tissues (e.g., bone, tendon, skin, blood vessels) are characterized by their anisotropic structure and mechanical properties, which are basically determined by the organization of collagen in fibrils and fibers and their alignment in the direction of preferential loading. This organization, in concomitance with the existing interactions at the molecular and supramolecular level, maximizes the contribution of collagen to the mechanical properties of the tissues. Even though the reconstituted fibrils that compose collagen gels are structurally identical to those observed in vivo, their random orientation, low density, and lack of inter-fibrillar crosslinks define the impaired mechanical properties.

In VTE, collagen gels are normally used as templates for the regeneration of the adventitia or the media. Notwithstanding the potential in promoting the formation of a tissue equivalent, the maturation of a vascular substitute becomes far less trivial. Even though proper compaction of the collagen gel may lead to important densification and realignment in a preferential direction, collagen aggregates still miss the covalent bonds that stabilize the lattice and switch the mechanical behavior from prevalently viscous to more elastic. Elastic recoil is not only a concern for the mature TEBV but also for the vascular construct that is subjected to mechanical conditioning. A vascular construct without recoil is destined to fail and the poor elasticity of reconstituted collagen gels is not encouraging. This outcome also derives from the way collagen gels are reconstituted. The dimensions and the degree of entanglements of reconstituted fibrils depend on the experimental conditions defined during the process of self-assembly. Considering that the most effective remodeling occurs when vascular cells are embedded in the lattice, researchers have mainly tried to reproduce the physiological conditions that foster cell-mediated remodeling. This approach leaves no possibility to modulate the experimental parameters and therefore to control the microstructure either. In addition, crosslinking becomes acceptable only in the presence of biological compounds that do not endanger normal cell metabolism.

As a result, for VTE applications, collagen gels and relative tissue equivalents have been often prepared in combination with supports that could preserve their integrity by minimizing the manipulation or by mediating mechanical solicitations. The wish for a completely biological, collagen gel-based tissue equivalent, with a mechanical profile that is adequate to the demands of cyclic conditioning, leads to the need of strengthening, stiffening, and reducing the viscous character of collagen gels. These objectives were addressed in this project substantially by modifying the microstructure of collagen lattices. This was achieved combining two techniques. The first consisting of optimizing the experimental conditions of collagen gelation, and the second involving the formation of crosslinking. Many of the effects of altered experimental conditions have been already addressed in previous investigations on collagen self-assembly and resulting microstructures. This project, in particular, extends the capability of tailoring the mechanical properties of collagen gels, as well as obtaining lattices with significantly improved strength and stiffness through a systematic study of the effects of the experimental conditions, and, most important, of the interactions between the different levels of these parameters. On the other hand, crosslinking treatments have been long investigated for their ability to increase the mechanical performances of collagen lattices; notwithstanding their effectiveness has been largely proven, their contribution alone was never considered sufficient to ensure the mechanical stability under cyclic conditioning. For what concerns the results obtained in this project, the chemical crosslinking carried out on the newly defined lattices proved to be particularly beneficial, most importantly in increasing the elastic recoil. The mechanical profile is then expected to be further improved by cell-mediated remodeling.

6.2 Developments of the Protocols for Collagen Gels

The protocol of collagen gel from which this project originated was developed by Boccafoschi et al.[154] The gel consisted of a blend of collagen (1.6 mg/ml), DMEM, $NaHCO_3$, sera, and cell suspension (2 x 10^6 SMCs / mL of gel). The protocol was conceived following the classical approach in VTE, i.e. optimize all the experimental conditions in order to maximize cell colonization and remodeling. From a mechanical point

of view, bare gels were particularly weak, impossible to manipulate without provoking liquid syneresis and changing the shape, difficult to mount and test in repeatable conditions, and presented low strength and no elasticity. The tissue equivalents derived embedding SMCs in these gels were obtained after 1 week of static culture and showed low strength (~ 18 mmHg) and low elasticity. It was clear that the properties of collagen lattices had to be considerably improved in order for them to be used as supporting templates under cyclic conditioning. A first improvement followed the increase of collagen concentration (2 mg/mL) in the gel. A further increase of collagen concentration was limited by the volume fraction available in the blend for the acid collagen solution and by the initial collagen concentration in this same solution (4 mg/mL): in fact, DMEM, sera, $NaHCO_3$, and culture medium occupied the 50 % of the total volume, leaving the other 50 % to the acid collagen solution (50 % x 4 mg/mL = 2 mg/mL). Further improvements were attempted through the modulation of pH and UV-C crosslinking as reported in the first article (Chap. 3). Both of these methods precluded the possibility to include cells in the gels from the beginning. In general, few methods are known to strengthen collagen gels in physiological conditions and in the presence of cells, including lysyl-oxidase mediated crosslinking – which requires cell transfection – transglutaminase-mediated crosslinking and glycation – which require long periods in culture to be effective and do not seem to provide outstanding improvements in terms of strength or elasticity – genipin-mediated crosslinking – which has generally been tested at room temperature and would deserve further investigation when applied in physiological conditions – and also fibril alignment by a strong magnetic field – which proved to be less effective than cell-mediated compaction.[92,112,118,244,278] On the other hand, cell-mediated compaction only partially increases the mechanical properties in the short term, while the concern about elasticity can be solved only with the maturation of the construct and the synthesis of elastin by the SMCs, an event that becomes significant in case of dynamic conditioning. These considerations lead to the choice of optimizing the mechanical properties of collagen gels before seeding cells. The modulation of pH and the introduction of UV-C crosslinking were the first attempts to modify the microstructure and introduce covalent bonds between neighboring fibrils. Even though improvements were shown, they were not sufficient to ensure the mechanical stability of collagen lattices under

cyclic conditioning, neither in terms of strength, nor in terms of recoil. The limits of these gels derive from the protocol of collagen gels and the concomitant mechanism of crosslinking as well as denaturation that characterizes UV-C crosslinking. Concerning the protocol of collagen gel, collagen was not concentrated enough, components like DMEM were not necessary in the absence of cells and the buffer contained in the culture medium complicated the modulation of pH; concerning UV-C crosslinking, this method was abandoned in successive studies because the formation of covalent bonds was counterbalanced by the cleavage of the collagen molecule, which determined a limited efficacy for this technique. The composition of collagen gels was then radically redefined, maintaining only the components that were strictly necessary to determine collagen self-assembly. Collagen concentration was increased (2.8 or 3.6 mg/mL), DMEM was replaced by a salt (NaCl) solution with the addition of a buffer (HEPES) in the case where gels were prepared at pH 7, and the weak base ($NaHCO_3$) was substituted with a strong one (NaOH) to minimize the volume fraction, the contribution to the ionic strength, and to widen the range of achievable pH. With these modifications, pH and ionic strength were easily modulated by varying the concentration of salts and bases or deciding for the presence of the buffer. Considering that the presence of amino acids or phosphates as contained in the DMEM would hinder the EDC-mediated crosslinking between collagen/collagen and collagen/GAG side groups, this simpler model supported the bond-formation between collagen and GAGs. Further modifications of the protocol for collagen gels consisted in introducing sodium carbonate (Na_2CO_3), in order to better stabilize the pH at 10 when required, as well as GAGs.

In addition, the protocol designed to embed cells into the gel was simplified: $NaHCO_3$ was replaced by NaOH, HEPES buffer was introduced to provide a better control of the pH, and the volume fraction reserved to the cell suspension was maximized. This protocol was designed mainly with the intent to validate the improvements in terms of mechanical properties of the gels obtained with optimized experimental conditions, and to compare the two different ways of combining collagen gel and vascular cells.

6.3 Modification of the Microstructure

Collagen gel microstructure was modified in two ways:

- By working on fibrils dimensions and interactions.
- By working on fibrils alignment and compaction via SMCs.

The first method is based on the modulation of the parameters that determine collagen self-assembly and result in isotropic lattices, while the second relies on SMCs' traction of collagen fibrils in the primary loading direction and produces highly anisotropic lattices. As shown in the third article (Chap. 5), cell-mediated compaction can be pursued on lattices formed according to the first method, so combining the advantages of the two approaches. Reversing the order of application of these procedures would benefit neither to cell-mediated remodeling – the modulation of the experimental condition endangering cell viability – nor to the optimization of the mechanical properties.

Several works report that the aspect ratio of collagen fibrils varies as a function of the experimental conditions, including pH, ionic strength, and temperature.[129,132,141] These effects have been related to the influence these parameters have on the interactions that drive collagen self-assembly.

Salt species, salt concentration and pH, all affect the electrostatic interactions that determine repulsion or attraction between side chains of collagen monomers in the same or different fibrils. Even though the reciprocal influence of ion species, ion concentration, and pH is quite complex, in general, an increase of pH or a decrease of ionic strength induce the formation of thinner fibrils. Higher ionic strength increases the solubility of collagen monomers according to the phenomenon of salting in, retarding fibril precipitation and favoring lateral aggregation, and so, the formation of thicker fibrils. On the other hand, a too high ionic strength may favor salting out and fast precipitation of collagen fibrils. The effect of pH depends on the isoelectric point, which in turn depends on salt type and concentration. In general, the solubility of a protein is lower at the isoelectric point, while at different pH collagen residues may result protonated (acid pH) or deprotonated (basic pH). It was proposed that fibrils formed at a more basic pH were thinner and stiffer because

more water molecules were expelled, while fibrils formed at an acidic pH were thicker for the higher hydration.[130] Other hypotheses suggest that a more basic pH may promote linear aggregation (longer and thinner fibrils) rather than lateral aggregation (shorter and thicker fibrils) through a mechanism in which deprotonation and electrostatic interactions between unusually charged amino acids favor end-to-end more than side-by-side interactions.[148]

Collagen self-assembly, as the folding of most proteins, is an entropy-driven process, in which collagen monomers assemble to minimize their free energy.[279] In particular, the free energy of collagen monomers is related to the presence of hydrophobic residues as well. When the temperature is increased, the entropy of the solvent increases and collagen monomers assemble to minimize the contact between water molecules and hydrophobic side chains. An increase of the temperature accelerates fibril precipitation, so limiting lateral aggregation and favoring the formation of thinner fibrils. The results from SEM images and turbidity measurements presented in the second article (Chap. 4) show that collagen fibrils formed in different conditions of pH, temperature, and ionic strength seem to follow the trends shown in previous reports.[129,130,132,140,141,144,147,148,153,157] In particular, at a higher pH, collagen fibrils appear thinner (Figure 4.2). As well, the turbidity values (Table 4.2) confirm that thinner fibrils were obtained at a lower ionic strength and higher temperatures. At the same time, higher precipitation rates were measured for higher temperatures, lower ionic strengths, and a pH closer to the isoelectric point.[131]

In conclusion, by lowering the temperature and increasing the ionic strength, the forces related to these parameters were reduced and collagen solubility and salting-in were favored against fibril formation. With the minimization of these forces, the effects of basic pH resulted increased as shown by the results from mechanical tests.

6.4 Collagen-GAG Blends and Crosslinking

GAGs are found in the form of HA or sulphated polysaccharides. Sulphated GAGs are associated to core proteins to form PGs. Part of the PGs (hyalectans) can form big agglomerates with HA, resulting highly hydrated and becoming responsible for the viscous

behavior of ECM and for the mechanical response under compression.[38,44] Another group of PGs (small leucine-rich PGs) influences the assembly of collagen fibrils and fibers as well as connects neighboring fibrils. In tissues like tendons, it was shown that these PGs play a complex role from the mechanical point of view, accounting for the viscous behavior of these tissues – related to their water content – and the stress transfer between connected structures.[26,48,109] These two types of PGs are also present in the ECM of blood vessels.

Several attempts to reproduce the entanglement between collagen and polysaccharidic chains as found in the native ECM implied the use of GAGs and collagen. GAGs do not have core proteins like PGs. Consequently they can spontaneously interact with collagen only through electrostatic interactions between the carboxyl groups present in the GAG chain and the protonated residues in the collagen molecule. These interactions are favored by an acidic pH or low ionic strength. In physiologic conditions, GAGs and collagen do not significantly interact to change the mechanical profile of the lattice. For these cases, several works attempted to stabilize collagen-GAG blends, obtained under different forms (sponge, gel), through covalent crosslinking. The most used methods are physical (e.g., thermal dehydration) or chemical (e.g., EDC-mediated crosslinking). EDC is a cytotoxic chemical agent that mediates zero-length crosslinks, i.e. the chemical agent or its derivatives are not incorporated in the lattice and can be washed away without leaving any trace in the lattice or concern for cell viability. The efficacy of EDC in forming amide bonds between carboxyl groups which are present in the GAG chains or in the collagen monomer (Asp or Glu) and amine residues (mainly Lys in the collagen molecule), resides on the number and proximity of reactive groups. These covalent bonds are formed between collagen-collagen or collagen-GAG side groups. The most used GAG is CS, but also HA has been applied with success.[199-202,210-215,218-220] The presence of both of these GAGs in the blood vessel wall suggests that collagen-GAG blends may complete collagen lattices from a structural and biological point of view. Chemical crosslinking is generally proven to stiffen collagen lattices and increase the ultimate stress.[111] Results from the third article (Chap. 5) show that crosslinked lattices are stiffer but present a lower ultimate tensile stress: this is determined by the different mechanical behavior and the different type of break that the samples experience. While in non-crosslinked samples, collagen fibrils slide past each other

and the reorganization of the lattice leads to liquid syneresis, plastic deformation and rupture, in crosslinked samples the lattice is minimally reorganized as shown by the brittle break. In other words, non-crosslinked samples were able to absorb a higher stress by viscous deformation, while viscosity and the capability to absorb stress were reduced in crosslinked samples.

The introduction of HA and the consequent reduction of collagen concentration do not appear particularly beneficial from a mechanical point of view but may present potential in promoting cell-mediated remodeling under cyclic conditioning.

UV-C crosslinking stiffens collagen lattices but, as EDC crosslinking, it depends on the number and proximity of reactive groups, which in this case are the aromatic side chains of Phenylalanine or Tyrosine. In addition, UV-C radiation induces cleavage and denaturation of the collagen molecules, therefore reducing the advantages that come with increasing UV-C doses to obtain higher crosslinking. This conformational change in part of the collagen content may explain the different proliferation rate of fibroblasts seeded on irradiated and non-irradiated collagen gels.

6.5 Mechanical Behavior

As shown and discussed by several authors, collagen gels and derived tissue equivalents present a non-linear, viscoelastic behavior similar to the one of biologic tissues, characterized by viscous dissipation and loop hysteresis under cyclic loading.[32,155,170,172] This is due to similarities in the structure and components of these lattices, mainly constituted by fibrous proteins and the entrapped viscous fluid. On the other hand, the contribution of each component depends on the state of aggregation and organization, not considering that native tissues are normally richer in ECM molecules than tissue equivalents. Consequently, even though the shape of the mechanical curve is similar, strength, stiffness, elasticity, and the type of break may differ considerably. Collagen lattices present a mechanical behavior that is time dependent. In particular it depends on the length and the rate of application of the load. This is a consequence of the viscous dissipation that occurs when the fluid flows through the lattice, and fibrils slide past each

other in response to a mechanical solicitation.[170] Lower the amount and strength of the interactions between fibrils, and the more accentuated this behavior is.

Testing the mechanical properties of collagen gels was particularly problematic at the beginning of this project because of their very low strength, low water retention, and thus low capacity to retain the original shape. These gels couldn't be handled, so they were tested in the moulds were they were set, and in this case with a hybrid compression-indentation test. This test was particularly helpful because it ensured repeatable measurements on gels that couldn't be extracted from moulds for tensile or unconfined compression tests without compromising their integrity. Three different regions were distinguished in the curve of the mechanical properties, which are consistent with the study of Davidenko et al.[199]

Mechanical tests evolved with the mechanical properties of collagen lattices: In fact, the optimization of the experimental conditions lead to gels stiff enough to be tested through ring tests and unconfined compression. In the first two articles, collagen gels were tested at room temperature and in a dry environment, while in the third article samples were tested in a thermo-regulated bath with PBS, in order to mimic the environmental conditions of pH, temperature and ionic strength experienced by vascular constructs during the maturation process.

The stiffness and the strength of collagen gels were increased throughout the three articles by increasing collagen concentration (from 1.6 to 3.6 mg/mL), the pH (from 7 to 10), and by decreasing the gelation temperature (from 37 to 4 ºC). In the particular condition of gel prepared at a pH of 10 and at 4 ºC, the increase of the ionic strength lead to higher mechanical properties (~ 4-fold) and resulted particularly interesting as a parameter by which to regulate the process and length of collagen self-assembly. As previously reported, when self-assembly is carried out in basic conditions, fibrils result thinner and longer, with an important contribution to the bulk mechanical properties of the lattice.[132,141] It has been proposed that the slenderness (or aspect ratio, i.e. the length-diameter ratio) of the fibrils, more then their diameter, is important in conferring strength and toughness to the lattice.[127,280] A high length-diameter ratio implies a higher total area exposed for the same

concentration of collagen: in this way more inter-fibril interactions are possible and the stress transfer becomes more effective. By reducing the influence of temperature and ionic strength on collagen precipitation, fibril formation was mostly driven by the interactions related to the basic pH: In this case, the formation of longer, thinner fibrils was promoted and the mechanical properties sensibly increased as shown in Figure 4.4-b.

In the first article (Chap. 3), the time-dependent behavior of collagen gels was tested by increasing the compression rate, with the stiffness increasing proportionally.

In the third article (Chap. 5), collagen lattices were subjected to cyclic loading: The presence of loop hysteresis as well as of the plastic deformation before a break confirmed that samples were experiencing creep deformation and viscous dissipation through the sliding of collagen fibrils past each other. The introduction of crosslinking in gels obtained by opportunely setting the experimental conditions, reduced the hysteresis and the permanent deformation, thus suggesting that the elastic recoil could be pursued by fixing neighboring fibrils with covalent bonds and by hindering the viscous slippage. The idea of increasing the elastic character of collagen lattices by crosslinking treatments was investigated, but with different preparation methods, by Yunoki et al.[281] They obtained highly elastic lattices by crosslinking and shrinking. The method proposed by these authors and the one presented in this project show that opportunely prepared collagen lattices can stand cyclic conditioning with low permanent deformation and a reduced risk of mechanical failure.

Alternatively, tissue equivalents' mechanical properties were increased by fostering cell-mediated realignment of collagen fibrils (Chap. 5).

6.6 Cell Viability and Remodeling

Collagen-based scaffolds are particularly attractive for how easy cells recognize the substrate and thus remodel the surroundings. In the past, collagen has often been preferred to synthetic materials for reasons related to these biological properties, which should be preserved by the methods employed to increase the mechanical properties. In this work, the mechanical properties of collagen gels have been increased by different means and the

capacity of cells to adhere, proliferate, or remodel the lattice has been assessed in order to establish the potential of each technique. Vascular cells (fibroblast or SMCs) proved to adhere on all the collagen gels. The modulation of the experimental conditions neither affected the proliferation nor prevented cell-mediated remodeling as shown in the second and third article (Chap. 4-5). The rate of remodeling depends on the degree of stability of the lattice and, as expected, was lower in gels that were stiffened by EDC crosslinking. Collagen substrate crosslinked by UV-C treatments elicited a lower rate of proliferation, the reason probably related to the conformational changes of the collagen triple helix. In general, all the techniques exploited to change the mechanical profile of collagen gels preserved the biological properties, even though EDC crosslinking is preferred compared to UV-C irradiation for the lack of secondary effects on collagen lattices. The potential of collagen gels to be remodeled and form tissue equivalents has been confirmed both in the case of cells embedded in the gels and in the case of cells seeded on the top. In particular, SMCs embedded in collagen gels showed a particular ease in reorganizing collagen fibrils as was shown by the fast compaction (~ 24 h) and rapid increase of the mechanical properties.

6.7 Limits of the Project

This project succeeded in increasing the strength, stiffness and elasticity of collagen gels, motivating the idea that collagen gels may be able to support cell-mediated remodeling under cyclic loading. Nonetheless, some fundamental points were not addressed and should be investigated further before assessing that the collagen lattices developed in this project will successfully support the regeneration of a fully functional TEBV. These points may be resumed as follows:

- Even though collagen gels formed by modulating the experimental parameters and crosslinked with EDC (Article 3, Chap. 5) showed an improved recoil that let suppose their mechanical stability under cyclic loading, this hypothesis was formulated following tests of one hundred cycles maximum and should be proved under a long-term conditioning. Moreover, the evolution under cyclic conditioning should be evaluated while promoting cell-mediated remodeling. This could affect

the mechanical behavior for mainly two reasons: firstly, living cells affect the bulk mechanical properties by actively contracting in response to traction or passively by working as junction between neighboring fibrils; secondly, living cells, moreover under mechanical conditioning, tend to remodel the microstructure and so modify the bulk mechanical properties as well.

- It should be confirmed that the maturation of collagen gels as developed in the third article – seeded with SMCs on the top – results in tissue equivalents with the mechanical and histological features of the medial layer. Moreover, this maturation process is far from being trivial and the proper definition of the culture conditions (e.g., use of supplements) would deserve more attention and investigation.
- Cell-mediated remodeling strongly depends on the features of cells used, including their type, phenotype, species and age of the source. While in this project murine and porcine cell types were used, from a clinical point of view, the potential of collagen lattices for tissue regeneration should be evaluated with human cells, paying particular attention to the influence of the age and conditions of the donor.
- This project focused on the development of a tissue equivalent mimicking the medial layer; nonetheless, the process that leads to the formation of the two remaining arterial layers should be defined and validated.

6.8 Future Perspectives

This project opens new possibilities in the use of collagen gels as scaffolds for the regeneration of the vascular tissue, yet leaves some questions to be answered in the future. In particular, a necessary step will be the validation of these lattices under extensive mechanical conditioning, following the remodeling by vascular cells. The mechanisms that trigger the desired cellular functions should be defined, in particular as:

- The proper mechanical conditioning in order to promote matrix remodeling and synthesis of the ECM components that are fundamental for the correct functioning of TEBVs – first of all elastin.

- The correct mix of chemicals, including growth supplements, cytokines, etc.

In addition, further studies may clarify the effects of different cellular origins and types, for example with the intent to exploit the great potential of progenitor and stem cells.

Concerning the starting composition of collagen gel-based scaffolds, other blends may be investigated: For example it would be interesting to include soluble elastin, not only to accentuate the elastic character of the resulting blend, but even to regulate cell phenotype.

The modulation of the experimental parameters and of the gelation rate may be used to affect not only the aspect ratio and the interactions of collagen fibrils, but even their distribution: the second article (Chap. 4) shows that gelation can be retarded by increasing the ionic strength or decreasing the temperature. This modulation may be associated to techniques (application of magnetic or electric fields) for the alignment of collagen fibrils and may result in higher mechanical properties in preferential directions. Fibril alignment by different means and consequent effects on cell behavior by contact guidance have been a matter of interest for different groups, attracted by the potential of regulating mechanical and biological aspects of the construct.[63,282,283]

The mechanical properties of collagen lattices whose fibrils have been realigned by cell-mediated compaction may know further improvements in terms of mechanical properties by the introduction of crosslinking treatments. In this case, the increased density of the lattice and the increased proximity between different fibrils would greatly increase the efficacy of the crosslinking treatment: More covalent bonds would be formed between neighboring fibrils, therefore lowering the possibility for collagen fibrils to slide past each other and increasing the contribution of the fibrils stretching to the stiffness of the lattice. Chemical crosslinking would imply cellular death, a case in which cells would be seeded again on the top of the lattice once the crosslinking is completed; otherwise natural compounds (e.g., genipin) may be used in order to ensure cell survival during the corsslinking process. The latter case needs further understanding on the ways natural compounds can be used in physiological conditions.

In conclusion, collagen gels prepared under opportunely defined experimental conditions prove to suit a wider range of applications in terms of mechanical requirements. With the addition of crosslinks, they may constitute the missing link between the attractiveness of collagen gels in the formation of tissue equivalents and their application under cyclic conditioning for the regeneration of the vascular tissues. The profile of these lattices could be further improved and enriched from the mechanical and biological point of view, and the proper modulation of vascular cells phenotype and ECM synthesis may determine the successful formation of vessel substitutes.

Appendix

This compendium is meant to complete the information given in Chapter III, IV, and V regarding the parameters and the protocols that were used for the mechanical characterization. Considering the wide range of bulk properties of collagen gel samples and the lack of specific standardization for testing these materials, the authors felt free to choose the test conditions and the type of data analysis without referring to any standard. Each section refers to a different scientific article. All the tests were carried out with an Instron 5848 Microtester (Instron Corporation, Norwood, MA, USA) at the Laval University. Data acquisition and pre-elaboration were supported by the Merlin software package. Data were then elaborated – re-sampling, differentiation, integration, mean and StD, etc. – with algorithms that were specifically defined for each test. These algorithms were designed in the Matlab R2009 programming environment (MathWorks, Natick, MA, USA).

A.1 Mechanical Testing in the First Article (Chapter III)

Samples were tested in a compression test mode. Disk-shaped gels (ø = 32 mm, height = 3.8 mm) were confined on the sides and on the bottom by the Petri dishes (i.d. = 32 mm) and were compressed by a circular plate (ø = 20 mm) that was fixed to a 5 N load cell (**Figure A.1**).

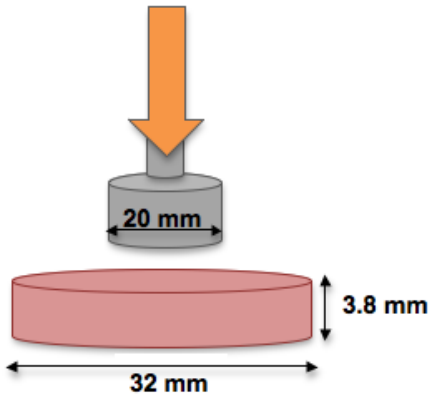

Figure A.1: Setup for compression test in the first article.

Tests were carried out at three different compression rates: 0.1, 1 and 10 mm/min. Samples were tested at room temperature, in contact with air, without mechanical preconditioning and with a single compression run. Compression rates were chosen according preliminary experiments. Results were expressed in terms of stress/strain and stiffness/strain where the stiffness is defined by Equation 3.3. The stress/strain and the stiffness/strain behaviors are shown in Figure 3.3. As reported in Chap. 3, the stiffness was calculated in the region that was considered more representative of the bulk properties of the gels.

Here reported the algorithm designed for data analysis:

```
%definizione variabili
passo=0.2; %passo di campionamento
gp=5; %grado polinomio interpolante
nc=54;%numero campioni
rc=1; %cm, raggio del piatto di compressione
ac=(rc)^2*pi; %cm^2, area del piatto di compressione
%lettura da file, eliminazione ripetizioni, determinazione deformazione
%percentuale
Fd=[];
for k=1:nc
   fd=fopen([num2str(k),'.dat'],'r+');
   Fd=[Fd fd];
end
%definizione della deformazione percentuale massima per campionamento
temp=[];
for k=1:nc
   ve=fscanf(Fd(k),'%g %g',[2 inf]);
   ve=ve';
   temp=[temp max((1-(ve(:,1)/ve(1,1)))*100)];
end
dmx=min(temp);
df_p=[0:passo:dmx];
def=df_p';
%campionamento, media, errore standard e derivata
Dati=[]; %matrice con tutti i dati campionati
iDati=[]; %mattrice cont tutti i dati interpolati (vettori dei coefficienti di interpolazione)
mDati=[]; %matrice con media dei dati (sulle tre ripetizioni)
eDati=[]; %matrice con gli errori delle medie
dDati=[]; %matrice con le derivate delle inerpolazioni di tutti i dati
```

```
mdDati=[]; %matrice con le medie delle derivate
edDati=[]; %matrice con gli errori delle medie delle derivate
dati=[]; %vettore provvisorio di immagazzinamento
po=[];  %vettore provvisorio di immagazzinamento delle interpolazioni
Fd=[];
for k=1:nc
   fd=fopen([num2str(k),'.dat'],'r+');
   Fd=[Fd fd];
end
for k=1:nc
   vet=fscanf(Fd(k),'%g %g',[2 inf]);
   vet=vet';
   k2=1;
   while k2<length(vet);
      if vet(k2,1)==vet(k2+1,1)
         vet(k2,:)=[];
      end
      k2=k2+1;
   end
   v1=(1-(vet(:,1)/vet(1,1)))*100;
   v2=-vet(:,2)*10/ac; %qui decido di mettere tutto in kPa
   dati=interp1(v1,v2,def,'spline');
   Dati=[Dati dati];
   po=polyfit(def,dati,gp);
   iDati=[iDati po'];
   dDati=[dDati (polyval(polyder(po),df_p))'];
end
for k=1:3:nc
   M=[];
   dM=[];
   for k1=k:k+2
      M=[M;Dati(:,k1)'];
      dM=[dM;dDati(:,k1)'];
   end
   mDati=[mDati (mean(M))'];
   eDati=[eDati (std(M))'];
   mdDati=[mdDati (mean(dM))'];
   edDati=[edDati (std(dM))'];
end
Dicitura=[7.5 7.5 7.5 7.5 7.5 7.5 7.5 7.5 7.5 10 10 10 10 10 10 10 10 10;0.1 0.1 0.1 1 1 1 10 10 10 0.1 0.1 0.1 1 1 1 10 10 10;0 35 70 0
35 70 0 35 70 0 35 70 0 35 70 0 35 70];
```

```
Salv=[7 7 7 7 7 7 7 7 7 10 10 10 10 10 10 10 10 10;0 0 0 1 1 1 10 10 10 0 0 0 1 1 1 10 10 10;0 35 70 0 35 70 0 35 70 0 35 70 0 35 70 0 35 70];

cont=nc/3;

%per test statistici

pro=[];

for k=1:3:nc

   pro=[pro [vmd(k);vmd(k+1);vmd(k+2)]];

end

for k=1:cont-1

   for k1=k+1:cont

      testt(pro(:,k),pro(:,k1))

      k

      k1

   end

end

%vmd rappresenta la variabile dipendente, le variabili indipendenti sono

%UVc, pH e velocit‡ di compressione

pH=[7.5 7.5 7.5 7.5 7.5 7.5 7.5 7.5 7.5 7.5 7.5 7.5 7.5 7.5 7.5 7.5 7.5 7.5 7.5 7.5 7.5 7.5 7.5 7.5 7.5 7.5 7.5 7.5 7.5 7.5 10 10 10 10 10 10 10 10 10 10 10 10 10 10 10 10 10 10 10 10 10 10 10 10 10 10 10 10 10 10];

UVc=[0 0 0 35 35 35 70 70 70 0 0 0 35 35 35 70 70 70 0 0 0 35 35 35 70 70 70 0 0 0 35 35 35 70 70 70 0 0 0 35 35 35 70 70 70 0 0 0 35 35 35 70 70 70 ];

velo=[0.1 0.1 0.1 0.1 0.1 0.1 0.1 0.1 0.1 1 1 1 1 1 1 1 1 1 10 10 10 10 10 10 10 10 10 0.1 0.1 0.1 0.1 0.1 0.1 0.1 0.1 0.1 1 1 1 1 1 1 1 1 1 10 10 10 10 10 10 10 10 10];

anovan(vmd,{pH UVc velo},3);

vmd2=vmd;

pH2=pH;

UVc2=UVc;

velo2=velo;

cn=nc;

k=1;

while k<=cn

   if UVc2(k)==35

      UVc2(k)=[];

      pH2(k)=[];

      velo2(k)=[];

      vmd2(k)=[];

      cn=cn-1;

   else k=k+1;

   end

end

anovan(vmd2,{pH2 UVc2 velo2},3);
```

The influence of the boards of the Petri dish was investigated by testing the same gels in Petri dishes with different diameters: 35 mm and 60 mm. No differences were found, thus indicating that the results were not affected by the choice of the diameter of the dish.

A.2 Mechanical Testing in the Second Article (Chapter IV)

Cylindrical samples (ø = 11 mm, height = 5.5 mm) were tested in compression mode with a circular plate (ø = 20 mm) attached to a 5 N load cell. Samples were preconditioned with three cycles (0 - 2%) and tested in contact with air at 0.2 mm/s and room temperature (**Figure A.2**).

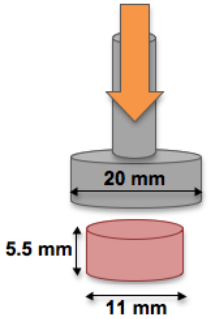

Figure A.2: Setup for compression tests in the second article.

Compressive modulus (CM) and compressive strain energy (CSE) were defined as reported in Chapter IV. The following code was defined for data analysis.

```
%Algoritmo per l'elaborazione dei dati da test di compressione
passo=0.01; %passo di campionamento (=strain mm/mm)
gp=5; %grado polinomio interpolante
ntrat=2*3*7;%numero trattamenti
nc=94;%numero campioni
%dc=0.011;
%rc=0.01; %[m], raggio del piatto di compressione
%ac=(rc)^2*pi;%[m^2], area del piatto di compressione
%conv=(1/ac)/1000;% da N in KPa
lsi=0.15;%limite stiffness inferiore
lss=0.3;%limite stiffness superiore
lii=0;%limite integrale inferiore
lis=0.4;%limite integrale superiore
lLMi=0.15;%limite inferiore per il calcolo del Linear Modulus
```

```
lLMs=0.3;%limite superiore per il calcolo del Linear Modulus
%lettura da file, eliminazione ripetizioni, determinazione deformazione
%DATA:
%riga1: nome trattamento
%riga2: # campione
%riga3: dati in mm e N per tutti i campioni
%riga4: dati in strain e stress(kPa)
%riga5: matrice a 3 colonne con def, medie, StD
%riga6: vettore coefficienti di interpolazione grado 5
%riga7: parametro di errore dell'interpolazione grado 5
%riga8: vettore derivata
%riga9: derivate e StD derivate
%riga10: vettore integrale
%riga11: integrale tra estremi definiti diviso l'intervallo di integrazione
%riga12: media e StD integrale per ogni trattamento
%riga13: coefficiente angolare della retta di interpolazione nella regione
%di interesse per tutti i campioni
%riga14: media e StD coefficiente angolare della retta di interpolazione nella regione
%di interesse per ogni trattamento
%riga15: vettore coefficienti di interpolazione grado 1 (regressione)
%riga16: parametro di errore dell'interpolazione grado 1
%riga17: retta di interpolazione: vettore, x:0:30 in funzione dei coeff. di
%interpolazione grado 1
%riga18: media delle derivate tra lsi (limite stiffness inf) e lss per ogni
%campione
%riga19: media delle medie delle derivate nella regione di interesse e StD
DATA=cell(19,nc);
for c=1:nc
   DATA{2,c}=num2str(c);
   switch c
      case {1,2}
         DATA{1,c}={'4C' '80mM' 'pH7'};
      case {3,4}
         DATA{1,c}={'4C' '80mM' 'pH10'};
      case {5,6,7}
         DATA{1,c}={'4C' '100mM' 'pH7'};
      case {8,9,10}
         DATA{1,c}={'4C' '100mM' 'pH10'};
      case {11,12,13}
         DATA{1,c}={'4C' '120mM' 'pH7'};
      case {14,15,16}
```

```
    DATA{1,c}={'4C' '120mM' 'pH10'};
case {17,18,19}
    DATA{1,c}={'4C' '140mM' 'pH7'};
case {20,21}
    DATA{1,c}={'4C' '140mM' 'pH10'};
case {22,23,24}
    DATA{1,c}={'4C' '160mM' 'pH7'};
case {25,26,27}
    DATA{1,c}={'4C' '160mM' 'pH10'};
case {28,29}
    DATA{1,c}={'4C' '180mM' 'pH7'};
case {30,31,32}
    DATA{1,c}={'4C' '180mM' 'pH10'};
case {33,34,35}
    DATA{1,c}={'4C' '200mM' 'pH7'};
case {36,37,38}
    DATA{1,c}={'4C' '200mM' 'pH10'};
case {39,40}
    DATA{1,c}={'21C' '80mM' 'pH7'};
case {41,42}
    DATA{1,c}={'21C' '80mM' 'pH10'};
case {43,44}
    DATA{1,c}={'21C' '100mM' 'pH7'};
case {45,46}
    DATA{1,c}={'21C' '100mM' 'pH10'};
case {47,48}
    DATA{1,c}={'21C' '120mM' 'pH7'};
case {49,50}
    DATA{1,c}={'21C' '120mM' 'pH10'};
case {51,52}
    DATA{1,c}={'21C' '140mM' 'pH7'};
case {53,54}
    DATA{1,c}={'21C' '140mM' 'pH10'};
case {55,56}
    DATA{1,c}={'21C' '160mM' 'pH7'};
case {57,58}
    DATA{1,c}={'21C' '160mM' 'pH10'};
case {59,60}
    DATA{1,c}={'21C' '180mM' 'pH7'};
case {61,62}
    DATA{1,c}={'21C' '180mM' 'pH10'};
```

```
        case {63,64}
            DATA{1,c}={'21C' '200mM' 'pH7'};
        case {65,66}
            DATA{1,c}={'21C' '200mM' 'pH10'};
        case {67,68}
            DATA{1,c}={'37C' '80mM' 'pH7'};
        case {69,70}
            DATA{1,c}={'37C' '80mM' 'pH10'};
        case {71,72}
            DATA{1,c}={'37C' '100mM' 'pH7'};
        case {73,74}
            DATA{1,c}={'37C' '100mM' 'pH10'};
        case {75,76}
            DATA{1,c}={'37C' '120mM' 'pH7'};
        case {77,78}
            DATA{1,c}={'37C' '120mM' 'pH10'};
        case {79,80}
            DATA{1,c}={'37C' '140mM' 'pH7'};
        case {81,82}
            DATA{1,c}={'37C' '140mM' 'pH10'};
        case {83,84}
            DATA{1,c}={'37C' '160mM' 'pH7'};
        case {85,86}
            DATA{1,c}={'37C' '160mM' 'pH10'};
        case {87,88}
            DATA{1,c}={'37C' '180mM' 'pH7'};
        case {89,90}
            DATA{1,c}={'37C' '180mM' 'pH10'};
        case {91,92}
            DATA{1,c}={'37C' '200mM' 'pH7'};
        case {93,94}
            DATA{1,c}={'37C' '200mM' 'pH10'};
    end
end
for t=1:nc
    temp=csvread([num2str(DATA{2,t}),'.raw']);
    temp=[temp(:,2),temp(:,4)];
    c=1;
    temp1=[];
    while temp(c,2)>min(temp(:,2))
        if ((temp(c,2)<0)&&(temp(c,1)<=temp(1,1)))
```

```
        temp1=[temp1;temp(c,:)];
    end
    c=c+1;
end
temp=temp1;
c=1;
while c<length(temp(:,1));
    if (temp(c,1)==temp(c+1,1))||(temp(c,2)==temp(c+1,2))
        temp(c,:)=[];
        c=c-1;
    end
    c=c+1;
end
DATA{3,t}=temp;
%switch t
    %case {1,2,3,4,5,6,7,8,9,10,11,12,13,14,15,16,17,18}
        dc=0.011;
    %case {19,20,21,22,23,24,25,26,27}
        %dc=0.016;
%end
ac=(dc/2)^2*pi;
conv=(1/ac)/1000;
temp=[1-(temp(:,1)/temp(1,1)),(-temp(:,2)*conv)];%vettore in strain (mm/mm) e in kPa
%verifica che non ci siano ripetizioni creati dal Merlin
c=1;
while c<length(temp(:,1));
    if (temp(c,1)==temp(c+1,1))
        temp(c,:)=[];
    else c=c+1;
    end
end
def=((round(min(temp(:,1))*1000)/1000):passo:(round(max(temp(:,1))*1000)/1000))';
temp=[def,interp1(temp(:,1),temp(:,2),def,'spline')];
DATA{4,t}=temp;
po=[];
c=1;
temp1=[];
while temp(c,2)<max(temp(:,2))
    temp1=[temp1;temp(c,:)];
    c=c+1;
end
```

```
    [po,S]=polyfit(temp1(:,1),temp1(:,2),gp);
    DATA{6,t}=po;
    DATA{7,t}=S;
    DATA{8,t}=[temp1(:,1),(polyval(polyder(po),temp1(:,1)))];
    temd=[temp1(:,1),(polyval(polyder(po),temp1(:,1)))];
    temdm=[];
    for c=((lsi*100)-1):(passo*100):((lss*100)-1)
        temdm=[temdm,temd(c,2)];
    end
    DATA{18,t}=mean(temdm);
    DATA{10,t}=polyint(po);
    DATA{11,t}=polyval(polyint(po),lis)-polyval(polyint(po),lii);
    xLM=(lLMi:passo:lLMs)';
    yLM=interp1(temp1(:,1),temp1(:,2),xLM);
    [LM,LMe]=polyfit(xLM,yLM,1);%calcolo Linear Modulus
    DATA{13,t}=LM(1);
end
DatiAnova=[];
Res=zeros(ntrat,6);
k=1;% questo tratto dell'algoritmo conta sul fatto che ripetizioni dello stesso trattamento si susseguano nella matrice DATA
while k<=nc
    temp=DATA{4,k};
    temd=DATA{8,k};
    de=temp(:,1);
    dd=temd(:,1);
    M=temp(:,2);
    Md=temd(:,2);
    Mi=DATA{11,k};
    MLM=DATA{13,k};
    stiff=DATA{18,k};
    c=k+1;
    while strcmp(DATA{1,c},DATA{1,k})
        temp1=DATA{4,c};
        temd1=DATA{8,c};
        Mi=[Mi,DATA{11,c}];
        MLM=[MLM,DATA{13,c}];
        stiff=[stiff,DATA{18,c}];
        det=(max(de(1,1),temp1(1,1)):passo:min(max(de(:,1)),max(temp1(:,1))))';
        M=[interp1(de,M,det),interp1(temp1(:,1),temp1(:,2),det)];
        de=det;
        ddt=(max(dd(1,1),temd1(1,1)):passo:min(max(dd(:,1)),max(temd1(:,1))))';
```

```
        Md=[interp1(dd,Md,ddt),interp1(temd1(:,1),temd1(:,2),ddt)];
        dd=ddt;
         c=c+1;
         if c>nc
            break
         end
    end
    xm=de;
    ym=mean(M,2);
    em=std(M,0,2);
    xd=dd;
    yd=mean(Md,2);
    ed=std(Md,0,2);
    DatiAnova=[DatiAnova;Mi',MLM',stiff'];
    DATA{5,k}=[xm,ym,em];
    DATA{9,k}=[xd,yd,ed];
    DATA{12,k}=[mean(Mi),std(Mi)];
    DATA{14,k}=[mean(MLM),std(MLM)];
    xr=(lLMi:passo:lLMs)';
    yr=interp1(xm,ym,xr);
    [pr,Sr]=polyfit(xr,yr,1);
    DATA{15,k}=pr;
    DATA{16,k}=Sr;
    DATA{19,k}=[mean(stiff),std(stiff)];
    Res(k,:)=[mean(Mi),std(Mi),mean(MLM),std(MLM),mean(stiff),std(stiff)];
       k=c;
end
NomeDati=cell(nc,1);
pH=cell(nc,1);
T=cell(nc,1);
IS=cell(nc,1);
nf=3;
tio=cell(1,nf);
for k=1:nc
    NomeDati{k,1}=DATA{1,k};
    tio=DATA{1,k};
    T{k,1}=tio{1,1};
    IS{k,1}=tio{1,2};
    pH{k,1}=tio{1,3};
end
Rep=cell(nc,1);
```

```
rip=1;
Rep{1,1}=rip;
for k=2:nc
    if strcmp(NomeDati{k,1},NomeDati{k-1,1})
        rip=rip+1;
    else rip=1;
    end
    Rep{k,1}=rip;
end
for c=1:nc
    if strcmp(NomeDati{c,1},'4C-80mM-pH7')
            T{c,1}='4';
            IS{c,1}='80';
            pH{c,1}='7';
    elseif strcmp(NomeDati{c,1},'4C-80mM-pH10')
            T{c,1}='4';
            IS{c,1}='80';
            pH{c,1}='10';
        elseif strcmp(NomeDati{c,1},'4C-100mM-pH7')
            T{c,1}='4';
            IS{c,1}='100';
            pH{c,1}='7';
        elseif strcmp(NomeDati{c,1},'4C-100mM-pH10')
            T{c,1}='4';
            IS{c,1}='100';
            pH{c,1}='10';
        elseif strcmp(NomeDati{c,1},'4C-120mM-pH7')
            T{c,1}='4';
            IS{c,1}='120';
            pH{c,1}='7';
        elseif strcmp(NomeDati{c,1},'4C-120mM-pH10')
            T{c,1}='4';
            IS{c,1}='120';
            pH{c,1}='10';
        elseif strcmp(NomeDati{c,1},'4C-140mM-pH7')
            T{c,1}='4';
            IS{c,1}='140';
            pH{c,1}='7';
        elseif strcmp(NomeDati{c,1},'4C-140mM-pH10')
            T{c,1}='4';
            IS{c,1}='140';
```

```
    pH{c,1}='10';
elseif strcmp(NomeDati{c,1},'4C-160mM-pH7')
    T{c,1}='4';
    IS{c,1}='160';
    pH{c,1}='7';
elseif strcmp(NomeDati{c,1},'4C-160mM-pH10')
    T{c,1}='4';
    IS{c,1}='160';
    pH{c,1}='10';
elseif strcmp(NomeDati{c,1},'4C-180mM-pH7')
    T{c,1}='4';
    IS{c,1}='180';
    pH{c,1}='7';
elseif strcmp(NomeDati{c,1},'4C-180mM-pH10')
    T{c,1}='4';
    IS{c,1}='180';
    pH{c,1}='10';
elseif strcmp(NomeDati{c,1},'4C-200mM-pH7')
    T{c,1}='4';
    IS{c,1}='200';
    pH{c,1}='7';
elseif strcmp(NomeDati{c,1},'4C-200mM-pH10')
    T{c,1}='4';
    IS{c,1}='200';
    pH{c,1}='10';
elseif strcmp(NomeDati{c,1},'21C-80mM-pH7')
    T{c,1}='21';
    IS{c,1}='80';
    pH{c,1}='7';
elseif strcmp(NomeDati{c,1},'21C-80mM-pH10')
    T{c,1}='21';
    IS{c,1}='80';
    pH{c,1}='10';
elseif strcmp(NomeDati{c,1},'21C-100mM-pH7')
    T{c,1}='21';
    IS{c,1}='100';
    pH{c,1}='7';
elseif strcmp(NomeDati{c,1},'21C-100mM-pH10')
    T{c,1}='21';
    IS{c,1}='100';
    pH{c,1}='10';
```

```
elseif strcmp(NomeDati{c,1},'21C-120mM-pH7')
    T{c,1}='21';
    IS{c,1}='120';
    pH{c,1}='7';
elseif strcmp(NomeDati{c,1},'21C-120mM-pH10')
    T{c,1}='21';
    IS{c,1}='120';
    pH{c,1}='10';
elseif strcmp(NomeDati{c,1},'21C-140mM-pH7')
    T{c,1}='21';
    IS{c,1}='140';
    pH{c,1}='7';
elseif strcmp(NomeDati{c,1},'21C-140mM-pH10')
    T{c,1}='21';
    IS{c,1}='140';
    pH{c,1}='10';
elseif strcmp(NomeDati{c,1},'21C-160mM-pH7')
    T{c,1}='21';
    IS{c,1}='160';
    pH{c,1}='7';
elseif strcmp(NomeDati{c,1},'21C-160mM-pH10')
    T{c,1}='21';
    IS{c,1}='160';
    pH{c,1}='10';
elseif strcmp(NomeDati{c,1},'21C-180mM-pH7')
    T{c,1}='21';
    IS{c,1}='180';
    pH{c,1}='7';
elseif strcmp(NomeDati{c,1},'21C-180mM-pH10')
    T{c,1}='21';
    IS{c,1}='180';
    pH{c,1}='10';
elseif strcmp(NomeDati{c,1},'21C-200mM-pH7')
    T{c,1}='21';
    IS{c,1}='200';
    pH{c,1}='7';
elseif strcmp(NomeDati{c,1},'21C-200mM-pH10')
    T{c,1}='21';
    IS{c,1}='200';
    pH{c,1}='10';
elseif strcmp(NomeDati{c,1},'37C-80mM-pH7')
```

```
    T{c,1}='37';
    IS{c,1}='80';
    pH{c,1}='7';
elseif strcmp(NomeDati{c,1},'37C-80mM-pH10')
    T{c,1}='37';
    IS{c,1}='80';
    pH{c,1}='10';
elseif strcmp(NomeDati{c,1},'37C-100mM-pH7')
    T{c,1}='37';
    IS{c,1}='100';
    pH{c,1}='7';
elseif strcmp(NomeDati{c,1},'37C-100mM-pH10')
    T{c,1}='37';
    IS{c,1}='100';
    pH{c,1}='10';
elseif strcmp(NomeDati{c,1},'37C-120mM-pH7')
    T{c,1}='37';
    IS{c,1}='80';
    pH{c,1}='7';
elseif strcmp(NomeDati{c,1},'37C-120mM-pH10')
    T{c,1}='37';
    IS{c,1}='120';
    pH{c,1}='10';
elseif strcmp(NomeDati{c,1},'37C-140mM-pH7')
    T{c,1}='37';
    IS{c,1}='140';
    pH{c,1}='7';
elseif strcmp(NomeDati{c,1},'37C-140mM-pH10')
    T{c,1}='37';
    IS{c,1}='140';
    pH{c,1}='10';
elseif strcmp(NomeDati{c,1},'37C-160mM-pH7')
    T{c,1}='37';
    IS{c,1}='160';
    pH{c,1}='7';
elseif strcmp(NomeDati{c,1},'37C-160mM-pH10')
    T{c,1}='37';
    IS{c,1}='160';
    pH{c,1}='10';
elseif strcmp(NomeDati{c,1},'37C-180mM-pH7')
    T{c,1}='37';
```

```
        IS{c,1}='180';
        pH{c,1}='7';
    elseif strcmp(NomeDati{c,1},'37C-180mM-pH10')
        T{c,1}='37';
        IS{c,1}='180';
        pH{c,1}='10';
    elseif strcmp(NomeDati{c,1},'37C-200mM-pH7')
        T{c,1}='37';
        IS{c,1}='200';
        pH{c,1}='7';
    elseif strcmp(NomeDati{c,1},'37C-200mM-pH10')
        T{c,1}='37';
        IS{c,1}='200';
        pH{c,1}='10';
  end
end
p=anovan(DatiAnova(:,1),{pH IS T},'model','interaction');
```

Square-section toroidal samples (cross-sectional area: 5 mm × 6 mm, i.d. = 22 mm, n = 2) were placed between two freely rotating hooks (ø = 8 mm), the upper one being fixed to a 5 N load cell, and were preconditioned with three cycles (0 - 2%) and tested in contact with air at 0.2 mm/s and room temperature (**Figure A.3**). Two black strips (1 mm × 5 mm) were applied on the samples and the deformation was followed using a video camera (Figure 2.6-c). The tensile modulus (TM) and the ultimate tensile stress (UTS) were defined as reported in Chapter IV.

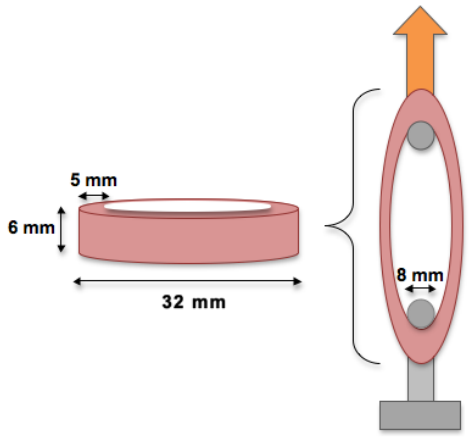

Figure A.3: Setup for tensile tests in the second article.

The code presented below was designed for the analysis of data in the case of tensile tests.

```
%Algoritmo per l'elaborazione dei dati da test di compressione
passo=0.002; %passo di campionamento (mm/mm)
gp=5; %grado polinomio interpolante
ntrat=7;%numero trattamenti
nc=14;%numero campioni
nf=3;%#fattori
ri_d=0.022;%diametro interno dell'anello (m)
su_d=0.007;%diametro del supporto cilindrico su cui si poggia l'anello al momento del test (m)
cLM=4;%da il range nel quale calcolare il Linear Modulus come media degli utlimi cLM valori della derivata prima
%lettura da file, eliminazione ripetizioni, determinazione deformazione
%DATA:
%riga1: nome trattamento
%riga2: # campione
%riga3: dati in strain (mm/mm) e Stress (kPa) per tutti i campioni
%riga4: dati in strain (mm/mm) e Stress (kPa) interpolati
%riga5: matrice a 3 colonne con strain, medie, StD
%riga6: vettore coefficienti di interpolazione grado 5 e parametro di
%errore
%riga7: vettore derivata
%riga8: derivate e StD derivate
%riga9: vettore integrale
%riga10: coeff interp lineare e parametro di errore
%riga11: vettore con integrale tra estremi definiti, LM calcolato come linearizzazione degli ultimi cLM punti, Stiffness calcolata come media degli ultimi cLM valori della
%derivata I, max Stress e max Strain
%righe12`20: la stessa cosa delle righe 2`10 ma per lo StrainVideo
DATA=cell(20,nc);
for c=1:nc
   DATA{2,c}=num2str(c);
   switch c
      case {1,2}
         DATA{1,c}={'4c' '80mM' 'pH10'};
      case {3,4}
         DATA{1,c}={'4c' '140mM' 'pH10'};
      case {5,6}
         DATA{1,c}={'4c' '200mM' 'pH10'};
      case {7,8}
         DATA{1,c}={'21c' '80mM' 'pH10'};
      case {9,10}
```

```
        DATA{1,c}={'21c' '140mM' 'pH10'};
    case {11,12}
        DATA{1,c}={'21c' '200mM' 'pH10'};
    case {13,14}
        DATA{1,c}={'37c' '140mM' 'pH7'};
  end
end

for t=1:nc
  switch t
    case {1,2,3,4,5,6,9,10,11,12,13,14}
      wid=0.005;
      thi=0.006;
      len=(ri_d-su_d)*pi/2;%calcolo distanza fra supporti all'inizio
    case {7,8}
      wid=0.005;
      thi=0.006;
      len=0.031;
  end
  ac=2*wid*thi;%moltiplicato per due perchË ci sono i due lembi dell'anello
  conv=(1/ac)/1000;
  temp=csvread([num2str(DATA{2,t}),'.raw']);
  temp=[temp(:,2)/(1000*len),temp(:,5)*conv];%vettore in strain[mm/mm] e in kPa
  c=1;
  temp1=[];
  while c<length(temp(:,2))&&(temp(c,2)<max(temp(:,2)))
    if (temp(c,2)>=0)&&(temp(c,1)>=temp(1,1))
      temp1=[temp1;temp(c,:)];
    end
    c=c+1;
  end
  temp=temp1;
  c=1;
  while c<length(temp(:,1));
    if (temp(c+1,1)-temp(c,1))<0.00005
      temp(c,:)=[];
    else c=c+1;
    end
  end
  DATA{3,t}=temp;
  %calcolo vettore interpolato
```

```
    def=((round(min(temp(:,1))*1000)/1000):passo:(round(max(temp(:,1))*1000)/1000))';
    lii=min(def);%limite integrale inferiore
    lis=max(def);%limite integrale superiore
    temp=[def,interp1(temp(:,1),temp(:,2),def,'spline')];
    DATA{4,t}=temp;
    [po,S]=polyfit(temp(:,1),temp(:,2),gp);
    DATA{6,t}={po,S};
    temd=[temp(:,1),(polyval(polyder(po),temp(:,1)))];
    DATA{7,t}=temd;
    DATA{9,t}=polyint(po);
    xLM=(temp(length(temp(:,2))-cLM,1):passo:temp(length(temp(:,2)),1))';
    yLM=interp1(temp(:,1),temp(:,2),xLM);
    [po1,S1]=polyfit(xLM,yLM,1);%calcolo Linear Modulus
    DATA{10,t}={po1,S1};
    stiff=[];
    for cont=(length(temd(:,2))-cLM):length(temd(:,2))
        stiff=[stiff,temd(cont,2)];
    end
    DATA{11,t}=[polyval(polyint(po),lis)-polyval(polyint(po),lii),DATA{10,t}{1,1}(1,1),mean(stiff),max(temp(:,2)),max(temp(:,1))];
end
Ris=[];
RisM=zeros(ntrat,10);%matrice resultati. Righe: media e StD di integrale, linear modulus calcolato cme interpolazione lineare degli
ultimi cLM punti, Stiffness, Max Stress, Max Strain; sulle colonne i trattamenti
k=1;% questo tratto dell'algoritmo conta sul fatto che ripetizioni dello stesso trattamento si susseguano nella matrice DATA
while k<=nc
    temp=DATA{4,k};
    temd=DATA{7,k};
    de=temp(:,1);
    dd=temd(:,1);
    M=temp(:,2);
    Md=temd(:,2);
    Mi=DATA{11,k}(1,1);
    MLM=DATA{11,k}(1,2);
    Stiff=DATA{11,k}(1,3);
    MmaxStress=DATA{11,k}(1,4);
    MmaxStrain=DATA{11,k}(1,5);
    c=k+1;
    while
(strcmp(DATA{1,c}{1,1},DATA{1,k}{1,1})&&strcmp(DATA{1,c}{1,2},DATA{1,k}{1,2})&&strcmp(DATA{1,c}{1,3},DATA{1,k}{1,3}))
        temp1=DATA{4,c};
        temd1=DATA{7,c};
        Mi=[Mi,DATA{11,c}(1,1)];
```

```
        MLM=[MLM,DATA{11,c}(1,2)];
        Stiff=[Stiff,DATA{11,c}(1,3)];
        MmaxStress=[MmaxStress,DATA{11,c}(1,4)];
        MmaxStrain=[MmaxStrain,DATA{11,c}(1,5)];
        det=(max(de(1,1),temp1(1,1)):passo:min(max(de(:,1)),max(temp1(:,1))))';
        M=[interp1(de,M,det),interp1(temp1(:,1),temp1(:,2),det)];
        de=det;
        ddt=(max(dd(1,1),temd1(1,1)):passo:min(max(dd(:,1)),max(temd1(:,1))))';
        Md=[interp1(dd,Md,ddt),interp1(temd1(:,1),temd1(:,2),ddt)];
        dd=ddt;
         c=c+1;
         if c>nc
            break
         end
    end
    xm=de;
    ym=mean(M,2);
    em=std(M,0,2);
    xd=dd;
    yd=mean(Md,2);
    ed=std(Md,0,2);
    Ris=[Ris;Mi',MLM',Stiff',MmaxStress',MmaxStrain'];
    DATA{5,k}=[xm,ym,em];
    DATA{8,k}=[xd,yd,ed];
RisM(k,:)=[mean(Mi),std(Mi),mean(MLM),std(MLM),mean(Stiff),std(Stiff),mean(MmaxStress),std(MmaxStress),mean(MmaxStrain),std(
MmaxStrain)];
    k=c;
end
for t=1:nc
    wid=0.005;
    thi=0.006;
    ac=2*wid*thi;%moltiplicato per due perchË ci sono i due lembi dell'anello
    conv=(1/ac)/1000;
    temp=csvread([num2str(DATA{2,t}),'.raw']);
    temp=[temp(:,4)/100,temp(:,5)*conv];%vettore in strainVideo[mm/mm] e in kPa
    c=1;
    check=0;
    temp1=[];
    while c<=length(temp(:,2))&&(temp(c,2)<max(temp(:,2)))
        if temp(c,1)==min(temp(:,1))
            check=1;
```

```
        end
        if (temp(c,2)>0)&&check
            temp1=[temp1;[temp(c,1)-min(temp(:,1)),temp(c,2)]];
        end
        c=c+1;
    end
    temp=temp1;
    c=1;
    while c<length(temp(:,1));
        if (temp(c+1,1)-temp(c,1))<0.00005
            temp(c,:)=[];
        else c=c+1;
        end
    end
    DATA{12,t}=temp;
    %calcolo vettore interpolato
    def=((round(min(temp(:,1))*1000)/1000):passo:(round(max(temp(:,1))*1000)/1000))';
    lii=min(def);%limite integrale inferiore
    lis=max(def);%limite integrale superiore
    temp=[def,interp1(temp(:,1),temp(:,2),def,'spline')];
    DATA{13,t}=temp;
    [po,S]=polyfit(temp1(:,1),temp1(:,2),gp);
    DATA{15,t}={po,S};
    temd=[temp1(:,1),(polyval(polyder(po),temp1(:,1)))];
    DATA{16,t}=temd;
    DATA{18,t}=polyint(po);
    xLM=(temp(length(temp(:,2))-cLM,1):passo:temp(length(temp(:,2)),1))';
    yLM=interp1(temp(:,1),temp(:,2),xLM);
    [po1,S1]=polyfit(xLM,yLM,1);%calcolo Linear Modulus
    DATA{19,t}={po1,S1};
    stiff=[];
    for cont=(length(temd(:,2))-cLM):length(temd(:,2))
        stiff=[stiff,temd(cont,2)];
    end
    DATA{20,t}=[polyval(polyint(po),lis)-polyval(polyint(po),lii),DATA{19,t}{1,1}(1,1),mean(stiff),max(temp(:,2)),max(temp(:,1))];
end
RisVideo=[];
RisMVideo=zeros(ntrat,10);%matrice resultati. Righe: media e StD di linear modulus calcolato cme max della derivata, Max Stress, Max Strain e integrale; sulle colonne i trattamenti
k=1;% questo tratto dell'algoritmo conta sul fatto che ripetizioni dello stesso trattamento si susseguano nella matrice DATA
while k<=nc
```

```
temp=DATA{13,k};
temd=DATA{16,k};
de=temp(:,1);
dd=temd(:,1);
M=temp(:,2);
Md=temd(:,2);
Mi=DATA{20,k}(1,1);
MLM=DATA{20,k}(1,2);
Stiff=DATA{20,k}(1,3);
MmaxStress=DATA{20,k}(1,4);
MmaxStrain=DATA{20,k}(1,5);
c=k+1;
while
(strcmp(DATA{1,c}{1,1},DATA{1,k}{1,1})&&strcmp(DATA{1,c}{1,2},DATA{1,k}{1,2})&&strcmp(DATA{1,c}{1,3},DATA{1,k}{1,3}))
    temp1=DATA{13,c};
    temd1=DATA{16,c};
    Mi=[Mi,DATA{20,c}(1,1)];
    MLM=[MLM,DATA{20,c}(1,2)];
    Stiff=[Stiff,DATA{20,c}(1,3)];
    MmaxStress=[MmaxStress,DATA{20,c}(1,4)];
    MmaxStrain=[MmaxStrain,DATA{20,c}(1,5)];
    det=(max(de(1,1),temp1(1,1)):passo:min(max(de(:,1)),max(temp1(:,1))))';
    M=[interp1(de,M,det),interp1(temp1(:,1),temp1(:,2),det)];
    de=det;
    ddt=(max(dd(1,1),temd1(1,1)):passo:min(max(dd(:,1)),max(temd1(:,1))))';
    Md=[interp1(dd,Md,ddt),interp1(temd1(:,1),temd1(:,2),ddt)];
    dd=ddt;
    c=c+1;
    if c>nc
       break
    end
end
xm=de;
ym=mean(M,2);
em=std(M,0,2);
xd=dd;
yd=mean(Md,2);
ed=std(Md,0,2);
RisVideo=[RisVideo;Mi',MLM',Stiff',MmaxStress',MmaxStrain'];
DATA{14,k}=[xm,ym,em];
DATA{17,k}=[xd,yd,ed];
```

```
RisMVideo(k,:)=[mean(Mi),std(Mi),mean(MLM),std(MLM),mean(Stiff),std(Stiff),mean(MmaxStress),std(MmaxStress),mean(MmaxStrain
),std(MmaxStrain)];
    k=c;
end
NomeDati=cell(nc,1);
Temp=cell(nc,1);
IS=cell(nc,1);
pH=cell(nc,1);
tio=cell(1,nf);
for k=1:nc
    NomeDati{k,1}=DATA{1,k};
    tio=DATA{1,k};
    Temp{k,1}=tio{1,1};
    IS{k,1}=tio{1,2};
    pH{k,1}=tio{1,3};
end

%Rep=cell(nc,1);
%rip=1;
%Rep{1,1}=rip;
%for k=2:nc
    %if strcmp(NomeDati{k,1},NomeDati{k-1,1})
        %rip=rip+1;
    %else rip=1;
    %end
    %Rep{k,1}=rip;
%end
AnInt=anovan(Ris(:,1),{pH IS Temp},'model','interaction');
AnLM=anovan(Ris(:,2),{pH IS Temp},'model','interaction');
AnStiff=anovan(Ris(:,3),{pH IS Temp},'model','interaction');
AnMaxStress=anovan(Ris(:,4),{pH IS Temp},'model','interaction');
AnMaxStrain=anovan(Ris(:,5),{pH IS Temp},'model','interaction');
p=anovan(DatiAnovaVideo(:,1),{pH IS Temp},'model','interaction');
[p,tbl,stats] = anova1(Ris(:,1),[1,1,2,2,3,3,4,4,5,5,6,6,7,7]');
[c,m] = multcompare(stats);
[p,tbl,stats] = anova1(Ris(:,2),[1,1,2,2,3,3,4,4,5,5,6,6,7,7]');
[c,m] = multcompare(stats);
[p,tbl,stats] = anova1(Ris(:,3),[1,1,2,2,3,3,4,4,5,5,6,6,7,7]');
[c,m] = multcompare(stats);
[p,tbl,stats] = anova1(Ris(:,4),[1,1,2,2,3,3,4,4,5,5,6,6,7,7]');
[c,m] = multcompare(stats);
```

```
[p,tbl,stats] = anova1(Ris(:,5),[1,1,2,2,3,3,4,4,5,5,6,6,7,7]');
[c,m] = multcompare(stats);
[p,tbl,stats] = anova1(RisVideo(:,1),[1,1,2,2,3,3,4,4,5,5,6,6,7,7]');
[c,m] = multcompare(stats);
[p,tbl,stats] = anova1(RisVideo(:,2),[1,1,2,2,3,3,4,4,5,5,6,6,7,7]');
[c,m] = multcompare(stats);
[p,tbl,stats] = anova1(RisVideo(:,3),[1,1,2,2,3,3,4,4,5,5,6,6,7,7]');
[c,m] = multcompare(stats);
[p,tbl,stats] = anova1(RisVideo(:,4),[1,1,2,2,3,3,4,4,5,5,6,6,7,7]');
[c,m] = multcompare(stats);
[p,tbl,stats] = anova1(RisVideo(:,5),[1,1,2,2,3,3,4,4,5,5,6,6,7,7]');
[c,m] = multcompare(stats);
Riel=RisVideo;
Riel(4,:)=[];Riel(3,:)=[];Riel(2,:)=[];Riel(1,:)=[];
[p,tbl,stats] = anova1(Riel(:,2),[3,3,4,4,5,5,6,6,7,7]');
[c,m] = multcompare(stats);
[p,tbl,stats] = anova1(Riel(:,3),[3,3,4,4,5,5,6,6,7,7]');
[c,m] = multcompare(stats);
[p,tbl,stats] = anova1(Riel(:,1),[3,3,4,4,5,5,6,6,7,7]');
[c,m] = multcompare(stats);
[p,tbl,stats] = anova1(Riel(:,4),[3,3,4,4,5,5,6,6,7,7]');
[c,m] = multcompare(stats);
[p,tbl,stats] = anova1(Riel(:,5),[3,3,4,4,5,5,6,6,7,7]');
[c,m] = multcompare(stats);
figure;plot(DATA{3,1}(:,1),DATA{3,1}(:,2),'-',DATA{4,1}(:,1),DATA{4,1}(:,2),'.-
',DATA{3,2}(:,1),DATA{3,2}(:,2),'*',DATA{4,2}(:,1),DATA{4,2}(:,2),'+');
figure;plot(DATA{3,1}(:,1),DATA{3,1}(:,2),'-',DATA{4,1}(:,1),(polyval(DATA{6,1}{1,1},DATA{4,1}(:,1))),'*');
figure;plot(DATA{3,1}(:,1),DATA{3,1}(:,2),'-');
figure;plot(DATA{4,1}(:,1),(polyval(DATA{6,1}{1,1},DATA{4,1}(:,1))),'*');
```

The compression and tensile rate and the preconditioning protocol were defined consistently with the work of Seliktar et al.[93]

A.3 Mechanical Testing in the Third Article (Chapter V)

Cyclic uniaxial tensile tests were carried out on ring-shaped (i.d. = 22 mm). Samples were placed between two freely rotating hooks (ø = 8 mm), the upper one being fixed to a 10 N load cell, in a thermoregulated bath (T = 37 ºC) containing 1X PBS. The setup is shown in Figure 5.1. The samples were stretched by separating the hooks up to a distance (= 22 mm) corresponding to the complete extension of the rings, and then left for 10 minutes to reach

the temperature of the bath. They were then cyclically tested at 5 %·s^{-1} according to two different stretching protocols. In the first one (SP1), samples were stretched under five increasing loads for ten cycles each. In the second one (SP2), samples were stretched one hundred times under a fixed load. The applied loads were defined considering a given transmural pressure that acts on a tubular construct during cyclic conditioning. The Equation 5.3, 5.4, 5.5 were obtained from Equation 5.2, which in turn represents the relation between the wall tension (T), the internal (p_{int}) and the external (p_{ext}) pressure, the internal (r_{int}) and the external (r_{ext}) radius, in a thick-walled vessel as already reported by Fung et al., Azuma et al., and Quick et al.:[264,265,284]

$$T = p_{\text{int}} r_{\text{int}} - p_{\text{ext}} r_{ext}$$

The hysteresis, defined as the loop area divided by the area under the loading curve, the maximal strain (Max Strain) and the permanent deformation (PDef) after each cycle, the ultimate tension (UT) and the ultimate strain (US) were calculated with the following algorithms.[168,172,266]

Protocol SP1

```
passo=0.002;
ntrat=5;%numero trattamenti
nc=24;%numero campioni
cLM=4; %da il range nel quale calcolare il Linear Modulus come media degli utlimi cLM valori della derivata prima
DATA=cell(6,nc);%matrice generale 1.nome campione 2.numero campione 3.matrice per ogni campione 4.parametri estratti per ogni campione
for c=1:nc
   DATA{2,c}=num2str(c);
   switch c
      case {1,2,3,4,5}
         DATA{1,c}={'TypeA'};
      case {6,7,8,9}
         DATA{1,c}={'TypeB'};
      case {10,11,12,13,14}
         DATA{1,c}={'TypeB+HA'};
      case {15,16,17,18,19}
         DATA{1,c}={'TypeB+Cr'};
      case {20,21,22,23,24}
         DATA{1,c}={'TypeB+HA+Cr'};
   end
```

```
end
lfc1=0.10842;
lfc2=0.22041;
lfc3=0.33241;
lfc4=0.44440;
lfc5=0.55639;
lf1=0.21;
lf2=0.45;
lf3=0.69;
lf4=0.93;
lf5=1.17;
len=24;%lunghezza campione in mm
plf=0.01;%limite  forza per la valutazione deformazione plastica
pldf=0.3;%limite  derivata forza per la valutazione deformazione plastica

for c1=1:nc
   %ac=wid(t)*thi(t);%moltiplicato per due perchË ci sono i due lembi dell'anello
   %conv=(1/ac)/1000;
   vgrezzi=csvread([num2str(DATA{2,c1}),'.raw']);
   vgrezzi=[vgrezzi(:,2)/len,vgrezzi(:,4)];
   %figure;plot(vgrezzi(:,1),vgrezzi(:,2));

   c2=1;
   while c2<length(vgrezzi(:,1))
      if abs(vgrezzi(c2+1,1)-vgrezzi(c2,1))<0.0001
         vgrezzi(c2,:)=[];
      else c2=c2+1;
      end
   end
   prov=vgrezzi;

   c2=1;
   while c2<length(vgrezzi(:,1))
      %if
((vgrezzi(c2+1,1)>vgrezzi(c2,1))&&(vgrezzi(c2+1,2)<vgrezzi(c2,2)))||((vgrezzi(c2+1,1)<vgrezzi(c2,1))&&(vgrezzi(c2+1,2)>vgrezzi(c2,
2)))
      if ((vgrezzi(c2+1,2)-vgrezzi(c2,2))/(vgrezzi(c2+1,1)-vgrezzi(c2,1)))<=0.001
         vgrezzi(c2+1,:)=[];
      else c2=c2+1;
      end
   end
   %figure;plot(vgrezzi(:,1),vgrezzi(:,2),'b-',prov(:,1),prov(:,2),'r-');
```

```
maxLoad=max(vgrezzi(:,2));

c2=1;
while vgrezzi(c2,1)<vgrezzi(c2+1,1)
   c2=c2+1;
end
while vgrezzi(c2,1)>vgrezzi(c2+1,1)
   c2=c2+1;
end

if vgrezzi(1,1)>vgrezzi(c2,1)
   vgrezzi=[[vgrezzi(c2,1);vgrezzi(:,1)],[vgrezzi(c2,2);vgrezzi(:,2)]];
end

vgrezzi=[(vgrezzi(:,1)-vgrezzi(1,1))*len/(len-vgrezzi(1,1)),vgrezzi(:,2)];

c2=1;
while c2<length(vgrezzi(:,1))
   if vgrezzi(c2,1)<0||vgrezzi(c2,2)<0
      vgrezzi(c2,:)=[];
   else c2=c2+1;
   end
end
temp=vgrezzi;%parte per togliere la parte della rottura
c2=length(temp(:,1));
while temp(c2,2)<0.5*max(temp(:,2))
   c2=c2-1;
end
c3=c2;
maxStrain=0;
while not(temp(c3-2,2)<temp(c3-1,2)&&temp(c3-1,2)>temp(c3,2))
   c3=c3-1;
end
maxStrain=temp(c3-1,2);

if temp(c2,1)>temp(c2-1,1)
   c2=length(temp(:,1));
   while temp(c2,1)>temp(c2-1,1)
      temp(c2,:)=[];
      c2=c2-1;
```

```
    end
  end
  maxStrain=max(temp(:,1));
  %figure;plot(temp(:,1),temp(:,2));
  %figure;plot(vgrezzi(:,1),vgrezzi(:,2));
  vgrezzi=temp;

  c2=1;
  nsemicicli=0;
  while c2<length(vgrezzi(:,1))
    while c2<length(vgrezzi(:,1))&&vgrezzi(c2,1)<vgrezzi(c2+1,1)
      c2=c2+1;
    end
    nsemicicli=nsemicicli+1;
    while c2<length(vgrezzi(:,1))&&vgrezzi(c2,1)>vgrezzi(c2+1,1)
      c2=c2+1;
    end
    nsemicicli=nsemicicli+1;
  end
  c2=1;
  c3=1;
  ncicli=fix(nsemicicli/2);
  DataCycle=cell(8,nsemicicli);%matrice dati per ogni campione, sulle colonne i cicli,
%sulle righe: 1,dati grezzi dei cicli 2,dati da polinomio gp grado 3,coeff vettore interp
% 4,derivata 5,integrale della curva 6,interpolazione lineare di primo
% grado 7,vettore con integrale tra estremi definiti, LM, Stiffness, Max
% Load, Max Strain
  while c2<=(nsemicicli)
    strain=[];
    force=[];
    while c3<length(vgrezzi)
      if vgrezzi(c3,1)<vgrezzi(c3+1,1)
        strain=[strain;vgrezzi(c3,1)];
        force=[force;vgrezzi(c3,2)];
        c3=c3+1;
      else strain=[strain;vgrezzi(c3,1)];
        force=[force;vgrezzi(c3,2)];
        break
      end
    end
    force=force-min(force);
```

```
switch c1
   case {1,2,3,4,5}
      if c2<=20
         force=force*(lfc1/max(force));
      elseif (c2>20)&&(c2<=40)
         force=force*(lfc2/max(force));
      elseif (c2>40)&&(c2<=60)
         force=force*(lfc3/max(force));
      elseif (c2>60)&&(c2<=80)
         force=force*(lfc4/max(force));
      elseif c2>80
         force=force*(lfc5/max(force));
      end
   otherwise
      if c2<=20
         force=force*(lf1/max(force));
      elseif (c2>20)&&(c2<=40)
         force=force*(lf2/max(force));
      elseif (c2>40)&&(c2<=60)
         force=force*(lf3/max(force));
      elseif (c2>60)&&(c2<=80)
         force=force*(lf4/max(force));
      elseif c2>80
         force=force*(lf5/max(force));
      end
end
DataCycle{1,c2}=[strain,force];
def=linspace(strain(1),strain(end));
def=def';
temp=[def,interp1(strain,force,def)];

vet=[];
for c4=1:50
   [po,S]=polyfit(temp(:,1),temp(:,2),c4);
   vet=[vet,S.normr];
end
for c4=1:length(vet)
   if vet(c4)==min(vet)
      break
   end
end
```

```
[po,S]=polyfit(temp(:,1),temp(:,2),c4);
temp=[def,polyval(po,def)];
DataCycle{2,c2}=temp;
DataCycle{3,c2}={po,S};
temd=[temp(:,1),(polyval(polyder(po),temp(:,1)))];
DataCycle{4,c2}=temd;
DataCycle{5,c2}=polyint(po);
xLM=(temp(length(temp(:,2))-cLM,1):passo:temp(length(temp(:,2)),1))';
yLM=interp1(temp(:,1),temp(:,2),xLM);
[po1,S1]=polyfit(xLM,yLM,1);%calcolo Linear Modulus
DataCycle{6,c2}={po1,S1};
stiff=[];
for cont=(length(temd(:,2))-cLM):length(temd(:,2))
   stiff=[stiff,temd(cont,2)];
end
for cont1=length(temd(:,1)):-1:1
   pdef=temd(cont1,1);
   if temd(cont1,2)<=pldf %&& temp(cont1,2)<=plf
      break
   end
end
DataCycle{7,c2}=[polyval(polyint(po),max(def))-
polyval(polyint(po),min(def)),DataCycle{6,c2}{1,1}(1,1),mean(stiff),pdef,max(temp(:,1))];
c2=c2+1;

strain=[];
force=[];
forceP=[];
while c3<length(vgrezzi)
   if vgrezzi(c3,1)>vgrezzi(c3+1,1)
      strain=[strain;vgrezzi(c3,1)];
      force=[force;vgrezzi(c3,2)];
      c3=c3+1;
   else strain=[strain;vgrezzi(c3,1)];
      force=[force;vgrezzi(c3,2)];
      break
   end
end
force=force-min(force);
switch c1
```

```
    case {1,2,3,4,5}
        if c2<=20
            force=force*(lfc1/max(force));
        elseif (c2>20)&&(c2<=40)
            force=force*(lfc2/max(force));
        elseif (c2>40)&&(c2<=60)
            force=force*(lfc3/max(force));
        elseif (c2>60)&&(c2<=80)
            force=force*(lfc4/max(force));
        elseif c2>80
            force=force*(lfc5/max(force));
        end
    otherwise
        if c2<=20
            force=force*(lf1/max(force));
        elseif (c2>20)&&(c2<=40)
            force=force*(lf2/max(force));
        elseif (c2>40)&&(c2<=60)
            force=force*(lf3/max(force));
        elseif (c2>60)&&(c2<=80)
            force=force*(lf4/max(force));
        elseif c2>80
            force=force*(lf5/max(force));
        end
end
DataCycle{1,c2}=[strain,force];
def=linspace(strain(1),strain(end));
def=def';
temp=[def,interp1(strain,force,def)];

vet=[];
for c4=1:50
    [po,S]=polyfit(temp(:,1),temp(:,2),c4);
    vet=[vet,S.normr];
end
for c4=1:length(vet)
    if vet(c4)==min(vet)
        break
    end
end
```

```
    [po,S]=polyfit(temp(:,1),temp(:,2),c4);
    temp=[def,polyval(po,def)];
    DataCycle{2,c2}=temp;
    DataCycle{3,c2}={po,S};
    temd=[temp(:,1),(polyval(polyder(po),temp(:,1)))];
    DataCycle{4,c2}=temd;
    DataCycle{5,c2}=polyint(po);
    %xLM=(temp(length(temp(:,2))-cLM,1):passo:temp(length(temp(:,2)),1))';
    %yLM=interp1(temp(:,1),temp(:,2),xLM);
    %[po1,S1]=polyfit(xLM,yLM,1);%calcolo Linear Modulus
    %DataCycle{6,t}={po1,S1};
    %stiff=[];
    %for cont=(length(temd(:,2))-cLM):length(temd(:,2))
      %stiff=[stiff,temd(cont,2)];
    %end
    for cont1=1:length(temd(:,1))
      pdef=temd(cont1,1);
      if temd(cont1,2)<=pldf %&& temp(cont1,2)<=plf
        break
      end
    end
    DataCycle{7,c2}=[polyval(polyint(po),max(def))-polyval(polyint(po),min(def)),0,0,pdef,max(temp(:,1))];
    c2=c2+1;
  end
  for c2=1:2:nsemicicli-1
    DataCycle{8,c2}=[(DataCycle{7,c2}(1)-
DataCycle{7,c2+1}(1))*100/(DataCycle{7,c2}(1));maxLoad;DataCycle{7,c2+1}(4);DataCycle{7,c2}(5);maxStrain];%sulle tre righe ho
l'isteresi, il max load e il max strain
  end
  vet1=[];
  vet2=[];
  vet3=[];
  for c2=1:nsemicicli
    vet1=[vet1;DataCycle{1,c2}];
    vet2=[vet2;DataCycle{2,c2}];
    vet3=[vet3,DataCycle{8,c2}];
  end
  %figure;plot(vgrezzi(:,1),vgrezzi(:,2),'g-',vet1(:,1),vet1(:,2),'b-',vet2(:,1),vet2(:,2),'r-');
  DATA{3,c1}=DataCycle;
  DATA{4,c1}=vet3;
  DATA{5,c1}=vet2;
  DATA{6,c1}=vet1;
```

```
end

RIS=cell(ntrat,5);%risultati per tutti i campioni, 1.isteresi, 2.strain, 3.MaxLoad, 4.MaxStrain
RISm=cell(ntrat,5);%risultati con media e std per tutti i trattamenti, 1.isteresi, 2.strain, 3.MaxLoad, 4.MaxStrain
RISmSE=cell(ntrat,5);%risultati con media e SE per tutti i trattamenti, 1.isteresi, 2.strain, 3.MaxLoad, 4.MaxStrain
k=1;% questo tratto dell'algoritmo conta sul fatto che ripetizioni dello stesso trattamento si susseguano nella matrice DATA
ctrat=1;
while k<=nc
   temp=DATA{4,k};
   MHyste=temp(1,:);
   MmaxLoad=max(temp(2,:));
   mStrain=temp(3,:);
   MStrain=temp(4,:);
   MmaxStrain=max(temp(5,:));
   nrip=1;
   c1=k+1;
   while strcmp(DATA{1,c1}{1,1},DATA{1,k}{1,1})
      temp1=DATA{4,c1};
      MmaxLoad=[MmaxLoad,max(temp1(2,:))];
      MmaxStrain=[MmaxStrain,max(temp1(5,:))];
      if length(temp1(4,:))>length(MStrain)
         c2=length(temp1(4,:));
         while c2>length(MStrain)
            temp1(:,c2)=[];
            c2=c2-1;
         end
      elseif length(temp1(4,:))<length(MStrain)
          c2=length(MStrain);
         while c2>length(temp1(4,:))
            mStrain(:,c2)=[];
            MStrain(:,c2)=[];
            MHyste(:,c2)=[];
            c2=c2-1;
         end
      end
      MHyste=[MHyste;temp1(1,:)];
      mStrain=[mStrain;temp1(3,:)];
      MStrain=[MStrain;temp1(4,:)];
      c1=c1+1;
      nrip=nrip+1;
      if c1>nc
```

```
        break
      end
    end
    RIS{ctrat,1}=MHyste;
    RIS{ctrat,2}=MmaxLoad;
    RIS{ctrat,3}=mStrain;
    RIS{ctrat,4}=MStrain;
    RIS{ctrat,5}=MmaxStrain;
    RISm{ctrat,1}=[mean(MHyste);std(MHyste)]';
    RISm{ctrat,2}=[mean(MmaxLoad),std(MmaxLoad)];
    RISm{ctrat,3}=[mean(mStrain);std(mStrain)]';
    RISm{ctrat,4}=[mean(MStrain);std(MStrain)]';
    RISm{ctrat,5}=[mean(MmaxStrain),std(MmaxStrain)];
    RISmSE{ctrat,1}=[mean(MHyste);std(MHyste)/sqrt(nrip)]';
    RISmSE{ctrat,2}=[mean(MmaxLoad),std(MmaxLoad)/sqrt(nrip)];
    RISmSE{ctrat,3}=[mean(mStrain);std(mStrain)/sqrt(nrip)]';
    RISmSE{ctrat,4}=[mean(MStrain);std(MStrain)/sqrt(nrip)]';
    RISmSE{ctrat,5}=[mean(MmaxStrain),std(MmaxStrain)/sqrt(nrip)];
    ctrat=ctrat+1;
    k=c1;
end
```

Protocol SP2

```
%ALGORITMO CICLI
passo=0.002;
ntrat=5;%numero trattamenti
nc=16;%numero campioni
cLM=4; %da il range nel quale calcolare il Linear Modulus come media degli utlimi cLM valori della derivata prima
DATA=cell(6,nc);%matrice generale 1.nome campione 2.numero campione 3.matrice per ogni campione 4.parametri estratti per ogni campione
for c=1:nc
    DATA{2,c}=num2str(c);
    switch c
        case {1,2,3,4,5}
            DATA{1,c}={'TypeA'};
        case {6,7,8}
            DATA{1,c}={'TypeB'};
        case {9,10,11}
            DATA{1,c}={'TypeB+HA'};
        case {12,13,14}
```

```
        DATA{1,c}={'TypeB+Cr'};
    case {15,16}
        DATA{1,c}={'TypeB+HA+Cr'};
  end
end
lfc1=0.10842;
lfc2=0.22041;
lfc3=0.33241;
lfc4=0.44440;
lfc5=0.55639;
lf1=0.21;
lf2=0.45;
lf3=0.69;
lf4=0.93;
lf5=1.17;
len=24;%lunghezza campione in mm
plf=0.01;%limite  forza per la valutazione deformazione plastica
pldf=0.3;%limite  derivata forza per la valutazione deformazione plastica

for c1=1:nc
  %ac=wid(t)*thi(t);%moltiplicato per due perchË ci sono i due lembi dell'anello
  %conv=(1/ac)/1000;
  vgrezzi=csvread([num2str(DATA{2,c1}),'.raw']);
  vgrezzi=[vgrezzi(:,2)/len,vgrezzi(:,4)];
  %figure;plot(vgrezzi(:,1),vgrezzi(:,2));

  c2=1;
  while c2<length(vgrezzi(:,1))
    if abs(vgrezzi(c2+1,1)-vgrezzi(c2,1))<0.0001
      vgrezzi(c2,:)=[];
    else c2=c2+1;
    end
  end
  prov=vgrezzi;

  c2=1;
  while c2<length(vgrezzi(:,1))
    %if
((vgrezzi(c2+1,1)>vgrezzi(c2,1))&&(vgrezzi(c2+1,2)<vgrezzi(c2,2)))||((vgrezzi(c2+1,1)<vgrezzi(c2,1))&&(vgrezzi(c2+1,2)>vgrezzi(c2,
2)))
    if ((vgrezzi(c2+1,2)-vgrezzi(c2,2))/(vgrezzi(c2+1,1)-vgrezzi(c2,1)))<=0.001
      vgrezzi(c2+1,:)=[];
```

```
    else c2=c2+1;
    end
end
%figure;plot(vgrezzi(:,1),vgrezzi(:,2),'b-',prov(:,1),prov(:,2),'r-');

maxLoad=max(vgrezzi(:,2));

c2=1;
while vgrezzi(c2,1)<vgrezzi(c2+1,1)
    c2=c2+1;
end
while vgrezzi(c2,1)>vgrezzi(c2+1,1)
    c2=c2+1;
end

if vgrezzi(1,1)>vgrezzi(c2,1)
    vgrezzi=[[vgrezzi(c2,1);vgrezzi(:,1)],[vgrezzi(c2,2);vgrezzi(:,2)]];
end

vgrezzi=[(vgrezzi(:,1)-vgrezzi(1,1))*len/(len-vgrezzi(1,1)),vgrezzi(:,2)];

c2=1;
while c2<length(vgrezzi(:,1))
    if vgrezzi(c2,1)<0||vgrezzi(c2,2)<0
        vgrezzi(c2,:)=[];
    else c2=c2+1;
    end
end
maxStrain=0;
temp=vgrezzi;%parte per togliere la parte della rottura
c2=length(temp(:,1));
while temp(c2,2)<0.5*max(temp(:,2))
    c2=c2-1;
end
if temp(c2,1)>temp(c2-1,1)
    c2=length(temp(:,1));
    while temp(c2,1)>temp(c2-1,1)
        if temp(c2-2,2)<temp(c2-1,2)&&temp(c2-1,2)>temp(c2,2)
            maxStrain=temp(c2-1,2);
        end
        temp(c2,:)=[];
```

```
        c2=c2-1;
    end
  else maxStrain=max(temp(:,1));
  end
  %figure;plot(temp(:,1),temp(:,2));
  %figure;plot(vgrezzi(:,1),vgrezzi(:,2));
  vgrezzi=temp;

  c2=1;
  nsemicicli=0;
  while c2<length(vgrezzi(:,1))
    while c2<length(vgrezzi(:,1))&&vgrezzi(c2,1)<vgrezzi(c2+1,1)
      c2=c2+1;
    end
    nsemicicli=nsemicicli+1;
    while c2<length(vgrezzi(:,1))&&vgrezzi(c2,1)>vgrezzi(c2+1,1)
      c2=c2+1;
    end
    nsemicicli=nsemicicli+1;

  end
  c2=1;
  c3=1;
  ncicli=fix(nsemicicli/2);
  DataCycle=cell(8,nsemicicli);%matrice dati per ogni campione, sulle colonne i cicli,
%sulle righe: 1,dati grezzi dei cicli 2,dati da polinomio gp grado 3,coeff vettore interp
% 4,derivata 5,integrale della curva 6,interpolazione lineare di primo
% grado 7,vettore con integrale tra estremi definiti, LM, Stiffness, Max
% Load, Max Strain
  while c2<=(nsemicicli)
    strain=[];
    force=[];
    while c3<length(vgrezzi)
      if vgrezzi(c3,1)<vgrezzi(c3+1,1)
        strain=[strain;vgrezzi(c3,1)];
        force=[force;vgrezzi(c3,2)];
        c3=c3+1;
      else strain=[strain;vgrezzi(c3,1)];
        force=[force;vgrezzi(c3,2)];
        break
      end
```

```
end
force=force-min(force);
switch c1
   case {1,2,3,4,5}
      force=force*(lfc1/max(force));
   otherwise
      force=force*(lf1/max(force));
end
DataCycle{1,c2}=[strain,force];
def=linspace(strain(1),strain(end));
def=def';
temp=[def,interp1(strain,force,def)];

vet=[];
for c4=1:50
   [po,S]=polyfit(temp(:,1),temp(:,2),c4);
   vet=[vet,S.normr];
end
for c4=1:length(vet)
   if vet(c4)==min(vet)
      break
   end
end

[po,S]=polyfit(temp(:,1),temp(:,2),c4);
temp=[def,polyval(po,def)];
DataCycle{2,c2}=temp;
DataCycle{3,c2}={po,S};
temd=[temp(:,1),(polyval(polyder(po),temp(:,1)))];
DataCycle{4,c2}=temd;
DataCycle{5,c2}=polyint(po);
xLM=(temp(length(temp(:,2))-cLM,1):passo:temp(length(temp(:,2)),1))';
yLM=interp1(temp(:,1),temp(:,2),xLM);
[po1,S1]=polyfit(xLM,yLM,1);%calcolo Linear Modulus
DataCycle{6,c2}={po1,S1};
stiff=[];
for cont=(length(temd(:,2))-cLM):length(temd(:,2))
   stiff=[stiff,temd(cont,2)];
end
for cont1=length(temd(:,1)):-1:1
   pdef=temd(cont1,1);
```

```
        if temd(cont1,2)<=pldf %&& temp(cont1,2)<=plf
            break
        end
    end
    DataCycle{7,c2}=[polyval(polyint(po),max(def))-
polyval(polyint(po),min(def)),DataCycle{6,c2}{1,1}(1,1),mean(stiff),pdef,max(temp(:,1))];
    c2=c2+1;

    strain=[];
    force=[];
    while c3<length(vgrezzi)
        if vgrezzi(c3,1)>vgrezzi(c3+1,1)
            strain=[strain;vgrezzi(c3,1)];
            force=[force;vgrezzi(c3,2)];
            c3=c3+1;
        else strain=[strain;vgrezzi(c3,1)];
            force=[force;vgrezzi(c3,2)];
            break
        end
    end
    force=force-min(force);
    switch c1
        case {1,2,3,4,5}
            force=force*(lfc1/max(force));
        otherwise
            force=force*(lf1/max(force));
    end
    DataCycle{1,c2}=[strain,force];
    def=linspace(strain(1),strain(end));
    def=def';
    temp=[def,interp1(strain,force,def)];

    vet=[];
    for c4=1:50
        [po,S]=polyfit(temp(:,1),temp(:,2),c4);
        vet=[vet,S.normr];
    end
    for c4=1:length(vet)
        if vet(c4)==min(vet)
            break
        end
```

```
    end

    [po,S]=polyfit(temp(:,1),temp(:,2),c4);
    temp=[def,polyval(po,def)];
    DataCycle{2,c2}=temp;
    DataCycle{3,c2}={po,S};
    temd=[temp(:,1),(polyval(polyder(po),temp(:,1)))];
    DataCycle{4,c2}=temd;
    DataCycle{5,c2}=polyint(po);
    %xLM=(temp(length(temp(:,2))-cLM,1):passo:temp(length(temp(:,2)),1))';
    %yLM=interp1(temp(:,1),temp(:,2),xLM);
    %[po1,S1]=polyfit(xLM,yLM,1);%calcolo Linear Modulus
    %DataCycle{6,t}={po1,S1};
    %stiff=[];
    %for cont=(length(temd(:,2))-cLM):length(temd(:,2))
      %stiff=[stiff,temd(cont,2)];
    %end
    for cont1=1:length(temd(:,1))
      pdef=temd(cont1,1);
      if temd(cont1,2)<=pldf %&& temp(cont1,2)<=plf
        break
      end
    end
    DataCycle{7,c2}=[polyval(polyint(po),max(def))-polyval(polyint(po),min(def)),0,0,pdef,max(temp(:,1))];
    c2=c2+1;
  end
  for c2=1:2:nsemicicli-1
    DataCycle{8,c2}=[(DataCycle{7,c2}(1)-
DataCycle{7,c2+1}(1))*100/(DataCycle{7,c2}(1));maxLoad;DataCycle{7,c2+1}(4);DataCycle{7,c2}(5);maxStrain];%sulle tre righe ho
l'isteresi, il max load e il max strain
  end
  vet1=[];
  vet2=[];
  vet3=[];
  for c2=1:nsemicicli
    vet1=[vet1;DataCycle{1,c2}];
    vet2=[vet2;DataCycle{2,c2}];
    vet3=[vet3,DataCycle{8,c2}];
  end
  %figure;plot(vet1(:,1),vet1(:,2),'-',vet2(:,1),vet2(:,2),'red');
  DATA{3,c1}=DataCycle;
  DATA{4,c1}=vet3;
```

```
    DATA{5,c1}=vet2;
    DATA{6,c1}=vet1;
end
RIS=cell(ntrat,5);%risultati per tutti i campioni, 1.isteresi, 2.strain, 3.MaxLoad, 4.MaxStrain
RISm=cell(ntrat,5);%risultati con media e std per tutti i trattamenti, 1.isteresi, 2.strain, 3.MaxLoad, 4.MaxStrain
RISmSE=cell(ntrat,5);%risultati con media e SE per tutti i trattamenti, 1.isteresi, 2.strain, 3.MaxLoad, 4.MaxStrain
k=1;% questo tratto dell'algoritmo conta sul fatto che ripetizioni dello stesso trattamento si susseguano nella matrice DATA
ctrat=1;
while k<=nc
    temp=DATA{4,k};
    MHyste=temp(1,:);
    MmaxLoad=max(temp(2,:));
    mStrain=temp(3,:);
    MStrain=temp(4,:);
    MmaxStrain=temp(5,:);
    nrip=1;
    c1=k+1;
    while strcmp(DATA{1,c1}{1,1},DATA{1,k}{1,1})
        temp1=DATA{4,c1};
        MmaxLoad=[MmaxLoad,max(temp1(2,:))];
        MmaxStrain=[MmaxStrain,temp1(5,:)];
        if length(temp1(4,:))>length(MStrain)
            c2=length(temp1(4,:));
            while c2>length(MStrain)
                temp1(:,c2)=[];
                c2=c2-1;
            end
        elseif length(temp1(4,:))<length(MStrain)
             c2=length(MStrain);
            while c2>length(temp1(4,:))
                mStrain(:,c2)=[];
                MStrain(:,c2)=[];
                MHyste(:,c2)=[];
                c2=c2-1;
            end
        end
        MHyste=[MHyste;temp1(1,:)];
        mStrain=[mStrain;temp1(3,:)];
        MStrain=[MStrain;temp1(4,:)];
        c1=c1+1;
        nrip=nrip+1;
```

```
    if c1>nc
      break
    end
  end
  RIS{ctrat,1}=MHyste;
  RIS{ctrat,2}=MmaxLoad;
  RIS{ctrat,3}=mStrain;
  RIS{ctrat,4}=MStrain;
  RIS{ctrat,5}=MmaxStrain;
  RISm{ctrat,1}=[mean(MHyste);std(MHyste)]';
  RISm{ctrat,2}=[mean(MmaxLoad),std(MmaxLoad)];
  RISm{ctrat,3}=[mean(mStrain);std(mStrain)]';
  RISm{ctrat,4}=[mean(MStrain);std(MStrain)]';
  RISm{ctrat,5}=[mean(MmaxStrain),std(MmaxStrain)];
  RISmSE{ctrat,1}=[mean(MHyste);std(MHyste)/sqrt(nrip)]';
  RISmSE{ctrat,2}=[mean(MmaxLoad),std(MmaxLoad)/sqrt(nrip)];
  RISmSE{ctrat,3}=[mean(mStrain);std(mStrain)/sqrt(nrip)]';
  RISmSE{ctrat,4}=[mean(MStrain);std(MStrain)/sqrt(nrip)]';
  RISmSE{ctrat,5}=[mean(MmaxStrain),std(MmaxStrain)/sqrt(nrip)];
  ctrat=ctrat+1;
  k=c1;
end
```

References

[1] Nerem, R. M., Sambanis, A. "Tissue Engineering: From Biology to Biological Substitutes", *Tissue Eng* **1995,** *1*, 3.

[2] Langer, R. "Tissue Engineering", *Mol Ther* **2000,** *1*, 12.

[3] Stegemann, J. P., Hong, H., Nerem, R. M. "Mechanical, biochemical, and extracellular matrix effects on vascular smooth muscle cell phenotype", *J Appl Physiol* **2005,** *98*, 2321.

[4] Ratner, B. D., Bryant, S. J. "Biomaterials: Where We Have Been and Where We Are Going", *Annu Rev Biomed Eng* **2004,** *6*, 41.

[5] Place, E. S., Evans, N. D., Stevens, M. M. "Complexity in biomaterials for tissue engineering", *Nat Mater* **2009,** *8*, 457.

[6] Stock, U., Vacanti, J. P. "Tissue Engineering: Current State and Prospects ", *Annu Rev Med* **2001,** *52*, 443.

[7] Sachlos, E., Czernuszka, J. T. "Making tissue engineering scaffolds work. Review: the application of solid freeform fabrication technology to the production of tissue engineering scaffolds", *Eur Cell Mater* **2003,** *5*, 29.

[8] Liu, C., Xia, Z. F., Czernuszka, J. T. "Three-dimensional scaffolds for tissue engineering", *Chem Eng Res Des* **2007,** *85*, 1051.

[9] Chan-Park, M. B., Shen, J. Y., Cao, Y., Xiong, Y., Liu, Y., Rayatpisheh, S., Kang, G. C.-W., Greisler, H. P. "Biomimetic control of vascular smooth muscle cell morphology and phenotype for functional tissue-engineered small-diameter blood vessels", *J Biomed Mater Res A* **2009,** *88A*, 1104.

[10] Vats, A., Tolley, N. S., Polak, J. M., Gough, J. E. "Scaffolds and biomaterials for tissue engineering: a review of clinical applications", *Clin Otolaryngol* **2003,** *28*, 165.

[11] Arosarena, O. "Tissue engineering", *Facial Plast Surg* **2005,** *13*, 233.

[12] Boland, E. D., Espy, P. G., Bowlin, G. L., "Tissue Engineering Scaffolds". In *Encyclopedia of Biomaterials and Biomedical Engineering*, Inc., M. D., Ed. 270 Madison Avenue, New York, New York, 10016, 2004; pp 1630.

[13] Venkatraman, S., Boey, F., Lao, L. L. "Implanted cardiovascular polymers: Natural, synthetic and bio-inspired", *Prog Polym Sci* **2008,** *33*, 853.

[14] Hoenig, M. R., Campbell, G. R., Rolfe, B. E., Campbell, J. H. "Tissue-Engineered Blood Vessels: Alternative to Autologous Grafts?", *Arterioscl Throm Vasc* **2005,** *25*, 1128.

[15] Bilodeau, K., Couet, F., Boccafoschi, F., Mantovani, D. "Design of a Perfusion Bioreactor Specific to the Regeneration of Vascular Tissues Under Mechanical Stresses", *Artif Organs* **2005,** *29*, 906.

[16] Barron, V., Lyons, E., Stenson-Cox, C., Mchugh, P. E., Pandit, A. "Bioreactors for Cardiovascular Cell and Tissue Growth : A Review", *Ann Biomed Eng* **2003,** *31*, 1017.

[17] Couet, F., Rajan, N., Mantovani, D. "Macromolecular Biomaterials for Scaffold-based Vascular Tissue Engineering", *Macromol Biosci* **2007,** *7*, 701.

[18] Bouten, C. V. C., Dankers, P. Y. W., Driessen-Mol, A., Pedron, S., Brizard, A. M. A., Baaijens, F. P. T. "Substrates for cardiovascular tissue engineering", *Adv Drug Deliver Rev* **2011,** *63*, 221.

[19] Rhodin, J. A. G., Terjung, R., "Architecture of the Vessel Wall". In *Handbook of Physiology*, Berne, R. M., Ed. John Wiley & Sons, Inc.: 1979; Vol. 2, pp 1.

[20] Wagenseil, J. E., Mecham, R. P. "Vascular Extracellular Matrix and Arterial Mechanics", *Physiol Rev* **2009,** *89*, 957.

[21] Isenberg, B. C., J., W. "Building structure into engineered tissues", *Mater Today* **2006,** *9*, 54.

[22] Humphrey, J. D., *Vascular Growth and Remodeling*, John Wiley & Sons, Inc.: 2006.

[23] Gelse, K., Poschl, E., Aigner, T. "Collagens--structure, function, and biosynthesis", *Adv Drug Deliv Rev* **2003,** *55*, 1531.

[24] Voet, D., Voet, J. G., "Three-Dimensional Structures of Proteins - Fibrous Proteins - Collagen". In *Biochemistry*, 3rd ed.; International, W., Ed. John Wiley and sons Inc: 2004; pp 233.

[25] Seliktar, D., Nerem, R. M., "Blood Vessel Substitute". In *Methods for tissue engineering*, Atala, A.; Lanza, P., Eds. Academic Press: 2002; pp 891.

[26] Silver, F. H., Freeman, J. W., Seehra, G. P. "Collagen self-assembly and the development of tendon mechanical properties", *J Biomech* **2003,** *36*, 1529.

[27] Ravi, S., Qu, Z., Chaikof, E. L. "Polymeric Materials for Tissue Engineering of Arterial Substitutes", *Vascular.* **2009,** *17*, 1.

[28] Wallace, D. G., Rosenblatt, J. "Collagen gel systems for sustained delivery and tissue engineering", *Adv Drug Deliv Rev* **2003,** *55*, 1631.

[29] Rajan, N., Lagueux, J., Couet, F., Pennock, W., Sionkowska, A., Mantovani, D. "Low Doses of Ultraviolet Radiation Stimulate Cell Activity in Collagen-based Scaffolds", *Biotechnol Prog* **2008,** *24*, 884.

[30] Guyton, A. C., Hall, J. E., "Quadro Generale dell Circolazione e Principi dell'Emodinamica". In *Fisiologia Medica*, IX ed.; EdiSES: Naples, Italy, 1999; pp 165.

[31] Lanzer, P., Topol, E. J., *Pan vascular medicine: integrated clinical management*, Springer: 2002.

[32] Holzapfel, G. A., "Collagen in Arterial Walls: Biomechanical Aspects". In *Collagen: Structure and Mechanics*, Fratzl, P., Ed. Springer: 2008; pp 285.

[33] Dela Paz, N., D'amore, P. "Arterial versus venous endothelial cells", *Cell Tissue Res* **2009,** *335*, 5.

[34] Van De Vosse, F. N. "Mathematical modelling of the cardiovascular system", *J Eng Math* **2003,** *47*, 175.

[35] Li, J. K.-J., *Dynamics of the vascular system*, World Scientific Publishing: 2004.

[36] Kelleher, C. M., Mclean, S. E., Mecham, R. P., Gerald, P. S., "Vascular Extracellular Matrix and Aortic Development". In *Current Topics in Developmental Biology*, Academic Press: 2004; Vol. Volume 62, pp 153.

[37] Vito, R. P., Dixon, S. A. "Blood Vessel Constitutive Models - 1995-2002", *Annu Rev Biomed Eng* **2003,** *5*, 413.

[38] Iozzo, R. V. "Matrix Proteoglycans: From Molecular Design to Cellular Function", *Annu Rev Biochem* **1998,** *67*, 609.

[39] Zhang, W. J., Liu, W., Cui, L., Cao, Y. "Tissue engineering of blood vessel", *J Cell Mol Med* **2007,** *11*, 945.

[40] Pankajakshan, D., Agrawal, D. K. "Scaffolds in tissue engineering of blood vessels", *Can J Physiol Pharmacol* **2010,** *88*, 855.

[41] Voet, D., Voet, J. G., "Sugars and Polysaccharides-Glycosaminoglycas-Hyaluronic Acid". In *Biochemistry*, Wiley, Ed. John Wiley and sons Inc: 2004; pp 368.

[42] Beckman, M. J., Shields, K. J., Diegelmann, R. F., "Collagen". In *Encyclopedia of Biomaterials and Biomedical Engineering*, Marcel Dekker, Inc.: New York, 2004; pp 324.

[43] Patel, A., Fine, B., Sandig, M., Mequanint, K. "Elastin biosynthesis: The missing link in tissue-engineered blood vessels", *Cardiovasc Res* **2006,** *71*, 40.

[44] Gandhi, N. S., Mancera, R. L. "The Structure of Glycosaminoglycans and their Interactions with Proteins", *Chem Biol Drug Des* **2008,** *72*, 455.

[45] Gupta, V., Grande-Allen, K. J. "Effects of static and cyclic loading in regulating extracellular matrix synthesis by cardiovascular cells", *Cardiovasc Res* **2006,** *72*, 375.

[46] Kenagy, R. D., Plaas, A. H., Wight, T. N. "Versican Degradation and Vascular Disease", *Trends Cardiovas Med* **2006,** *16*, 209.

[47] Ferdous, Z., Grande-Allen, K. J. "Utility and Control of Proteoglycans in Tissue Engineering", *Tissue Eng* **2007,** *13*, 1893.

[48] Redaelli, A., Vesentini, S., Soncini, M., Vena, P., Mantero, S., Montevecchi, F. M. "Possible role of decorin glycosaminoglycans in fibril to fibril force transfer in relative mature tendons--a computational study from molecular to microstructural level", *J Biomech* **2003,** *36*, 1555.

[49] Wess, T. J., "Collagen Fibrillar Structure and Hierarchies". In *Collagen: Structure and Mechanics*, Fratzl, P., Ed. Springer: 2008; pp 15.

[50] Who, Fact sheet Nº 317 - Cardiovascular diseases. (18-02-2011),

[51] Stegemann, J. P., Kaszuba, S. N., Rowe, S. L. "Review: Advances in Vascular Tissue Engineering Using Protein-Based Biomaterials", *Tissue Eng* **2007,** *13*, 2601.

[52] Teebken, O. E., Haverich, A. "Tissue Engineering of Small-Diameter Vascular Grafts", *Graft* **2002,** *5*, 14.

[53] Hoerstrup, S. P., Zund, G., Sodian, R., Schnell, A. M., Grunenfelder, J., Turina, M. I. "Tissue engineering of small caliber vascular grafts", *Eur J Cardiothorac Surg* **2001,** *20*, 164.

[54] Kannan, R. Y., Salacinski, H. J., Butler, P. E., Hamilton, G., Seifalian, A. M. "Current status of prosthetic bypass grafts: A review", *J Biomed Mater Res B* **2005,** *74B*, 570.

[55] Rashid, S. T., Salacinski, H. J., Fuller, B. J., Hamilton, G., Seifalian, A. M. "Engineering of bypass conduits to improve patency", *Cell Proliferat* **2004,** *37*, 351.

[56] Berglund, J. D., Galis, Z. S. "Designer blood vessels and therapeutic revascularization", *Br J Pharmacol* **2003,** *140*, 627.

[57] Nerem, R. M., Seliktar, D. "Vascular Tissue Engineering", *Annu Rev Biomed Eng* **2001,** *3*, 225.

[58] Vorp, D. A., Maul, T., Nieponice, A. "Molecular aspects of vascular tissue engineering", *Front Biosci* **2005,** *10*, 768.

[59] Kakisis, J. D., Liapis, C. D., Breuer, C., Sumpio, B. E. "Artificial blood vessel: The Holy Grail of peripheral vascular surgery", *J Vasc Surg* **2005,** *41*, 349.

[60] Niklason, L. E., Seruya, M., "Small-Diameter Vascular Grafts". In *Methods for tissue engineering*, Atala, A.; Lanza, P., Eds. Academic Press: 2002; pp 905.

[61] Chlupác, J., Filová, E., Bacáková, L. "Blood Vessel Replacement: 50 years of Development and Tissue Engineering Paradigms in Vascular Surgery", *Physiol Res* **2009,** *58*, 119.

[62] Isenberg, B. C., Williams, C., Tranquillo, R. T. "Small-Diameter Artificial Arteries Engineered In Vitro", *Circ Res* **2006,** *98*, 25.

[63] Tranquillo, R. T. "The tissue-engineered small-diameter artery", *Ann N Y Acad Sci* **2002,** *961*, 251.

[64] Gong, Z., Niklason, L. E. "Blood Vessels Engineered from Human Cells", *Trends Cardiovasc Med* **2006,** *16*, 153.

[65] Opitz, F., Schenke-Layland, K., Cohnert, T. U., Stock, U. A. "Phenotypical Plasticity of Vascular Smooth Muscle Cells‚ÄìEffect of In Vitro and In Vivo Shear Stress for Tissue Engineering of Blood Vessels", *Tissue Eng* **2007,** *13*, 2505.

[66] Aami, ANSI/AAMI VP20-94. In *Cardiovascular Implants - Vascular Graft Prostheses* 1994; p 29.

[67] Badylak, S. F., Lantz, G. C., Coffey, A., Geddes, L. A. "Small intestinal submucosa as a large diameter vascular graft in the dog", *J Surg Res* **1989,** *47*, 74.

[68] Lantz, G. C., Badylak, S. F., Hiles, M. C., Coffey, A. C., Geddes, L. A., Kokini, K., Sandusky, G. E., Morff, R. J. "Small intestinal submucosa as a vascular graft: a review", *J Invest Surg* **1993,** *6*, 297.

[69] Sandusky, G. E., Lantz, G. C., Badylak, S. F. "Healing Comparison of Small Intestine Submucosa and ePTFE Grafts in the Canine Carotid Artery", *J Surg Res* **1995,** *58*, 415.

[70] Wilson, G. J., Yeger, H., Klement, P., Lee, J. M., Courtman, D. W. "Acellular Matrix Allograft Small Caliber Vascular Prostheses", *ASAIO J* **1990,** *36*, M340.

[71] Huynh, T., Abraham, G., Murray, J., Brockbank, K., Hagen, P.-O., Sullivan, S. "Remodeling of an acellular collagen graft into a physiologically responsive neovessel", *Nat Biotech* **1999,** *17*, 1083.

[72] Inoue, Y., Anthony, J. P., Lleon, P., Young, D. M. "Acellular Human Dermal Matrix as a Small Vessel Substitute", *J reconstr Microsurg* **1996,** *12*, 307.

[73] Thomas, A. C., Campbell, G. R., Campbell, J. H. "Advances in vascular tissue engineering", *Cardiovasc Pathol* **2003,** *12*, 271.

[74] Campbell, J. H., Efendy, J. L., Campbell, G. R. "Novel vascular graft grown within recipient's own peritoneal cavity", *Circ Res* **1999,** *85*, 1173.

[75] Campbell, J. H., Walker, P., Chue, W.-L., Daly, C., Cong, H.-L., Xiang, L., Campbell, G. R. "Body cavities as bioreactors to grow arteries", *Int Congr Ser* **2004,** *1262*, 118.

[76] Chue, W.-L., Campbell, G. R., Caplice, N., Muhammed, A., Berry, C. L., Thomas, A. C., Bennett, M. B., Campbell, J. H. "Dog peritoneal and pleural cavities as bioreactors to grow autologous vascular grafts", *J Vasc Surg* **2004,** *39*, 859.

[77] Niklason, L. E., Gao, J., Abbott, W. M., Hirschi, K. K., Houser, S., Marini, R., Langer, R. "Functional Arteries Grown in Vitro", *Science* **1999,** *284*, 489.

[78] Shum-Tim, D., Stock, U., Hrkach, J., Shinoka, T., Lien, J., Moses, M. A., Stamp, A., Taylor, G., Moran, A. M., Landis, W., Langer, R., Vacanti, J. P., Mayer, J. E., Jr. "Tissue engineering of autologous aorta using a new biodegradable polymer", *Ann Thorac Surg* **1999,** *68*, 2298.

[79] Watanabe, M., Shin'oka, T., Tohyama, S., Hibino, N., Konuma, T., Matsumura, G., Kosaka, Y., Ishida, T., Imai, Y., Yamakawa, M., Ikada, Y., Morita, S. "Tissue-

engineered vascular autograft: Inferior vena cava replacement in a dog model", *Tissue Eng* **2001,** *7*, 429.

[80] Shin'oka, T., Imai, Y., Ikada, Y. "Transplantation of a tissue-engineered pulmonary artery", *New Engl J Med* **2001,** *344*, 532.

[81] Dahl, S. L. M., Kypson, A. P., Lawson, J. H., Blum, J. L., Strader, J. T., Li, Y., Manson, R. J., Tente, W. E., Dibernardo, L., Hensley, M. T., Carter, R., Williams, T. P., Prichard, H. L., Dey, M. S., Begelman, K. G., Niklason, L. E. "Readily Available Tissue-Engineered Vascular Grafts", *Sci Transl Med* **2011,** *3*, 1.

[82] L'heureux, N., Paquet, S., Labbe, R., Germain, L., Auger, F. A. "A completely biological tissue-engineered human blood vessel", *Faseb J* **1998,** *12*, 47.

[83] L'heureux, N., Dusserre, N., Konig, G., Victor, B., Keire, P., Wight, T. N., Chronos, N. A. F., Kyles, A. E., Gregory, C. R., Hoyt, G., Robbins, R. C., Mcallister, T. N. "Human tissue-engineered blood vessels for adult arterial revascularization", *Nat Med* **2006,** *12*, 361.

[84] L'heureux, N., Dusserre, N., Marini, A., Garrido, S., De La Fuente, L., Mcallister, T. "Technology Insight: the evolution of tissue-engineered vascular grafts[mdash]from research to clinical practice", *Nat Clin Pract Cardiovasc Med* **2007,** *4*, 389.

[85] L'heureux, N., Mcallister, T. N., De La Fuente, L. M. "Tissue-Engineered Blood Vessel for Adult Arterial Revascularization", *New Engl J Med* **2007,** *357*, 1451.

[86] Konig, G., Mcallister, T. N., Dusserre, N., Garrido, S. A., Iyican, C., Marini, A., Fiorillo, A., Avila, H., Wystrychowski, W., Zagalski, K., Maruszewski, M., Jones, A. L., Cierpka, L., De La Fuente, L. M., L'heureux, N. "Mechanical properties of completely autologous human tissue engineered blood vessels compared to human saphenous vein and mammary artery", *Biomaterials* **2009,** *30*, 1542.

[87] Weinberg, C. B., Bell, E. "A blood vessel model constructed from collagen and cultured vascular cells", *Science* **1986,** *231*, 397.

[88] L'heureux, N., Germain, L., Labbe, R., Auger, F. A. "In vitro construction of a human blood vessel from cultured vascular cells: A morphologic study", *J Vasc Surg* **1993,** *17*, 499.

[89] Kanda, K., Matsuda, T., Oka, T. "In vitro reconstruction of hybrid vascular tissue. Hierarchic and oriented cell layers", *ASAIO J* **1993,** *39*, M561.

[90] Hirai, J., Kanda, K., Oka, T., Matsuda, T. "Highly oriented, tubular hybrid vascular tissue for a low pressure circulatory system", *ASAIO J* **1994,** *40*, M383.

[91] Tranquillo, R. T., Girton, T. S., Bromberek, B. A., Triebes, T. G., Mooradian, D. L. "Magnetically orientated tissue-equivalent tubes: application to a circumferentially orientated media-equivalent", *Biomaterials* **1996,** *17*, 349.

[92] Girton, T. S., Oegema, T. R., Tranquillo, R. T. "Exploiting glycation to stiffen and strengthen tissue equivalents for tissue engineering", *J Biomed Mat Res* **1998,** *46*, 87.

[93] Seliktar, D., Black, A. R., Vito, R., P. , Nerem, R. M. "Dynamic Mechanical Conditioning of Collagen-Gel Blood Vessel Constructs Induces Remodeling In Vitro", *Ann Biomed Eng* **2000,** *28*, 351.

[94] Ye, Q., Zund, G., Benedikt, P., Jockenhoevel, S., Hoerstrup, S. P., Sakyama, S., Hubbell, J. A., Turina, M. "Fibrin gel as a three dimensional matrix in cardiovascular tissue engineering", *Eur J Cardio-Thorac* **2000,** *17*, 587.

[95] Grassl, E. D., Oegema, T. R., Tranquillo, R. T. "Fibrin as an alternative biopolymer to type-I collagen for the fabrication of a media equivalent", *J Biomed Mater Res* **2002,** *60*, 607.

[96] Long, J. L., Tranquillo, R. T. "Elastic fiber production in cardiovascular tissue-equivalents", *Matrix Biol* **2003,** *22*, 339.

[97] Cummings, C. L., Gawlitta, D., Nerem, R. M., Stegemann, J. P. "Properties of engineered vascular constructs made from collagen, fibrin, and collagen-fibrin mixtures", *Biomaterials* **2004,** *25*, 3699.

[98] Zavan, B., Vindigni, V., Lepidi, S., Iacopetti, I., Avruscio, G., Abatangelo, G., Cortivo, R. "Neoarteries grown in vivo using a tissue-engineered hyaluronan-based scaffold", *FASEB J* **2008,** *22*, 2853.

[99] Lepidi, S., Abatangelo, G., Vindigni, V., Deriu, G. P., Zavan, B., Tonello, C., Cortivo, R. "In vivo regeneration of small-diameter (2 mm) arteries using a polymer scaffold", *Faseb J* **2006,** *20*, 103.

[100] Berglund, J. D., Nerem, R. M., Sambanis, A. "Incorporation of Intact Elastin Scaffolds in Tissue-Engineered Collagen-Based Vascular Grafts", *Tissue Eng* **2004,** *10*, 1526.

[101] Buttafoco, L., Engbers-Buijtenhuijs, P., Poot, A. A., Dijkstra, P. J., Vermes, I., Feijen, J. "Physical characterization of vascular grafts cultured in a bioreactor", *Biomaterials* **2006,** *27*, 2380.

[102] Kanda, K., Matsuda, T. "Behavior of arterial wall cells cultured on periodically stretched substrates", *Cell Transplant* **1993,** *2*, 475.

[103] Isenberg, B. C., Tranquillo, R. T. "Long-term cyclic distention enhances the mechanical properties of collagen-based media-equivalents", *Ann Biomed Eng* **2003,** *31*, 937.

[104] Kim, B.-S., Nikolovski, J., Bonadio, J., Mooney, D. J. "Cyclic mechanical strain regulates the development of engineered smooth muscle tissue", *Nat Biotechnol* **1999,** *17*, 979.

[105] Kaully, T., Kaufman-Francis, K., Lesman, A., Levenberg, S. "Vascularization‚ÄîThe Conduit to Viable Engineered Tissues", *Tissue Eng Pt B-Rev* **2009,** *15*, 159.

[106] Stenzel, K. H., Miyata, T., Rubin, A. L. "Collagen as a Biomaterial", *Annu Rev Biophys Bio* **1974,** *3*, 231.

[107] Kadler, K. E., Holmes, D. F., Trotter, J. A., A., C. J. "Collagen fibril formation", *Biochem J* **1996,** *316*, 1.

[108] Drury, J. L., Mooney, D. J. "Hydrogels for tissue engineering: scaffold design variables and applications", *Biomaterials* **2003,** *24*, 4337.

[109] Ottani, V., Martini, D., Franchi, M., Ruggeri, A., Raspanti, M. "Hierarchical structures in fibrillar collagens", *Micron* **2002,** *33*, 587.

[110] Gupta, H. S., "Nanoscale Deformation Mechanisms in Collagen". In *Collagen: Structure and mechanics*, Fratzl, P., Ed. Springer: 2008; pp 155.

[111] Avery, N. C., Bailey, A. J., "Restraining Cross-Links Responsible for the Mechanical Properties of Collagen Fibers: Natural and Artificial". In *Collagen: Structure and Mechanics*, Fratzl, P., Ed. Springer: 2008; pp 81.

[112] Koob, T. J., "Collagen fixation". In *Encyclopedia of Biomaterials and Biomedical Engineering*, Marcel Dekker: 2004; pp 335.

[113] Chevallay, B., Herbage, D. "Collagen-based biomaterials as 3D scaffold for cell cultures: applications for tissue engineering and gene therapy", *Med Biol Eng Comput* **2000,** *38*, 211.

[114] Khang, G., Lee, S. J., Kim, M. S., Lee, H. B., *Biomaterials: Tissue Engineering and Scaffolds*, John Wiley & Sons, Inc.: 2006.

[115] Rajan, N., Habermehl, J., Cote, M.-F., Doillon, C. J., Mantovani, D. "Preparation of ready-to-use, storable and reconstituted type I collagen from rat tail tendon for tissue engineering applications", *Nat Protoc* **2007,** *1*, 2753.

[116] Lynn, A. K., Yannas, I. V., Bonfield, W. "Antigenicity and immunogenicity of collagen", *J Biomed Mater Res B* **2004,** *71B*, 343.

[117] Mitchell, S. L., Niklason, L. E. "Requirements for growing tissue-engineered vascular grafts", *Cardiovasc Pathol* **2003,** *12*, 59.

[118] Elbjeirami, W. M., Yonter, E. O., Starcher, B. C., West, J. L. "Enhancing mechanical properties of tissue-engineered constructs via lysyl oxidase crosslinking activity", *J Biomed Mater Res A* **2003,** *66A*, 513.

[119] Hermanson, G. T., "Bioconjugate Reagents". In *Bioconjugate Techniques*, Academic Press: 1996; p 217.

[120] Davidson, R. J., Cooper, D. R. "The Effect of Ultraviolet Irradiation on Acid-Soluble Collagen", *Biochem J* **1967,** *105*, 965.

[121] Payne, K. J., Veis, A. "Fourier transform ir spectroscopy of collagen and gelatin solutions: Deconvolution of the amide I band for conformational studies", *Biopolymers* **1988,** *27*, 1749.

[122] Doyle, B. B., Bendit, E. G., Blout, E. R. "Infrared Spectroscopy of Collagen and Collagen-Like Polypeptides", *Biopolymers* **1975,** *14*, 937.

[123] Metreveli, N., Namicheishvili, L., Jariashvili, K., Mrevlishvili, G., Sionkowska, A. "Mechanisms of the Influence of UV Irradiation on Collagen and Collagen-Ascorbic Acid Solutions", *Int J Photoenergy* **2006,** *2006*, 1.

[124] Kaminska, A., Sionkowska, A. "Photochemical transformations in collagen in the presence Beta-carotene", *J Photoch Photobio A* **1996,** *96*, 123.

[125] Kaminska, A., Sionkowska, A. "Effect of UV radiation on the infrared spectra of collagen", *Polym Degrad Stabil* **1996,** *51*, 19.

[126] Sionkowska, A. "Modification of collagen films by ultraviolet irradiation", *Polym Degrad Stabil* **2000,** *68*, 147.

[127] Sander, E. A., Barocas, V. H., "Biomimetic Collagen Tissues: Collagenous Tissue Engineering and Other Applications". In *Collagen: Structure and Mechanics*, Fratzl, P., Ed. Springer: 2008; pp 475.

[128] Hulmes, D. J., "Collagen Diversity, Synthesis and Assembly". In *Collagen: Structure and Mechanics*, Fratzl, P., Ed. Springer: 2008; pp 31.

[129] Wood, G. C., Keech, M. K. "The Formation of Fibrils from Collagen Solutions-The Effect of Experimental Conditions: Kinetic and Electron-Microscope Studies ", *Biochem J* **1960,** *75*, 588.

[130] Rosenblatt, J., Devereux, B., Wallace, D. G. "Injectable collagen as a pH-sensitive hydrogel", *Biomaterials* **1994,** *15*, 985.

[131] Wallace, D. G. "The relative contribution of electrostatic interactions to stabilization of collagen fibrils", *Biopolymers* **1990,** *29*, 1015.

[132] Roeder, B. A., Kokini, K., Sturgis, J. E., Robinson, J. P., Voytik-Harbin, S. L. "Tensile Mechanical Properties of Three-Dimensional Type I Collagen Extracellular Matrices With Varied Microstructure", *J Biomed Eng* **2002,** *124*, 214.

[133] Comper, W. D., Veis, A. "Characterization of nuclei in in vitro collagen fibril formation", *Biopolymers* **1977,** *16*, 2133.

[134] Forgacs, G., Newman, S. A., Hinner, B., Maier, C. W., Sackmann, E. "Assembly of Collagen Matrices as a Phase Transition Revealed by Structural and Rheologic Studies ", *Biophys J* **2003,** *84*, 1272.

[135] Helseth, D. L., Jr, Veis, A. "Collagen self-assembly in vitro. Differentiating specific telopeptide-dependent interactions using selective enzyme modification and the addition of free amino telopeptide. ", *J Biol Chem* **1981,** *256*, 7118.

[136] Comper, W. D., Veis, A. "The mechanism of nucleation for in vitro collagen fibril formation", *Biopolymers* **1977,** *16*, 2113.

[137] Amadori, L., Rajan, N., Vesentini, S., Mantovani, D. "Atomic Force and Confocal Microscopic Studies of Collagen-Cell-based Scaffolds for Vascular Tissue Engineering", *Adv Mat Res* **2007,** *15-17*, 83.

[138] Yang, Y.-L., Kaufman, L. J. "Rheology and Confocal Reflectance Microscopy as Probes of Mechanical Properties and Structure during Collagen and Collagen/Hyaluronan Self-Assembly", *Biophys J* **2009,** *96*, 1566.

[139] Yang, Y.-L., Leone, L. M., Kaufman, L. J. "Elastic Moduli of Collagen Gels Can Be Predicted from Two-Dimensional Confocal Microscopy", *Biophys J* **2009,** *97*, 2051.

[140] Raub, C. B., Suresh, V., Krasieva, T., Lyubovitsky, J., Mih, J. D., Putnam, A. J., Tromberg, B. J., George, S. C. "Noninvasive Assessment of Collagen Gel Microstructure and Mechanics Using Multiphoton Microscopy", *Biophys J* **2007,** *92*, 2212.

[141] Raub, C. B., Unruh, J., Suresh, V., Krasieva, T., Lindmo, T., Gratton, E., Tromberg, B. J., George, S. C. "Image Correlation Spectroscopy of Multiphoton Images Correlates with Collagen Mechanical Properties", *Biophys J* **2008,** *94*, 2361.

[142] Wood, G. C. "The Formation of Fibrils from Collagen Solutions. A Mechanism of Collagen-Fibril Formation. ", *Biochem J* **1960,** *75*, 598.

[143] Vogel, K. G., Paulsson, M., Heinegard, D. "Specific inhibition of type I and type II collagen fibrillogenesis by the small proteoglycan of tendon.", *Biochem J* **1984,** *223*, 587.

[144] Williams, B. R., Gelman, R. A., Poppke, D. C., Piez, K. A. "Collagen fibril formation. Optimal in vitro conditions and preliminary kinetic results", *J Biol Chem* **1978,** *253*, 6578.

[145] Silver, F. H., Christensen, D. L., "Assembly of Biological Molecules - Collagen Self-Assembly". In *Biomaterials Science and Biocompatibility*, Springer: 1999; pp 174.

[146] Hofmann, H., Fietzek, P. P., Kühn, K. "The Role of Polar and Hydrophobic Interactions for the Molecular Packing of Type I Collagen : A Three-dimensional Evaluation of the Amino Acid Sequence", *J Mol Biol* **1978,** *125*, 137.

[147] Rosenblatt, J., Devereux, B., Wallace, D. G. "Effect of electrostatic forces on the dynamic rheological properties of injectable collagen biomaterials.", *Biomaterials* **1992,** *13*, 878.

[148] Christiansen, D. L., Huang, E. K., Silver, F. H. "Assembly of type I collagen: fusion of fibril subunits and the influence of fibril diameter on mechanical properties", *Matrix Biol* **2000,** *19*, 409.

[149] Freudenberg, U., Behrens, S. H., Welzel, P. B., M¸Ller, M., Grimmer, M., Salchert, K., Taeger, T., Schmidt, K., Pompe, W., Werner, C. "Electrostatic Interactions Modulate the Conformation of Collagen I", *Biophys J* **2007,** *92*, 2108.

[150] Bianchi, E., Conio, G. "The Role of pH, Temperature, Salt Type, and Salt Concentration on the Stability of the Crystalline, Helical, and Randomly Coiled Forms of Collagen", *J Biol Chem* **1967,** *242*, 1361.

[151] Usha, R., Ramasami, T. "Effect of pH on Dimensional Stability of Rat Tail Tendon Collagen Fiber", *J Appl Polym Sci* **2000,** *75*, 1577.

[152] Li, Y., Asadi, A., Monroe, M. R., Douglas, E. P. "pH effects on collagen fibrillogenesis in vitro: Electrostatic interactions and phosphate binding", *Mat Sci Eng C* **2009,** *29*, 1643.

[153] Rosenblatt, J., Devereux, B., Wallace, D. C. "Dynamic Rheological Studies of Hydrophobic Interactions in Injectable Collagen Biomaterials", *J Appl Polym Sci* **1993,** *50*, 953.

[154] Boccafoschi, F., Rajan, N., Habermehl, J., Mantovani, D. "Preparation and Characterization of a Scaffold for Vascular Tissue Engineering by Direct-Assembling of Collagen and Cells in a Cylindrical Geometry", *Macromol Biosci* **2007,** *7*, 719.

[155] Wakatsuki, T., Kolodney, M. S., Zahalak, G. I., Elson, E. L. "Cell Mechanics Studied by a Reconstituted Model Tissue", *Biophys J* **2000,** *79*, 2353.

[156] Gross, J., Kirk, D. "The Heat Precipitation of Collagen from Neutral Salt Solutions: Some Rate-Regulating Factors", *J Biol Chem* **1958,** *233*, 355.

[157] Cooper, A. "Thermodynamic Studies of the Assembly in vitro of Native Collagen Fibrils", *Biochem J* **1970,** *118*, 355.

[158] Gelman, R. A., Piez, K. A. "Collagen Fibril Formation in Vitro. A Quasielastic Light-Scattering Study of Early Stages.", *J Biol Chem* **1980,** *255*, 8098.

[159] Na, G., Butz, L., Carroll, R. "Mechanism of in vitro collagen fibril assembly. Kinetic and morphological studies", *J Biol Chem* **1986,** *261*, 12290.

[160] Na, G. C., Phillips, L. J., Freire, E. I. "In vitro collagen fibril assembly: thermodynamic studies", *Biochemistry* **1989,** *28*, 7153.

[161] Silver, F. H., Ebrahimi, A., Snowhill, P. B. "Viscoelastic Properties of Self-Assembled Type I Collagen Fibers: Molecular Basis of Elastic and Viscous Behaviors ", *Connect Tissue Res* **2002,** *43*, 569.

[162] Olde Damink, L. H. H., Dijkstra, P. J., Van Luyn, M. J. A., Van Wachem, P. B., Nieuwenhuis, P., Feijen, J. "Cross-linking of dermal sheep collagen using a water-soluble carbodiimide", *Biomaterials* **1996,** *17*, 765.

[163] Barnes, C. P., Pemble, C. W., Brand, D. D., Simpson, D. G., Bowlin, G. L. "Cross-Linking Electrospun Type II Collagen Tissue Engineering Scaffolds with Carbodiimide in Ethanol", *Tissue Eng* **2007,** *13*, 1593.

[164] Wrobel, N., Schinkinger, M., Mirsky, V. M. "A Novel Ultraviolet Assay for Testing Side Reactions of Carbodiimides", *Anal Biochem* **2002,** *305*, 135.

[165] Gilles, M. A., Hudson, A. Q., Borders, C. L. "Stability of water-soluble carbodiimides in aqueous solution", *Anal Biochem* **1990,** *184*, 244.

[166] Bell, E., Ivarsson, B., Merrill, C. "Production of a Tissue-Like Structure by Contraction of Collagen Lattices by Human Fibroblasts of Different Proliferative Potential in vitro", *PNAS* **1979,** *76*, 1274.

[167] Barocas, V. H., Girton, T. S., Tranquillo, R. T. "Engineered alignment in media equivalents: Magnetic prealignment and Mandrel compaction", *J Biomech Eng* **1998,** *120*, 660.

[168] Silver, F. H., "Viscoelastic Mechanical Properties of Tissues". In *Mechanosensing and Mechanochemical Transduction in Extracellular Matrix*, Springer US: 2006; pp 181.

[169] Fratzl, P., "Collagen: Structure and Mechanics, an Introduction". In *Collagen: Structure and Mechanics*, Fratzl, P., Ed. Springer: 2008; pp 1.

[170] Silver, F. H., Landis, W. J., "Viscoelasticity, Energy Storage and Transmission and Dissipation by Extracellular Matrices in Vertebrates". In *Collagen: Structure and Mechanics*, Fratzl, P., Ed. Springer: 2008; pp 133.

[171] Hayashi, K., "Mechanical Properties of Soft Tissues and Arterial Walls". In *Biomechanics of soft tissue in cardiovascular systems*, Holzapfel, G. A.; Ogden, R. W., Eds. Springer: 2003; p 15.

[172] Wagenseil, J. E., Wakatsuki, T., Okamoto, R. J., Zahalak, G. I., Elson, E. L. "One-Dimensional Viscoelastic Behavior of Fibroblast Populated Collagen Matrices", *J Biomech Eng* **2003,** *125*, 719.

[173] Faury, G. "Function–structure relationship of elastic arteries in evolution: from microfibrils to elastin and elastic fibres ", *Pathol Biol* **2001,** *49* 310.

[174] Dobrin, P. B. "Mechanical properties of arterises", *Physiol Rev* **1978,** *58*, 397.

[175] Dobrin, P. B. "Mechanical Behavior of Vascular Smooth Muscle in Cylindrical Segments of Arteries in Vitro ", *Ann Biomed Eng* **1984,** *12*, 497.

[176] Pryse, K. M., Nekouzadeh, A., Genin, G. M., Elson, E. L., Zahalak, G. I. "Incremental Mechanics of Collagen Gels: New Experiments and a New Viscoelastic Model", *Ann Biomed Eng* **2003,** *31*, 1287.

[177] Wu, C.-C., Ding, S.-J., Wang, Y.-H., Tang, M.-J., Chang, H.-C. "Mechanical properties of collagen gels derived from rats of different ages", *J Biomat Sci-Polym E* **2005,** *16*, 1261.

[178] Neel, E. A. A., Cheema, U., Knowles, J. C., Brown, R. A., Nazhat, S. N. "Use of multiple unconfined compression for control of collagen gel scaffold density and mechanical properties", *Soft Matter* **2006,** *2*, 986.

[179] Chandran, P. L., Barocas, V. H. "Microstructural Mechanics of Collagen Gels in Confined Compression: Poroelasticity, Viscoelasticity, and Collapse", *J Biomech Eng* **2004,** *126*, 152.

[180] Girton, T. S., Barocas, V. H., Tranquillo, R. T. "Confined compression of a tissue-equivalent: collagen fibril and cell alignment in response to anisotropic strain", *J Biomech Eng* **2002,** *124*, 568.

[181] Lee, C. H., Singla, A., Lee, Y. "Biomedical applications of collagen", *Int J Pharm* **2001,** *221*, 1.

[182] Peng, L., Cheng, X. R., Wang, J. W., Xu, D. X., Wang, G. "Preparation and Evaluation of Porous Chitosan/Collagen Scaffolds for Periodontal Tissue Engineering", *J Bioact Compat Pol* **2006,** *21*, 207.

[183] Lee, J. E., Kim, K. E., Kwon, I. C., Ahn, H. J., Lee, S.-H., Cho, H., Kim, H. J., Seong, S. C., Lee, M. C. "Effects of the controlled-released TGF-[beta]1 from chitosan microspheres on chondrocytes cultured in a collagen/chitosan/glycosaminoglycan scaffold", *Biomaterials* **2004,** *25*, 4163.

[184] Tsai, S.-P., Hsieh, C.-Y., Hsieh, C.-Y., Wang, D.-M., Huang, L. L.-H., Lai, J.-Y., Hsieh, H.-J. "Preparation and cell compatibility evaluation of chitosan/collagen composite scaffolds using amino acids as crosslinking bridges", *J Appl Polym Sci* **2007,** *105*, 1774.

[185] Zhang, L., Ao, Q., Wang, A., Lu, G., Kong, L., Gong, Y. D., Zhao, N. M., Zhang, X. "A sandwich tubular scaffold derived from chitosan for blood vessel tissue engineering.", *J Biomed Mater Res A* **2006,** *77*, 277.

[186] Jockenhoevel, S., Zund, G., Hoerstrup, S. P., Chalabi, K., Sachweh, J. S., Demircan, L., Messmer, B. J., Turina, M. "Fibrin gel - advantages of a new scaffold in cardiovascular tissue engineering", *Eur J Cardio-thorac* **2001,** *19*, 424.

[187] Grassl, E. D., Oegema, T. R., Tranquillo, R. T. "A fibrin-based arterial media equivalent", *J Biomed Mater Res A* **2003,** *66*, 550.

[188] Swartz, D. D., Russell, J. A., Andreadis, S. T. "Engineering of fibrin-based functional and implantable small-diameter blood vessels", *Am J Physiol Heart Circ Physiol* **2005,** *288*, H1451.

[189] Rowe, S. L., Stegemann, J. P. "Interpenetrating Collagen-Fibrin Composite Matrices with Varying Protein Contents and Ratios", *Biomacromolecules* **2006,** *7*, 2942.

[190] Sell, S. A., Mcclure, M. J., Garg, K., Wolfe, P. S., Bowlin, G. L. "Electrospinning of collagen/biopolymers for regenerative medicine and cardiovascular tissue engineering", *Adv Drug Deliver Rev* **2009,** *61*, 1007.

[191] Lv, Q., Feng, Q., Hu, K., Cui, F. "Three-dimensional fibroin/collagen scaffolds derived from aqueous solution and the use for HepG2 culture", *Polymer* **2005,** *46*, 12662.

[192] Boland, E. D., Matthews, J. A., Pawlowski, K. J., Simpson, D. G., Wnek, G. E., Bowlin, G. L. "Electrospinning collagen and elastin: preliminary vascular tissue engineering", *Front Biosci* **2004,** *9*, 1422.

[193] Li, M., Mondrinos, M. J., Gandhi, M. R., Ko, F. K., Weiss, A. S., Lelkes, P. I. "Electrospun protein fibers as matrices for tissue engineering", *Biomaterials* **2005,** *26*, 5999.

[194] Buttafoco, L., Kolkman, N. G., Poot, A. A., Dijkstra, P. J., Vermes, I., Feijen, J. "Electrospinning collagen and elastin for tissue engineering small diameter blood vessels", *J Control Release* **2005,** *101*, 322.

[195] Daamen, W. F., Van Moerkerk, H. T. B., Hafmans, T., Buttafoco, L., Poot, A. A., Veerkamp, J. H., Van Kuppevelt, T. H. "Preparation and evaluation of molecularly-defined collagen-elastin-glycosaminoglycan scaffolds for tissue engineering", *Biomaterials* **2003,** *24*, 4001.

[196] Daamen, W. F., Nillesen, S. T. M., Wismans, R. G., Reinhardt, D. P., Hafmans, T., Veerkamp, J. H., Van Kuppevelt, T. H. "A Biomaterial Composed of Collagen and Solubilized Elastin Enhances Angiogenesis and Elastic Fiber Formation Without Calcification", *Tissue Eng Pt A* **2008,** *14*, 349.

[197] Stitzel, J., Liu, J., Lee, S. J., Komura, M., Berry, J., Soker, S., Lim, G., Van Dyke, M., Czerw, R., Yoo, J. J., Atala, A. "Controlled fabrication of a biological vascular substitute", *Biomaterials* **2006,** *27*, 1088.

[198] Mori, M., Yamaguchi, M., Sumitomo, S., Takai, Y. "Hyaluronan-based Biomaterials in Tissue Engineering", *Acta Histochem Cytochem* **2004,** *37*, 1.

[199] Davidenko, N., Campbell, J. J., Thian, E. S., Watson, C. J., Cameron, R. E. "Collagen-hyaluronic acid scaffolds for adipose tissue engineering", *Acta Biomater* **2010,** *6*, 3957.

[200] Park, S.-N., Park, J.-C., Kim, H. O., Song, M. J., Suh, H. "Characterization of porous collagen/hyaluronic acid scaff old modified by 1-ethyl-3-(3-dimethylaminopropyl)carbodiimide cross-linking", *Biomaterials* **2002,** *23*, 1205.

[201] Wang, T.-W., Spector, M. "Development of hyaluronic acid-based scaffolds for brain tissue engineering", *Acta Biomater* **2009,** *5*, 2371.

[202] Lin, Y.-K., Liu, D.-C. "Studies of Novel Hyaluronic Acid-collagen Sponge Materials Composed of Two Different Species of Type I Collagen", *J Biomat Appl* **2007,** *21*, 265.

[203] Voet, D., Voet, J. G., "Sugars and Polysaccharides - Glycosaminoglycans". In *Biochemistry*, Wiley, Ed. John Wiley and sons Inc: 2004; pp 368.

[204] Obrink, B. "The influence of glycosaminoglycans on the formation of fibers from monomeric tropocollagen in vitro", *Eur J Biochem* **1973,** *34*, 129.

[205] Mathews, M. B., Decker, L. "The Effect of Acid Mucopolysaccharides and Acid Mucopolysaccharide-Proteins on Fibril Formation from Collagen Solutions ", *Biochem. J.* **1968,** *109*, 517.

[206] Mathews, M. B. "The Interaction of Collagen and Acid Mucopolysaccharides - A Model for Connective Tissue", *Biochem J* **1965,** *96*, 710.

[207] Keech, M. K. "The Formation of Fibrils from Collagen Solutions IV. Effect of Mucopolysaccharides and Nucleic Acids: An Electron Microscope Study ", *J Biophys Biochem Cyt* **1961,** *9*, 193.

[208] Wood, G. C. "The Formation of Fibrils from Collagen Solutions - 3. Effect of Chondroitin Sulphate and Some other Naturally Occurring Polyanions on the Rate of Formation ", *Biochem J* **1960,** *75*, 605.

[209] Parry, D. A. D., Flint, M. H., Gillard, G. C., Craig, A. S. "A role for glycosaminoglycans in the development of collagen fibrils", *FEBS Letters* **1982,** *149*, 1.

[210] Ellis, D. L., Yannas, I. V. "Recent advances in tissue synthesis in vjvo by use of collagen- glycosaminoglycan copolymers ", *Biomaterials* **1996,** *17*, 291.

[211] Powell, H. M., Boyce, S. T. "EDC cross-linking improves skin substitute strength and stability", *Biomaterials* **2006,** *27*, 5821.

[212] Lee, C. R., Grodzinsky, A. J., Spector, M. "The effects of cross-linking of collagen-glycosaminoglycan scaffolds on compressive stiffness, chondrocyte-mediated contraction, proliferation and biosynthesis", *Biomaterials* **2001,** *22*, 3145.

[213] Kataropoulou, M., Henderson, C., Grant, H. "The influence of glycosaminoglycans and crosslinking agents on the phenotype of hepatocytes cultured on collagen gels", *Hum Exp Toxicol* **2003,** *22*, 65.

[214] Hanthamrongwit, M., Reid, W. H., Grant, M. H. "Chondroitin-6-sulphate incorporated into collagen gels for the growth of human keratinocytes: the effect of cross-linking agents and diamines", *Biomaterials* **1996,** *17*, 775.

[215] Flanagan, T. C., Wilkins, B., Black, A., Jockenhoevel, S., Smith, T. J., Pandit, A. S. "A collagen-glycosaminoglycan co-culture model for heart valve tissue engineering applications", *Biomaterials* **2006,** *27*, 2233.

[216] Pieper, J. S., Hafmans, T., Veerkamp, J. H., Van Kuppevelt, T. H. "Development of tailor-made collagen-glycosaminoglycan matrices: EDC/NHS crosslinking, and ultrastructural aspects - an ultrastructural study using cupromeronic blue", *Biomaterials* **2000,** *21*, 581.

[217] Pieper, J. S., Oosterhof, A., Dijkstra, P. J., Veerkamp, J. H., Van Kuppevelt, T. H. "Preparation and characterization of porous crosslinked collagenous matrices containing bioavailable chondroitin sulphate", *Biomaterials* **1999,** *20*, 847.

[218] Osborne, C., Barbenel, J., Smith, D., Savakis, M., Grant, M. "Investigation into the tensile properties of collagen/chondroitin-6-sulphate gels: the effect of crosslinking agents and diamines", *Med Biol Eng Comput* **1998,** *36*, 129.

[219] Osborne, C. S., Reid, W. H., Grant, M. H. "Investigation into cell growth on collagen/chondroitin-6-sulphate gels: the effect of crosslinking agents and diamines", *J Mater Sci-Mater M* **1997,** *8*, 179.

[220] Osborne, C. S., Reid, W. H., Grant, M. H. "Investigation into the biological stability of collagen/chondroitin-6-sulphate gels and their contraction by fibroblasts and keratinocytes: the effect of crosslinking agents and diamines", *Biomaterials* **1999,** *20*, 283.

[221] Docherty, R., Forrester, J. V., Lackie, J. M., Gregory, D. W. "Glycosaminoglycans facilitate the movement of fibroblasts through threedimensional collagen matrices", *J Cell Sci* **1989,** *92*, 263.

[222] Mackay, J., Mensah, G., *The atlas of heart disease and stroke*, 1st edition; World Health Organization: 2004.

[223] Ratcliffe, A. "Tissue engineering of vascular grafts", *Matrix Biol* **2000,** *19*, 353.

[224] Boccafoschi, F., Habermehl, J., Vesentini, S., Mantovani, D. "Biological performances of collagen-based scaffolds for vascular tissue engineering", *Biomaterials* **2005,** *26*, 7410.

[225] Habermehl, J., Skopinska, J., Boccafoschi, F., Sionkowska, A., Kaczmarek, H., Laroche, G., Mantovani, D. "Preparation of ready-to-use, stockable and reconstituted collagen", *Macromol Biosci* **2005,** *5*, 821.

[226] Krishnan, L., Weiss, J. A., Wessman, M. D., Hoying, J. B. "Design and Application of a Test System for Viscoelastic Characterization of Collagen Gels", *Tissue Eng* **2004,** *10*, 241.

[227] Zeng, D., Ferrari, A., Ulmer, J., Veligodskiy, A., Fischer, P., Spatz, J., Ventikos, Y., Poulikakos, D., Kroschewskiy, R. "Three-Dimensional Modeling of Mechanical Forces in the Extracellular Matrix during Epithelial Lumen Formation", *Biophys J* **2006,** *90*, 4380.

[228] Sionkowska, A., Kaminska, A. "Thermal helix-coil transition in UV irradiated collagen from rat tail tendon", *Int J Biol Macromol* **1999,** *24*, 337.

[229] Ohan, M. P., Weadock, K. S., Dunn, M. G. "Synergistic effects of glucose and ultraviolet irradiation on the physical properties of collagen", *J Biomed Mater Res* **2002,** *60*, 384.

[230] Sionkowska, A. "Photochemical transformations in collagen in the presence of melanin", *J Photoch Photobio A* **1999,** *124*, 91.

[231] Cooper, D. R., Davidson, R. J. "The Effect of Ultraviolet Irradiation on Soluble Collagen", *Biochem J* **1965,** *97*, 139.

[232] Kaminska, A., Sionkowska, A. "The effect of UV radiation on the thermal parameters of collagen degradation", *Polym Degr Stab* **1996,** *51*, 15.

[233] Miles, C. A., Sionkowska, A., Hulin, S. L., Sims, T. J., Avery, N. C., Bailey, A. J. "Identification of an Intermediate State in the Helix-Coil Degradation of Collagen by Ultraviolet Light", *J Biol Chem* **2000,** *275*, 33014.

[234] Sionkowska, A., Wess, T. "Mechanical properties of UV irradiated rat tail tendon (RTT) collagen", *Int J Biol Macromol* **2004,** *34*, 9.

[235] Fujimori, E. "Ultraviolet Light-Induced Change in Collagen Macromolecules", *Biopolymers* **1965,** *3*, 115.

[236] Lee, J. E., Park, J. C., Hwang, Y. S., Kim, J. K., Kim, J. G., Suh, H. "Characterization of UV-irradiated Dense/porous Collagen Membranes: Morphology, Enzymatic Degradation, and Mechanical Properties", *Yonsei Med J* **2001,** *42*, 172.

[237] Weadock, K. S., Miller, E. J., Bellincampi, L. D., Zawadsky, J. P., Dunn, M. G. "Physical crosslinking of collagen fibers: comparison of ultraviolet irradiation and dehydrothermal treatment", *J Biomed Mater Res* **1995,** *29*, 1373.

[238] Sionkowska, A., Wisniewski, M., Skopinska, J., Poggi, G. F., Marsano, E., Maxwell, C. A., Wess, T. J. "Thermal and mechanical properties of UV irradiated collagen/chitosan thin films", *Polym Degr Stab* **2006,** *91*, 3026.

[239] Pek, Y. S., Spectorb, M., Yannas, I. V., Gibson, L. J. "Degradation of a collagen–chondroitin-6-sulfate matrix by collagenase and by chondroitinase", *Biomaterials* **2004,** *25*, 473.

[240] Nam, K., Kimura, T., Kishida□, A. "Preparation and characterization of cross-linked collagen–phospholipid polymer hybrid gels", *Biomaterials* **2007,** *28*, 1.

[241] Muyonga, J. H., Cole, C. G. B., Duodu, K. G. "Fourier transform infrared (FTIR) spectroscopic study of acid soluble collagen and gelatin from skins and bones of young and adult Nile perch (Lates niloticus)", *Food Chem* **2004,** *86*, 325.

[242] Sinha, R. P., Häder, D.-P. "UV-induced DNA damage and repair: a review", *Phoch Photobio Sci* **2002,** *1*, 225.

[243] Fry, R. J. M., Ley, R. D. "The Mechanisms of Radiation Carcinogenesis", *Radiat Phys Chem* **1984,** *24*, 329.

[244] Orban, J. M., Wilson, L. B., Kofroth, J. A., El-Kurdi, M. S., Maul, T. M., Vorp, D. A. "Crosslinking of collagen gels by transglutaminase", *J Biomed Mater Res A* **2004,** *68A*, 756.

[245] Chen, R.-N., Ho, H.-O., Sheu, M.-T. "Characterization of collagen matrices crosslinked using microbial transglutaminase", *Biomaterials* **2005,** *26*, 4229.

[246] Lee, J. M., Edwards, H. H. L., Pereira, C. A., Samii, S. I. "Crosslinking of tissue-derived biomaterials in 1-ethyl-3-(3-dimethylaminopropyl)-carbodiimide (EDC)", *J Mater Sci-Mater M* **1996,** *7*, 531.

[247] Duan, X., Sheardown, H. "Crosslinking of collagen with dendrimers", *J Biomed Mater Res A* **2005,** *75A*, 510.

[248] Bellincampi, L. D., Dunn, M. G. "Effect of Crosslinking Method on Collagen Fiber–Fibroblast Interactions", *J Appl Polym Sci* **1997,** *63*, 1493.

[249] Caruso, A. B., Dunn, M. G. "Changes in mechanical properties and cellularity during long-term culture of collagen fiber ACL reconstruction scaffolds", *J Biomed Mater Res* **2005,** *73A*, 388.

[250] Who, Fact sheet Nº 317 - Cardiovascular diseases. http://www.who.int/mediacentre/factsheets/fs317/en/index.html, (07-05-2010),

[251] Atala, A., Lanza, R. P., *Methods of Tissue Engineering*, Academic Press: 2002.

[252] Gobeaux, F., Mosser, G., Anglo, A., Panine, P., Davidson, P., Giraud-Guille, M. M., Belamie, E. "Fibrillogenesis in Dense Collagen Solutions: A Physicochemical Study", *J Mol Biol* **2008,** *376*, 1509.

[253] Achilli, M., Lagueux, J., Mantovani, D. "On the Effects of UV-C and pH on the Mechanical Behavior, Molecular Conformation and Cell Viability of Collagen-Based Scaffold for Vascular Tissue Engineering", *Macromol Biosci* **2010,** *10*, 307.

[254] Berglund, J. D., Mohseni, M. M., Nerem, R. M., Sambanis, A. "A biological hybrid model for collagen-based tissue engineered vascular constructs", *Biomaterials* **2003,** *24*, 1241.

[255] Gentleman, E., Lay, A. N., Dickerson, D. A., Nauman, E. A., Livesay, G. A., Dee, K. C. "Mechanical characterization of collagen fibers and scaffolds for tissue engineering", *Biomaterials* **2003,** *24*, 3805.

[256] Harris, J. R., Reiber, A. "Influence of saline and pH on collagen type I fibrillogenesis in vitro: Fibril polymorphism and colloidal gold labelling", *Micron* **2007,** *38*, 513.

[257] Couet, F., Mantovani, D. "How to Optimize Maturation in a Bioreactor for Vascular Tissue Engineering: Focus on a Decision Algorithm for Experimental Planning", *Ann Biomed Eng* **2010,** *38*, 2877.

[258] Bilodeau, K., Mantovani, D. "Bioreactors for Tissue Engineering: Focus on Mechanical Constraints. A Comparative Review", *Tissue Eng* **2006,** *12*, 1.

[259] Achilli, M., Mantovani, D. "Tailoring Mechanical Properties of Collagen-Based Scaffolds for Vascular Tissue Engineering: The Effects of pH, Temperature and Ionic Strength on Gelation", *Polymers* **2010,** *2*, 664.

[260] Xuejun Xin, Borzachiello, A., Netti, P. A., Ambrosio, L., Nicolais, L. "Hyaluronic-acid-based semi-interpenetrating materials", *J Biomat Sci-Polym E* **2004,** *15*, 1223.

[261] Travis, J. A., Hughes, M. G., Wong, J. M., Wagner, W. D., Geary, R. L. "Hyaluronan Enhances Contraction of Collagen by Smooth Muscle Cells and Adventitial Fibroblasts : Role of CD44 and Implications for Constrictive Remodeling", *Circ Res* **2001,** *88*, 77.

[262] Li, C.-Q., Huang, B., Luo, G., Zhang, C.-Z., Zhuang, Y., Zhou, Y. "Construction of collagen II/hyaluronate/chondroitin-6-sulfate tri-copolymer scaffold for nucleus pulposus tissue engineering and preliminary analysis of its physico-chemical properties and biocompatibility", *J Mater Sci-Mater M* **2010,** *21*, 741.

[263] Tomihata, K., Ikada, Y. "Crosslinking of hyaluronic acid with water-soluble carbodiimide", *J Biomed Mater Res* **1997,** *37*, 243.

[264] Azuma, T., Oka, S. "Circumferential Tension in the Wall of Bent Blood Vessels", *Microvasc Res* **1974,** *7*, 10.

[265] Quick, C. M., Li, J. K. J., Weizsicker, H. W., Noordergraaf, A. In *Laplace's Law adapted to a blood vessel with two-phase wall structure*, Bioeng. Conf., Bar Harbor, ME , USA, 22-23 May, 1995; Bar Harbor, ME , USA, 1995; pp 1.

[266] Vawter, D. L., Fung, Y. C., West, J. B. "Elasticity of excised dog lung parenchyma", *J Appl Physiol* **1978,** *45*, 261.

[267] Feng, Z., Yamato, M., Akutsu, T., Nakamura, T., Okano, T., Umezu, M. "Investigation on the Mechanical Properties of Contracted Collagen Gels as a Scaffold for Tissue Engineering", *Artif Organs* **2003,** *21*, 84.

[268] Wille, J., Elson, E., Okamoto, R. "Cellular and Matrix Mechanics of Bioartificial Tissues During Continuous Cyclic Stretch", *Ann Biomed Eng* **2006,** *34*, 1678.

[269] Baguneid, M., Murray, D., Salacinski, H. J., Fuller, B., Hamilton, G., Walker, M., Seifalian, A. M. "Shear-stress preconditioning and tissue-engineering-based paradigms for generating arterial substitutes", *Biotechnol Appl Bioc* **2004,** *39*, 151.

[270] Ma, L., Gao, C., Mao, Z., Zhou, J., Shen, J. "Biodegradability and cell-mediated contraction of porous collagen scaffolds: the effect of lysine as a novel crosslinking bridge", *J Biomed Mater Res A* **2004,** *71*, 334.

[271] Everaerts, F., Torrianni, M., Van Luyn, M., Van Wachem, P., Feijen, J., Hendriks, M. "Reduced calcification of bioprostheses, cross-linked via an improved carbodiimide based method", *Biomaterials* **2004,** *25*, 5523.

[272] Song, E., Kim, S. Y., Chun, T., Byun, H.-J., Lee, Y. M. "Collagen scaffolds derived from a marine source and their biocompatibility", *Biomaterials* **2006,** *27*, 2951.

[273] Everaerts, F., Torrianni, M., Hendriks, M., Feijen, J. "Biomechanical properties of carbodiimide crosslinked collagen: Influence of the formation of ester crosslinks", *J Biomed Mater Res* **2008,** *85A*, 547.

[274] Saito, H., Murabayashi, S., Mitamura, Y., Taguchi, T. "Characterization of alkali-treated collagen gels prepared by different crosslinkers", *J Mater Sci-Mater M* **2008,** *19*, 1297.

[275] Niklason, L. E., Abbott, W., Gao, J., Klagges, B., Hirschi, K. K., Ulubayram, K., Conroy, N., Jones, R., Vasanawala, A., Sanzgiri, S., Langer, R. "Morphologic and mechanical characteristics of engineered bovine arteries", *J Vasc Surg* **2001,** *33*, 628.

[276] Hoerstrup, S. P., Kadner, A., Breymann, C., Maurus, C. F., Guenter, C. I., Sodian, R., Visjager, J. F., Zund, G., Turina, M. I. "Living, autologous pulmonary artery conduits tissue engineered from human umbilical cord cells", *Ann Thorac Surg* **2002,** *74*, 46.

[277] Stegemann, J. P., Nerem, R. M. "Phenotype modulation in vascular tissue engineering using biochemical and mechanical stimulation", *Ann Biomed Eng* **2003,** *31*, 391.

[278] Sung, H. W., Chang, W. H., Ma, C. Y., Lee, M. H. "Crosslinking of biological tissues using genipin and/or carbodiimide", *J Biomed Mater Res A* **2003,** *64*, 427.

[279] Voet, D., Voet, J. G., "Protein Folding, Dynamics, and Structural Evolution - Folding Pathways". In *Biochemistry*, 3rd ed.; International, W., Ed. John Wiley & Sons Inc: 2004; p 1616.

[280] Goh, K. L., Meakin, J. R., Aspden, R. M., Hukins, D. W. L. "Stress transfer in collagen fibrils reinforcing connective tissues: Effects of collagen fibril slenderness and relative stiffness", *J Theor Biol* **2007,** *245*, 305.

[281] Yunoki, S., Mori, K., Suzuki, T., Nagai, N., Munekata, M. "Novel elastic material from collagen for tissue engineering", *J Mater Sci-Mater M* **2007,** *18*, 1369.

[282] Lai, E. S., Anderson, C. M., Fuller, G. G. "Designing a tubular matrix of oriented collagen fibrils for tissue engineering", *Acta Biomater* **2011,** *7*, 2448.

[283] Chen, S., Hirota, N., Okuda, M., Takeguchi, M., Kobayashi, H., Hanagata, N., Ikoma, T. "Microstructures and rheological properties of tilapia fish-scale collagen hydrogels with aligned fibrils fabricated under magnetic fields", *Acta Biomater* **2011,** *7*, 644.

[284] Fung, Y. C., "On the Law of Laplace". In *Biomechanics: Mechanical Properties of Living Tissues*, Springer: New York, 1993; pp 14.